JOHANNES GUTENBERG UNIVERSITÄT MAINZ

Elektrochemische Si-Bindungsknüpfung

Dissertation

zur Erlangung des akademischen Grades
„Doktor der Naturwissenschaften“ (*Dr. rer. nat.*)
vorgelegt dem Fachbereich 09: Chemie, Pharmazie, Geographie und Geowissenschaften
der Johannes Gutenberg-Universität Mainz

eingereicht von

ALEXANDER DAVID BECK

geboren in Rosenheim

Januar 2023

Datum der Promotionsprüfung: 4. August 2023

Meiner Familie

Weisheit beruht auf Erfahrung. Erfahrung ist oft das Ergebnis mangelnder Weisheit.

(Sir Terence David John Pratchett, 1948 – 2015)

Erklärung

Die experimentelle und schriftliche Ausarbeitung dieser Arbeit wurde von Oktober 2019 bis Januar 2023 am Consortium für elektrochemische Industrie der Wacker Chemie AG unter der Leitung von Dr. Stefan Haufe (Abteilung RD-A/MUC, Wacker Chemie AG) und unter Betreuung durch Prof. Dr. S. R. Waldvogel, Department Chemie (FB 09, Johannes Gutenberg-Universität Mainz) durchgeführt. Hiermit erkläre ich, dass die vorliegende Dissertation von mir selbständig, ohne fremde Hilfe und mit keinen anderen als den darin angegebenen Hilfsmitteln angefertigt wurde, und dass die wörtlichen oder dem Inhalt nach aus fremden Arbeiten entnommenen Stellen, Zeichnungen, Skizzen, bildlichen Darstellungen und dergleichen als solche genau kenntlich gemacht sind.

München, 06.08.2023

_____

Alexander Beck

Danksagung

Auflistung aller Publikationen

[1] A. D. Beck, S. Haufe, S. R. Waldvogel, *ChemElectroChem* **2023**, im Druck.
[DOI: 10.1002/celc.202201149]

[2] A. D. Beck, L. Schäffer, S. Haufe, S. R. Waldvogel, *Eur. J. Org. Chem.* **2022**, e202201253.
[DOI: 10.1002/ejoc.202201253]

[3] R. Baierl, A. Kostenko, F. Hanusch, A. D. Beck, S. Inoue, *Eur. J. Org. Chem.* **2022**, e202201072.
[DOI: 10.1002/ejoc.202201072]

[4] A. D. Beck, S. Haufe, S. R. Waldvogel, *ChemElectroChem* **2022**, *9*, e202200840.
[DOI: 10.1002/celc.202200840]

[5] A. D. Beck, S. Haufe, J. Tillmann, S. R. Waldvogel, *ChemElectroChem* **2022**, *9*, e202101374.
[DOI: 10.1002/celc.202101374]

Patente

[1] „Verfahren zur Herstellung von Organosiliciumverbindungen“, A. D. Beck, S. Haufe, Patentanmeldung vom 20.05.2022 am EPA (2022P00019WO).

Konferenzbeiträge

[1] Posterpräsentation: Electrochemistry 2022 (27.09.2022 - 30.09.2022, Berlin), am 28.09.2022, *Electrochemical metal-free catalyzed silicon-carbon bond formation*.

Abstrakt

Die Konversion von Chlor- und Hydrosilanen hin zu werthaltigen Materialien sowie die Erzeugung von Siloxanen basiert bisher auf konventionellen chemischen Syntheserouten, verbunden mit dem Einsatz von Oxidations- und Reduktionsmitteln bei hohen Temperaturen. Bei den hier aufgeführten Arbeiten wurden elektrochemische Ansätze mit Ziel einer Si-Si- und Si-C-Bindungsknüpfung untersucht, die Strom als „grüne“ Alternative zu den bisher genutzten Prozessen etablieren sollen.

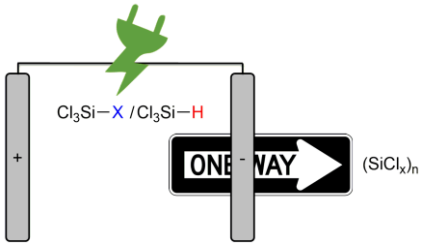

Die stark steigende Nachfrage nach Nano- und Mikroelektronik erfordert neue und umweltfreundliche Reaktionswege für die Herstellung eines der wichtigsten Substrate für die Produktion von Halbleitermaterialien: Si_2Cl_6. Die vorliegende Studie befasst sich mit den Möglichkeiten und Herausforderungen der selektiven elektrochemischen Bildung von Si_2Cl_6 ausgehend von mehrfach Halogen-funktionalisierten Silanen, sowohl durch Cyclovoltammetrie-Messungen wie auch durch elektrochemische Synthese. Die kathodische Dehalodimerisierung von $SiCl_4$ und der Ansatz des Halogenaustauschs für eine leichtere Substratreduktion werden in Betracht gezogen. Eine halogenidfreie anodische Dehydrodimerisierung von $HSiCl_3$ wird untersucht, einschließlich der Lewis-sauren Aktivierung der Si-H-Bindung. Darüber hinaus wurde auch der Einsatz tertiärer Amine, für die Benkeser-ähnliche *in situ*-Erzeugung eines $SiCl_3$-Anions studiert. Das Zielmolekül Si_2Cl_6 ist stark anfällig gegenüber einer direkten elektrochemischen Konversion, was die anodische und kathodische Elektrosynthese äußerst herausfordernd gestaltet.

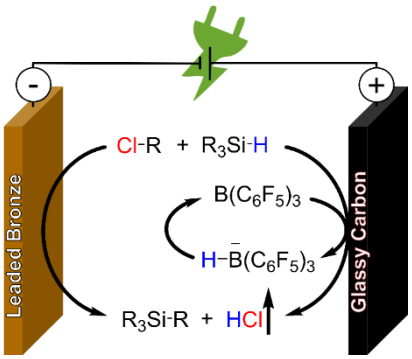

Die Anwendungsmöglichkeiten von $B(C_6F_5)_3$ erstrecken sich in zahlreiche Gebiete der organischen und anorganischen Chemie. Eine elektrochemische Umsetzung von Hydrosilanen unter Verwendung von $B(C_6F_5)_3$ zur Erhöhung der Ausbeute oder der Substratbandbreite wurde jedoch bisher nicht beschrieben. Die vorliegende Arbeit befasst sich mit der Verwendung von Lewis-sauren Boranen, insbesondere $B(C_6F_5)_3$, für die Aktivierung von Hydrosilanen in Gegenwart eines kommerziell erhältlichen Elektrolyten zur Erzeugung von Si-C-Bindungen. Die Benzylierung und Allylierung von Hydrosilan-Spezies wird in Gegenwart katalytischer Mengen von $B(C_6F_5)_3$ mit einer Ausbeute von bis zu 86% erfolgreich realisiert. Ein Screening der Elektroden-materialien ergab, dass Bleibronzen für die kathodische Umwandlung ohne Kontaminierung des Elektrolyten durch Schwermetalle am besten geeignet sind. Untersuchungen mittels Cyclovoltammetrie zeigen, dass $B(C_6F_5)_3$ das Hydrosilan aktiviert und so den nukleophilen Zugang fördert, was zu einer erheblichen Steigerung der Ausbeute und Anreicherung des Zielprodukts im Reaktionsgemisch führt.

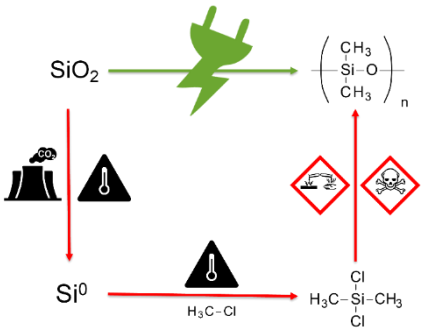

Die Nachfrage nach Alternativen zum industriellen, hoch energieintensiven Verfahren zur Erzeugung von Silikonen ausgehend von Siliziumdioxid veranlasste eine kritische Bewertung des zuvor beschriebenen direkten elektrochemischen Weges. Die erfolgreiche Methylierung verschiedener SiO_2-Quellen zu zyklischen Methylsiloxanen

konnte über eine elektrochemische Reduktionsreaktion erreicht werden. Im Gegensatz zu früheren Annahmen geht die Reaktion nicht von Methanol als Methylradikalquelle aus, was zu einer Methoxylierung des Elektrolytlösungsmittels führt. Es hat sich gezeigt, dass Methylammoniumkationen die direkte Umsetzung ermöglichen, stark abhängig von der Stabilisierung des Radikal-Zwischenprodukts durch den Elektrolyten. THF / $Bu_4NCF_3SO_3$ ist das einzige anwendbare System mit Ausbeuten unter 14 %, bezogen auf die Methylammoniumkationen für die höchste bisher erhaltene Produktmenge. Mechanistische Erkenntnisse zeigen, dass die Methylierung nicht über die vermeintliche Hydrolyse des Dimethoxydimethylsilan-Zwischenprodukts erfolgt, sondern über eine direkte Konversion, wie vergleichende Untersuchungen eines FENTON-ähnlichen Verfahrens zeigen. Weiterhin sind zyklische Methylsiloxane anfällig für eine nachfolgende elektrochemische Äquilibrierung, die maßgeblich durch das Elektrolytlösemittel dirigiert wird.

Inhaltsverzeichnis

1 Einleitung und Motivation

Das Gebiet der Elektrosynthese schafft eine umweltfreundliche Alternative zu herkömmlichen Syntheserouten[1] und erlebte in den vergangenen Jahren eine wahre Renaissance für künftige Syntheseanwendungen.[2] Im Bereich der Nachhaltigkeit kann diese Schlüsseltechnologie durch die Vermeidung stöchiometrischer Mengen an Oxidations- und Reduktionsmitteln glänzen.[3] Der Einsatz von Strom als Reagenz, besonders aus regenerativen Quellen, ermöglicht so „grüne" Prozesse und stellt damit einen entscheidenden Wegbereiter zu klimafreundlichen Verfahren dar.[4] Im Themenbereich der Reaktionssicherheit, ein für industrielle Anwendungen hochrelevantes Gebiet, punktet die Elektrosynthese durch die einfache Möglichkeit des Strom-Abschaltens. Ein thermisches „Durchgehen" der Reaktion kann so effektiv unterbunden werden und ermöglicht inhärente Reaktionssicherheit.[5]

Als eines der forschungsintensivsten Chemieunternehmen der Welt entwickelt WACKER seit über 100 Jahren chemische Spezialprodukte. Hierbei werden aktuell ca. 65% des Umsatzes basierend auf dem Grundstoff Silizium erzeugt.[6] Mit einem Portfolio von mehr als 3200 Produkten können so insbesondere Kunden im Bereich der Chemie-, Bau-, Elektro-, Elektrotechnik- und Photovoltaikindustrie bedient werden.[6] Die Unternehmensstruktur von WACKER gliedert sich hierbei in die vier Geschäftsbereiche Silicones, Polymers, Polysilicon und Biosolutions. Um die ambitionierten Nachhaltigkeitsziele mit dem Erreichen der Klimaneutralität bis 2045 verwirklichen zu können,[7] die WACKER verfolgt, werden unterschiedlichste Ansätze auf eine industrielle Machbarkeit überprüft. Dazu zählt ebenfalls die mögliche Elektrifizierung von Syntheseprozessen. Als europäischer Marktführer im Bereich der Silikone,[6] ist sowohl die Konversion von reaktiven Chlor-[8] und Hydrosilanen[9] zu werthaltigen Produkten wie auch die Untersuchung neuartiger, direkter Zugänge zu Silikonen[10] ein hoch relevantes Themengebiet. So lassen sich beispielsweise organofunktionelle Silane erzeugen, mithilfe derer das gewünschte Eigenschaftsprofil im Silikonprodukt bestimmt werden kann.[11] Weiterhin ist die Anzahl und Art der funktionellen Gruppen ausschlaggebend für weitere Produktmerkmale und entscheidet so über ein breites Spektrum von Silikonölen, -emulsionen, -elastomeren und -harzen.[12] Die Untersuchung von elektrochemischen Syntheserouten im Bereich

der Silane und Siloxane kann so einen entscheidenden Beitrag für die Nachhaltigkeitsziele leisten.

[1] a) D. Cantillo, *Chem. Commun.* **2022**, *58*, 619–628; b) C. Kingston, M. D. Palkowitz, Y. Takahira, J. C. Vantourout, B. K. Peters, Y. Kawamata, P. S. Baran, *Acc. Chem. Res.* **2020**, *53*, 72–83; c) M. C. Leech, K. Lam, *Nat. Rev. Chem.* **2022**, *6*, 275–286; d) A. Shatskiy, H. Lundberg, M. D. Kärkäs, *ChemElectroChem* **2019**, *6*, 4067–4092; e) S. R. Waldvogel, B. Janza, *Angew. Chem., Int. Ed.* **2014**, *53*, 7122–7123; *Angew. Chem.*, **2014**, *126*, 7248–7249; f) Y. Yuan, A. Lei, *Nat. Commun.* **2020**, *11*, 802.

[2] D. Pollok, S. R. Waldvogel, *Chem. Sci.* **2020**, *11*, 12386–12400.

[3] a) M. D. Kärkäs, *Chem. Soc. Rev.* **2018**, *47*, 5786–5865; b) R. D. Little, K. D. Moeller, *Chem. Rev.* **2018**, *118*, 4483–4484; c) J. L. Röckl, D. Pollok, R. Franke, S. R. Waldvogel, *Acc. Chem. Res.* **2020**, *53*, 45–61; d) S. R. Waldvogel, S. Lips, M. Selt, B. Riehl, C. J. Kampf, *Chem. Rev.* **2018**, *118*, 6706–6765; e) A. Wiebe, T. Gieshoff, S. Möhle, E. Rodrigo, M. Zirbes, S. R. Waldvogel, *Angew. Chem., Int. Ed.* **2018**, *57*, 5594–5619; *Angew. Chem.*, **2018**, *130*, 5694–5721; f) M. Yan, Y. Kawamata, P. S. Baran, *Chem. Rev.* **2017**, *117*, 13230–13319.

[4] B. A. Frontana-Uribe, R. D. Little, J. G. Ibanez, A. Palma, R. Vasquez-Medrano, *Green Chem.* **2010**, *12*, 2099–2119.

[5] E. J. Horn, B. R. Rosen, P. S. Baran, *ACS Cent. Sci.* **2016**, *2*, 302–308.

[6] "Geschäftsbericht 2021 Wacker Chemie AG - Geschäftsbericht 2021. Chemie – die Lösungsindustrie für eine nachhaltige Welt", gefunden unter https://www.wacker.com/cms/de-de/about-wacker/wacker-at-a-glance/annual-report/detail.html (Aufgerufen am: 17.01.2023), **2022**.

[7] "Race to Zero", gefunden unter https://www.wacker.com/cms/de-de/about-wacker/sustainability/overview/sustainability.html (Aufgerufen am: 17.01.2023), **2022**.

[8] A. D. Beck, S. Haufe, J. Tillmann, S. R. Waldvogel, *ChemElectroChem* **2022**, *9*, e202101374.

[9] A. D. Beck, S. Haufe, S. R. Waldvogel, *ChemElectroChem* **2022**, *9*, e202200840.

[10] A. D. Beck, L. Schäffer, S. Haufe, S. R. Waldvogel, *Eur. J. Org. Chem.* **2022**, e202201253.

[11] E. P. Plueddemann, *Silane Coupling Agents*, Springer New York, Boston, MA, **1982**.

[12] J. Ackermann, V. Damrath, *Chem. Unserer Zeit* **1989**, *23*, 86–99.

1.1 Die elektrochemische Konversion von Chlor- und Hydrosilanen

Zu diesem Kapitel wurde ein Manuskript veröffentlicht:
A. D. Beck, S. Haufe, S. R. Waldvogel*, *General Concepts and Recent Advances in the Electrochemical Transformation of Chloro- and Hydrosilanes*, *ChemElectroChem* **2023**, im Druck. [DOI: 10.1002/celc.202201149] *Korrespondenzautor
Erläuterung meines Beitrags: Das komplette Manuskript wurde von mir verfasst. Die Finalisierung der Veröffentlichung wurde von mir unter Betreuung von Dr. Stefan Haufe und Prof. Dr. Siegfried R. Waldvogel abgeschlossen.

Zusammenfassung

Organosiliziumverbindungen nehmen eine tragende Rolle in einer Vielzahl von Anwendungen ein, die sich von Materialwissenschaften,[1] Pharmazie[2] und Transport[3] bis hin zu Elektronikbauteilen erstrecken.[4] Traditionelle Syntheserouten basieren dabei häufig auf GRIGNARD-artigen Reaktionen,[5] WURTZ-analogen Konversionen mittels Alkalimetallen[6] oder auf Edelmetall-katalysierten, vorzugsweise Palladium-basierten, Systemen.[7] Entgegen den meist harschen Reaktionsbedingungen, die aus industrieller Sicht nicht nur einen Sicherheitsaspekt, sondern auch eine ökonomische Entscheidung darstellen, ermöglicht die Elektrochemie hier neuartige Ansätze. Syntheserouten zu Organosiliziumverbindungen können sich so bei geeigneten Parametern über anodische[8–12] und kathodische[13,14] Konversionen sicher und nachhaltig gestalten lassen. Besonders die gute kommerzielle Verfügbarkeit von hochwertigem Equipment, welches für Synthesearbeiten und Analytik benötigt wird, erleichtert den Einstieg in die Welt der elektrochemischen Silankonversion und führte in den vergangenen Jahren zu einer Renaissance unter Entwicklung von innovativen Syntheseverfahren.[8–12,15–19]

Der Umgang mit Chlor- und Hydrosilanen stellt jedoch eine Besonderheit unter den elektrochemischen Konversionen dar. Die hohe Anfälligkeit für Hydrolyse[15,20–24] schließt nicht nur die Verwendung von protischen Lösemitteln aus, sie bedingt auch die absolut wasserfreie Arbeit mit allen Komponenten. Vom Lösemittel und Leitsalz, über die eingesetzten Substrate und Additive bis hin zu Reaktionsgefäßen und Elektrodenmaterialien ist der Ausschluss von Feuchtigkeit eine Voraussetzung. Besonders in elektrochemischen Analysetechniken, wie der Cyclovoltammetrie (CV)

kam[20,22–24] und kommt[25] es so häufig zu Fehlinterpretationen, da Reduktionssignale des entstehenden Chlorwasserstoffs als solche von Chlorsilanen aufgefasst werden können. Darüber hinaus können die Nukleophilie des Lösemittels,[16,20,26,27,28] stabilisierende Eigenschaften von Leitsalz-Ionen[10–12,29–34] und Additive, wie Komplexbildner,[35–37] den Reaktionsverlauf ausschlaggebend beeinflussen. Eine Vielzahl an unerwünschten Nebenreaktionen, von der Äquilibrierung[32,38] über den Halogenaustausch,[29,39–43] bis zu nukleophilen Additionen[20,26] oder der Hydrolyse[15,20–24] können auftreten, wenn notwendige Komponenten für die Konversion nicht mit Bedacht gewählt werden.

Erfüllen alle Bestandteile die notwendigen Voraussetzungen, lassen sich Organosiliziumverbindungen über diverse Syntheseprotokolle erzeugen. Grundsätzlich ist hierbei die Reaktionsführung über den anodischen oder kathodischen Verlauf nach dem Ausgangsmaterial zu unterscheiden (Schema 1): Chlorsilane können durch kathodische Konversion unter Abspaltung von Chlorid reduziert, Hydrosilane unter Freisetzung von Protonen oxidiert werden.

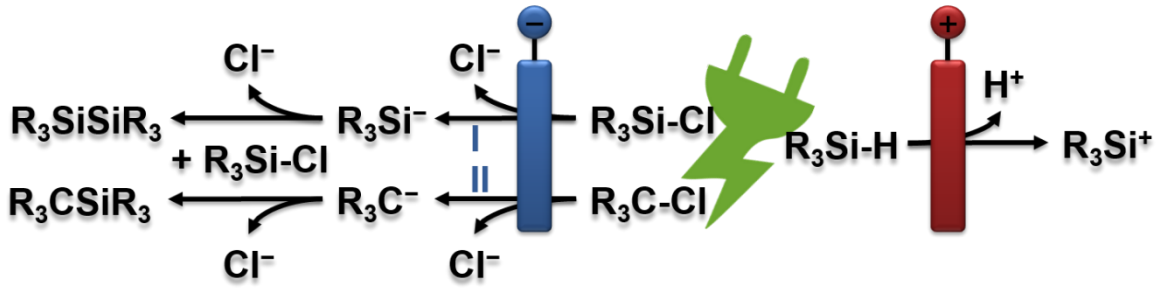

Schema 1. Elektrochemische Konversion von Chlor- und Hydrosilanen: Reduktiver Zugang zu Si-Si- (Route **I**) und Si-C-Bindung (Route **II**) unter Erzeugung eines Anions mit nukleophilem Angriff auf ein elektrophiles Chlorsilan[31,40,44,45] und oxidativer Zugang durch Erzeugung eines Silylkations.[29,46]

Für Chlorsilane kommt es hierbei zu einer Reduktion bis zum Silylanion (Schema 1, **I**),[31,40,44,45] falls keine abfangenden Substrate, wie ungesättigte Kohlenwasserstoffe,[19] in der Reaktionslösung vorliegen. Dieses Silylanion erzeugt unter nukleophilem Angriff auf ein weiteres elektrophiles Chlorsilan eine Si-Si-Bindungsknüpfung.[28] Über diese Route sind je nach Anzahl der Chloratome am Silan ein breites Spektrum an Verbindungen, von Dimeren[13,23,31–33,39–41,44,47,48–50] über Oligomeren[31,40,44,45,49–51,52] bis hin zu Polymeren[28,31,32,39,40,45,48,51,53,54] und sogar die Abscheidung von elementarem Silizium[55] zugänglich. Anstelle des Chlorsilans können auch organische Verbindungen reduziert werden, die beispielsweise als Carbanion (Schema 1, **II**) analog eine

nukleophile Substitution am Chlorsilan eingehen.[18,35–37,56,57–59] Durch Abspaltung von Chlorid können so Si-C-Bindungen erzeugt werden. Das jeweils freigesetzte Chlorid muss im Reaktionsverlauf abgefangen werden, um keine störenden Nebenreaktionen, wie Chlorierung des Lösemittels,[57–59] zu verursachen. Während bereits Abfangreaktionen wie die Chlorierung von Alkenen[13] oder *in situ* erzeugten Protonen[13,14] eingesetzt wurden, ist die Opferanode nach wie vor das Mittel der Wahl und bestimmt maßgeblich den Reaktionsverlauf. Neben dem Abfangen von Chlorid sind das Stabilisieren des reduzierten Intermediats durch *in situ* erzeugte ionische Verbindungen[19,31,34,54,60] und sogar der Schutz vor Überreduktion des Zielprodukts[35] Eigenschaften, die sich durch den Einsatz einer Opferanode nutzen lassen.

Hydrosilane als Ausgangsmaterial können über den anodischen Reaktionsweg oxidiert werden. Das Oxidationspotential befindet sich meist in hohen anodischen Bereichen und die direkte Oxidation unterliegt damit harschen Bedingungen.[8,11,61] Neben der geringeren Substratvielfalt und höheren Preisen der Hydrosilane im Vergleich zu Chlorsilanen, ist dies der Hauptgrund für die überschaubare Anzahl an wissenschaftlichen Studien zur direkten anodischen Konversion. Häufiger hat sich in den vergangenen Jahren der Einsatz von Mediatoren in der Oxidation von Hydrosilanen bewährt. Die Aktivierung der Si-H-Bindung durch Borane, wie sie in dieser Arbeit behandelt werden (Schema 2, links),[12,42] wie auch die radikalische Mediation über *N*-oxyle (Schema 2, rechts),[8–11] beispielsweise durch Oxidation von *N*-Hydroxyphthalimid (NHPI) zur reaktiven Radikalspezies Phthalimido-*N*-oxyl (PINO), stellen Optionen für milde Reaktionsbedingungen dar. Besonders die Wasserstoffatom-Transfer (HAT)-Reaktion mit einem Hydrosilan hat Aufmerksamkeit erlangt[62] und kann so zur Darstellung von Silanolen,[8] Silanonen,[9] Dibenzosilolen[10] und zur Silyl-Oxygenierung von Alkenen[11] eingesetzt werden.

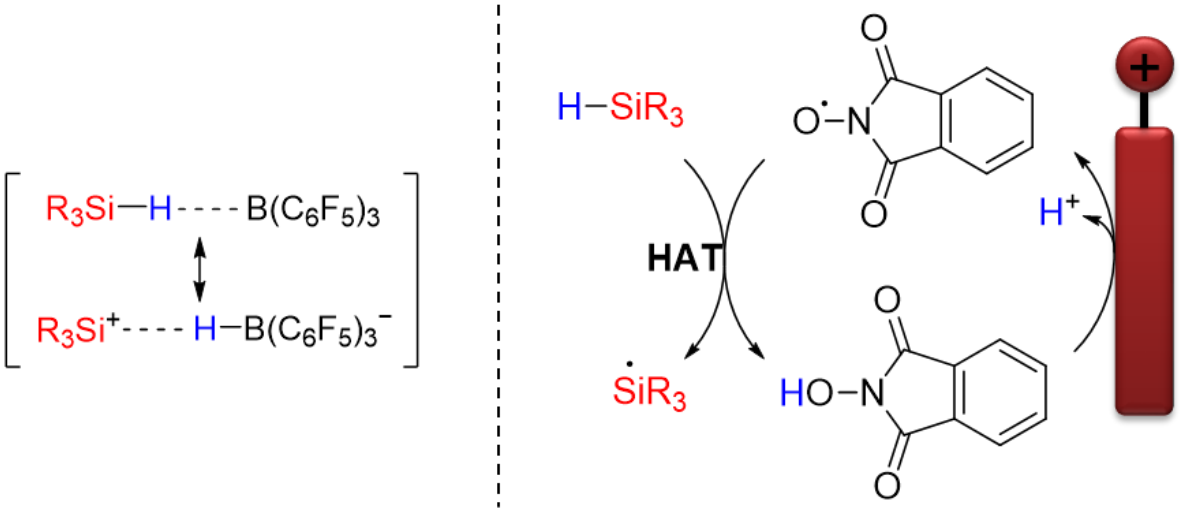

Schema 2. Aktivierung von Hydrosilanen: Durch Lewis-saure Borane wie $B(C_6F_5)_3$[12,42] (links) und durch HAT Reaktion mittels NHPI / PINO[8–11] (rechts).

[1] a) T. Kalnin, V. Gulbis, *Corrosion protection*. *Processes, management and technologies*, Nova Science Publishers, New York, **2009**; b) E. B. Wyman, M. C. Skief, *Organosilanes*. *Properties, performance, and applications*, Nova Science Publishers, New York, **2010**.

[2] a) A. K. Franz, S. O. Wilson, *J. Med. Chem.* **2013**, *56*, 388–405; b) A. Ramirez, K. A. Woerpel, *Org. Lett.* **2005**, *7*, 4617–4620; c) G. A. Showell, J. S. Mills, *Drug Discovery Today* **2003**, *8*, 551–556.

[3] a) N. Auner, J. Weis *Organosilicon chemistry VI*. *From molecules to materials*, Wiley-VCH, Weinheim, Chichester, **2008**; b) E. Pouget, J. Tonnar, P. Lucas, P. Lacroix-Desmazes, F. Ganachaud, B. Boutevin, *Chem. Rev.* **2010**, *110*, 1233–1277.

[4] a) L. Du, W. Chu, H. Miao, D. Wang, C. Xu, Y. Ding, *Eur. J. Inorg. Chem.* **2015**, *2015*, 3205–3211; b) R. A. Ovanesyan, D. M. Hausmann, S. Agarwal, *ACS Appl. Mater. Interfaces* **2015**, *7*, 10806–10813; c) R. A. Ovanesyan, D. M. Hausmann, S. Agarwal, *ACS Appl. Mater. Interfaces* **2018**, *10*, 19153–19161; d) R. A. Ovanesyan, N. Leick, K. M. Kelchner, D. M. Hausmann, S. Agarwal, *Chem. Mater.* **2017**, *29*, 6269–6278.

[5] a) S. Bähr, W. Xue, M. Oestreich, *ACS Catal.* **2019**, *9*, 16–24; b) Z. Li, X. Cao, G. Lai, J. Liu, Y. Ni, J. Wu, H. Qiu, *J. Organomet. Chem.* **2006**, *691*, 4740–4746; c) G. Martin, F. S. Kipping, *J. Chem. Soc., Trans.* **1909**, *95*, 302–314; d) R. Robison, F. S. Kipping, *J. Chem. Soc., Trans.* **1908**, *93*, 439–456.

[6] a) J. Koe, *Polym. Int.* **2009**, *58*, 255–260; b) K. Meenu, D. S. Bag, R. Lagarkha, R. Tomar, A. K. Gupta, *Curr. Organocatal.* **2019**, *6*, 193–221.

[7] a) R. E. Grote, E. R. Jarvo, *Org. Lett.* **2009**, *11*, 485–488; b) Z.-D. Huang, R. Ding, P. Wang, Y.-H. Xu, T.-P. Loh, *Chem. Commun.* **2016**, *52*, 5609–5612.

[8] H. Liang, L.-J. Wang, Y.-X. Ji, H. Wang, B. Zhang, *Angew. Chem., Int. Ed.* **2021**, *60*, 1839–1844; *Angew. Chem.*, **2021**, *133*, 1867–1872.

[9] K. Okamoto, S. Nagahara, Y. Imada, R. Narita, Y. Kitano, K. Chiba, *J. Org. Chem.* **2021**, *86*, 15992–16000.

[10] P. Han, M. Yin, H. Li, J. Yi, L. Jing, B. Wei, *Adv. Synth. Catal.* **2021**, *363*, 2757–2761.

[11] J. Ke, W. Liu, X. Zhu, X. Tan, C. He, *Angew. Chem., Int. Ed.* **2021**, *60*, 8744–8749; *Angew. Chem.*, **2021**, *133*, 8826–8831.

[12] A. D. Beck, S. Haufe, S. R. Waldvogel, *ChemElectroChem* **2022**, *9*, e202200840.

[13] C. Jammegg, S. Graschy, E. Hengge, *Organometallics* **1994**, *13*, 2397–2400.

[14] A. Popp, R. Weidner, H. Stüger, C. Grogger, B. Loidl (Consortium für elektrochemische Industrie GmbH), DE 10 2004 029 258 A1, **2004**.

[15] V. Jouikov, C. Biran, M. Bordeau, J. Dunoguès, *Electrochim. Acta* **1999**, *45*, 1015–1024.

[16] S. Soualmi, M. Dieng, A. Ourari, D. Gningue-Sall, V. Jouikov, *Electrochim. Acta* **2015**, *158*, 457–469.

[17] V. V. Zhuikov, *Russ. J. Electrochem.* **2000**, *36*, 117–127.

[18] C. Grogger, B. Loidl, H. Stueger, T. Kammel, B. Pachaly, *J. Electrochem. Soc.* **2013**, *160*, G88-G92.

[19] L. Lu, J. C. Siu, Y. Lai, S. Lin, *J. Am. Chem. Soc.* **2020**, *142*, 21272–21278.

[20] R. Corriu, G. Dabosi, M. Martineau, *J. Organomet. Chem.* **1978**, *150*, 27–38.

[21] R. Corriu, G. Dabosi, M. Martineau, *J. Organomet. Chem.* **1981**, *222*, 195–199.

[22] R. Corriu, G. Dabosi, M. Martineau, *J. Organomet. Chem.* **1980**, *186*, 19–24.

[23] R. J. P. Corriu, G. Dabosi, M. Martineau, *J. Chem. Soc., Chem. Commun.* **1979**, 457b.

[24] W. G. Boberski, A. L. Allred, *J. Organomet. Chem.* **1975**, *88*, 73–77.

[25] M. Hoddenbagh, D. Foucher, D. Worsfold, *Electrochemical Studies of Chlorine Containing Silanes*, ChemRxiv, Cambridge: Cambridge Open Engage, **2021**.

[26] R. Corriu, G. Dabosi, M. Martineau, *J. Organomet. Chem.* **1980**, *186*, 25–37.

[27] a) J. L. Brefort, R. J. P. Corriu, C. Guerin, B. J. L. Henner, W. W. C. Wong Chi Man, *Organometallics* **1990**, *9*, 2080–2085; b) R. D. Miller, J. Michl, *Chem. Rev.* **1989**, *89*, 1359–1410.

[28] M. Okano, K. Takeda, T. Toriumi, H. Hamano, *Electrochim. Acta* **1998**, *44*, 659–666.

[29] A. Kunai, T. Kawakami, E. Toyoda, T. Sakurai, M. Ishikawa, *Chem. Lett.* **1993**, *22*, 1945–1948.

[30] Y. Kimata, H. Suzuki, S. Satoh, A. Kuriyama, *Organometallics* **1995**, *14*, 2506–2511.

[31] S. Kashimura, M. Ishifune, *J. Synth. Org. Chem. Jpn.* **2000**, *58*, 966–974.

[32] C. Grogger, B. Loidl, H. Stueger, T. Kammel, B. Pachaly, *J. Organomet. Chem.* **2006**, *691*, 105–110.

[33] Y. Kogai, M. Ishifune, K. Uchida, S. Kashimura, *Electrochemistry* **2005**, *73*, 419–423.

[34] B. K. Peters, K. X. Rodriguez, S. H. Reisberg, S. B. Beil, D. P. Hickey, Y. Kawamata, M. Collins, J. Starr, L. Chen, S. Udyavara, K. Klunder, T. J. Gorey, S. L. Anderson, M. Neurock, S. D. Minteer, P. S. Baran, *Science* **2019**, *363*, 838–845.

[35] P. Pons, C. Biran, M. Bordeau, J. Dunoguès, *J. Organomet. Chem.* **1988**, *358*, 31–37.

[36] D. Deffieux, M. Bordeau, C. Biran, J. Dunogues, *Organometallics* **1994**, *13*, 2415–2422.

[37] M. Bordeau, P. Clavel, A. Barba, M. Berlande, C. Biran, N. Roques, *Tetrahedron Lett.* **2003**, *44*, 3741–3744.

[38] a) L. G. Mahone, D. R. Weyenberg, *J. Organomet. Chem.* **1968**, *12*, 231–233; b) K. Moedritzer, J. R. van Wazer, *J. Organomet. Chem.* **1968**, *12*, 69–77; c) D. R. Weyenberg, A. E. Bey, P. J. Ellison, *J. Organomet. Chem.* **1965**, *3*, 489–492; d) F. C. Whitmore, E. W. Pietrusza, L. H. Sommer, *J. Am. Chem. Soc.* **1947**, *69*, 2108–2110.

[39] A. Kunai, E. Toyoda, T. Kawakami, M. Ishikawa, *Organometallics* **1992**, *11*, 2899–2903.

[40] S. Kashimura, M. Ishifune, N. Yamashita, H.-B. Bu, M. Takebayashi, S. Kitajima, D. Yoshiwara, Y. Kataoka, R. Nishida, S. Kawasaki Si, H. Murase, T. Shono, *J. Org. Chem.* **1999**, *64*, 6615–6621.

[41] J. Ohshita, K. Hino, T. Iwawaki, A. Kunai, *J. Organomet. Chem.* **2009**, *625*, 138–143.

[42] A. D. Beck, S. Haufe, J. Tillmann, S. R. Waldvogel, *ChemElectroChem* **2022**, *9*, e202101374.

[43] A. H. Schmidt, M. Russ, *Chem. Ber.* **1981**, *114*, 1099–1110.

[44] E. Hengge, H. Firgoi, *J. Organomet. Chem.* **1981**, *212*, 155–161.

[45] E. Hengge, G. Litscher, *Monatsh. Chem.* **1978**, *109*, 1217–1225.

[46] N. T. Berberova, *Russ. J. Electrochem.* **2000**, *36*, 174–182.

[47] a) P. Boudjouk, B. H. Han, K. R. Anderson, *J. Am. Chem. Soc.* **1982**, *104*, 4992–4993; b) R. Corriu, G. Dabosi, M. Martineau, *J. Organomet. Chem.* **1980**, *188*, 63–72; c) E. Hengge, C. Jammegg, W. Kalchauer (Wacker Chemie GmbH), EP 0629718 A1, **1994**; d) E. Hengge, G. Litscher, *Angew. Chem., Int. Ed.* **1976**, *15*, 370; *Angew. Chem.*, **1976**, *88*, 414; e) S. Kashiwamura, R. Nishida, T. Shono (Osaka Gas Co., Ltd.), JP 3264683 A2, **1991**.

[48] R. Nishida, S. Kawasaki, H. Murase (Osaka Gas Co., Ltd.), EP 0671487 B1, **1995**.

[49] E. Hengge, Ch. Jammegg in *Organosilicon Chemistry I*, John Wiley & Sons, Ltd, **2008**, pp. 27–29.

[50] A. Kunai, T. Kawakami, E. Toyoda, M. Ishikawa, *Organometallics* **1991**, *10*, 893–895.

[51] S. Kashimura, M. Ishifune, H.-B. Bu, M. Takebayashi, S. Kitajima, D. Yoshihara, R. Nishida, S. Kawasaki, H. Murase, T. Shono, *Tetrahedron Lett.* **1997**, *38*, 4607–4610.

[52] a) M. Ishifune, Y. Kogai, H. Iijima, Y. Kera, N. Yamashita, S. Kashimura, *Electrochemistry* **2004**, *72*, 159–164; b) A. Kunai, T. Kawakami, E. Toyoda, M. Ishikawa, *Organometallics* **1991**, *10*, 2001–2003.

[53] a) M. Bordeau, C. Biran, M.-P. Léger-Lambert, J. Dunoguès, *J. Chem. Soc., Chem. Commun.* **1991**, 1476–1477; b) M. Elangovan, A. Muthukumaran, M. Anbu Kulandainathan, *Eur. Polym. J.* **2005**, *41*, 2450–2460; c) T. Fujiki, M. Ishifune, S. Kashiwamura, S. Kawasaki, H. Murase, H. Sakamoto (Osaka Gas Co., Ltd.), JP 2006188620 A2, **2006**; d) M. Ishifune, Y. Kogai, H. Iijima, Y. Kera, N. Yamashita, S. Kashimura, *J. Macromol. Sci., Part A: Pure Appl.Chem.* **2004**, *41*, 373–386; e) K. Jian, C. Shao, H. Wang, J. Wang, Y. Wu, Z. Xie (National Defense Univ. of Science and Technology), CN 106245056 A, **2016**; f) S. Kawasaki, H. Murase, R. Nishida (Osaka Gas Co., Ltd.), JP 3692434 B2, **2005**; g) A. Mavrič, A. Badasyan, G. Mali, M. Valant, *Eur. Polym. J.* **2017**, *90*, 162–170; h) M. Okano, H. Fukai, M. Arakawa, H. Hamano, *Electrochem. Commun.* **1999**, *1*, 223–226; i) M. Okano, K. Nakamura, K. Yamada, N. Hosoda, M. Wasaka, *Electrochemistry* **2006**, *74*, 956–958; j) T. Shono, S. Kashimura, R. Nishida, S. Kawasaki (Osaka Gas Co., Ltd.), EP 0446578 A2, **1991**; k) T. Shono, S. Kashimura, R. Nishida, S. Kawasaki (Osaka Gas Co., Ltd.), EP 0558760 B1, **1993**; l) T. Kugita, D. Ohtani, M. Okano, K. Mochida, *Denki Kagaku (1961-1998)* **1994**, *522–523*; m) M. Umezawa, H. Ichikawa, T. Ishikawa, T. Nonaka, *Denki Kagaku (1961-1998)* **1991**, *59*, 421–426; n) A. Watanabe, T.

Komatsubara, M. Matsuda, Y. Yoshida, S. Tagawa, *J. Photopolym. Sci. Technol.* **1992**, *5*, 545–546.

[54] T. Shono, S. Kashimura, M. Ishifune, R. Nishida, *J. Chem. Soc., Chem. Commun.* **1990**, 1160–1161.

[55] a) A. K. Agrawal, A. E. Austin, *J. Electrochem. Soc.* **1981**, *128*, 2292–2296; b) N. Downes, Q. Cheek, S. Maldonado, *J. Electrochem. Soc.* **2021**, *168*, 22503; c) J. Gobet, H. Tannenberger, *J. Electrochem. Soc.* **1988**, *135*, 109–112; d) Q. P. Ma, W. Liu, B. C. Wang, Q. S. Meng, *Adv. Mater. Res.* **2009**, *79-82*, 1635–1638; e) T. Munisamy, A. J. Bard, *Electrochim. Acta* **2010**, *55*, 3797–3803; f) Y. Nishimura, Y. Fukunaka, T. Nohira, R. Hagiwara, *ECS Trans.* **2008**, *11*, 13–24; g) Y. Tsuyuki, T. Fujimura, M. Kunimoto, Y. Fukunaka, P. Pianetta, T. Homma, *J. Electrochem. Soc.* **2017**, *164*, D994-D998.

[56] a) M. Bordeau, C. Biran, P. Pons, M. P. Leger-Lambert, J. Dunogues, *J. Org. Chem.* **1992**, *57*, 4705–4711; b) V. Jouikov, V. Krasnov, *J. Organomet. Chem.* **1995**, *498*, 213–219; c) B. I. Martynov, A. A. Stepanov, *J. Fluorine Chem.* **1997**, *85*, 127–128; d) C. Moreau, F. Serein-Spirau, C. Biran, M. Bordeau, P. Gerval, *Organometallics* **1998**, *17*, 2797–2804; e) C. Moreau, F. Serein-Spirau, M. Bordeau, C. Biran, *Organometallics* **2001**, *20*, 1910–1917; f) C. Moreau, F. Serein-Spirau, M. Bordeau, C. Biran, J. Dunoguès, *J. Organomet. Chem.* **1996**, *522*, 213–221.

[57] T. Shono, Y. Matsumura, S. Katoh, N. Kise, *Chem. Lett.* **1985**, *14*, 463–466.

[58] J. Yoshida, K. Muraki, H. Funahashi, N. Kawabata, *J. Org. Chem.* **1986**, *51*, 3996–4000.

[59] J. Yoshida, K. Muraki, H. Funahashi, N. Kawabata, *J. Organomet. Chem.* **1985**, *284*, C33-C35.

[60] C. Duprat, C. Biran, M. Bordeau, T. Constantieux, P. Gerval, J. Dunoguès, *J. Chem. Soc., Chem. Commun.* **1995**, 2107.

[61] H. F. T. Klare, L. Albers, L. Süsse, S. Keess, T. Müller, M. Oestreich, *Chem. Rev.* **2021**, *121*, 5889–5985.

[62] L.-Q. Ren, N. Li, J. Ke, C. He, *Org. Chem. Front.* **2022**, *9*, 6400–6415.

ChemElectroChem
Review
doi.org/10.1002/celc.202201149
Chemistry Europe
European Chemical Societies Publishing
www.chemelectrochem.org

General Concepts and Recent Advances in the Electrochemical Transformation of Chloro- and Hydrosilanes

Alexander D. Beck,[a, b] Stefan Haufe,[a] and Siegfried R. Waldvogel*[b]

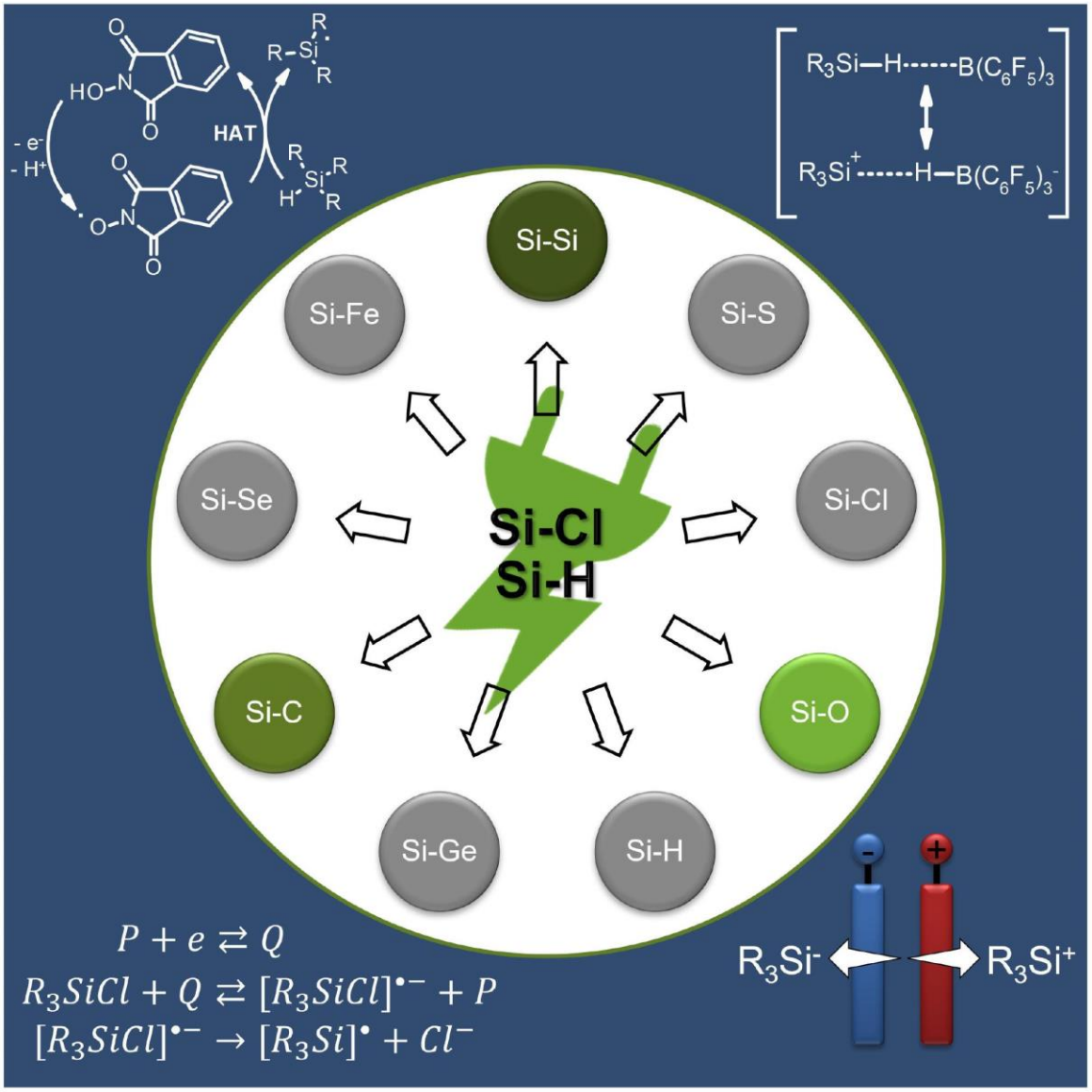

ChemElectroChem
Review
doi.org/10.1002/celc.202201149
Chemistry Europe
European Chemical Societies Publishing

Organosilanes play an important role in organic synthesis as well as in a variety of further areas, ranging from life science to transportation. Especially, the electrochemical access has become increasingly important in the past years and developed into an essential topic due to new conceptual approaches and mediated reaction control. With the commercial availability of high-quality electrochemical equipment, the technical requirements for electro- conversion are at hand to a wide audience. This results in the need for a concise survey of electrochemical silane transformation, appropriate for novices as well as experts alike. This review provides an overview of the most relevant work in this field, identifies common obstacles in working with chlorosilanes and hydrosilanes and bridges the gap between known techniques and novel methods with respect to their electrochemical conversion. The historical development is outlined with reference to the various cathodic as well as anodic conversions and should encourage to expand the research field of electrochemical silane transformation.

1. Introduction

Organosilicon compounds and silanes play a relevant role not only in organic chemistry,[1,2] but also in the fields of materials science,[3] pharmaceuticals,[4] transportation,[5,6] electronics and photonics,[5,6,7] life sciences and medical solutions,[5,6,8] as well as energy applications.[5] Due to their exceptional chemical and physical properties and unique Si bond construction features, a wide range of applications is established, leading to high demand. However, conventional synthetic routes for the preparation of organosilicon compounds are often based on Grignard-type conversions,[9] alkali metal-directed trans-formations such as Wurtz-type reactions,[10] or noble metal-catalyzed systems such as palladium based setups,[11] which represents not only a safety concern, but also environmental and cost considerations for industrial applications. This is very much in favor of the field of electrosynthesis which is experiencing a renaissance, providing an environmentally benign alternative to traditional synthesis protocols,[12] and emerging as a key discipline for future synthesis applications.[13] This methodology can easily pay off for compounds with highly added value.[14] The significant advantages of electrosynthesis are the avoidance of stoichiometric or even larger amounts of oxidizers or reducing agents and elevated temperatures.[15] Therefore, there is little or no reagent waste generated, and when renewable electricity is used, such processes become highly sustainable.[16] In addition, because the electricity can be simply switched off, thermal runaway reactions are not possible, making this method inherently safe.[17] However, several parameters and counter reactions seem to play a crucial role for success.[18,19] With modern screening and optimization techniques, determining the appropriate parameters can be accomplished in reasonable time.[20]

While the field of electrochemical synthesis of organosilanes and silane compounds is constantly expanding and new, exciting concepts are being published, to our knowledge, no review has appeared since 2000 on the holistic view of synthesis routes starting from hydro- and halosilanes.[21–26] Whereas there are reviews regarding the electrochemical synthesis of organosilicon species,[2,21–28] formation of polysilanes,[29,30] the electro-deposition of silicon starting from halosilanes,[31–34] and silyl radical driven conversions,[35] this review is focused on the electrochemical Si bond formation starting from chloro- and hydrosilanes. Ionic as well as the radical related type of conversion are the scope of the present analysis, further providing a general view on common obstacles regarding the work with chloro- and hydrosilanes. In addition, a compact overview of existing concepts of Si bond formation will be given, with emphasis on new methods as well as on the use of sacrificial anodes, continuing to play a major role in electrochemical conversion today. Reviews regarding the cleavage of Si bonds with the release of a "silyl super proton",[24,25] and functionalization of carbon in β-position to a Si-atom are already known and beyond the scope of this work.[25]

2. Useful information for electrochemical silane synthesis

For easier understanding of the work described here regarding the synthetic decisions and choice of parameters, some details on the work with halo- and hydrosilanes are first pointed out.

2.1. Solvent and additives

As in most systems of electro organic synthesis, a solvent is required for the electrolyte system. The solubility and dissociation of supporting electrolyte is mandatory, featuring sufficient conductivity. Further prerequisites are a suitable electrochemical window and inert behavior towards the substrates and intermediates. In addition, some special features must be considered in the conversion of halo- and hydrosilanes. Depending on the steric demand and electrophilic properties, these compounds are very prone to hydrolysis,[36–38] which requires working in aprotic solvents. In most cases, the solvent used must not contain any traces of moisture, which can otherwise easily result in misinterpretations, as we will outline

[a] *A. D. Beck, Dr. S. Haufe*
Wacker Chemie AG Consortium für elektrochemische Industrie
Zielstattstraße 20, 81379 München (Germany)
[b] *A. D. Beck, Prof. S. R. Waldvogel*
Department Chemie
Johannes Gutenberg-Universität Mainz
Duesbergweg 10–14, 55128 Mainz (Germany)
URL:https://www.aksw.uni-mainz.de/
E-mail:
E-mail: waldvogel@uni-mainz.de

ChemElectroChem
Review
doi.org/10.1002/celc.202201149
Chemistry Europe
European Chemical Societies Publishing

in the further sections through conclusions from the literature (*vide infra*).[39–41] Especially, mechanistic studies based on cyclic voltammetry (CV) easily allow for misleading conclusions. Even traces of water can enable rapid hydrolysis of the halosilanes with formation of hydrogen halide, i. e. the formation of HCl by hydrolysis of chlorosilanes (Scheme 1, a). This results in the detection of relatively low cathodic reduction signals, which can be misinterpreted as the reduction potential of the halosilanes.[37] In particular, the hydrolysis of chlorosilanes occurs almost quantitatively, so that Corriu and co-workers have developed a polarographic method for water determination on this reaction, allowing accuracy comparable to the Karl-Fischer titration.[37]

The kinetics of the described hydrolysis can further be promoted by the use of nucleophilic solvents, such as *N*,*N*-dimethylformamide (DMF), tetramethyl urea (TMU), dimethyl sulfoxide (DMSO) or hexamethyl phosphoroustriamide (HMPT).[36,42] This effect can be explained by the coordination of halosilanes by nucleophilic solvents to form a pentacoordinated state (Scheme 1, b).[42–44] Favoring further nucleophilic attack on the silicon atom by water, for example, results in acceleration of hydrolysis or allows racemization of the product.[42] Pentacoordination can also be used specifically to support reactions with nucleophilic attack on the halosilane and thus increase the desired yield.[43,49] However, the determination of redox potentials can be impaired by this effect, making investigations using cyclic voltammetry difficult to compare and therefore ideally being conducted in non-nucleophilic solvents.[50]

In addition to coordinating properties, polarity plays a particularly important role in low-nucleophilic solvents. Increasing polarity increases the stabilization of reductively generated

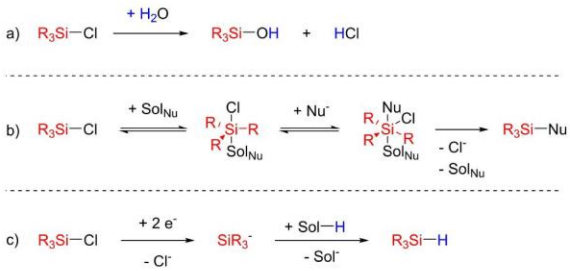

Scheme 1. Possible solvent interaction with halosilanes (Sol = solvent, Nu = -nucleophile): a) hydrolysis of chlorosilanes by residual water in the electrolyte solvent,[36–38] b) coordination of chlorosilane by a nucleophilic solvent and acceleration of further nucleophilic access,[36,42–44] c) role of solvent as hydrogen donor with subsequent formation of Si–H bond.[41,45–48]

intermediates, which has been exploited selectively in the past, for example, for the synthesis of long-chain polysilanes.[51,52] By using 1,2-dimethoxyethane (DME) instead of tetrahydrofuran (THF), higher molecular masses of the polysilanes can thus be obtained.[52] Simultaneously, the stabilization of the intermediate is also related to acidity of the solvent. If the solvent represents a hydrogen donor, a proton can be abstracted from the solvent if the reactivity of the silyl species is sufficient, and thus an undesirable Si–H bond can be formed (Scheme 1, c). Acetonitrile (MeCN) in particular has been frequently discussed in this regard in the past.[41,45–47] However, proton abstraction can also occur with the use of DME as a solvent, as shown by Dessey and co-workers.[48] Further reactions caused by the choice of solvent is siloxane formation due to the high oxophilicity of silyl intermediates, generated from halo- and

Alexander D. Beck received his B. Sc. degree in chemistry and biochemistry from Ludwig-Maximilians-University Munich for studies on the synthesis in liquid ammonia with lithium and silicon and his M. Sc. degree in chemistry for the investigation of a redox initiator system by electron spin resonance spectroscopy (Prof. Dr. K. Karaghiosoff) in cooperation with Wacker Chemie AG. He is currently working on his Ph.D. project on the electrochemical Si bond formation at Wacker Chemie AG, Munich, under the supervision of Prof. Dr. S. R. Waldvogel from the Johannes Gutenberg University Mainz.

Stefan Haufe studied chemistry in Bielefeld and received his Ph.D. in 2001 from the Technical University of Munich (Prof. U. Stimming). He started his industrial career at Proton Motor GmbH, Starnberg and Sartorius AG, Goettingen in the field of fuel cell development. Since 2008, he has been working at Wacker Chemie AG, Munich, first as a group leader and from 2017 as Director of Lithium-Ion Battery Application Technology in Corporate R&D. He is responsible for the development of Si-based anode active materials and for various other electro-chemical topics relevant to WACKER.

Siegfried R. Waldvogel studied chemistry in Konstanz and received his Ph.D. in 1996 from University of Bochum/Max Planck Institute for Coal Research (Prof. M. T. Reetz). After postdoctoral research in La Jolla, CA (Prof. J. Rebek, Jr.), he started his own research at the Universities of Münster and Bonn. He became full professor at JGU Mainz in 2010. His research interests are novel electro-organic transformations including bio-based feedstocks. In 2018, he cofounded ESy-Labs GmbH, which provides custom electrosynthesis and contract R&D.

ChemElectroChem | Review
doi.org/10.1002/celc.202201149
Chemistry Europe
European Chemical Societies Publishing

hydrosilanes, especially in the presence of oxygen donors such as carbonates.[47] Another option is the use of solvent as a sacrificial system with respect to the electrochemical counter-reaction, for example by trapping chloride species in the anodic oxidation by means of chlorination of the solvent.[53–55]

2.2. Supporting electrolyte

The second component of the electrolyte, which has a decisive influence onto the course of reaction in the electrochemical conversion of halo- and hydrosilanes, is the supporting electrolyte. Anhydrous features represent also a prerequisite, which otherwise results in the undesired formation of Si–O bonds,[45] potentially coating the electrode surface.[39] Furthermore, the conductivity,[47] as well as the electron transfer, depending on the ions selected, contributes significantly to the desired conversion.[56] However, increase of conductivity is possible by using mixed salts, for example, the combination of LiCl and $MgCl_2$ in a 2:1 ratio results in the increase of conductivity by a factor of 100 compared to the individual components.[57] This impact is probably due to aggregation and dissociation effects, which gives rise to increased solubility of the supporting electrolyte. Halosilanes also take over a particular role concerning the subject of supporting electrolyte. Thus, halogen-containing components can result in halogen exchange at the silane. These effects have been described in particular for the conversion of chlorosilanes to fluorosilanes based on BF_4^- and $CF_3CO_2^-$ (Scheme 2, a).[47,58–60] Fluorosilanes as electrochemically outstandingly stable species are usually no longer accessible for further conversions. Transformation to bromosilanes is also possible via this simple halogen exchange, for example by mixing the chlorosilanes with alkali and alkaline earth metal bromides in MeCN at room temperature (Scheme 2, a).[61,62] However, the effect can be suppressed by the addition of nucleophilic additives such as HMPT.[63]

Another unique feature of halo- and hydrosilanes is the equilibration of functional groups, especially the hydrogen and halo substituents. Thus, in the presence of $AlCl_3$,[68] or especially by typical supporting electrolyte components such as quaternary ammonium ions,[64–66] catalytic exchange of the two functional groups can occur. As Weyenberg and co-workers have found,[64] this reaction is also possible on non-alkylated halosilanes, such as $HSiCl_3$. Thus, equilibration to $SiCl_4$ and H_2SiCl_2 is already possible at room temperature. For monohalogenated silanes, this can also result in conversion to perchlorinated silanes by the electrolyte (Scheme 2, b),[67] which can lead to undesirable electrochemical polymerizations. Although the mechanism is not fully understood, a nucleophilic attack via a halide ion is presumed.[64] By changing the supporting electrolyte components to alkali and alkaline-earth metal ions, this equilibration can be suppressed.[67]

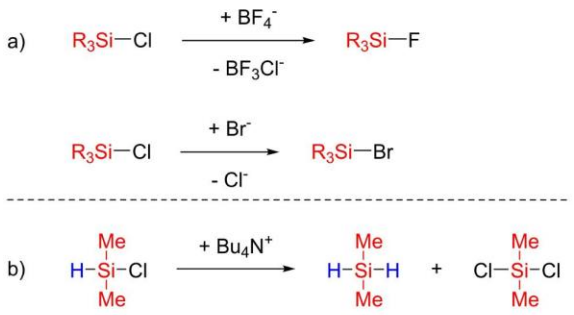

Scheme 2. Possible interactions of supporting electrolyte with halosilanes: a) halogen exchange at chlorosilane,[47,58–62] b) equilibration reaction of hydrochlorosilanes via tetraalkylammonium cations.[64–67]

Another important function of the supporting electrolyte is the stabilization of the silyl intermediate in the reaction. Anodically generated silyl species, i.e. via the oxidation of hydrosilanes, can be well stabilized by weakly coordinating anions, such as ClO_4^-,[60,69,70] BF_4^-,[71] and PF_6^-.[72] Mg^{2+} has been shown to be particularly suitable for the stabilization of cathodically generated intermediates, which has a positive effect on the yield obtained by electrochemical conversion.[56,67,73,74] One reason for this could be the catalytic influence due to the mild Lewis acidity of the most commonly used $MgCl_2$, which is also known in organic synthesis and is already addressed in a more detailed review.[75] In this context, the concentration of the supporting electrolyte can also have an impact on product formation, e.g. increased chain length in reductive polysilane synthesis.[56]

2.3. Sacrificial anode materials

Next, the most underestimated properties of sacrificial anodes will be surveyed, which will accompany the field of reductive conversion of halosilanes. Conversion of halosilanes releases the corresponding halides, e.g. chloride in the case of chlorosilanes. To prevent interfering side reactions these must be removed from the reaction mixture. Hengge and co-workers have already investigated various possibilities, such as the use of stable SiC anodes to oxidize chloride to chlorine.[76] However, due to the requirement of aprotic solvents, this results in solvent chlorination, an effect that is specifically exploited in some cases as a sacrificial electrolyte, such as DMF.[53–55]

The anodic conversion of cyclohexene as sacrificial agent and selective chlorination of the C=C double bond has also been investigated (Scheme 3, a).[63] This use of the halogenation of alkenes has proven to be a versatile halide shuttle by generation of vicinal dihalogenides and has sparked renewed interest in current organic synthesis.[77] Another possibility is the use of a hydrogen anode, to electrochemically generate protons in-situ at the anode surface to capture free chloride ions and release them as gaseous hydrogen chloride (Scheme 3, b).[63,78] In literature of electrochemical silane conversion this concept is hardly exploited, probably due to the technical complexity.

The most popular and simple alternative to these methods is the use of sacrificial anodes, metallic electrodes which trap the free halides as metal halides due to their low potential oxidation in the course of the reaction (Scheme 3, c).[19] Depending on the solubility of the metal ion in the electrolyte,

ChemElectroChem | Review
doi.org/10.1002/celc.202201149
Chemistry Europe
European Chemical Societies Publishing

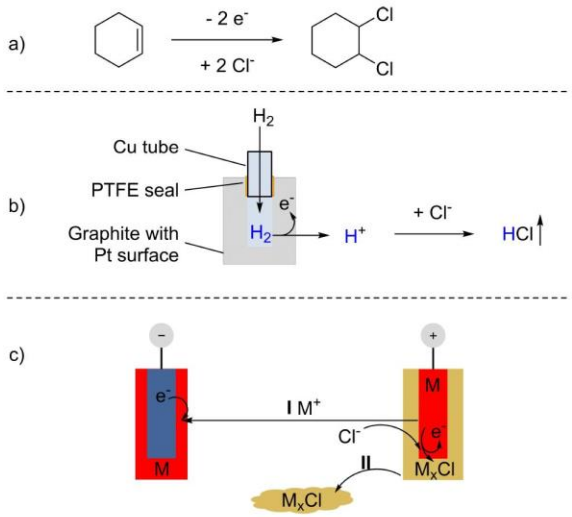

Scheme 3. Possibilities to remove chlorides from the electrolyte: a) anodic chlorination of cyclohexene as sacrificial agent,[63] b) anodic generation of protons via the porous hydrogen anode to form gaseous hydrogen chloride,[63,78] c) formation of metal chloride via the oxidation of a sacrificial metal anode with possible coating of the cathode material at respective reduction potentials (M = metal).[79–82]

coating of the anode surface by the metal halide can occur, as for example on silver by AgCl.[79] However, no passivation layers have yet been observed in the context of halosilane reduction that represent a complete isolation of the anode,[79] and thus result in the premature termination of the electrochemical conversion. Presumably, dissolution, or precipitation of the metal chloride from the solution occurs, preventing complete anode isolation. When using sacrificial anodes, the reduction potentials of the soluble components should be considered. Usually, dissolved metal halides are present in the reaction mixture in addition to the reactant, product, and intermediate species. The appropriate choice of anode material can serve as reductive protection of the product. Preventing over-reduction of the target molecule, and achieving high product selectivity can be obtained via deposition of the dissolved metal ion instead of product reduction at the cathode, as reported by Pons and co-workers.[82] However, if the reduction potential is inappropriate, metallic coating of the cathode occurs as main reaction (Scheme 3, c **I**), lowering the Faradaic yield.[79–81] Otherwise, the metal chloride precipitates off the mixture depending on their solubility (Scheme 3, c **II**). According to suitable oxidation potentials (Table 1), Mg,[56–58,67,73,83–89] Al,[80,82,85,90,91] Zn,[82,92] Ni,[85] Cu,,[59,85,93–95] Ag,[79] and Hg[81,96,97] could be used as sacrificial anode materials.

In addition, sacrificial anodes can interfere further in the reaction than just trapping undesired halides. In presence of an active metallic surface with low oxidation potential, this may result in Grignard-type conversions. Faradaic yields far exceeding 100% can occur,[57,83,84,99] questioning the simple switch-off of the synthesis route and rendering the change to alternative anode materials futile. In particular, easily reducible substrates, such as organic bromides can be affected. As Ishifune and co-workers demonstrated,[73] pre-electrolysis with Mg electrodes to form Mg(0) and subsequent reduction at Pt electrodes allows the formation of a Si–Si bond, in contrast to electrolysis in the absence of Mg. The active Mg species is mandatory for the desired Grignard-type conversion, although it can be cathodically restored. Current-free experiments are used in recent studies to test the Grignard-type influence of sacrificial anodes.[88]

Oxidation of the sacrificial anode leads to the formation of corresponding cations, which can interfere in the reaction process analogue to supporting electrolyte components. Especially, the stabilization of the generated intermediate influences reaction properties and differs in yield and selectivity compared to sacrificial anode-free systems.[56,74,85,88] This effect could be used by Biran, Bordeau and co-workers to generate selectively Si–Al intermediates at low temperatures in the reduction of chlorosilanes on Al sacrificial anodes that are stable and storable for several weeks.[90] Only by the addition of further chlorosilanes the desired Si–Si bond linkage is obtained, demonstrating the high stabilization by released ions in the use of sacrificial anodes.

2.4. Tripwires with cyclic voltammetry

As highlighted in the previous chapters, hydro- and in particular halosilanes involve some peculiarities, such as hydrolysis, equilibration, halogen exchange or nucleophilic addition by the solvent. Besides influences on the reactivity, the redox potential of the investigated silane can be shifted, thus easily resulting in misunderstandings in cyclic voltammetry. In addition to the mandatory need for anhydrous electrolytes due to

Table 1. Standard oxidation potential of sacrificial anode materials commonly used for electrosynthesis with chlorosilanes.

Entry	Metal oxidation	Potential[a] E^0 [V]	Ref.
1	$Mg \rightarrow Mg^{2+} + 2e^-$	−2.37	[98]
2	$Al \rightarrow Al^{3+} + 3e^-$	−1.66	[98]
3	$Zn \rightarrow Zn^{2+} + 2e^-$	−0.76	[98]
4	$Ni \rightarrow Ni^{2+} + 2e^-$	−0.26	[98]
5	$Cu \rightarrow Cu^{2+} + 2e^-$	0.52	[98]
6	$Ag \rightarrow Ag^{+} + e^-$	0.80	[98]
7	$Hg \rightarrow Hg^{2+} + 2e^-$	0.85	[98]

[a] Potential vs. SHE at 25 °C and 1 atm.

ChemElectroChem | Review doi.org/10.1002/celc.202201149 | Chemistry Europe European Chemical Societies Publishing

hydrolysis,[39–41] supporting electrolyte components, such as Mg^{2+},[100] and nucleophilic solvents can result in significant potential shifts.[50] Halogenated substrates are also dependent on the choice of electrode material, so the reduction process differs depending on the material. On non-catalytically active electrodes, such as glassy carbon, a concerted mechanism presumably occurs; on catalytically active surfaces, such as Ag, Cu, Pd, or mixtures thereof, the intermediate is stabilized via electrode surface interaction and thus more easily reducible,[101] also discussed in previous reviews.[102]

Since no standard electrolytes and electrode materials have yet been established for CV studies of hydro- and halosilanes, it is futile to compare reduction potentials of halosilanes in different environments, as shown by Jouikov.[24] In the past,[39,50,67,103,104–106] as well as in more recent studies,[43,61,107] reduction potentials of halosilanes are therefore found in a wide potential window, especially the frequently investigated Me_3SiCl (Table 2, entries 1–6). However, within an identical electrolyte and electrode system, clear trends can be identified for the reduction potential of halosilanes:

- Increase in steric demand of organic substituents shifts the reduction potential to more negative regime (Table 2, entries 7–11),
- resonance stabilizing substituents shift the potential to less negative potentials (Table 2, entries 11–13),
- a less electronegative halide substituent lead to less negative reduction potential (Table 2, entries 14–16),
- higher homologues of the 4th main group are more easily reducible (Table 2, entries 17–20).

However, CV data are to be interpreted with care, as they are often a basis for mechanistic interpretations. Besides the lack of direct comparability, the interpretation depends on the choice of electrolyte. Thus, there is still disagreement about the reduction of chlorosilanes, since in principle both a 1-electron and a 2-electron process can occur, which induces the reduction to the radical or anion. Parallel reduction to the radical anion and diradical with further decomposition to the neutral radical and anion is discussed as well.[109] While for analogue Ge,[39,40,110] Sn[42,48] and Pb[48] compounds clearly distinguishable reduction signals can be detected and assigned to the respective reduction step, the interpretation of chlorosilanes is more complex. The mostly irreversible reduction takes place at highly cathodic potentials. In addition, a reversible signal often occurs in the low cathodic range, which can be caused by traces of moisture and accompanying HCl formation,[36,39–41] or by the presence of oxygen,[24,63] if not carefully dried and prepared, at best in a glovebox. Mechanistic conclusions based on CV studies without synthetic evidence should therefore be treated with caution, since standing alone they leave much room for interpretation.[107] One trend by which the verisimilitude to the discussion of chlorosilane reduction can be estimated is the decreasing reduction potential of oligo- and polychlorosilanes with increasing Si–Si chain length.[41,61] Reduction of chlorosilanes in the low cathodic range should accordingly allow readily accessible reduction to silicon deposition, which is not the case in practice.[105,111,112,113] Corriu and co-workers, who have worked extensively on the subject of hydrolysis of chlorosilanes in the electrolyte, were able to show that reversible reduction potentials in the less negative regime often correspond to the reduction of HCl and do not provide evidence for a 2-electron process.[37] Holm and co-workers referred the reduction of Ph_3Si radical by photo modulated CV studies to −1.39 V vs. SCE,[114] thus, the reduction of the radical to the anion seems to be much easier than from the chlorosilane to the radical. The two-step reduction presumably occurs via a consecutive highly cathodic process if the reactive species is not trapped by a suitable substrate, such as an alkene.[88]

Table 2. Overview of reduction potential of halosilanes.

Entry	Substrate	Potential [V] vs. SCE	Conditions	Ref.
1	Me_3SiCl[a]	−0.1[c]	DME, Bu_4NClO_4, Pt	[63]
2	Me_3SiCl[a]	−0.5[c]	DMF, Et_4NClO_4, Pt	[50]
3	Me_3SiCl[a]	−1.1[c]	PhOMe, Bu_4NClO_4, Pt	[50]
4	Me_3SiCl[b]	−2.2[d]	DME, Bu_4NClO_4, Pt	[81]
5	Me_3SiCl[a]	<-3.0[c]	DMF, Et_4NOTs, Pb	[108]
6	Me_3SiCl[a]	−3.1[c]	THF | Bu_4NClO_4 | GC	[88]
7	Me_2SiCl_2[a]	−2.3[d]	MeCN, Et_4NClO_4 | Pt	[109]
8	$EtMeSiCl_2$[a]	−2.4[d]	MeCN, Et_4NClO_4, Pt	[109]
9	nPrMeSiCl$_2$[a]	−2.6[d]	MeCN, Et_4NClO_4, Pt	[109]
10	nHexMeSiCl$_2$[a]	−2.9[d]	MeCN, Et_4NClO_4, Pt	[109]
11	cHexMeSiCl$_2$[a]	−3.2[d]	MeCN, Et_4NClO_4, Pt	[109]
12	$PhMeSiCl_2$[a]	−3.1[d]	MeCN, Et_4NClO_4, Pt	[109]
13	Ph_2SiCl_2[a]	−3.0[d]	MeCN, Et_4NClO_4, Pt	[109]
14	Ph_3SiF[b]	−2.2[e]	THF, Bu_4NI, dme	[110]
15	Ph_3SiCl[b]	−2.0[e]	THF, Bu_4NI, dme	[110]
16	Ph_3SiBr[b]	−1.9[e]	THF, Bu_4NI, dme	[110]
17	Ph_3SiCl[a]	−3.1[d]	DME, Bu_4NClO_4, dme	[48]
18	Ph_3GeCl[a]	−2.8[d]	DME, Bu_4NClO_4, dme	[48]
19	Ph_3SnCl[a]	−1.6[d]	DME, Bu_4NClO_4, dme	[48]
20	Ph_3PbCl[a]	−1.4[d]	DME, Bu_4NClO_4, dme	[48]

DME = 1,2-dimethoxyethane, DMF = *N*,*N*-dimethylformamide, OTs = $H_3CC_6H_4SO_2^-$, THF = tetrahydrofuran, GC = glassy carbon, MeCN = acetonitrile, dme = dropping mercury electrode, [a] Value of E_p [b] Value of $E_{1/2}$ [c] measured vs. SCE [d] vs. 0.001 M Ag/$AgClO_4$, converted to SCE by the respective author [e] referenced to sat. Ag/AgI, converted to SCE (−0.44 V vs. SCE) by the respective author.

ChemElectroChem | Review
doi.org/10.1002/celc.202201149
Chemistry Europe
European Chemical Societies Publishing

However, for future CV studies, it would be a good practice to check whether hydrolysis resulted in HCl formation. In addition to prior Karl-Fischer titration of the electrolyte,[61,70] it is very easy to show in-situ by cyclic voltammetry whether HCl formation has occurred.[38,115] For this purpose, the start of the CV is selected in the oxidative regime. If no oxidation potential of chloride can be detected in the first run, the subsequently measured reduction signals are independent of HCl. In the second cycle an oxidation signal of chloride should be visible, caused by reductive cleavage of the Si–Cl bond.[38,115] The same applies to synthesis. Here a pre-electrolysis at low potentials, if conducted by potentiostatic means or with low applied charge until cathodic hydrogen gas evolution ceased, if conducted via galvanostatic conditions is generally used to remove traces of HCl.[43,58,82–84,99,106,116,117] The disiloxane species formed via hydrolysis are generally non-reactive towards further electrochemical conversions.

3. Electrochemical silane synthesis

The electrochemical synthesis of silane species started in the '70s with the reductive coupling to form Si–Si bonds by Hengge and Litscher.[96] This easy and controllable alternative to the hitherto known Wurtz-type pathway was especially useful for the conversion of chlorosilanes. Instead of using alkali metals for the desired conversion towards the Si bond formation, electrons could be applied as reagents leading to mild reaction conditions. Since their pioneering discovery, much has developed in the field of reductive as well as oxidative synthesis. In the following, we will give a brief overview of various possibilities, as well as recent advances achieved via new and exciting synthetic aspects, especially regarding the field of mediated electrochemistry.

3.1. Cathodic conversion

For the reductive coupling of halide species towards Si bonds, two possibilities arise. Reduction of the halosilane itself (Scheme 4, a) or of an organic halide with trapping of the nucleophilic intermediate by the electrophilic halosilane (Scheme 4, b). The course of reaction depends on the presence of organic moieties with sufficient reduction potential, as well as appropriate stability of the carbanion for selective nucleophilic attack at the halosilane.

While the reduction of organic substrates generally results in the formation of a carbanion, the state of reduction of halosilanes is a frequently discussed topic and depends on stabilization of the intermediate and presence of trapping agents, as unsaturated hydrocarbons,[118] as we will see later. As mentioned, it is difficult to discuss mechanistic aspects based on cyclic voltammograms alone, which is why attempts were made to convert two chlorosilane species with different reduction potentials in the same cell (Scheme 4, c). Formation of the radical anion (pathway **I**) should lead to only the dimer of the more easily reducible substrate under cleavage of

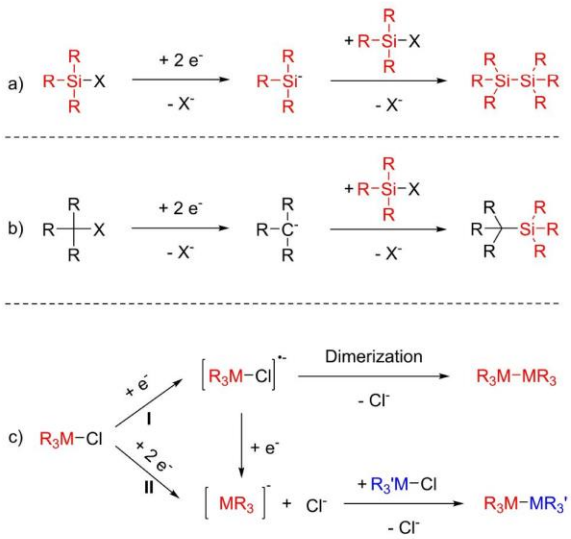

Scheme 4. Pathways for the cathodic conversion of halosilanes: a) reduction of the halosilane species, b) trapping of an electrogenerated carbanion by a halosilane, c) discussed electrochemical pathway of radical anion vs. anion (M = Si, Ge).[56,58,81,97]

chloride. The anionic 2-electron process (pathway **II**) would form a mixture of dimers arising from both chlorosilanes due to trapping of the formed silyl anion nucleophile. However consecutive reduction of the radical to the anion at the electrode surface is possible. In independent studies, Hengge and co-workers,[81,97] as well as Kashimura and co-workers,[56,58] could show with different sacrificial anodes and electrolytes that the mixed dimer is the only product arising, clearly indicating the anionic pathway or very fast consecutive reduction in the absence of trapping agents. In analogy synthetic approaches by electrolyzing a mixture of chlorosilanes and -germanes at increasingly cathodic potentials were conducted.[110] With germanium species being able to form radicals (pathway **I**), the selective dimerization to Ge–Ge bonds can be achieved. Choosing more negative cathodic potentials, Ge is further reduced to the anionic form (pathway **II**), generating Ge–Ge and Ge–Si bonds by nucleophilic attack of the respective electrophilic species.

3.1.1. Si–Si bond formation

The general idea of reductive access to Si–Si bonds via conversion of halosilanes is straightforward, given the effects mentioned above. The simplest product to achieve is via a dimerization reaction of monochlorosilanes (Scheme 4, a). Although the reduction potential of Me_3SiCl is still unresolved, dimerization to $Me_3Si\text{-}SiMe_3$ has been shown using electrolyte compositions with high cathodic stability such as THF, HMPT and DME in combination with low coordinating supporting electrolytes such as Bu_4NClO_4, Et_4NBF_4 or $LiClO_4$ at sacrificial,[58,96,119,120] as well as inert anode materials.[63,76,121] In

ChemElectroChem | Review
doi.org/10.1002/celc.202201149
Chemistry Europe
European Chemical Societies Publishing

addition to the symmetric dimerization of Ph_3SiCl,[40,58,76,81,96,110] $Me_2PhSiCl$,[56,73,79] $MePh_2SiCl$,[47,58,79] HMe_2SiCl,[67] $HPhMeSiCl$,[67] HPh_2SiCl,[67] $H_2PhSiCl$,[67] and alkoxychloro-silanes,[59] various asymmetric disilanes were prepared in high yields in undivided cells using the sacrificial anode technique.[79,97] Usage of hydrochlorosilanes enables easily further product functionalization. The dimerization of organofunctional chlorosilanes possessing amine groups were so far unsuccessful due to very high reduction potentials, exceeding the electrolytic stability.[67] However, different approaches via reductive mediation of chlorosilanes have been attempted to lower the reduction potential for the desired conversion. Phosphonium salts,[38] nitrobenzene derivatives,[38] and aromatic compounds,[38,43,115] constitute possible substrates as redox mediators. They exhibit the typical CV characteristics of active mediators. A reversible cathodic potential is detectable, due to the generation of a radical anion that is significantly less negative than the chlorosilane to be converted (Scheme 5). Further, by the addition of chlorosilane, the reversibility of the mediator signal disappears, and the current density rises, indicating electron transfer from the mediator radical anion to the chlorosilane.

The general idea of redox mediators is the convenient generation of a redox active species, here the radical anion Q by reduction of the mediator starting material P (Equation 1). This generated radical anion transfers the electron to the actual substrate, here a chlorosilane, in a chemical reaction step and is itself oxidized back to P in the process (Equation 2). In a stepwise reaction, cleavage of chloride occurs with generation of the desired substrate radical species (Equation 3), to allow for further dimerization.

$$P + e^- \leftrightarrow Q \tag{1}$$

$$R_3SiCl + Q \leftrightarrow [R_3SiCl]^{\bullet -} + P \tag{2}$$

$$[R_3SiCl]^{\bullet -} \rightarrow [R_3Si]^{\bullet} + Cl^- \tag{3}$$

One challenge in the study of mediators is the hydrolysis of chlorosilanes. In some cases after only a few minutes,[38] the mediator shows reductive reversibility again, since electron transfer to the hydrolyzed silane is no longer possible. Instead of equation 2, re-oxidation of the radical anion Q back to P takes place (Equation 1). In particular, sterically non-hindered alkylchlorosilanes are very sensitive to hydrolysis, so that they have not yet proved suitable for this mediated bulk electrolysis. Another obstacle is the high electrophilicity of chlorosilane species. As shown by Jouikov and co-workers,[43] in competition with the pure electron transfer, substrate-mediator addition may occur (Equation 4).

$$R_3SiCl + Q \rightarrow R_3SiQ + Cl^- \tag{4}$$

Even with poorly nucleophilic delocalized anion radicals as anthracene, and further aromatic derivatives, this reaction is highly efficient. Si–C bond formation to the mediator occurs in high yield with subsequent (di-)silylation of the mediator as the main reaction (Scheme 6), allowing the desired dimerization of chlorosilanes only in traces. Depending on the selected mediator, Si–N bond formation as for benzonitrile due to negative charge localization on the N atom can occur. Si–O bond formation of the oxophilic chlorosilane with used methyl benzoate as mediator is another possibility. By choosing more sterically demanding chlorosilane species as *t*-$BuMe_2SiCl$, the desired electron transfer is dominating compared to S_N-like nucleophilic addition. Simultaneously, the high bulkiness of the chlorosilane results in H-abstraction by the reduced silyl species with formation of Si–H bonds instead of the dimerization to Si–Si bonds.[43]

Apart from mediated techniques, sacrificial anodes, especially Mg are taking a special role in the chlorosilane conversion. In the dimerization of $Me_2PhSiCl$ shown by Ishifune and co-workers,[73] the presence of an active Mg species is essential for the conversion. In absence of Mg no product is formed, while pre-electrolysis to provide Mg for further reduction at Pt electrodes enables the dimerization. However, pre-electrolysis to generate Mg and addition of the chlorosilane under current-less conditions also forms the dimer in low yields, indicating the Grignard-type conversion in some cases with Mg electrodes. Using the sacrificial anode technique, formation of metal chlorides at the anode surface may increase the electrical resistance, therefore the use of ultrasonication in a symmetrical electrode setup with switching polarity to remove the metal

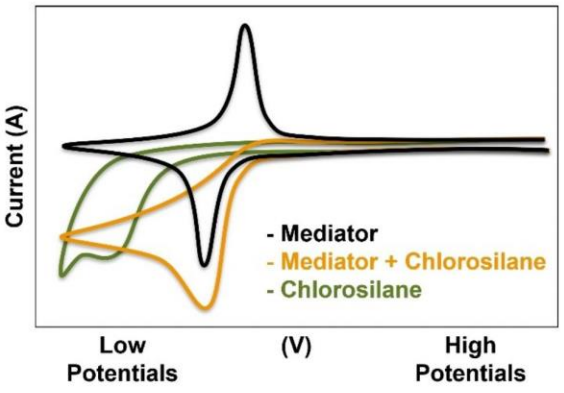

Scheme 5. Schematic mediator functionality, visible in a typical CV measurement.[43]

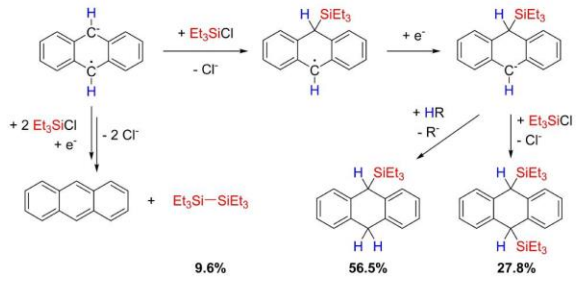

Scheme 6. Undesired silylation of the anthracene redox mediator as main reaction with the use of chlorosilane substrates.[43]

ChemElectroChem | Review
doi.org/10.1002/celc.202201149
Chemistry Europe
European Chemical Societies Publishing

chloride surface layer of the electrode,[120] as well as additional supporting electrolytes,[119] are some used tricks to provide high conductivity and generate high product yields.

Entering the field of dichlorosilanes, so far only the use of sterically highly demanding mesityl groups results in dimerization,[122] allowing the special case of a Si=Si double bond. Aside this rarity, the additional degree of freedom by the use of dichlorosilanes results in Si–Si chain formation. By selective mixing of di- and monochlorosilanes, with the monochlorosilanes present in significant excess as chain terminators, synthesis of oligosilanes in various chain lengths can be achieved. The first representatives to be obtained are the corresponding trisilanes via end capping of a dichlorosilane by monochlorosilanes.[56,79,81,87,94,123] Accordingly, tetrasilanes are achieved via the dimerization of monochlorodisilanes,[94] or by end capping of dichlorodisilanes.[56,58] Pentasilanes are accessible via reductive conversion of dichloromonosilanes and monochlorodisilanes.[94] Using hydrochlorosilanes as end capping agents, the resulting H-terminated oligosilanes can be functionalized for further Si–Si elongation. As shown by Ishifune and co-workers,[87] and Kashimura and co-workers,[56] chlorination with benzoyl peroxide (BPO) and carbon tetrachloride yields dichlorotrisilanes, which can be further elongated to pentasilanes according to the same procedure of reductive elongation (Scheme 7).[56]

However, oligosilanes consisting of only the sterically demanding Ph_2Si units tend to cyclization and the formation of $[Ph_2Si]_4$,[76,97] instead of linear products as for methylated or mixed sterically demanding silanes. By analogy, cyclic methylsilanes such as $[Me_2Si]_5$ or $[Me_2Si]_6$ can also be obtained by significant lowering of the concentration of the starting material.[76]

In non-diluted systems in the absence of monochlorosilanes as chain terminators, reduction of dichlorosilanes results in polysilane formation.[67] Mechanistically, the process is comparable to the previous reductive Si–Si bond formation, with reduction of the substrate to the anion and nucleophilic attack on another chlorosilane.[124] As shown by Okano and co-workers,[51] the polysilane synthesis proceeds from the reduction of the monomeric species with the formation of dimers and short-chain oligomers (Scheme 8, a). The extension of the Si–Si backbone results in easier reducibility, so that further chain elongation to polysilanes starts from oligomeric structures. At the same time, the Si–Si backbone can be reductively cleaved again to generate anionic intermediates as an undesired side reaction (Scheme 8, b),[51,125] a process becoming more dominant with increasing chain length. In addition, "back-biting" reactions can occur above a certain chain length, with termination of the chain growth by ring closure (Scheme 8, c), with cleavage of chloride via path **I** or cleavage of an anionic oligosilane via path **II**.

Scheme 7. Synthesis of oligosilanes via reductive coupling, followed by chlorination of hydrosilanes, BPO = benzoyl peroxide.[56,87]

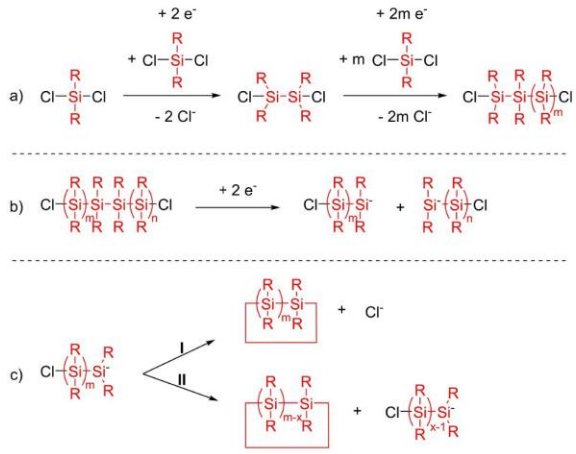

Scheme 8. Mechanistic details on the formation of polysilanes starting of dichlorosilanes:[51,56,125,126] a) formation of di- and oligosilanes via reductive transformation, b) reductive cleavage of polysilanes to anionic intermediates, c) "back-biting" reactions with the cleavage of chloride (**I**) or anionic oligosilanes (**II**).

With dichlorodisilanes and -oligosilanes as starting material, "back-biting" reactions dominate the early stage of reaction and cooling of the reaction to 0 °C is needed to shift the kinetics towards chain elongation instead of ring closure.[56,126]

Especially in the synthesis of polysilanes, stabilization of the anionic polysilane intermediate plays a crucial part of the desired reaction. Polarity of the solvent,[47,51,52,127] as well as cationic species help to generate long chain polysilanes. Therefore, Mg as sacrificial anode material and subsequent as Mg^{2+} solvated species shows not only outstanding performance relating to yield and chain length,[56,58,85,128,129,130] but does allow the product formation in some cases in the first place.[58] Again, to prevent coating of the anode material, sonication,[56,129,131] as well as switching polarity,[56,80,129,131] are established methods. As Kunai and co-workers showed,[47] the combination of polar solvents, low coordinating supporting electrolytes, high substrate concentration and high applied charge can achieve polysilanes with molecular weights exceeding 100 kDa, outperforming the Wurtz-type polysilane formation. In special cases polysilanes can be generated in the absence of a solvent, using only the dichlorosilane monomer with a complexing agent, such as HMPT, to solubilize the anodic generated metal chloride.[91] The less toxic tris(*N*,*N*-tetramethylene) phosphoric triamide (TPPA) might be a suitable stabilizing agent as well, as shown in the synthesis of organosilicon compounds.[132] The synthesis of functionalized polysilanes with more challenging side chains, such as hydroxy-related,[56,123] or vinyl groups,[133] not accessible via the Wurtz route, can be achieved via the mild electrochemical reduction with molecular masses above 16 kDa.

ChemElectroChem | Review
doi.org/10.1002/celc.202201149
Chemistry Europe
European Chemical Societies Publishing

The same applies for the convenient synthesis of block copolysilanes with Mg sacrificial anodes.[130,131,134]

Changing the reactant to trichlorosilanes provides access to polysilane networks. Defined structures with high molecular masses of up to over 60 kDa and good optical properties in the visible region can be achieved for sterically demanding silanes with octyl,[135] butyl,[135,136] *t*-butyl,[136] phenyl,[136,137] and *c*-hexyl groups,[136] inaccessible via Wurtz reaction. Polymeric networks were also generated with sterically low demanding silanes such as $MeSiCl_3$,[136] $HSiCl_3$[97] and $SiCl_4$[97] in DME. Further information on the synthesis of polysilane structures can be found in additional literature.[29]

Choosing high cathodic potentials in a potentiostatic setup with perchlorinated chlorosilanes, reductive transformation up to the deposition of elemental silicon can be achieved. So far, the amorphous film thickness is still in the range of some µm.[105,111,113,138] However, electrodeposition of silicon at different electrode surfaces at room temperature is in the focus of research, and already covered by comprehensive reviews.[31–34]

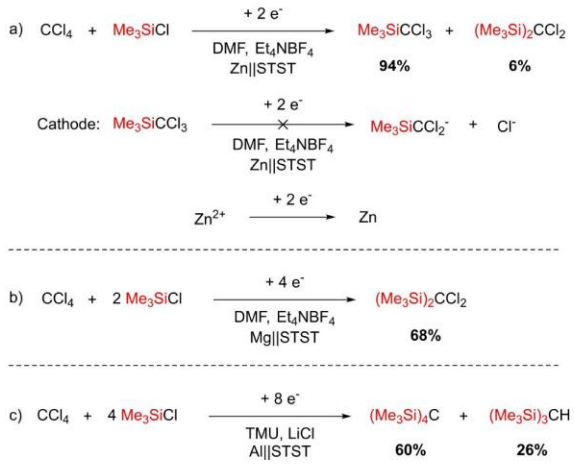

Scheme 9. Multiple silylation of perchlorinated alkanes (STST = stainless steel):[82] a) selective monosilylation of CCl_4 via Zn anode, b) enabling the disilylation of CCl_4 via Mg anode, c) successful tri- and tetrasilylation of CCl_4 via Al anode.

3.1.2. Si-C bond formation

As mentioned earlier, reductive coupling with halosilanes to form Si–C bonds yielding organosilanes typically originates from organic halides. In the course of the reaction, these organic halides are reduced to the respective carbanions, acting as strong nucleophiles to attack the electrophilic halosilanes. This nucleophilic trap functionality has long been considered to be the only role for halosilanes in cathodic Si–C bond formation,[25] exhibiting a wide repertoire of examples.[24] However, we will highlight additional possibilities for the reductive conversion towards organosilanes below.

This conceptual summary will start with the general principles of the classic nucleophilic trap function. Depending on the organic substrate, it is possible to achieve multiple silylation at an organic halide. As shown by Pons and co-workers,[82] choosing the organic halides CCl_4, $CHCl_3$ and CH_2Cl_2 mono-, di-, tri- and tetrasilylation in polar solvents as DMF and TMU are accessible. However, care must be taken regarding the choice of anode material using the sacrificial anode technique, due to the reduction potential shift of the silylated organic halide. Starting with CCl_4 the monosilylation with Me_3SiCl as nucleophile trap is possible at a Zn anode in excellent yields and selectivity (Scheme 9, a). The same applies for fluorohalocarbons, as shown by Martynov.[92] However, to achieve a higher degree of silylation, the anode material must be changed, otherwise coating of the cathode with Zn metal occurs.[82] With Mg as anode material, disilylation is possible with 68% yield, by doubling the applied charge compared to the monosilylation (Scheme 9, b). For the tri- and tetrasilylation, Al is a suitable sacrificial anode material, leading to about 60% of $(Me_3Si)_4C$ (Scheme 9, c). A comparable result is obtained for the use of $CHCl_3$ and the corresponding mono-, di- and trisilylation depending on the anode material. Silylation of the high cathodically reducible CH_2Cl_2 is more challenging and HMPT as additional complexing agent needs to be used with an Al anode for the desired conversion.

Analogue, Bordeau and co-workers have shown,[116] that multiple silylation of the aromatic system of aryl halides is possible. After monosilylation of PhBr to $PhSiMe_3$, the use of Al as sacrificial anode with HMPT as additional complexing agent allows for the partial reduction of the aromatic ring, generating a strong carbanion to be trapped by Me_3SiCl, yielding the tri- and pentasilylated cyclic (di)enes (Scheme 10, a). The same applies for the multiple silylation of *o*-dichlorobenzene by Biran, Bordeau and co-workers.[139] Again, the combination of Al sacrificial anode material and additional HMPT complexing agent allows selective mono-, di- and tetrasilylation, first by

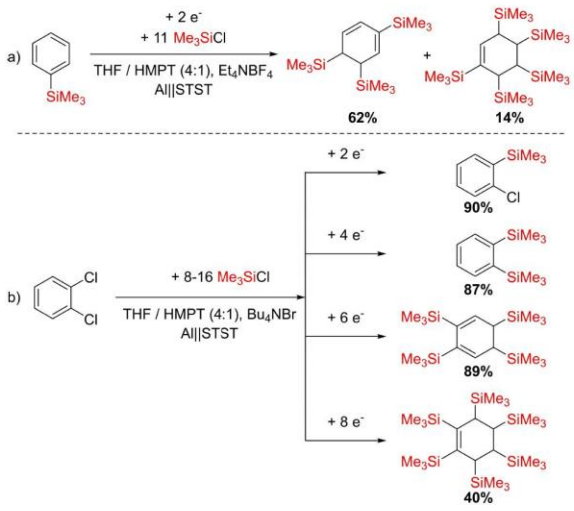

Scheme 10. Multiple silylation of aromatic systems (STST = stainless steel): a) di- and tetrasilylation of the aromatic system of trimethylphenylsilane,[116] b) mono-, di-, tetra-, and hexasilylation of *o*-dichlorobenzene.[139]

ChemElectroChem | Review
doi.org/10.1002/celc.202201149
Chemistry Europe
European Chemical Societies Publishing

reduction of the C–Cl bond and further by partial reduction of the aromatic ring (Scheme 10, b). Even hexasilylation can be achieved in yields of 40%, however with increasing reduction potential, side reactions for the overreduction of electrolyte components rise.

Conversely, multiple silylation can also be achieved by using a di- or perchlorosilane. As shown by Jouikov and co-workers,[117] the reduction of α,ω-dihalides with methylated and vinylated dichlorosilanes using an Al anode leads to the formation of cyclic silanes. Respective compounds can also be obtained without sacrificial anode, but with the sacrificial electrolyte DMF in a divided cell. While silacyclopropyl derivatives are inaccessible due to the high ring tension, corresponding silacyclobutyl, especially -pentyl, -hexyl and also -heptyl systems can be generated in particular with α,ω-dibromides (Scheme 11). However, reduction potential of the organic dihalide rises with increasing chain length. The use of α,ω-dibromides, which have suitable reduction potentials, results in the highest yields and even allows dicyclic structures starting from $SiCl_4$ as nucleophile trap. Selectivity can be achieved by the slow generation of nucleophiles, here via low current densities in combination with an excess of chlorosilane. The subsequent ring formation is supported by a 5- or 6-coordinated transition state.

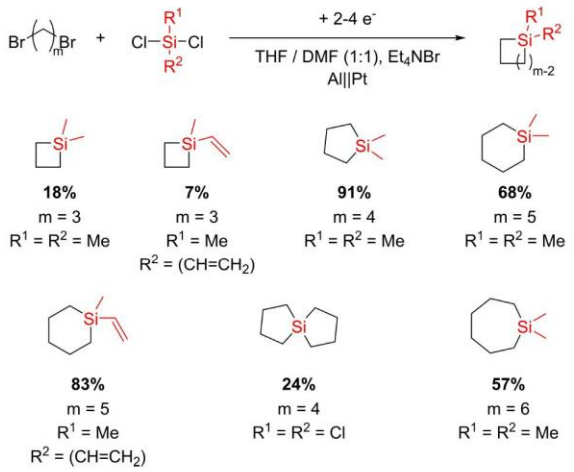

Scheme 11. Multiple silylation of α,ω-dibromides with di- and tetrachlorosilanes leading to cyclic silanes.[117]

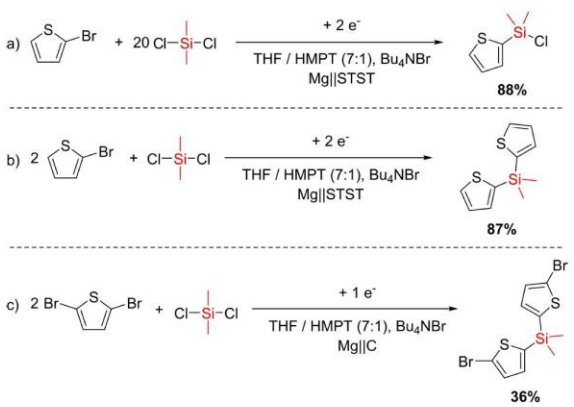

Scheme 12. Selective silylation of mono- and dihalothiophenes with dichlorosilanes (STST = stainless steel): a) with retention of Si–Cl bond,[84,99] b) complete conversion of dichlorosilane,[84] c) retention of C–Br bond after reductive silylation.[83]

Comparably, the reduction of halothiophenes with dichlorosilanes as nucleophilic traps leads to the respective silylation, as shown by Biran, Bordeau and co-workers.[83,84,99] Again, the sacrificial anode technique, here with the use of Mg as most promising material in an electrolyte with additional HMPT as complexing agent was used. Applying the above-mentioned principles,[117] low current densities of 1 mA/cm² in combination with an twentyfold excess of dichlorosilane are favored to yield the single silylated product with retention of one Si–Cl bond (Scheme 12, a).[84] Changing the substrate ratio to 2:1 of halothiophene to dichlorosilane, results in dual Si–C bond formation to the thiophene species (Scheme 12, b). In the conversion of dihalothiophenes, low current densities and applied charge allowed the retention of C–Br bond after single silylation (Scheme 12, c). However, it should be noted, that Faradaic yields are fare above 100%, indicating a Grignard-type influence on the conversion.[83,84]

As Bordeau and co-workers showed,[140] even more difficult substrates are accessible with this technique. Via the use of a sacrificial anode based on Al and HMPT complexing agent, the silylation of ethyl trifluoroacetate to the respective ethyltrimethylsilyl ketal could be achieved (Scheme 13). Low temperatures of −25 °C and a fifteenfold excess of chlorosilane were needed to favor the formation of the desired ketal over the silylation of the trifluoro substituent.

While halothiophenes, especially bromothiophenes, show a reduction potential in the low reductive range, *p*-substituted halobenzenes are much more difficult to reduce. For the single Si–C bond formation high excess of dichlorosilane is needed. However, due to similar reduction potentials of halobenzenes and dichlorosilanes, the excess of dichlorosilane leads to polysilane formation as main reaction. To specifically target the halobenzenes, Bordeau and co-workers,[99] applied a redox mediator system for the reductive Si–C bond formation. Instead of the organic moieties, seen in the reductive formation of Si–Si bonds,[38,43,115] a Ni(0) redox mediator was used here. An excess of 2,2′-bipyridine (bipy) was applied, as has been shown promising in the reductive coupling of allyl chlorides and α-chloro esters with carbonyl compounds.[141] The reduction potential of the Ni(bpy)Br_2 is at an easily achievable −1.2 V vs. SCE compared to the reduction of the desired *p*-bromoanisole with −2.45 V vs. SCE.[99] Via the mediated technique, the

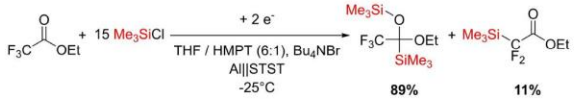

Scheme 13. Selective silylation of ethyl trifluoroacetate to the respective ethyltrimethylsilyl ketal (STST = stainless steel).[140]

ChemElectroChem | Review
doi.org/10.1002/celc.202201149
Chemistry Europe
European Chemical Societies Publishing

conversion of starting material could be increased from the non-mediated 13% to 98%, with very good isolated yield for the silylated anisole (Scheme 14). This technique further allowed the successful reductive coupling of haloaryls, halopyridines and halofurans with chlorosilanes to organofunctional silanes.[99] However, the mediator system faces its limitations when the reduction potentials of mediator and substrate compete, i.e. by NO_2-substituted aryls.

The use of easily reducible organic substrates that show high stabilization of the resulting carbanion, such as allyl,[53–55] benzyl,[53] vinyl,[54,55] and some aryl systems,[54,55] allows the avoidance of additional stabilizing components such as Mg^{2+} or HMPT at high current densities of up to 75 mA/cm^2. Redox mediators for selective silylation and even the sacrificial anode technique can be omitted for these substrates. Instead of the oxidized metal, the solvent DMF scavenges the oxidized chloride, unless substrates without electron-withdrawing groups are used in an undivided cell. Product chlorination occurs in this case (Scheme 15, a). However, high amounts of applied charge are needed for the conversion, especially in the undivided cell (Scheme 15, b), indicating side reactions of the chlorinated electrolyte. In contrast, Pons and co-workers,[49] were able to show silylation of benzyl halides without chlorination as a side reaction with a lower amount of charge using the sacrificial anode technique. As Kawabata and co-workers demonstrated,[54,55] in addition to the use of organic halides, acetoxy, carbonate or sulfone compounds are conceivable for the formation of carbanions, although with lower yields. However, chloro- and hydrochlorosilanes are the sole possible nucleophile traps for the desired conversion so far.

Grogger and co-workers,[57] achieved the formation of further organofunctional silanes starting from hydrochlorosilanes via the Mg sacrificial anode technique. However, due to the equilibration reaction of hydrochlorosilanes by tetraalkylammonium cations as mentioned earlier (Scheme 2, b), a suitable supporting electrolyte needs to be used. The 2:1 mixture of LiCl and $MgCl_2$ in THF represents an interesting special case here. The conductivity is increased by a factor of 100 compared to the individual components, due to ion aggregation with the low dissociating $MgCl_2$, shifting equation 5 to the right:

$$Li^+ + MgCl_2 \leftrightarrow [ClMgClLi^+] \quad (5)$$

Suppression of the equilibration reaction is achieved. Further the conversion of the alkoxysilane $Me_2Si(OMe)_2$ as nucleophile trap could be successfully conducted for different organic halides. However, a Grignard effect for organic bromides results in significantly lower necessary applied charges.

Leaving the realm of nucleophilic trapping functionality of chlorosilanes, the situation is reversed. In the presence of an organic unsaturated hydrocarbon, the reduction takes place at the halosilane, being subsequently trapped by the unsaturated hydrocarbon species. As Ohno and co-workers demonstrated,[89] via this reductive pathway the β-silylation of different aryl acrylates, nitriles and ketones could be achieved in yields up to 79% (Scheme 16). The use of sacrificial anodes, especially Mg is mandatory for the conversion. This indicates a necessity of the stabilization of the silyl intermediate by suitable cations like Mg^{2+}.

However, no mechanistic details were unraveled at that time. In this regard, Lin and co-workers,[88] have recently published an exciting mechanistic elucidation. By using alkenes and alkynes as unsaturated hydrocarbon species for the

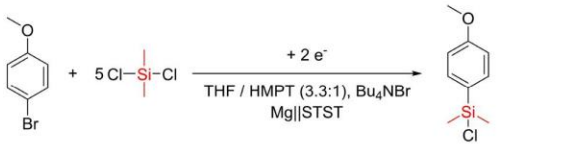

Scheme 14. Ni(0) redox mediator for the reductive conversion of halobenzenes as *p*-bromoanisole and Me_2SiCl_2, generating higher conversion and yield (STST = stainless steel).[99]

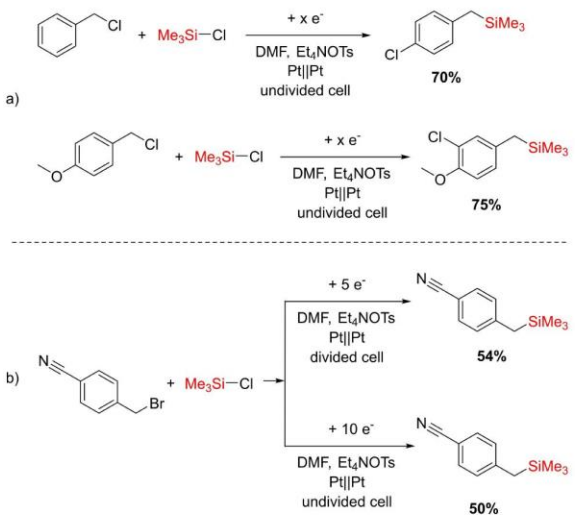

Scheme 15. Silylation of benzylic halides: a) chlorination of the product as side reaction in absence of a sacrificial anode in an undivided cell,[53] b) high applied charge needed for the conversion in absence of a sacrificial anode in an undivided cell.[53]

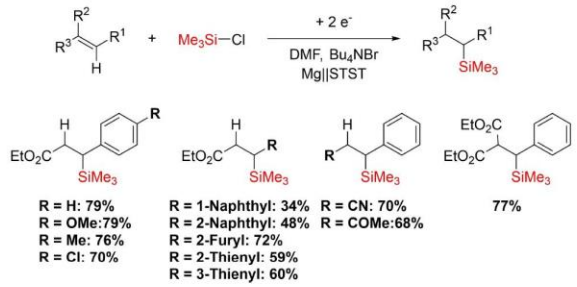

Scheme 16. Silylation of unsaturated hydrocarbon species by the reduction of chlorosilanes via the Mg sacrificial anode technique (STST = stainless steel).[89]

ChemElectroChem | Review
doi.org/10.1002/celc.202201149
Chemistry Europe
European Chemical Societies Publishing

trapping reaction of reduced silyl intermediates, a wide range of mono- and disilylated products could be obtained. High tolerance towards functional groups as boronates, tertiary amines, thioethers, alcohols and ketones, was reported by the described technique. Although they used a different type of electrolyte system (THF/Bu_4NClO_4) compared to the work of Ohno and co-workers (DMF/Bu_4NBr),[89] the subsequent silylation of unsaturated hydrocarbons with the use of sacrificial anode materials is similar. In their investigation, they clarified that the reaction originates from the chlorosilane. Substrate activation with Mg could be excluded by current-less conditions in the presence of Mg powder. According to the CV data, the potential of the alkene is a significant 0.7 V more negative compared to the cathodic potential of the chlorosilane. Supported by density functional theory (DFT) calculations and radical probe experiments based on the ring opening of a vinyl cyclopropane, the cathodic generation of silyl radicals with Mg assisted cleavage of Cl^- is proposed (Scheme 17). It is assumed that the presence of alkenes or alkynes results in a scavenging reaction of the silyl radical prior to any further reduction to the anion, as observed for the Si–Si bond formation. After the scavenging, a second reduction generates the anionic species. This leads to the subsequent mono- or disilylated product, depending on the availability of further electrophilic species (El). With weakly acidic substrates, allowing the cleavage of protons as El, such as MeCN, the anionic intermediate is hydrosilylated. Cyclic substrates containing Si–Si bonds could be obtained in high yields by using dichlorooligosilanes, via the "back biting" reaction, referring to the Si–Si bond formation of polysilanes (Scheme 8, c pathway I). The non-appearance of Si–Si bond cleavage in these cases demonstrates the wide range of applicable species.

In a similar work, Kunai and co-workers,[95] studied the addition of dichlorosilanes to an excess of dienes. By the use of a copper sacrificial anode, they generated the respective silacyclopent-3-enes in various electrolyte systems, including THF/Bu_4NClO_4 as used by Lin and co-workers.[88] Demonstrated by CV studies, the reduction takes place at the dichlorosilane with the diene serving as a trapping reagent. However, they assumed the formation of a silyl anion via two-electron reduction with consecutive ring formation. Given the mechanistic details of Lin and co-workers,[88] it is very likely that the reduction of dichlorosilanes also proceeds via a comparable radical pathway. Presumably, the corresponding silyl radical is scavenged by the diene in this case. Subsequently, reduction to the anion and consecutive ring closure by nucleophilic attack on the electrophilic silane occurs. However, formation of a copolymer via nucleophilic attack at another dichlorosilane was mentioned.

Comparable studies were also conducted by Jouikov and co-workers.[106] Here, Me_3SiCl was reduced in the presence of phenylacetylene. CV studies again show that the reduction should occur at the chlorosilane. In this case, the reduction potentials of the two substrates are very close, less than 0.1 V, suggesting a possible additional anionic course. Based on studies of Si–Si bond formation, it is believed that a silyl radical would be immediately further reduced to the corresponding anion. However, experiments in a potentiostatic driven ECE type flow cell (Scheme 18), which allows reduction to the anion and subsequent oxidation to the radical, show that the substrate stoichiometry is crucial for the resulting product. With an excess of chlorosilane, mainly the disilylated product is

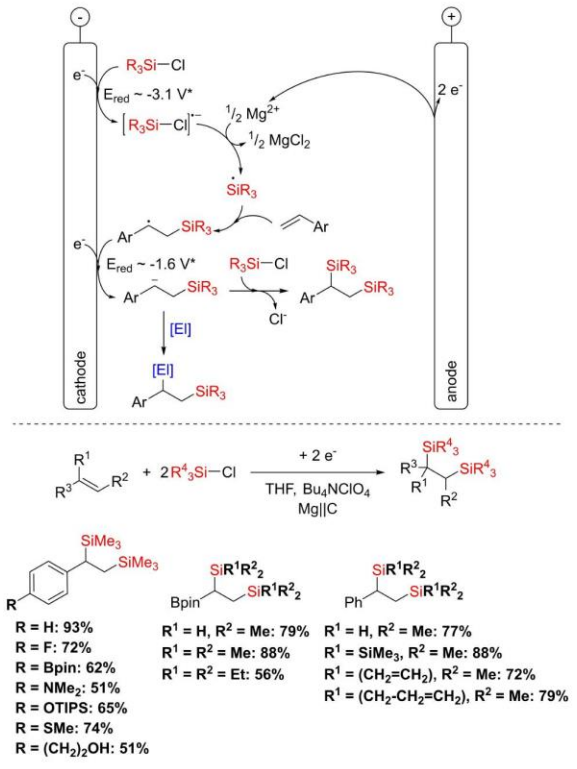

Scheme 17. Proposed reaction mechanism of the silylation of unsaturated hydrocarbon species by the reduction of chlorosilanes by Lin and co-workers (top, El = electrophilic species; *vs. SCE), reaction equation, conditions, and yield range of some relevant representatives of the electrochemical conversion (bottom, Bpin = 4,4,5,5-tetramethyl-1,3,2-dioxaborolan-2-yl, TIPS = triisopropylsilyl).[88]

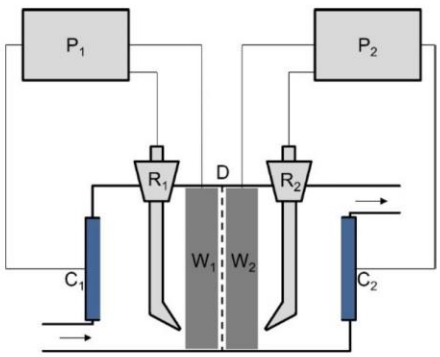

Scheme 18. Setup of the ECE type flow cell, to allow radical formation via the potentiostatic driven reduction and subsequent oxidation of substrates by Jouikov and co-workers (P_1, P_2 = potentiostat; R_1, R_2 = reference electrode; D = insulating porous diaphragm; C_1, C_2 = counter electrode; W_1, W_2 = working electrode).[106]

ChemElectroChem | Review
doi.org/10.1002/celc.202201149
Chemistry Europe
European Chemical Societies Publishing

obtained. Here, the reaction is assumed to proceed via radical addition to the triple bond, which is consistent with the results of Lin and co-workers.[88] However, if the stoichiometry is changed to a higher amount of alkyne, competition by the anionic route is supposed.

Another exciting publication by Jouikov and co-workers,[142] describes the combination of 2,2′-bipyridine (bipy) complexation of chlorosilanes with the trapping strategy using reactive C=C double bonds. Bipy as an adduct forms a hexacoordinated state with monochlorosilanes (Scheme 19) and chlorogermanes.[143] This results in a redox mediated type of reductive conversion, shifting the reduction potential of bipy by more than 1.0 V into the less negative regime. Electrochemical reduction generates the corresponding radical anion of the complex, which was detected by ESR spectroscopy. After cleavage of chloride, the silyl radical is released from the complex, allowing bipy to be available again for the coordination of monochlorosilanes. In the further course, the silyl radical can be trapped either by α-phenyl-*N*-*t*-butyl-nitrone (PBN) to the stable spin adduct, or by reactive C=C double bonds of the glassy carbon (GC) cathode. In the absence of PBN, this results in silylation of the GC surface with a chemically and mechanically stable coating, leading to surface passivation. Thus, the easy and hydrolysis-stable coating of carbon materials can be achieved.

3.1.3. Further reductive Si bond formation

In addition to the Si–Si and Si–C bond formation, further bond types can be obtained via the reductive reaction pathway. These are addressed considerably less frequently in literature and are briefly outlined below. **Si–Ge** bond formation can be achieved via the reduction of halogermanes in the presence of halosilanes, as mentioned earlier. The reaction occurs at cathodic potentials, which allow the reduction via the radical to the anion (Scheme 4, c). The respective germyl anion leads to nucleophilic attack at the halosilane, forming a Si–Ge bond. A variety of Si–Ge bonds,[58,87,110,126] including polymeric products,[56,58,86,87,126] have been achieved in the past via the sacrificial anode technique.

Si–S and **Si–Se** bonds can be obtained in analogy to the discussed nucleophile trapping technique used for Si–C bond formation. As shown by Jouikov and co-workers,[104] the cathodic reduction of a dichalcogenide, e.g. PhSSPh or PhSeSePh, leads to the respective chalcogenide anion (Scheme 20, a). Acting as a strong nucleophile, Si-chalcogenide

Scheme 19. Electrochemical generation of detectable silyl radical anions via bipy coordination and subsequent silylation of unsaturated C=C bonds at the glassy carbon (GC) cathode surface.[142]

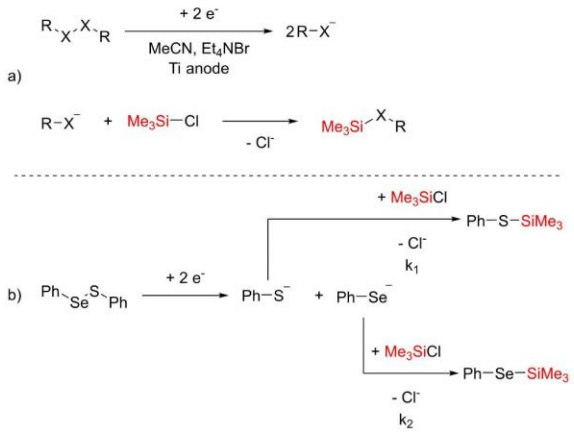

Scheme 20. Reductive silylation of dichalcogenides via the generation of strong chalcogenide nucleophiles (X = S, Se):[104] a) silylation via nucleophilic bond formation by chalcogenide anions, b) kinetic investigations showing the favored Si–Se bond formation due to higher nucleophilicity.

bonds can be formed in high yields. They further investigated reaction kinetics regarding the type of chalcogenide. By the use of PhSSePh as the substrate in large excess, concentration of both species can be neglected, and the order of reaction is similar (Scheme 20, b). By chromatographic observation of the conversion, they concluded that the $PhSe^-$ anion is the stronger nucleophile, achieving one order of magnitude faster Si bond formation for k_2 (Scheme 20, b). This is probably due to the bigger ion size, leading to the disfavoring of π-conjugation with the Ph-group and subsequent higher negative charge localization at Se^-.

Si-H bond formation can be achieved via the reduction of chlorosilanes in the presence of an H-donor. In some cases, the electrolyte solvent, such as DME,[48] or MeCN,[41] can be the source of protons and is used as the H-donor, generating electrolytic side reactions. In other cases, the H-donor, e.g. phenol,[110] or a diol,[144] is added as a substrate to provide protons in the course of the reaction. However, especially in the case of phenol, the formation of equimolar amounts of Si-O bonds occurs, due to the formation of PhO^- by proton abstraction. PhO^- represents a nucleophile, being trapped by available chlorosilanes to form the corresponding siloxane (Scheme 21). This reaction is electrochemically directed, as the phenol does not react with Ph_3SiCl at room temperature.

Si–O bond formation via reductive conversion has also been addressed in literature. However, the respective reaction pathways are considered special cases which are briefly described in the following. As reported by Jouikov and co-workers,[27,145–148] by electrochemical reduction of oxygen in different aprotic electrolytes, presumably the superoxide anion can be generated as a strong nucleophile in a divided cell. In the presence of reactive dichlorosilanes,[27,145–147] and dialkoxysilanes,[27,146–148] trapping of the above anion occurs, forming the highly reactive silanone intermediate $R_2Si{=}O$. If short-chain (cyclo)siloxanes are present as trapping reagents, extension of these frameworks occurs (Scheme 22). In the

ChemElectroChem | Review
doi.org/10.1002/celc.202201149
Chemistry Europe
European Chemical Societies Publishing

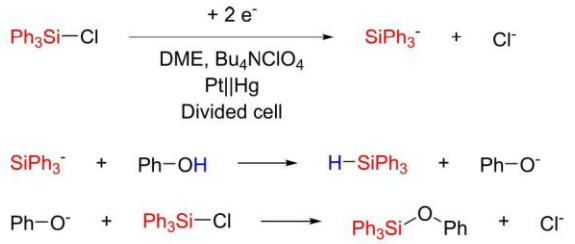

Scheme 21. Formation of equimolar amounts of siloxane and hydrosilane in the electrochemical conversion of chlorosilane with phenol.[110]

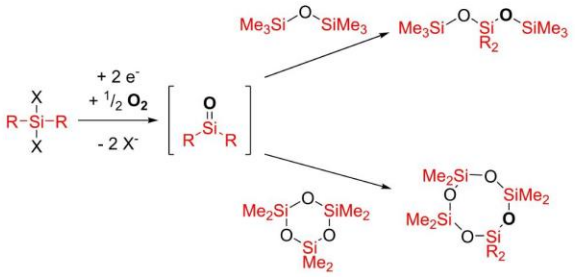

Scheme 22. Electrochemical conversion of chloro- and alkoxysilanes to silanones via the reactive superoxide intermediate as suggested by Jouikov and co-workers (X = Cl, OAlkyl).[27,145–147]

absence of these species, the silanone reacts with itself to form cyclic siloxanes, being available for further Si–O elongation.

Another special case involves the reduction of O_2 in the presence of CO_2, resulting in the formation of the reactive $C_2O_6^{2-}$.[149] By addition of monochlorosilanes, silylcarboxylic acids are obtained, dichlorosilanes are converted to cyclic siloxanes. However, the electrochemical conversion occurs here only for the preparation of the precursor molecule $C_2O_6^{2-}$, further silylation can be achieved via current-less conditions.

A further example of Si–O bond formation is the preparation of silyl enol ethers by electrochemically generated bases (EGBs).[150] Reduction of 2-pyrrolidone as a pre-base using the Mg sacrificial anode technique yields the Mg-stabilized base at temperatures of −75 °C. Addition of a ketone forms the Mg enolate, which is further trapped by an excess of Me_3SiCl. Here again, the electrochemical reduction is not applied for silylation, but for the preparation of the reactive precursor. The synthesis of silyl ethers is comparable,[151] with aldehydes and ketones serving as EGBs via reduction to the alkoxide anion. In this case, initial amounts of 0.05–0.5 *F* are sufficient, due to a catalytic cycle, generating the silyl ether compound.

In another special case, Me_3SiCl serves as a promoter for the hydrocoupling of α,β-unsaturated esters with aldehydes and ketones.[108] While the role of the chlorosilane is not clarified, an activation of the carbonyl compounds is suspected.

Si–Fe bonds could be prepared by the Mg sacrificial electrode technique.[152–154] In this process, cyclopentadienyl iron(II) dicarbonyl dimers (Fp_2) are reduced in the presence of chlorosilanes as nucleophile trapping agents in a THF/Bu_4NBr electrolyte (Scheme 23). While the respective substrates con-

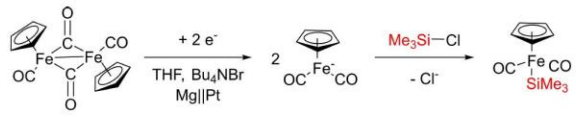

Scheme 23. Electrochemical Si–Fe bond formation via the generation of a strong Fp^- nucleophile being trapped by the chlorosilane.[152–154]

taining Si–Fe bonds could be isolated and crystallized, the reaction is shown to proceed slowly even in the current-less state, suggesting Grignard-type contribution in the reaction.

3.2. Anodic conversion

The anodic oxidation of silanes takes up a special role in literature. In contrast to the strongly electrophilic character of halosilanes, the desired bonds cannot be formed in the anodic conversion in the same diversity as is accessible for halosilanes by generating a nucleophile and subsequent trapping. Depending on the reaction conditions, oxidative conversion can be initiated via either the cationic or radical reaction pathway. Since hydrosilanes as starting compounds usually exhibit high oxidation potentials,[69,155] direct oxidation corresponds to relatively harsh reaction conditions that limits functional group tolerance, generating high reactive and strong electrophilic silyl cations.[156] Together with the more expensive and narrower range of available substrates compared to chlorosilanes, the electrochemical oxidation of hydrosilanes has been scarcely studied for a long time. This results in a much smaller number of publications on the subject compared to the cathodic conversion of halosilanes. However, the anodic approach to organosilanes is important from both a structural and technical point of view, due to the possible elimination of sacrificial anodes.[70] The oxidation of organosilanes for the synthesis of organic molecules, by cleavage of a "silyl super proton" is beyond the scope of this review and has been addressed in other work.[24,25]

In recent years, mediated strategies have developed in addition to the direct oxidation technique,[157] and have been adopted to the hydrosilane mediation. Here, oxidation of a mediator substrate, for example *N*-hydroxyphthalimide (NHPI), generates a reactive radical species in this case phthalimido-*N*-oxyl (PINO) (Scheme 24). By a hydrogen atom transfer (HAT) reaction with a hydrosilane, the silyl radical can thus be generated under mild reaction conditions, which in the further process either initiates a radical reaction or is itself oxidized to the cation due to the shift of the oxidation potential. While the purely radical reaction pathway has already been highlighted in a recent review,[35] synthetic tricks and electrochemical techniques that allow both radical and cationic conversion starting from hydrosilanes are presented below.

ChemElectroChem | Review
doi.org/10.1002/celc.202201149
Chemistry Europe
European Chemical Societies Publishing

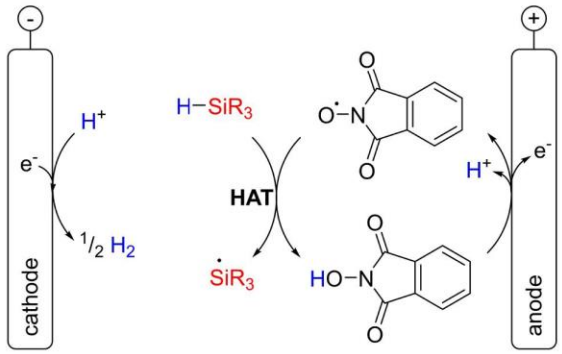

Scheme 24. NHPI/PINO mediated electrochemical oxidative transformation of hydrosilanes to silylradicals.[69,72,155]

3.2.1. Si-Si bond formation

The foundation for the oxidative Si–Si bond formation was laid by Kunai and co-workers in 1993.[60] They investigated the conversion towards disilanes starting from hydrosilanes in a DME/Bu_4NClO_4 electrolyte at platinum electrodes. In their work they demonstrated that hydrosilanes such as Me_2PhSiH can be oxidized at a GC anode at high potentials of 2.2 V vs. SCE. Presumably, the silyl cation is formed via a 2-electron oxidation and stabilized by the perchlorate anion of the supporting electrolyte (Scheme 25). Diffusion of the stabilized intermediate to the cathode and subsequent reduction is possible. The backwards reduction, probably to the silyl radical allows the corresponding dimerization (Scheme 25, **I**). Direct conversion to the corresponding disilane occurred in a yield of only 7.0% with an applied charge of 4.4 *F*. Parallel to the desired reduction, decomposition of the perchlorate supporting electrolyte anion is also possible (Scheme 25, **II**), resulting in the formation of the corresponding disiloxane in 15% yield. To increase the yield of the disilane, chlorination of the silyl cation by CuCl and $CuCl_2$ was investigated, leading to the corresponding chlorosilane in high yields up to 95% (Scheme 25, **III**). As a coupled one-pot reaction with formation of the chlorosilane and subsequent dimerization, 48% of the disilane could be prepared (Scheme 25, **IV**). However, for the corresponding conversion, the sacrificial anode technique based on Cu was necessary.

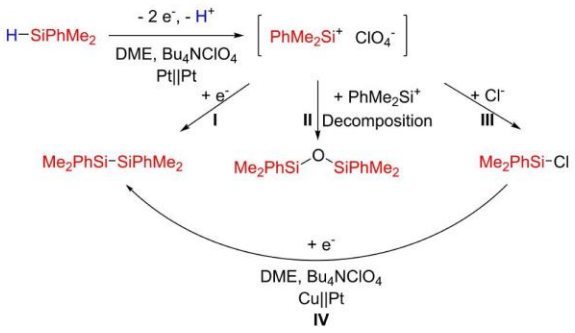

Scheme 25. Electrochemical oxidative conversion of hydrosilanes via the stabilized silyl cation to the disilane (**I**, **IV**), disiloxane (**II**) or chlorosilane (**III**).[60]

In recent studies,[61] Waldvogel and co-workers have demonstrated that the amount of charge required for Si–Si bond formation can be more than halved. The reaction of Kunai and co-workers is based on the presence of a silyl cation species which generates a Si–Si bond via subsequent reduction. By the addition of the strongly Lewis acidic borane $B(C_6F_5)_3$, the generation of a stabilized, activated silyl intermediate as silicon electrophile was sought, as has fundamentally expanded organic chemistry in recent years.[158] In the absence of coordinating substrates such as the supporting electrolyte, hydride abstraction can generate these silyl cationic intermediates, as a reactive species (Scheme 26, a).[159–161] In the presence of coordinating substrates such as the perchlorate anion, the formation of a silyl cation and borohydride has not yet been clearly confirmed by CV studies. However, CV measurements of the borohydride are difficult in the absence of suitable substrates due to the nature of the equilibrium, lying on the side of the non-activated hydrosilane.[162] However, a clear influence on the course of the reaction in the synthesis can be shown. Thus, the amount of charge necessary to generate 7% of the disilane decreases by more than half to 2.0 *F* by adding catalytic amounts of borane (Scheme 26, b). While the desired product could not be generated in high yield, this study demonstrates the potential use of Lewis acidic boranes for the electrochemical conversion of hydrosilanes.

Analogue to the synthesis of oligosilanes via the reductive reaction pathway with the use of dichlorosilanes, the oxidative process is accessible via the choice of dihydrosilanes, as Kimata and co-workers have shown.[71,163] Oxidation of $MePhSiH_2$ at a platinum anode yields a mixture of short-chain oligosilanes with Si–Si chain lengths of 2–5 as products. The use of the sterically more challenging Ph_2SiH_2 results exclusively in the formation of the dimer with 23% (Scheme 27). Unfortunately,

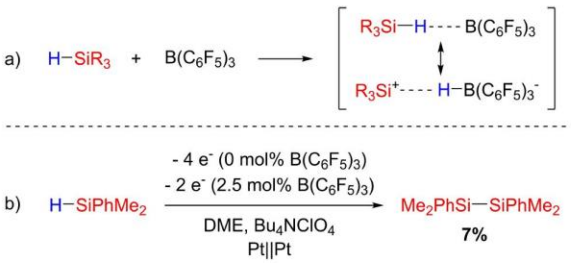

Scheme 26. The use of the Lewis acidic borane $B(C_6F_5)_3$: a) for the activation of hydrosilanes,[159–161] b) for the electrochemical conversion of hydrosilanes.[61]

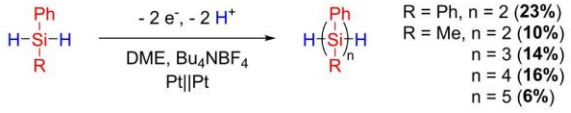

Scheme 27. Oxidative conversion of dihydrosilanes to di- and oligosilanes.[71,163]

ChemElectroChem | Review
doi.org/10.1002/celc.202201149
Chemistry Europe
European Chemical Societies Publishing

no further mechanistic studies were conducted. The formation of radical cations is assumed, but the cathodic access by the undivided cell could allow an analogous course as in the case of Kunai and co-workers.[60]

To further increase the Si–Si chain length during the oxidative conversion of hydrosilanes, it is necessary to switch to trihydrosilanes, as Kimata and co-workers have demonstrated.[71] Due to the lower steric requirements, the use of $PhSiH_3$ and $HexSiH_3$ allows the formation of average chain lengths of 6 and 10, respectively, enabling molecular weights to exceed 3 kDa (Scheme 28). However, linear oligosilanes and polysilanes are still obtained with the use of trihydrosilanes. Network structures, as known for the reductive pathway, are not formed via the oxidative reaction route. Similarly, higher chain lengths have not yet been formed via the described method. This fact can be explained by the high oxidation potential of the Si–H bond compared to the Si–Si bond. Analog to the reduction potential of Si–Si bonds, the oxidation potential decreases into the lower anodic regime with increasing chain length.[164] This fact is intensified by aryl groups compared to alkyl groups. If the oxidation potentials of Si–H and Si–Si bonds compete, the Si–Si bond is cleaved in a concurrent reaction, limiting the absolute chain length. Here again, a radical cation is assumed to be the intermediate of synthesis in the undivided cell.

3.2.2. Si-C bond formation

In contrast to the reductive Si–C bond formation via chlorosilanes as substrates, anodic access via hydrosilanes was hardly known until a few years ago. Only recently possible electrochemical reaction routes for this access have been described. Following the work in Si–Si bond formation,[61] Waldvogel and co-workers established the concept of Lewis acidic boranes as mediators for the conversion to Si–C bonds starting from hydrosilanes and enhancing the yields, i.e. for benzyldimethylphenylsilane from 12% to 86%.[70] As could be demonstrated in this study, contrary to previous assumptions,[165] the presence of a supporting electrolyte does not prevent the function of the borane by coordination. Rather, the interaction of supporting electrolyte and borane is necessary to stabilize the highly reactive intermediate (Scheme 29). Alternatively, a spontaneous reaction with the solvent DME occurs with the formation of the respective silyl ether. Various supporting electrolytes, such as perchlorates and tetrafluoroborates, have proven suitable for this stabilization. In the electrochemical conversion, the hydrosilane is activated by the addition of borane. In parallel, an organic halide is reduced at the cathode. In a subsequent step, the nucleophilic carbanion formed reacts with the activated,

Scheme 28. Oxidative conversion of trihydrosilanes to linear oligo- and polysilanes (n_{av} = average chain length).[71]

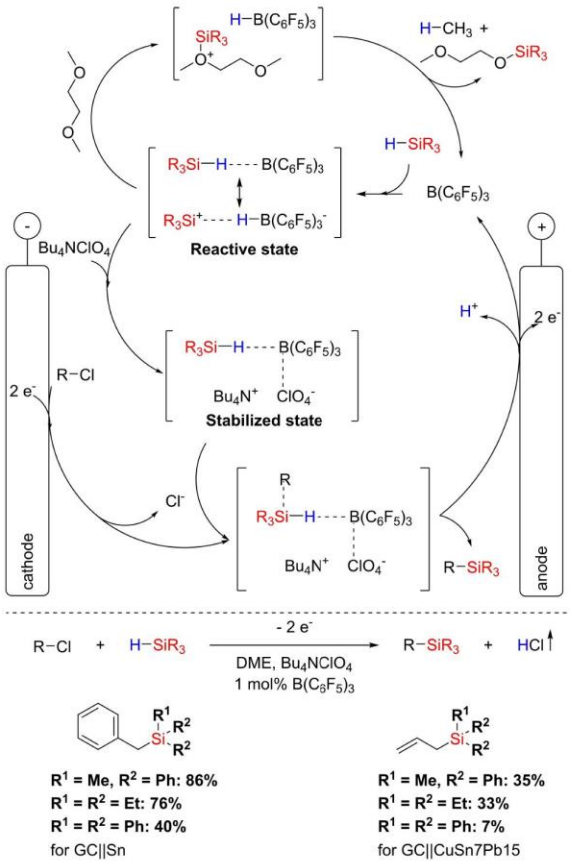

Scheme 29. Borane mediated electrochemical conversion of hydrosilanes to allyl and benzyl silanes as suggested by Waldvogel and co-workers (top), reaction equation, conditions, and yield range of relevant representatives of the electrochemical conversion (bottom).[70]

higher electrophilic hydrosilane, and Si–C bond formation occurs. The borane mediator is converted back to its initial state via oxidation at the anode to activate a hydrosilane again. At the anodic side, the regeneration of the borane yields protons to react with the cathodically produced chloride ions. Hydrogen chloride is formed and released from the reaction solution. This reaction path eliminates the need for the sacrificial anode technique to obtain a Si–C bond formation in presence of chloride ions. Besides its role as a mediator, the borane additionally serves as a protection against over-oxidation. This is comparable to the protection against over-reduction by metal ions as shown by Pons and co-workers on chlorosilanes.[82] The corresponding allylsilane can only be prepared in the presence of a borane mediator. As reported, allyldimethylphenylsilane is oxidized 0.58 V more readily than the hydrosilane starting material. Addition of the mediator shifts the oxidation potential of the hydrosilane by 0.88 V into the lower anodic regime and consequently prevents oxidation of the product. In addition to $B(C_6F_5)_3$, BCl_3 and BEt_3 have proved to be potentially mediators for the conversion of hydrosilanes towards benzyl and allyl functionalities.

ChemElectroChem | Review
doi.org/10.1002/celc.202201149
Chemistry Europe
European Chemical Societies Publishing

Another strategy to form Si–C bonds is the scavenging of radical intermediates by unsaturated hydrocarbons, in analogy to the reductive synthesis of Lin and co-workers.[88] As early as 2000, Berberova reported,[166] that electrochemical hydrosilylation is accessible via the anodic oxidation of hydrosilanes in the presence of C=C double bonds, as in acrylonitrile and cyclohexene. Direct oxidation of hydrosilanes demonstrated the formation of hydrogen as a radical dimerization product. This indicates a silyl radical cation as intermediate, which reacts in a subsequent reaction step to the silyl cation with elimination of a hydrogen radical (Scheme 30, a). Investigation of the limiting current using a ring-disk electrode allowed the lifetime of the radical cation to be calculated as 0.003 s, exceeding the stability of free radicals in solution. Via a pulsed electrolysis, it was further demonstrated that the hydrosilylation reaction occurring corresponds to a radical chain reaction, with the initiation proceeding electrochemically. The generated silyl radical cation is trapped by the unsaturated hydrocarbon and subsequent oxidation of a further hydrosilane occurs, continuing the process (Scheme 30, b). Only minor initial charge amounts already result in complete hydrosilylation by the emerging reaction. However, it was noted that only small supporting electrolyte cations as Li^+ and Na^+ could be successfully applied, as tetraalkylammonium cations block the anode, preventing the desired hydrosilane oxidation. Recent studies show a possible hydrosilylation of alkynes via the electrochemical reaction pathway.[167] However, the oxidation of Si–B bonds is beyond the scope of our review and has been already discussed elsewhere.[35]

Recent studies by He and co-workers,[69] have shown that the use of a HAT mediator generates a silyl radical that can be scavenged by unsaturated hydrocarbons. Again, small supporting electrolyte cations as Li^+ were beneficial for the desired oxidation. However, a special case is applied by consuming the mediator in the reaction, resulting in silyl-oxygenation of the C=C double bond rather than hydrosilylation (Scheme 31). NHPI and adjacent structures are oxidized to PINO radical derivatives, generating the silyl radical via a HAT reaction. The C=C double bond scavenges the silyl radical, resulting in the formation of an α-silyl alkyl radical, which allows the formation of the corresponding C–O bond by trapping another PINO radical derivative. The reduction of hydrogen is described as the cathodic reaction. The radical intermediate was confirmed by (2,2,6,6-tetramethylpiperidin-1-yl)oxyl (TEMPO) and radical clock experiments based on vinyl cyclopropane in analogy to Lin and co-workers.[88] Via this radical three-component reaction, a broad substrate base with diverse hydrosilanes, electron-deficient alkenes, and *N*-oxyl species could be obtained in high yields.

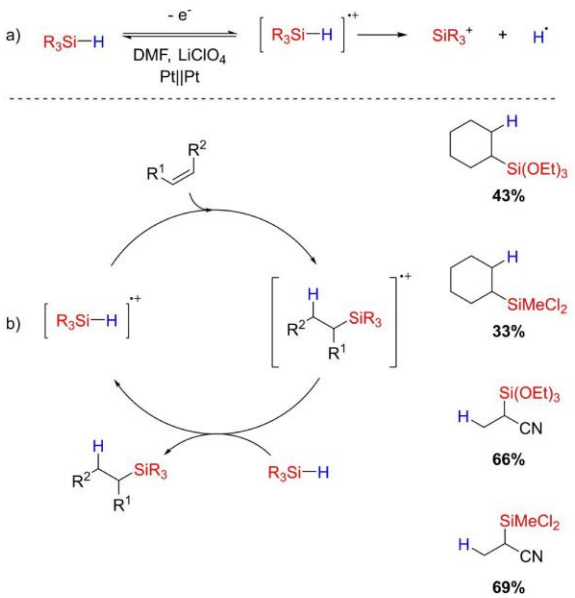

Scheme 30. Electrochemical oxidation of hydrosilanes:[166] a) formation of the silyl radical cation with subsequent reaction to the silyl cation under the release of hydrogen atom, b) catalytic cycle for the hydrosilylation of alkenes via electrochemical oxidative hydrosilane activation.

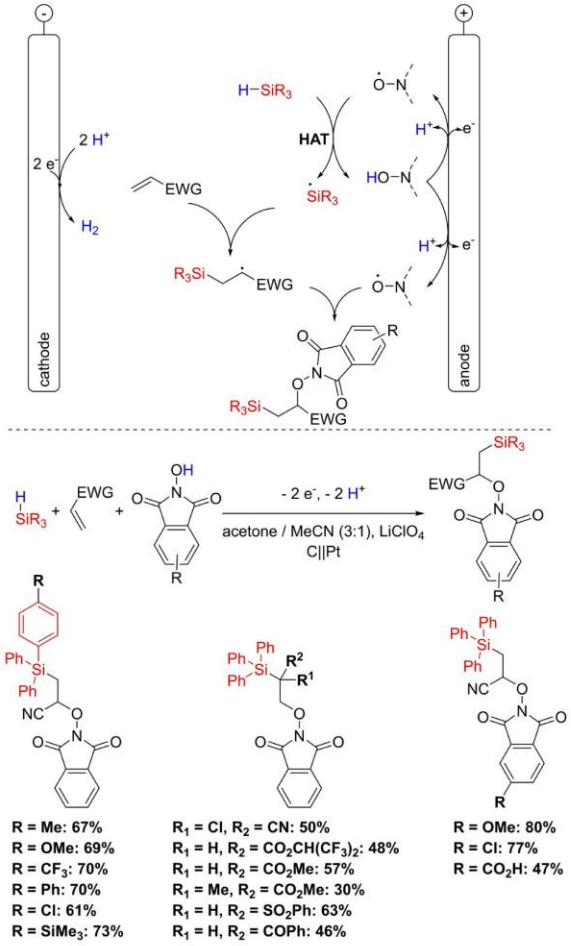

Scheme 31. Electrochemical silyl-oxygenation of activated alkenes via radical mediated HAT reaction with hydrosilanes as suggested by He and co-workers (top, EWG = electron withdrawing group), reaction equation, conditions, and yield range of some relevant representatives of the electrochemical conversion (bottom).[69]

ChemElectroChem | Review
doi.org/10.1002/celc.202201149
Chemistry Europe
European Chemical Societies Publishing

In addition to the previously described formation of intermolecular Si–C bonds, the electrochemical synthesis of intramolecular Si–C bonds is possible. Recently, Han and co-workers reported,[72] that dibenzosiloles can be obtained via an oxidative HAT reaction of hydrosilanes. Interestingly, the reaction requires the addition of 1,1,1,3,3,3-hexafluoro-2-propanol (HFIP) to increase the yields above 10%. Furthermore, pyridine is used to deprotonate NHPI to the respective anion, which is electrochemically oxidized to the PINO radical. The direct anodic oxidation seems to be prevented, probably due to the choice of the supporting electrolyte cation. The optimization of the reaction conditions starts with a tetraalkylammonium cation, which has a negative impact by at least partially blocking of the anodic access, as shown in previous studies.[69,166] By using the combination of HFIP and pyridine, the choice of the supporting electrolyte cation is of secondary importance, so that high yields can be achieved for various salt combinations. In this way, the used system circumvents the cationic anode blockage. The silyl radical is first formed by the HAT reaction in the course of the reaction (Scheme 32), analog to the work of He and co-workers,[69] as TEMPO studies show. Further anodic oxidation to the silyl cation occurs in the subsequent step. This silyl cation can be trapped as a silanol by the addition of water. The corresponding dibenzosilole is formed via a sila-Friedel-Crafts reaction with subsequent deprotonation, analogous to silicon electrophiles reported in the organic chemistry.[168]

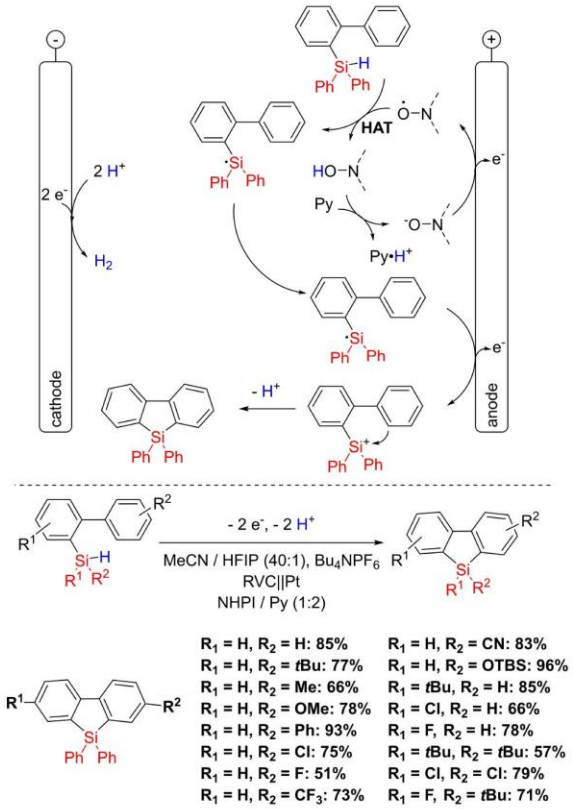

Scheme 32. Electrochemical HAT mediated conversion of hydrosilanes via sila-Friedel-Crafts reaction for the formation of dibenzosiloles as suggested by Han and co-workers (top), reaction equation, conditions, and yield range of some relevant representatives of the electrochemical conversion (bottom, HFIP = 1,1,1,3,3,3-hexafluoro-2-propanol, RVC = reticulated vitreous carbon, Py = pyridine, TBS = *t*-butyl dimethylsiloxyl).[72]

3.2.3. Further oxidative Si bond formations

In addition to Si–Si and Si–C bond formation, further coupling type reactions exist in the electrochemical oxidative synthesis of silanes, which will be briefly highlighted below. For the use of hydrosilanes as starting material, as is the focus of this review, additional **Si–H** bond formation is not established. However, an anodic route for the conversion to Si–H bonds starting from silicon as a sacrificial anode in hydride salt melts has been reported.[169]

In reference to the reductive synthesis of the **Si–O** bond to silanones, an oxidative approach is known. Via the hydrosilane mediated electrochemical reduction of amides to amines, the respective Si=O bond is formed as a consecutive reaction.[170] $PhSiH_3$ is converted to the silyl radical via a bromide mediator with a HAT reaction. In parallel, the reduction of the amide occurs, to generate the respective Si–C bond via recombination. In the course of the reaction, after [1,2]-brook rearrangement and subsequent oxidation to the silyl cation, the silanone is cleaved, with further conversion of the amide to the amine (Scheme 33).

Furthermore, silyl ethers can be prepared via the oxidative reaction pathway.[171] In this case, the oxidation does not start from a hydrosilane, but from easily oxidizable allyl and benzyl silanes. By anodic cleavage of the Si–C bond in an alcohol as electrolyte solvent, such as MeOH, the released silyl cation can be scavenged as the respective silyl ether.

The electrochemical access to silyl ethers and silanols starting from hydrosilanes was recently reported by Zhang and co-workers.[155] In their work, the activation of a hydrosilane via a HAT process plays a central role (Scheme 34). NHPI is oxidized in an anodic conversion to the PINO radical, which is facilitated by the presence of hydroxide ions. These occur in the reaction process due to the reduction of water, being the substrate for silanol formation. The hydroxide ions hence exhibit a comparable facilitating function in the anodic oxidation of NHPI as the HFIP/pyridine system of Han and co-workers.[72] In this study, tetrabutylammonium cations are again used exclusively as supporting electrolytes. After the HAT process, the silyl radical, which was verified by TEMPO trapping experiments, is further electrochemically oxidized to the silyl cation. The silyl cation reacts with water or the corresponding alcohol under the release of protons. The conversion of hydrosilanes to the respective silanols, disilanols and silyl ethers could thus be demonstrated over a broad substrate base. Due to the mild reaction conditions, the functional group tolerance is high, allowing even complex structures to be prepared.

As shown in previous studies,[60,70] **Si–Cl** bond formation starting from hydrosilanes is also possible, but not of economic interest. The corresponding Si–Cl bond can be obtained by

ChemElectroChem | Review
doi.org/10.1002/celc.202201149
Chemistry Europe
European Chemical Societies Publishing

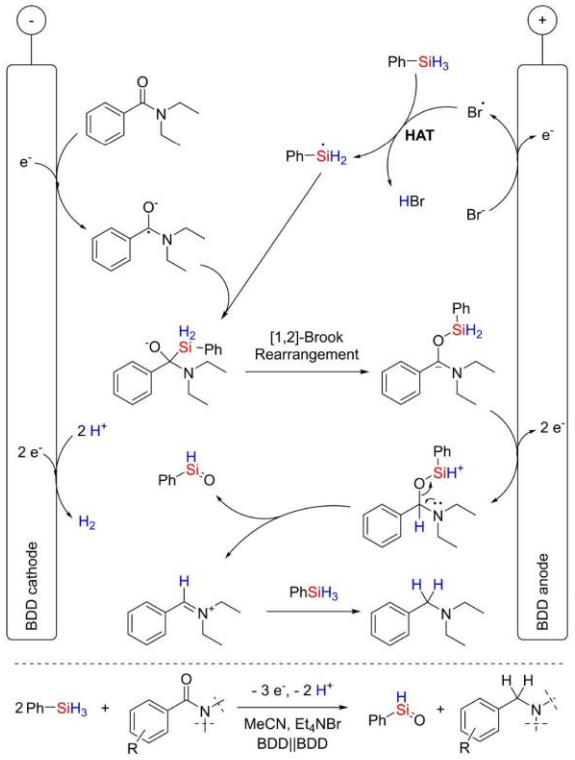

Scheme 33. Electrochemical conversion of silanes to silanones via a HAT reaction and subsequent oxidation to the silyl cation with consecutive reduction of an amide to an amine as suggested by Chiba and co-workers (top), reaction equation and conditions (bottom, BBD = boron-doped diamond).[170]

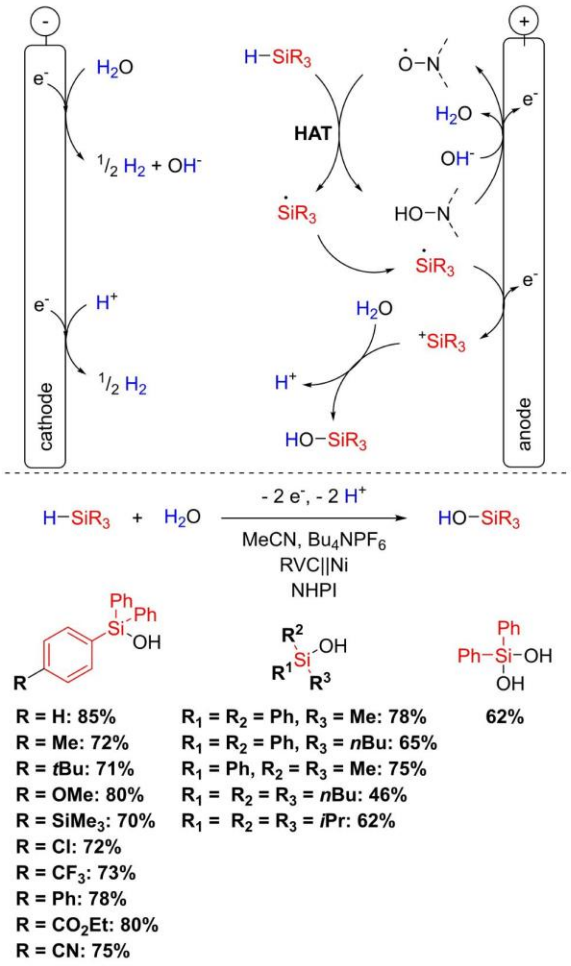

Scheme 34. Electrochemical HAT mediated oxidation of hydrosilanes to silanols as suggested by Zhang and co-workers (top), reaction equation, conditions, and yield range of some relevant representatives of the electrochemical conversion (bottom, RVC = reticulated vitreous carbon).[155]

oxidation of hydrosilanes in the presence of free chloride ions. The **Si–F** bond formation has not yet been described starting from hydrosilanes but should proceed analogously to the synthesis of the Si–Cl bond. Starting from tetraalkylsilanes,[46] and cyclosilanes,[172] the Si–F bond formation is described via cleavage of the corresponding Si–C or Si–Si bond in the presence of a fluoride ion. This fluoride ion can be provided, for example, as BF_4^- by the supporting electrolyte.

4. Conclusion

The electrochemical conversion of chlorosilanes and hydrosilanes is a safe and versatile method that has been applied successfully, although depending on a number of parameters. The solvent, supporting electrolyte and substrates require very dry conditions in order to exclude a hydrolysis reaction. Karl-Fischer titration and electroanalytical techniques are suitable for this verification and should be established together with a standardized electrolyte-electrode concept for the CV investigation of chlorosilanes and hydrosilanes for high comparability. Supporting electrolytes can cause stabilization of intermediates as well as exchange and equilibration reactions and should be chosen carefully.

The cathodic conversion of chlorosilanes provides a large number of publications that allow a profound comprehensibility. The reduction proceeds to the anion formation in the absence of appropriate trapping reagents, such as unsaturated hydrocarbons. This results in the generation of a nucleophile, and subsequent bond formation with another chlorosilane. High yields have been described with a variety of substrates via both silyl anions and carbanions. Mediator systems are gaining in importance, making the necessary reduction potentials more readily available. However, the high reactivity of chlorosilanes still leaves a wide field open for more stable mediator systems, yet metal ionic systems i.e., Ni-based ones show promising approaches. Trapping reactions of silyl radicals by unsaturated hydrocarbons further open up new synthetic possibilities and offer additional functionalization possibilities. Nevertheless, concepts for scavenging the cathodically released chloride, besides the mostly used sacrificial anodes, remain to be desired.

ChemElectroChem | Review
doi.org/10.1002/celc.202201149
Chemistry Europe
European Chemical Societies Publishing

Establishing gas anodes, i. e., hydrogen, and facilitating the easy commercial access may be a necessary step.

The oxidative conversion of hydrosilanes still leaves space for new electrochemical approaches. Direct conversion is limited by the high oxidation potential of hydrosilanes and has only been demonstrated on a marginal substrate range with low yields. Both activation by Lewis acid boranes for easier access to bond formation and radical mediated approaches show enormous features for future applications. Due to the mild conditions, a variety of substrate classes, as well as further mediation concepts, are conceivable. In addition, the use of Si–B compounds reveals novel possibilities for the electrochemical oxidative preparation of organosilanes.

Acknowledgements

Open Access funding enabled and organized by Projekt DEAL.

Conflict of Interest

The authors declare no conflict of interest.

Keywords: Anodic conversions · Cathodic conversions · Electrochemistry · Mediated Transformations · Silanes

[1] a) M. A. Brook, *Silicon in organic, organometallic, and polymer chemistry*, Wiley, New York, Weinheim, **2000**; b) T. H. Chan, D. Wang, *Chem. Rev.* **1995**, *95*, 1279–1292; c) A. Hosomi, *Acc. Chem. Res.* **1988**, *21*, 200–206; d) H. Sakurai, *Pure Appl. Chem.* **1982**, *54*, 1–22.
[2] J. Yoshida, K. Kataoka, R. Horcajada, A. Nagaki, *Chem. Rev.* **2008**, *108*, 2265–2299.
[3] a) T. Kalnin, V. Gulbis, *Corrosion protection. Processes, management and technologies*, Nova Science Publishers, New York, **2009**; b) E. B. Wyman, M. C. Skief, *Organosilanes. Properties, performance, and applications*, Nova Science Publishers, New York, **2010**.
[4] a) A. K. Franz, S. O. Wilson, *J. Med. Chem.* **2013**, *56*, 388–405; b) A. Ramirez, K. A. Woerpel, *Org. Lett.* **2005**, *7*, 4617–4620; c) G. A. Showell, J. S. Mills, *Drug Discovery Today* **2003**, *8*, 551–556.
[5] N. Auner, J. Weis *Organosilicon chemistry VI. From molecules to materials*, Wiley-VCH, Weinheim, Chichester, **2008**.
[6] E. Pouget, J. Tonnar, P. Lucas, P. Lacroix-Desmazes, F. Ganachaud, B. Boutevin, *Chem. Rev.* **2010**, *110*, 1233–1277.
[7] a) L. Du, W. Chu, H. Miao, D. Wang, C. Xu, Y. Ding, *Eur. J. Inorg. Chem.* **2015**, *2015*, 3205–3211; b) R. A. Ovanesyan, D. M. Hausmann, S. Agarwal, *ACS Appl. Mater. Interfaces* **2015**, *7*, 10806–10813; c) R. A. Ovanesyan, D. M. Hausmann, S. Agarwal, *ACS Appl. Mater. Interfaces* **2018**, *10*, 19153–19161; d) R. A. Ovanesyan, N. Leick, K. M. Kelchner, D. M. Hausmann, S. Agarwal, *Chem. Mater.* **2017**, *29*, 6269–6278.
[8] a) Y. Horii, K. Kannan, *Arch. Environ. Contam. Toxicol.* **2008**, *55*, 701–710; b) W. Johnson, W. F. Bergfeld, D. V. Belsito, R. A. Hill, C. D. Klaassen, D. C. Liebler, J. G. Marks, R. C. Shank, T. J. Slaga, P. W. Snyder, F. A. Andersen, *Int. J. Toxicol.* **2011**, *30*, 149S-227S; c) D. Seyferth, *Organometallics* **2001**, *20*, 4978–4992.
[9] a) S. Bähr, W. Xue, M. Oestreich, *ACS Catal.* **2019**, *9*, 16–24; b) Z. Li, X. Cao, G. Lai, J. Liu, Y. Ni, J. Wu, H. Qiu, *J. Organomet. Chem.* **2006**, *691*, 4740–4746; c) G. Martin, F. S. Kipping, *J. Chem. Soc. Trans.* **1909**, *95*, 302–314; d) R. Robison, F. S. Kipping, *J. Chem. Soc. Trans.* **1908**, *93*, 439–456.
[10] a) J. Koe, *Polym. Int.* **2009**, *58*, 255–260; b) K. Meenu, D. S. Bag, R. Lagarkha, R. Tomar, A. K. Gupta, *Curr. Organocatal.* **2019**, *6*, 193–221.
[11] a) R. E. Grote, E. R. Jarvo, *Org. Lett.* **2009**, *11*, 485–488; b) Z.-D. Huang, R. Ding, P. Wang, Y.-H. Xu, T.-P. Loh, *Chem. Commun.* **2016**, *52*, 5609–5612.
[12] a) D. Cantillo, *Chem. Commun.* **2022**, *58*, 619–628; b) C. Kingston, M. D. Palkowitz, Y. Takahira, J. C. Vantourout, B. K. Peters, Y. Kawamata, P. S. Baran, *Acc. Chem. Res.* **2020**, *53*, 72–83; c) M. C. Leech, K. Lam, *Nat. Chem. Rev.* **2022**, *6*, 275–286; d) A. Shatskiy, H. Lundberg, M. D. Kärkäs, *ChemElectroChem* **2019**, *6*, 4067–4092; e) S. R. Waldvogel, B. Janza, *Angew. Chem. Int. Ed.* **2014**, *53*, 7122–7123; *Angew. Chem.* **2014**, *126*, 7248–7249; f) Y. Yuan, A. Lei, *Nat. Commun.* **2020**, *11*, 802.
[13] D. Pollok, S. R. Waldvogel, *Chem. Sci.* **2020**, *11*, 12386–12400.
[14] a) S. Möhle, M. Zirbes, E. Rodrigo, T. Gieshoff, A. Wiebe, S. R. Waldvogel, *Angew. Chem. Int. Ed.* **2018**, *57*, 6018–6041; *Angew. Chem.* **2018**, *130*, 6124–6149; b) J. Seidler, J. Strugatchi, T. Gärtner, S. R. Waldvogel, *MRS Energy Sustainability* **2020**, *7*, E42.
[15] a) A. D. Beck, L. Schäffer, S. Haufe, S. R. Waldvogel, *Eur. J. Org. Chem.* **2022**, e202201253; b) M. D. Kärkäs, *Chem. Soc. Rev.* **2018**, *47*, 5786–5865; c) R. D. Little, K. D. Moeller, *Chem. Rev.* **2018**, *118*, 4483–4484; d) J. L. Röckl, D. Pollok, R. Franke, S. R. Waldvogel, *Acc. Chem. Res.* **2020**, *53*, 45–61; e) S. R. Waldvogel, S. Lips, M. Selt, B. Riehl, C. J. Kampf, *Chem. Rev.* **2018**, *118*, 6706–6765; f) A. Wiebe, T. Gieshoff, S. Möhle, E. Rodrigo, M. Zirbes, S. R. Waldvogel, *Angew. Chem. Int. Ed.* **2018**, *57*, 5594–5619; *Angew. Chem.* **2018**, *130*, 5694–5721; g) M. Yan, Y. Kawamata, P. S. Baran, *Chem. Rev.* **2017**, *117*, 13230–13319.
[16] B. A. Frontana-Uribe, R. D. Little, J. G. Ibanez, A. Palma, R. Vasquez-Medrano, *Green Chem.* **2010**, *12*, 2099–2119.
[17] E. J. Horn, B. R. Rosen, P. S. Baran, *ACS Cent. Sci.* **2016**, *2*, 302–308.
[18] S. B. Beil, D. Pollok, S. R. Waldvogel, *Angew. Chem. Int. Ed.* **2021**, *60*, 14750–14759; *Angew. Chem.* **2021**, *133*, 14874–14883.
[19] M. Klein, S. R. Waldvogel, *Angew. Chem. Int. Ed.* **2022**, e202204140; *Angew. Chem.* **2022**, e202204140.
[20] M. Dörr, M. M. Hielscher, J. Proppe, S. R. Waldvogel, *ChemElectroChem* **2021**, *8*, 2621–2629.
[21] E. M. Geniès, F. El Omar, *Electrochim. Acta* **1983**, *28*, 541–546.
[22] C. Biran, M. Bordeau, P. Pons, M.-P. Léger, J. Dunoguès, *J. Organomet. Chem.* **1990**, *382*, C17–C20.
[23] J. D. Dunitz, K. Hafner, S. Ito, J.-M. Lehn, K. N. Raymond, C. W. Rees, J. Thiem, F. Vögtle, E. Steckhan, *Topics in Current Chemistry, Vol. 170*, Springer Berlin Heidelberg, Berlin, Heidelberg, **1994**.
[24] V. V. Jouikov, *Russ. Chem. Rev.* **1997**, *66*, 509–540.
[25] J. Yoshida, *Electrochemistry V. Electrochemical reactions of organosilicon compounds*, Springer Berlin Heidelberg, **1994**.
[26] J. Chaussard, J.-C. Folest, J.-Y. Nedelec, J. Perichon, S. Sibille, M. Troupel, *Synthesis* **1990**, *1990*, 369–381.
[27] V. V. Jouikov, *ECS Trans.* **2008**, *15*, 317–323.
[28] L. Fleming, *Science of Synthesis. Category 1, Organometallics*, Georg Thieme Verlag, Stuttgart, **2002**.
[29] K. Subramanian, *J. Macromol. Sci. Polym. Rev.* **1998**, *38*, 637–650.
[30] A. D. S. Gomes, *New polymers for special applications*, InTech, Rijeka, Croatia, **2012**.
[31] D. Elwell, R. S. Feigelson, *Sol. Energy Mater.* **1982**, *6*, 123–145.
[32] D. Elwell, G. M. Rao, *J. Appl. Electrochem.* **1988**, *18*, 15–22.
[33] T. Homma, N. Matsuo, X. Yang, K. Yasuda, Y. Fukunaka, T. Nohira, *Electrochim. Acta* **2015**, *179*, 512–518.
[34] K. Yasuda, T. Nohira, *High Temp. Mater. Processes* **2022**, *41*, 247–278.
[35] L.-Q. Ren, N. Li, J. Ke, C. He, *Org. Chem. Front.* **2022**, *9*, 6400–6415.
[36] R. Corriu, G. Dabosi, M. Martineau, *J. Organomet. Chem.* **1978**, *150*, 27–38.
[37] R. Corriu, G. Dabosi, M. Martineau, *J. Organomet. Chem.* **1981**, *222*, 195–199.
[38] V. Jouikov, C. Biran, M. Bordeau, J. Dunoguès, *Electrochim. Acta* **1999**, *45*, 1015–1024.
[39] R. Corriu, G. Dabosi, M. Martineau, *J. Organomet. Chem.* **1980**, *186*, 19–24.
[40] R. J. P. Corriu, G. Dabosi, M. Martineau, *J. Chem. Soc. Chem. Commun.* **1979**, 457b.
[41] W. G. Boberski, A. L. Allred, *J. Organomet. Chem.* **1975**, *88*, 73–77.
[42] R. Corriu, G. Dabosi, M. Martineau, *J. Organomet. Chem.* **1980**, *186*, 25–37.
[43] S. Soualmi, M. Dieng, A. Ourari, D. Gningue-Sall, V. Jouikov, *Electrochim. Acta* **2015**, *158*, 457–469.
[44] J. L. Brefort, R. J. P. Corriu, C. Guerin, B. J. L. Henner, W. W. C. Wong Chi Man, *Organometallics* **1990**, *9*, 2080–2085.
[45] A. L. Allred, C. Bradley, T. H. Newman, *J. Am. Chem. Soc.* **1978**, *100*, 5081–5084.
[46] I. Y. Alyev, I. N. Rozhkov, I. L. Knunyants, *Tetrahedron Lett.* **1976**, *17*, 2469–2470.

ChemElectroChem | Review doi.org/10.1002/celc.202201149 | Chemistry Europe European Chemical Societies Publishing

[47] A. Kunai, E. Toyoda, T. Kawakami, M. Ishikawa, *Organometallics* **1992**, *11*, 2899–2903.
[48] R. E. Dessy, W. Kitching, T. Chivers, *J. Am. Chem. Soc.* **1966**, *88*, 453–459.
[49] P. Pons, C. Biran, M. Bordeau, J. Dunogues, S. Sibille, J. Perichon, *J. Organomet. Chem.* **1987**, *321*, C27–C29.
[50] P. Duchek, R. Ponec, V. Chvalovský, *J. Organomet. Chem.* **1984**, *271*, 101–106.
[51] M. Okano, K. Takeda, T. Toriumi, H. Hamano, *Electrochim. Acta* **1998**, *44*, 659–666.
[52] R. D. Miller, J. Michl, *Chem. Rev.* **1989**, *89*, 1359–1410.
[53] T. Shono, Y. Matsumura, S. Katoh, N. Kise, *Chem. Lett.* **1985**, *14*, 463–466.
[54] J. Yoshida, K. Muraki, H. Funahashi, N. Kawabata, *J. Org. Chem.* **1986**, *51*, 3996–4000.
[55] J. Yoshida, K. Muraki, H. Funahashi, N. Kawabata, *J. Organomet. Chem.* **1985**, *284*, C33–C35.
[56] S. Kashimura, M. Ishifune, *J. Synth. Org. Chem. Jpn.* **2000**, *58*, 966–974.
[57] C. Grogger, B. Loidl, H. Stueger, T. Kammel, B. Pachaly, *J. Electrochem. Soc.* **2013**, *160*, G88-G92.
[58] S. Kashimura, M. Ishifune, N. Yamashita, H.-B. Bu, M. Takebayashi, S. Kitajima, D. Yoshiwara, Y. Kataoka, R. Nishida, S. Kawasaki Si, H. Murase, T. Shono, *J. Org. Chem.* **1999**, *64*, 6615–6621.
[59] J. Ohshita, K. Hino, T. Iwawaki, A. Kunai, *J. Organomet. Chem.* **2009**, *625*, 138–143.
[60] A. Kunai, T. Kawakami, E. Toyoda, T. Sakurai, M. Ishikawa, *Chem. Lett.* **1993**, *22*, 1945–1948.
[61] A. D. Beck, S. Haufe, J. Tillmann, S. R. Waldvogel, *ChemElectroChem* **2022**, *9*, e202101374.
[62] A. H. Schmidt, M. Russ, *Chem. Ber.* **1981**, *114*, 1099–1110.
[63] C. Jammegg, S. Graschy, E. Hengge, *Organometallics* **1994**, *13*, 2397–2400.
[64] D. R. Weyenberg, A. E. Bey, P. J. Ellison, *J. Organomet. Chem.* **1965**, *3*, 489–492.
[65] L. G. Mahone, D. R. Weyenberg, *J. Organomet. Chem.* **1968**, *12*, 231–233.
[66] K. Moedritzer, J. R. Van Wazer, *J. Organomet. Chem.* **1968**, *12*, 69–77.
[67] C. Grogger, B. Loidl, H. Stueger, T. Kammel, B. Pachaly, *J. Organomet. Chem.* **2006**, *691*, 105–110.
[68] F. C. Whitmore, E. W. Pietrusza, L. H. Sommer, *J. Am. Chem. Soc.* **1947**, *69*, 2108–2110.
[69] J. Ke, W. Liu, X. Zhu, X. Tan, C. He, *Angew. Chem. Int. Ed.* **2021**, *60*, 8744–8749; *Angew. Chem.* **2021**, *133*, 8826–8831.
[70] A. D. Beck, S. Haufe, S. R. Waldvogel, *ChemElectroChem* **2022**, *9*, e202200840.
[71] Y. Kimata, H. Suzuki, S. Satoh, A. Kuriyama, *Organometallics* **1995**, *14*, 2506–2511.
[72] P. Han, M. Yin, H. Li, J. Yi, L. Jing, B. Wei, *Adv. Synth. Catal.* **2021**, *363*, 2757–2761.
[73] Y. Kogai, M. Ishifune, K. Uchida, S. Kashimura, *Electrochemistry* **2005**, *73*, 419–423.
[74] B. K. Peters, K. X. Rodriguez, S. H. Reisberg, S. B. Beil, D. P. Hickey, Y. Kawamata, M. Collins, J. Starr, L. Chen, S. Udyavara, K. Klunder, T. J. Gorey, S. L. Anderson, M. Neurock, S. D. Minteer, P. S. Baran, *Science* **2019**, *363*, 838–845.
[75] T. S. Daloee, F. K. Behbahani, *Mol. Diversity* **2020**, *24*, 463–476.
[76] E. Hengge, Ch. Jammegg, in *Organosilicon Chemistry I*, John Wiley & Sons, Ltd, **2008**, 27–29.
[77] X. Dong, J. L. Roeckl, S. R. Waldvogel, B. Morandi, *Science* **2021**, *371*, 507–514.
[78] A. Popp, R. Weidner, H. Stüger, C. Grogger, B. Loidl (Consortium für elektrochemische Industrie GmbH), DE 10 2004 029 258 A1, **2004**.
[79] A. Kunai, T. Kawakami, E. Toyoda, M. Ishikawa, *Organometallics* **1991**, *10*, 893–895.
[80] M. Umezawa, H. Ichikawa, T. Ishikawa, T. Nonaka, *Denki Kagaku (1961-1998)* **1991**, *59*, 421–426.
[81] E. Hengge, H. Firgoi, *J. Organomet. Chem.* **1981**, *212*, 155–161.
[82] P. Pons, C. Biran, M. Bordeau, J. Dunoguès, *J. Organomet. Chem.* **1988**, *358*, 31–37.
[83] C. Moreau, F. Serein-Spirau, C. Biran, M. Bordeau, P. Gerval, *Organometallics* **1998**, *17*, 2797–2804.
[84] C. Moreau, F. Serein-Spirau, M. Bordeau, C. Biran, J. Dunoguès, *J. Organomet. Chem.* **1996**, *522*, 213–221.
[85] T. Shono, S. Kashimura, M. Ishifune, R. Nishida, *J. Chem. Soc. Chem. Commun.* **1990**, ■■Dear author, if the journal has volumes, please add the journal number■■, 1160–1161.
[86] T. Shono, S. Kashimura, H. Murase, *J. Chem. Soc. Chem. Commun.* **1992**, ■■Dear author, if the journal has volumes, please add the journal number■■, 896–897.
[87] M. Ishifune, Y. Kogai, H. Iijima, Y. Kera, N. Yamashita, S. Kashimura, *Electrochemistry* **2004**, *72*, 159–164.
[88] L. Lu, J. C. Siu, Y. Lai, S. Lin, *J. Am. Chem. Soc.* **2020**, *142*, 21272–21278.
[89] T. Ohno, H. Nakahiro, K. Sanemitsu, T. Hirashima, I. Nishiguchi, *Tetrahedron Lett.* **1992**, *33*, 5515–5516.
[90] C. Duprat, C. Biran, M. Bordeau, T. Constantieux, P. Gerval, J. Dunoguès, *J. Chem. Soc. Chem. Commun.* **1995**, ■■Dear author, if the journal has volumes, please add the journal number■■, 2107.
[91] M. Bordeau, C. Biran, M.-P. Léger-Lambert, J. Dunoguès, *J. Chem. Soc. Chem. Commun.* **1991**, 1476–1477.
[92] B. I. Martynov, A. A. Stepanov, *J. Fluorine Chem.* **1997**, *85*, 127–128.
[93] L. A. Vermeulen, K. Smith, J. Wang, *Electrochim. Acta* **1999**, *45*, 1007–1014.
[94] A. Kunai, T. Kawakami, E. Toyoda, M. Ishikawa, *Organometallics* **1991**, *10*, 2001–2003.
[95] A. Kunai, T. Ueda, E. Toyoda, M. Ishikawa, *Bull. Chem. Soc. Jpn.* **1994**, *67*, 287–289.
[96] E. Hengge, G. Litscher, *Angew. Chem. Int. Ed.* **1976**, *15*, 370; *Angew. Chem.* **1976**, *88*, 414.
[97] E. Hengge, G. Litscher, *Monatsh. Chem.* **1978**, *109*, 1217–1225.
[98] D. R. Lide, *CRC Handbook of Chemistry and Physics*, CRC Press, Boca Raton, FL, **2005**.
[99] C. Moreau, F. Serein-Spirau, M. Bordeau, C. Biran, *Organometallics* **2001**, *20*, 1910–1917.
[100] A. Palma, B. A. Frontana-Uribe, J. Cárdenas, M. Saloma, *Electrochem. Commun.* **2003**, *5*, 455–459.
[101] a) S. Ardizzone, G. Cappelletti, P. R. Mussini, S. Rondinini, L. M. Doubova, *J. Organomet. Chem.* **2002**, *532*, 285–293; b) C. Durante, A. A. Isse, G. Sandonà, A. Gennaro, *Appl. Catal. B* **2009**, *88*, 479–489; c) L. Falciola, A. Gennaro, A. A. Isse, P. R. Mussini, M. Rossi, *J. Organomet. Chem.* **2006**, *593*, 47–56; d) A. A. Isse, G. Berzi, L. Falciola, M. Rossi, P. R. Mussini, A. Gennaro, *J. Appl. Electrochem.* **2009**, *39*, 2217–2225.
[102] a) P. Poizot, J. Simonet, *Electrochim. Acta* **2010**, *56*, 15–36; b) S. Rondinini, C. Locatelli, A. Minguzzi, A. Vertova, *Electrochemical Water and Wastewater Treatment. Chapter 1 - Electroreduction*, Butterworth-Heinemann, **2018**; c) M. Zhang, Q. Shi, X. Song, H. Wang, Z. Bian, *Environ. Sci. Pollut. Res. Int.* **2019**, *26*, 10457–10486.
[103] a) C. Biran, M. Bordeau, D. Bonafoux, D. Deffieux, C. Duprat, V. Jouikov, M. P. Léger-Lambert, C. Moreau, F. Serein-Spirau, *J. Chim. Phys.* **1996**, *93*, 591–600; b) W. G. Boberski, A. L. Allred, *J. Organomet. Chem.* **1975**, *88*, 65–72.
[104] V. Jouikov, L. Grigorieva, *Electrochim. Acta* **1996**, *41*, 2489–2491.
[105] J. Gobet, H. Tannenberger, *J. Electrochem. Soc.* **1988**, *135*, 109–112.
[106] V. Jouikov, G. Salaheev, *Electrochim. Acta* **1996**, *41*, 2623–2629.
[107] M. Hoddenbagh, D. Foucher, D. Worsfold, *Electrochemical Studies of Chlorine Containing Silanes*, ChemRxiv, Cambridge: Cambridge Open Engage, **2021**.
[108] T. Shono, H. Ohmizu, S. Kawakami, H. Sugiyama, *Tetrahedron Lett.* **1980**, *21*, 5029–5032.
[109] X. Wang, Y. Yuan, I. Cabasso, *J. Electrochem. Soc.* **2005**, *152*, E259–E264.
[110] R. Corriu, G. Dabosi, M. Martineau, *J. Organomet. Chem.* **1980**, *188*, 63–72.
[111] A. K. Agrawal, A. E. Austin, *J. Electrochem. Soc.* **1981**, *128*, 2292–2296.
[112] a) G. Martin, *J. Chem. Soc. Trans.* **1914**, *105*, 2836–2860; b) Y. Nishimura, Y. Fukunaka, *Electrochim. Acta* **2007**, *53*, 111–116.
[113] Y. Nishimura, Y. Fukunaka, T. Nohira, R. Hagiwara, *ECS Trans.* **2008**, *11*, 13–24.
[114] A. H. Holm, T. Brinck, K. Daasbjerg, *J. Am. Chem. Soc.* **2005**, *127*, 2677–2685.
[115] V. V. Zhuikov, *Russ. J. Electrochem.* **2000**, *36*, 117–127.
[116] M. Bordeau, C. Biran, P. Pons, M. P. Leger-Lambert, J. Dunogues, *J. Org. Chem.* **1992**, *57*, 4705–4711.
[117] V. Jouikov, V. Krasnov, *J. Organomet. Chem.* **1995**, *498*, 213–219.
[118] M. Oestreich, *Angew. Chem. Int. Ed.* **2016**, *55*, 494–499; *Angew. Chem.* **2016**, *128*, 504–509.
[119] R. Nishida, S. Kawasaki, H. Murase (Osaka Gas Co., Ltd.), EP 0671487 B1, **1995**.
[120] S. Kashiwamura, R. Nishida, T. Shono (Osaka Gas Co., Ltd.), JP 3264683 A2, **1991**.

ChemElectroChem | Review | doi.org/10.1002/celc.202201149 | Chemistry Europe | European Chemical Societies Publishing

[121] E. Hengge, C. Jammegg, W. Kalchauer (Wacker Chemie GmbH), EP 0629718 A1, **1994**.
[122] P. Boudjouk, B. H. Han, K. R. Anderson, *J. Am. Chem. Soc.* **1982**, *104*, 4992–4993.
[123] S. Kashimura, M. Ishifune, H.-B. Bu, M. Takebayashi, S. Kitajima, D. Yoshihara, R. Nishida, S. Kawasaki, H. Murase, T. Shono, *Tetrahedron Lett.* **1997**, *38*, 4607–4610.
[124] A. Mavrič, A. Badasyan, G. Mali, M. Valant, *Eur. Polym. J.* **2017**, *90*, 162–170.
[125] T. Kugita, D. Ohtani, M. Okano, K. Mochida, *Denki Kagaku (1961-1998)* **1994**, 522–523.
[126] M. Ishifune, S. Kashimura, Y. Kogai, Y. Fukuhara, T. Kato, H.-B. Bu, N. Yamashita, Y. Murai, H. Murase, R. Nishida, *J. Organomet. Chem.* **2000**, *611*, 26–31.
[127] M. Umezawa, M. Takeda, H. Ichikawa, T. Ishikawa, T. Koizumi, T. Fuchigami, T. Nonaka, *Electrochim. Acta* **1990**, *35*, 1867–1872.
[128] a) T. Fujiki, M. Ishifune, S. Kashiwamura, S. Kawasaki, H. Murase, H. Sakamoto (Osaka Gas Co., Ltd.), JP 2006188620 A2, **2006**; b) R. Nishida, S. Kawasaki, H. Murase (Osaka Gas Co., Ltd.), EP 0673960 A1, **1995**.
[129] T. Shono, S. Kashimura, R. Nishida, S. Kawasaki (Osaka Gas Co., Ltd.), EP 0558760 B1, **1993**.
[130] S. Kawasaki, H. Murase, R. Nishida (Osaka Gas Co., Ltd.), JP 3692434 B2, **2005**.
[131] T. Shono, S. Kashimura, R. Nishida, S. Kawasaki (Osaka Gas Co., Ltd.), EP 0446578 A2, **1991**.
[132] S. Kamio, T. Imagawa, M. Nakamoto, M. Oestreich, H. Yoshida, *Synthesis* **2021**, *53*, 4678–4681.
[133] a) M. Elangovan, A. Muthukumaran, M. Anbu Kulandainathan, *Eur. Polym. J.* **2005**, *41*, 2450–2460; b) K. Jian, C. Shao, H. Wang, J. Wang, Y. Wu, Z. Xie (National Defense Univ. of Science and Technology), CN 106245056A, **2016**.
[134] M. Ishifune, Y. Kogai, H. Iijima, Y. Kera, N. Yamashita, S. Kashimura, *J. Macromol. Sci. Part A: Pure Appl.Chem.* **2004**, *41*, 373–386.
[135] M. Okano, H. Fukai, M. Arakawa, H. Hamano, *Electrochem. Commun.* **1999**, *1*, 223–226.
[136] M. Okano, K. Nakamura, K. Yamada, N. Hosoda, M. Wasaka, *Electrochemistry* **2006**, *74*, 956–958.
[137] A. Watanabe, T. Komatsubara, M. Matsuda, Y. Yoshida, S. Tagawa, *J. Photopolym. Sci. Technol.* **1992**, *5*, 545–546.
[138] a) N. Downes, Q. Cheek, S. Maldonado, *J. Electrochem. Soc.* **2021**, *168*, 22503; b) Q. P. Ma, W. Liu, B. C. Wang, Q. S. Meng, *Adv. Mater. Res.* **2009**, *79–82*, 1635–1638; c) T. Munisamy, A. J. Bard, *Electrochim. Acta* **2010**, *55*, 3797–3803; d) Y. Tsuyuki, T. Fujimura, M. Kunimoto, Y. Fukunaka, P. Pianetta, T. Homma, *J. Electrochem. Soc.* **2017**, *164*, D994–D998.
[139] D. Deffieux, M. Bordeau, C. Biran, J. Dunogues, *Organometallics* **1994**, *13*, 2415–2422.
[140] M. Bordeau, P. Clavel, A. Barba, M. Berlande, C. Biran, N. Roques, *Tetrahedron Lett.* **2003**, *44*, 3741–3744.
[141] a) S. Durandetti, S. Sibille, J. Perichon, *J. Org. Chem.* **1989**, *54*, 2198–2204; b) S. Sibille, E. d'Incan, L. Leport, M.-C. Massebiau, J. Perichon, *Tetrahedron Lett.* **1987**, *28*, 55–58.
[142] M. Dieng, J. Simonet, V. Jouikov, *Electrochem. Commun.* **2015**, *53*, 33–36.
[143] M. Dieng, D. Gningue-Sall, V. Jouikov, *Main Group Met. Chem.* **2012**, *35*, 141–151.
[144] K. Inoue, H. Miyagawa, M. Murakami, N. Yanagawa (Mitsui Toatsu Chemicals), JP63250484 A2, **1988**.
[145] D. S. Fattakhova, V. V. Jouikov, M. G. Voronkov, *J. Organomet. Chem.* **2000**, *613*, 170–176.
[146] B. Martiz, R. Keyrouz, S. Gmouh, M. Vaultier, V. Jouikov, *Chem. Commun.* **2004**, 674–675.
[147] V. Jouikov, R. Keyrouz, *Silicon Chem.* **2003**, *2*, 141–146.
[148] R. Keyrouz, V. Jouikov, *New J. Chem.* **2003**, *27*, 902–904.
[149] K. N. Singh, S. Neuhold, C. Grogger, V. V. Jouikov, *Russ. J. Electrochem.* **2007**, *43*, 1170–1174.
[150] D. Bonafoux, M. Bordeau, C. Biran, J. Dunoguès, *J. Organomet. Chem.* **1995**, *493*, 27–32.
[151] M. Kimamura, H. Yamagishi, Y. Sawaki, *Denki Kagaku (1961-1998)* **1994**, *62*, 1119–1124.
[152] S. Neuhold, J. Albering, M. Flock, C. Grogger, *ECS Trans.* **2009**, *19*, 39–41.
[153] C. Grogger, H. Fallmann, G. Fürpaß, H. Stüger, G. Kickelbick, *J. Organomet. Chem.* **2003**, *665*, 186–195.
[154] J. Ruiz, F. Serein-Spirau, P. Atkins, D. Astruc, *C. R. Acad. Sci. Ser. IIb: Mec. Phys. Chim. Astron.* **1996**, *323*, 851–857.
[155] H. Liang, L.-J. Wang, Y.-X. Ji, H. Wang, B. Zhang, *Angew. Chem. Int. Ed.* **2021**, *60*, 1839–1844; *Angew. Chem.* **2021**, *133*, 1867–1872.
[156] H. F. T. Klare, L. Albers, L. Süsse, S. Keess, T. Müller, M. Oestreich, *Chem. Rev.* **2021**, *121*, 5889–5985.
[157] a) S. Coseri, *Catal. Rev.* **2009**, *51*, 218–292; b) R. Francke, R. D. Little, *Chem. Soc. Rev.* **2014**, *43*, 2492–2521; c) F. Wang, S. S. Stahl, *Acc. Chem. Res.* **2020**, *53*, 561–574.
[158] a) H. Fang, M. Oestreich, *Chem. Sci.* **2020**, *11*, 12604–12615; b) H. Fang, M. Oestreich, *Angew. Chem. Int. Ed.* **2020**, *59*, 11394–11398; *Angew. Chem.* **2020**, *132*, 11491–11495; c) H. Fang, G. Wang, M. Oestreich, *Org. Chem. Front.* **2021**, *8*, 3280–3285; d) H. Fang, K. Xie, S. Kemper, M. Oestreich, *Angew. Chem. Int. Ed.* **2021**, *60*, 8542–8546; *Angew. Chem.* **2021**, *133*, 8624–8628; e) H. F. T. Klare, M. Oestreich, *Dalton Trans.* **2010**, *39*, 9176–9184; f) P.-W. Long, T. He, M. Oestreich, *Org. Lett.* **2020**, *22*, 7383–7386; g) T. Robert, M. Oestreich, *Angew. Chem. Int. Ed.* **2013**, *52*, 5216–5218; h) A. Roy, M. Oestreich, *Chem. Eur. J.* **2021**, *27*, 8273–8276; i) J. C. L. Walker, H. F. T. Klare, M. Oestreich, *Nat. Rev. Chem.* **2020**, *4*, 54–62.
[159] D. J. Parks, J. M. Blackwell, W. E. Piers, *J. Org. Chem.* **2000**, *65*, 3090–3098.
[160] J. M. Blackwell, E. R. Sonmor, T. Scoccitti, W. E. Piers, *Org. Lett.* **2000**, *2*, 3921–3923.
[161] W. E. Piers, A. J. V. Marwitz, L. G. Mercier, *Inorg. Chem.* **2011**, *50*, 12252–12262.
[162] E. J. Lawrence, V. S. Oganesyan, D. L. Hughes, A. E. Ashley, G. G. Wildgoose, *J. Am. Chem. Soc.* **2014**, *136*, 6031–6036.
[163] Y. Kimata, H. Suzuki, S. Satoh, A. Kuriyama, *Chem. Lett.* **1994**, *23*, 1163–1164.
[164] A. Diaz, R. D. Miller, *J. Electrochem. Soc.* **1985**, *132*, 834–837.
[165] a) C.-C. Chang, T.-K. Chen, *J. Power Sources* **2009**, *193*, 834–840; b) C.-C. Chang, T.-K. Chen, L.-J. Her, G. T.-K. Fey, *J. Electrochem. Soc.* **2009**, *156*, A828–A832; c) G.-B. Han, J.-N. Lee, J. W. Choi, J.-K. Park, *Electrochim. Acta* **2011**, *56*, 8997–9003; d) E. J. Lawrence, V. S. Oganesyan, G. G. Wildgoose, A. E. Ashley, *Dalton Trans.* **2013**, *42*, 782–789; e) Y. M. Lee, J. E. Seo, N.-S. Choi, J.-K. Park, *Electrochim. Acta* **2005**, *50*, 2843–2848.
[166] N. T. Berberova, *Russ. J. Electrochem.* **2000**, *36*, 174–182.
[167] T. Biremond, P. Jubault, T. Poisson, *ACS Org. Inorg. Au* **2022**, *2*, 148–152.
[168] S. Bähr, M. Oestreich, *Angew. Chem. Int. Ed.* **2017**, *56*, 52–59; *Angew. Chem.* **2017**, *129*, 52–59.
[169] T. Nohira, Y. Ito, *Electrochemistry* **1999**, *67*, 635–642.
[170] K. Okamoto, S. Nagahara, Y. Imada, R. Narita, Y. Kitano, K. Chiba, *J. Org. Chem.* **2021**, *86*, 15992–16000.
[171] J. Yoshida, T. Murata, S. Isoe, *Tetrahedron Lett.* **1986**, *27*, 3373–3376.
[172] J. Y. Becker, E. Shakkour, R. West, *Tetrahedron Lett.* **1992**, *33*, 5633–5636.

Manuscript received: December 17, 2022
Revised manuscript received: January 6, 2023

1.2 Tris(pentafluorphenyl)boran $B(C_6F_5)_3$

Die Darstellung und Beschreibung von Tris(pentafluorphenyl)boran, $B(C_6F_5)_3$, durch MASSEY, PARK und STONE geht zurück auf das Jahr 1963.[1] Nach dieser Entdeckung mussten jedoch Jahrzehnte vergehen, bevor es zu einer Renaissance dieses Moleküls kam. Die außerordentlichen aktivierenden Eigenschaften für homogene Metallocen-ZIEGLER-NATTA-Katalysatoren im Bereich der Olefinpolymerisation[2] waren Auslöser des steigenden wissenschaftlichen Interesses und so wurde $B(C_6F_5)_3$ in den nachfolgenden Jahren zum Gegenstand zahlreicher Anwendungen in der organischen[3,4] und anorganischen Chemie[5]. Bei $B(C_6F_5)_3$ handelt es sich um einen thermisch stabilen Feststoff, dessen Lewis-Acidität vergleichbar ist mit BF_3 und BCl_3.[6] Im Vergleich zu den genannten Borhalogeniden ist die Handhabung jedoch einfach und sicher. Zusätzlich weist $B(C_6F_5)_3$ einen hohen sterischen Bedarf auf, sodass es trotz der entsprechenden Lewis-Acidität nicht in der Lage ist, dative Bindungen in Säure-Base-Addukten zu bilden.[7] Dieses Phänomen wird auch als "frustrierte Lewis-Paar"-Chemie (FLP) bezeichnet, und führte in den letzten Jahren zu neuartigen Reaktionswegen und -möglichkeiten, wie der Aktivierung kleiner Moleküle, unter anderem H_2,[7,8,9,10,11] CO,[7,8,11,12] CO_2,[7,8,11,13] N_2O[7,11,14,15] und SO_2[7,11,16] (Schema 3).

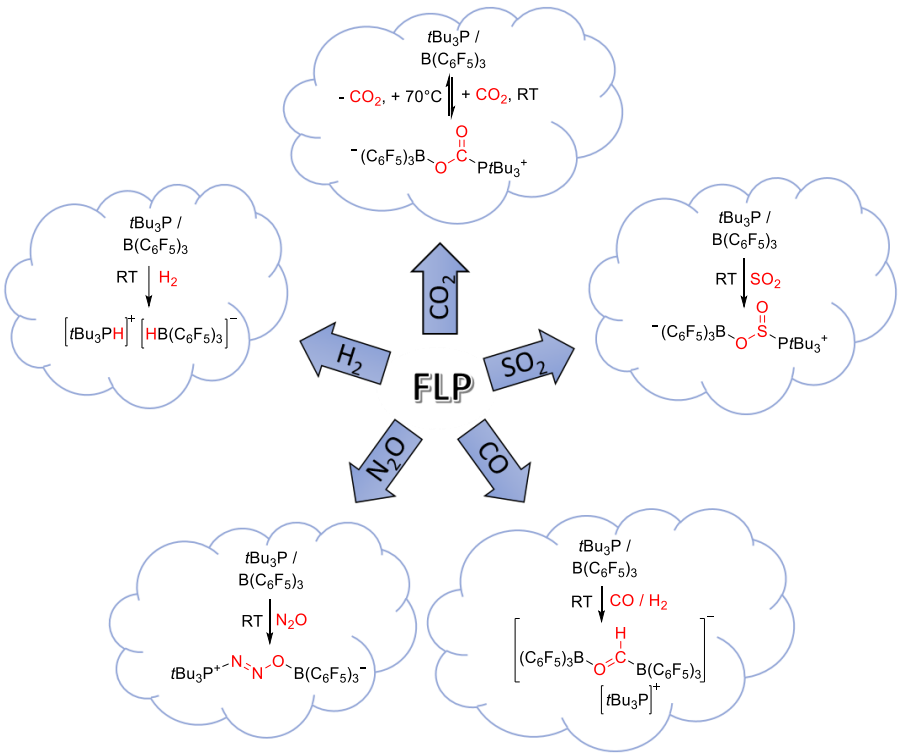

Schema 3. Aktivierung kleiner Moleküle durch die FLP Chemie basierend auf Lewis-aciden Boranen.[7,8,10,11,14–16]

Darüber hinaus ist auch die Aktivierung der Si-H-Bindung von Hydrosilanen mit $B(C_6F_5)_3$ möglich. Im Gegensatz zur üblichen Aktivierung durch Lewis-saure Substrate, wird hier jedoch nicht die Carbonylgruppe koordiniert. Während herkömmliche Lewis-Säuren durch Koordination am Carbonyl-Sauerstoff die C=O-Doppelbindung polarisieren und damit ein hoch elektrophiles Kohlenstoffatom erzeugen, führt $B(C_6F_5)_3$ **I** zur Bildung eines Addukts mit dem Hydrosilan. Durch teilweise Abstraktion des Hydrids kann es so zu dem hoch reaktiven Intermediat **II** kommen. Hier stehen das Addukt mit elongierter Si-H-Bindung und das Hydridoboran-stabilisierte Silylkation im Gleichgewicht (Schema 4).[17–19] Ein anschließender nukleophiler Angriff durch ein Carbonyl-Sauerstoff am elektropositiven Siliziumzentrum erzeugt das Hydridoboran-stabilisierte Ionenpaar **III**. Unter Hydrid-Transfer und Freisetzung der Silyletherspezies wird $B(C_6F_5)_3$ regeneriert und der katalytische Zyklus geschlossen.

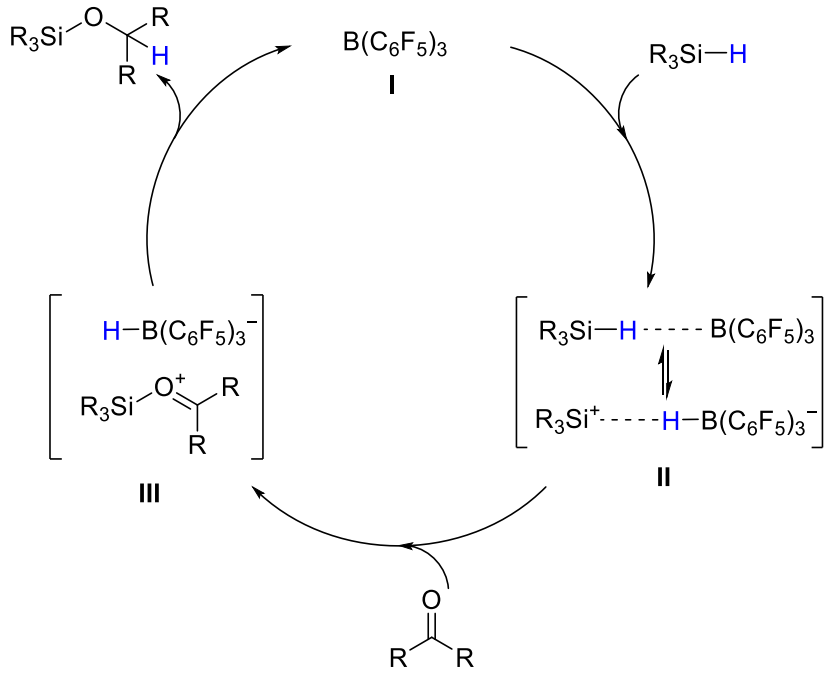

Schema 4. Aktivierung von Hydrosilanen durch $B(C_6F_5)_3$ und anschließende Hydrosilylierung von Carbonylverbindungen mit Regenerierung von $B(C_6F_5)_3$.[17,19,20,21]

Die Möglichkeit einer metallfreien Hydrosilan-Aktivierung durch $B(C_6F_5)_3$ hat in den vergangenen 20 Jahren für großes Aufsehen gesorgt, was eine breite Untersuchung synthetischer Routen initiiert hat. Durch den kommerziellen Zugang zu $B(C_6F_5)_3$ hat sich der Anwendungsbereich stark erweitert und eine Vielzahl katalytischer, Silan-basierter Umwandlungen konnte realisiert werden. Dazu zählen insbesondere die Silylierung von Alkoholen[22] und die Hydrosilylierung von Aldehyden,[23] Alkenen,[24,25]

Alkinen,[25] Enolen,[26] Estern,[23] Iminen,[18,21,27] und Ketonen.[21,23,28] Auch die Chlorierung von Hydrosilanen zu entsprechenden Chlorsilanen[29] sowie die Desoxygenierung von Alkoholen[3,30] und Carbonylverbindungen[30] wurden beleuchtet und tragen damit zum breiten Spektrum synthetischer Anwendungen bei.

In jüngster Zeit hat sich $B(C_6F_5)_3$ neben dem Feld der organischen Chemie auch auf dem Gebiet der Elektrochemie etabliert. Untersuchungen zum Reduktionspotential von $B(C_6F_5)_3$ standen im Mittelpunkt dieser Forschungen.[31,32] Die Messung des Reduktionspotentials von $B(C_6F_5)_3$ ist jedoch herausfordernd, sodass zuerst Versuche mit analogen Verbindungen, wie $MesB(C_6F_5)_3$ durchgeführt wurden, um das Potential zum ein-Elektronen-Übertrag abzuschätzen.[31] WILDGOOSE und Mitarbeiter[32] konnten später durch Verwendung eines $B(C_6F_5)_4^-$ haltigen Elektrolyten zeigen, dass das Reduktionspotential von $B(C_6F_5)_3$ bei −1.41 V vs. SCE in Dichlormethan liegt. Stärker komplexierende Anionen, wie Perchlorat führen zur teilweisen Deaktivierung von $B(C_6F_5)_3$, was die elektrochemische Untersuchung erschwert.[32,33] So konnte in bisherigen Studien gezeigt werden, dass durch die Verwendung von $B(C_6F_5)_3$ als Anionenrezeptor in Lithium-Ionen-Batterien die Festkörper-Elektrolyt-Interphase (SEI) stabilisiert werden kann[34] und die Zersetzung des Elektrolyten dadurch verhindert wird.[35] Auch erste elektrosynthetische Aspekte, insbesondere im Hinblick auf die Aktivierung von Wasserstoff[36,37] wurden beleuchtet, die eine Absenkung des Oxidationspotentials von H_2 um 910 mV[37] zeigen. Während sich das Potential von $B(C_6F_5)_3$ auch im Bereich der elektrochemischen Synthese demonstrieren lässt, steht möglichen Anwendungen noch ein weites Feld offen.

[1] a) A. G. Massey, A. J. Park, *J. Organomet. Chem.* **1964**, *2*, 245–250; b) A. G. Massey, A. J. Park, F. G. A. Stone, *Proc. Chem. Soc.* **1963**, *212*.

[2] a) T. J. Marks, *Acc. Chem. Res.* **1992**, *25*, 57–65; b) X. Yang, C. L. Stern, T. J. Marks, *J. Am. Chem. Soc.* **1994**, *116*, 10015–10031.

[3] V. Gevorgyan, M. Rubin, S. Benson, J.-X. Liu, Y. Yamamoto, *J. Org. Chem.* **2000**, *65*, 6179–6186.

[4] a) V. Gevorgyan, J.-X. Liu, Y. Yamamoto, *Chem. Commun.* **1998**, 37–38; b) R. L. Melen, *Chem. Commun.* **2014**, *50*, 1161–1174; c) D. J. Morrison, J. M. Blackwell, W. E. Piers, *Pure Appl. Chem.* **2004**, *76*, 615–623; d) D. J. Morrison, W. E. Piers, *Org. Lett.* **2003**, *5*, 2857–2860.

[5] a) A. Bernsdorf, H. Brand, R. Hellmann, M. Köckerling, A. Schulz, A. Villinger, K. Voss, *J. Am. Chem. Soc.* **2009**, *131*, 8958–8970; b) I. Krossing, I. Raabe, *Angew. Chem., Int. Ed.* **2004**, *43*, 2066–2090; *Angew. Chem.*, **2004**, *116*, 2116–2142; c) S. J. Lancaster, A. Rodriguez, A. Lara-Sanchez, M. D. Hannant, D. A. Walker, D. H. Hughes, M. Bochmann, *Organometallics* **2002**, *21*, 451–453; d) R. E. LaPointe, G. R. Roof, K. A. Abboud, J. Klosin, *J. Am. Chem. Soc.* **2000**, *122*, 9560–9561.

[6] a) M. A. Beckett, D. S. Brassington, S. J. Coles, M. B. Hursthouse, *Inorg. Chem. Commun.* **2000**, *3*, 530–533; b) H. Jacobsen, H. Berke, S. Döring, G. Kehr, G. Erker, R. Fröhlich, O. Meyer, *Organometallics* **1999**, *18*, 1724–1735.

[7] D. W. Stephan, G. Erker, *Angew. Chem., Int. Ed.* **2015**, *54*, 6400–6441; *Angew. Chem.*, **2015**, *127*, 6498–6541.

[8] D. W. Stephan, *Science* **2016**, *354*.

[9] a) L. Greb, P. Oña-Burgos, B. Schirmer, S. Grimme, D. W. Stephan, J. Paradies, *Angew. Chem., Int. Ed.* **2012**, *51*, 10164–10168; *Angew. Chem.*, **2012**, *124*, 10311–10315; b) G. C. Welch, D. W. Stephan, *J. Am. Chem. Soc.* **2007**, *129*, 1880–1881.

[10] D. W. Stephan, G. Erker, *Angew. Chem., Int. Ed.* **2010**, *49*, 46–76; *Angew. Chem.*, **2010**, *122*, 50–81.

[11] D. W. Stephan, G. Erker, *Chem. Sci.* **2014**, *5*, 2625–2641.

[12] R. Dobrovetsky, D. W. Stephan, *J. Am. Chem. Soc.* **2013**, *135*, 4974–4977.

[13] C. M. Mömming, E. Otten, G. Kehr, R. Fröhlich, S. Grimme, D. W. Stephan, G. Erker, *Angew. Chem., Int. Ed.* **2009**, *48*, 6643–6646; *Angew. Chem.*, **2009**, *121*, 6770–6773.

[14] E. Otten, R. C. Neu, D. W. Stephan, *J. Am. Chem. Soc.* **2009**, *131*, 9918–9919.

[15] E. Theuergarten, T. Bannenberg, M. D. Walter, D. Holschumacher, M. Freytag, C. G. Daniliuc, P. G. Jones, M. Tamm, *Dalton Trans.* **2014**, *43*, 1651–1662.

[16] M. Sajid, A. Klose, B. Birkmann, L. Liang, B. Schirmer, T. Wiegand, H. Eckert, A. J. Lough, R. Fröhlich, C. G. Daniliuc, S. Grimme, D. W. Stephan, G. Kehr, G. Erker, *Chem. Sci.* **2013**, *4*, 213–219.

[17] D. J. Parks, J. M. Blackwell, W. E. Piers, *J. Org. Chem.* **2000**, *65*, 3090–3098.

[18] J. M. Blackwell, E. R. Sonmor, T. Scoccitti, W. E. Piers, *Org. Lett.* **2000**, *2*, 3921–3923.

[19] W. E. Piers, A. J. V. Marwitz, L. G. Mercier, *Inorg. Chem.* **2011**, *50*, 12252–12262.

[20] a) T. Hackel, N. A. McGrath, *Molecules* **2019**, *24*, 432; b) A. Y. Houghton, J. Hurmalainen, A. Mansikkamäki, W. E. Piers, H. M. Tuononen, *Nat. Chem.* **2014**, *6*, 983–988.

[21] D. T. Hog, M. Oestreich, *Eur. J. Org. Chem.* **2009**, *2009*, 5047–5056.

[22] J. M. Blackwell, K. L. Foster, V. H. Beck, W. E. Piers, *J. Org. Chem.* **1999**, *64*, 4887–4892.

[23] D. J. Parks, W. E. Piers, *J. Am. Chem. Soc.* **1996**, *118*, 9440–9441.

[24] M. Rubin, T. Schwier, V. Gevorgyan, *J. Org. Chem.* **2002**, *67*, 1936–1940.

[25] W. Yuan, P. Smirnov, M. Oestreich, *Chem* **2018**, *4*, 1443–1450.

[26] J. M. Blackwell, D. J. Morrison, W. E. Piers, *Tetrahedron* **2002**, *58*, 8247–8254.

[27] a) J. Hermeke, M. Mewald, M. Oestreich, *J. Am. Chem. Soc.* **2013**, *135*, 17537–17546; b) K. Müther, J. Mohr, M. Oestreich, *Organometallics* **2013**, *32*, 6643–6646.

[28] S. Rendler, M. Oestreich, *Angew. Chem., Int. Ed.* **2008**, *47*, 5997–6000; *Angew. Chem.*, **2008**, *120*, 6086–6089.

[29] K. Chulsky, R. Dobrovetsky, *Angew. Chem., Int. Ed.* **2017**, *56*, 4744–4748; *Angew. Chem.*, **2017**, *129*, 4822–4826.

[30] W. Yang, L. Gao, J. Lu, Z. Song, *Chem. Commun.* **2018**, *54*, 4834–4837.

[31] S. A. Cummings, M. Iimura, C. J. Harlan, R. J. Kwaan, I. V. Trieu, J. R. Norton, B. M. Bridgewater, F. Jäkle, A. Sundararaman, M. Tilset, *Organometallics* **2006**, *25*, 1565–1568.

[32] E. J. Lawrence, V. S. Oganesyan, G. G. Wildgoose, A. E. Ashley, *Dalton Trans.* **2013**, *42*, 782–789.

[33] Y. M. Lee, J. E. Seo, N.-S. Choi, J.-K. Park, *Electrochim. Acta* **2005**, *50*, 2843–2848.

[34] G.-B. Han, J.-N. Lee, J. W. Choi, J.-K. Park, *Electrochim. Acta* **2011**, *56*, 8997–9003.

[35] a) C.-C. Chang, T.-K. Chen, *J. Power Sources* **2009**, *193*, 834–840; b) C.-C. Chang, T.-K. Chen, L.-J. Her, G. T.-K. Fey, *J. Electrochem. Soc.* **2009**, *156*, A828-A832.

[36] E. J. Lawrence, V. S. Oganesyan, D. L. Hughes, A. E. Ashley, G. G. Wildgoose, *J. Am. Chem. Soc.* **2014**, *136*, 6031–6036.

[37] E. J. Lawrence, T. J. Herrington, A. E. Ashley, G. G. Wildgoose, *Angew. Chem., Int. Ed.* **2014**, *53*, 9922–9925; *Angew. Chem.*, **2014**, *126*, 10080–10083.

1.3 Polysiloxane

Im Jahr 1901 entdeckte F. S. KIPPING unbeabsichtigt die erste Syntheseroute von Silikonen auf seinem ursprünglichen Ziel, der Darstellung einer Si=O-Doppelbindung.[1] Der Begriff „Silikon“, in Anlehnung an „Polysilicoketon“, leitet sich hierbei von der allgemeinen Formel einfacher linearer Strukturen $(R_2SiO)_n$ zu analogen Verbindungen mit C=O-Doppelbindung ab. Die damalige Betrachtung als diskrete R_2SiO Moleküle stellt so einen formalen Zusammenhang mit Ketonen $R_2C=O$ her.[2] Im wissenschaftlichen Sprachgebrauch ist die Struktureinheit Si-O-Si jedoch treffender als Siloxan zu bezeichnen, bzw. entsprechend als Polysiloxan. „Silikon“ beschreibt im Alltag hauptsächlich eine technische Anwendung.

Nach der Entdeckung durch KIPPING mussten jedoch Jahrzehnte vergehen,[3] ehe das Potential von Siloxanen erkannt und genutzt wurde.[4] Erst das Aufkommen des MÜLLER-ROCHOW-Prozesses,[5] der den industriellen Zugang zu Chlorsilanen als essentielles Zwischenprodukt ermöglichte, initiierte den rasanten Aufschwung der Silikonindustrie.[6] Polysiloxane haben sich seither in einem breiten Produktspektrum etabliert. Von Alltagsgegenständen bis hin zu industriellen Einsatzbereichen werden Polysiloxane verwendet. Das Produktionsvolumen hat seit ihrer Entdeckung nahezu kontinuierlich zugenommen und überstieg im Jahr 2020 weltweit 6.7 Megatonnen,[7] was auf die speziellen Eigenschaften von Polysiloxanen aufgrund der Si-O-Bindung zurückzuführen ist.[8] Diese sind insbesondere gutes dielektrisches Verhalten,[9] hohe thermische und oxidative Stabilität sowie ein hydrophober Charakter.[10–13] Die geringe Änderung der physikalischen Eigenschaften über weite Temperaturbereiche, niedrige Glasübergangstemperaturen und hohe Gasdurchlässigkeit, sind dabei auf die hohe Flexibilität der Polysiloxankette zurückzuführen .[14,15] Diese wird durch die längere Si-O-Bindung im Vergleich zu C-O-Bindungen, in Kombination mit einem größeren Winkel der Si-O-Si-Bindung als bei kohlenstoffanalogen Verbindungen, ermöglicht.[12,13]

In der Literatur sind verschiedene Zugänge zu Siloxanen bekannt, die aufgrund der hohen Verfügbarkeit und geringen Kosten von SiO_2 ausgehen:

- Die direkte thermische Alkoxylierung von SiO_2 durch Kohlensäureester[16–19] mit anschließender GRIGNARD-Alkylierung und Hydrolyse (Schema 5, a),
- die Umwandlung von SiO_2 mit Brenzcatechin zu dianionischen hexakoordinierten,[20–22] oder Ethylenglykol zu anionischen pentakoordinierten

Siliziumkomplexen,[23,24] mit anschließender GRIGNARD-Alkylierung zu den Silanolen (Schema 5, b) und Kondensation zu den entsprechenden Siloxanen,

- die säureinduzierte Alkoxylierung von Silikatmaterialien,[25]
- die carbothermische Reduktion von SiO_2 zu elementarem Silizium bei 1500–3000 °C,[4,16,23] Umsetzung zu (Methyl-)Chlorsilanen[4,5,16,23,25,26], Destillation des Chlorsilan Gemisches[16] und Hydrolyse zu den Siloxanen (Schema 5, c).

a) Direkte Alkoxylierung durch thermische Zersetzung von Kohlensäureestern

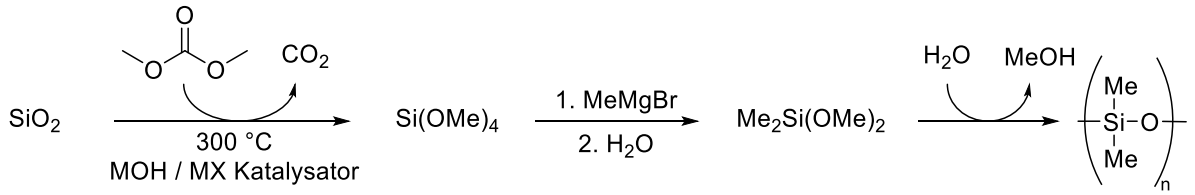

b) Umwandlung von SiO_2 über dianionische hexakoordinierte Siliziumkomplexe

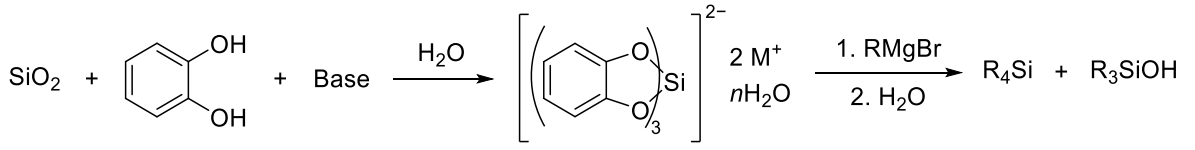

c) Carbothermische Reduktion, MÜLLER-ROCHOW-Prozess und Hydrolyse der Chlorsilane

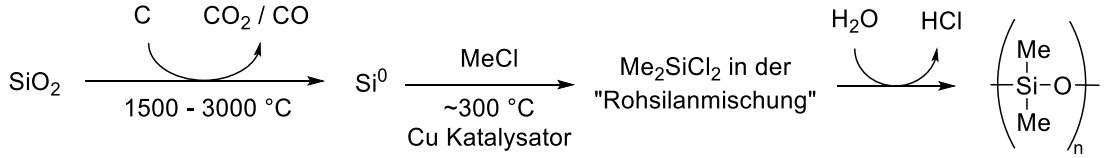

Schema 5. Synthetische Strategien für Polydimethylsiloxan, ausgehend von SiO_2: a) Thermische Alkoxylierung von SiO_2 durch Kohlensäureester (mit M als Erdalkalimetall, X als Halogenid);[16–19] b) Umwandlung von SiO_2 mit Brenzcatechin zu dianionischen hexakoordinierten Siliziumkomplexen (mit M als Erdalkalimetall);[20–22] c) Carbothermische Reduktion von SiO_2 über Chlorsilane zu Siloxanen.[4,5,16,23,25,26]

Industriell wird die carbothermische Reduktion von SiO_2 im Lichtbogenofen als Zugang zu Siloxanen eingesetzt. Das erhaltene elementare Silizium wird im MÜLLER-ROCHOW-Prozess[5] bei ca. 300 °C unter Kupfer-Katalyse mit Chlormethan zu den entsprechenden (Methyl-)Chlorsilanen umgesetzt (Tabelle 1).[4,5,16,23,25,26] Hierbei stellt Dimethyldichlorsilan das Hauptprodukt der „Rohsilanmischung“ dar, die einer Destillation[16] unterzogen wird, bevor es zur Umsetzung zu den Siloxanen kommt.

Tabelle 1: Typische Zusammensetzung einer „Rohsilanmischung“ des MÜLLER-ROCHOW-Prozesses.[a][27]

Eintrag	Verbindung	Siedepunkt [°C]	Anteil der „Rohsilanmischung“ [Gew.-%]
1	$(CH_3)_2SiCl_2$	70	70-90
2	$(CH_3)SiCl_3$	66	5-15
3	$(CH_3)_3SiCl$	57	2-4
4	$(CH_3)HSiCl_2$	41	1-4
5	$(CH_3)_2HSiCl$	35	0.1-0.5

[a] Typische Reaktionsbedingungen: 0,5-3 Gew.-% Kupferkatalysator; Zink oder Zinkoxid als Promotor; 250-320 °C.[27]

Die aufgetrennten (Methyl-)Chlorsilane können durch Hydrolyse zu den Silanolen konvertiert werden. Im industriellen Bereich hat sich die Methanolyse aufgrund der höheren Wirtschaftlichkeit etabliert, bei dem Methylchlorid freigesetzt wird, welches als Kreisprozess für den MÜLLER-ROCHOW-Prozess verwendet werden kann.[28,29] Für das Hauptprodukt, dem Dimethyldichlorsilan kann hierbei zwischen dem BAYER-Verfahren hin zu den zyklischen Siloxanen D_3 und D_4 als Hauptprodukt und dem WACKER-Verfahren zu linearen Verbindungen unterschieden werden (Schema 6).[30] Das BAYER-Verfahren findet bei 165 °C unter $ZnCl_2$ Katalyse statt, mit den zyklischen Strukturen. Im WACKER-Verfahren werden bei 100 °C lineare Oligosiloxane mit endständiger Silanol-Funktion erzeugt.[30]

Die weitere Polymerisation der linearen Oligo- oder Cyclosiloxane kann über drei mögliche Routen erfolgen (Schema 6), die von den Monomeren abhängig sind:[2]

- Polykondensation, bei der lineare Oligosiloxane thermisch, unter Wasserabspaltung, in hochmolekulare Polysiloxane überführt werden. Hier liegt kein Gleichgewicht zwischen linearen und zyklischen Verbindungen vor und die Polymerisation wird mit hohem Anteil an linearen Strukturen durch Zugabe von Kettenterminatoren, wie Silylaminen und Disilazanen gestoppt.[11,29]
- Ringöffnungspolymerisation (ROP), die ionisch, radikalisch, peroxidisch oder durch Plasma initiiert werden kann.[15] Hierbei wird die Ringspannung (bei D_3) und Entropie zur Linearisierung der zyklischen Strukturen angewendet. Es stellt sich ein Gleichgewicht zwischen linearen und zyklischen Siloxanen ein, welches sich durch Temperatur und Promotoren wie DMSO verschieben lässt.[11,29] Die Molekulargewichtsverteilung lässt sich über diesen Prozess gut steuern.
- Äquilibrierung, die parallel zur ROP ablaufen kann und durch Zugabe von Katalysatoren das Einstellen des Gleichgewichts zwischen linearen und zyklischen Siloxanen beschreibt.[31] Durch destillative Entfernung der zyklischen

Polysiloxane kann das Gleichgewicht zu höhermolekularen linearen Polysiloxanen verschoben oder ein Gemisch von Polysiloxanen zu einheitlicher Kettenlänge überführt werden.[11,29]

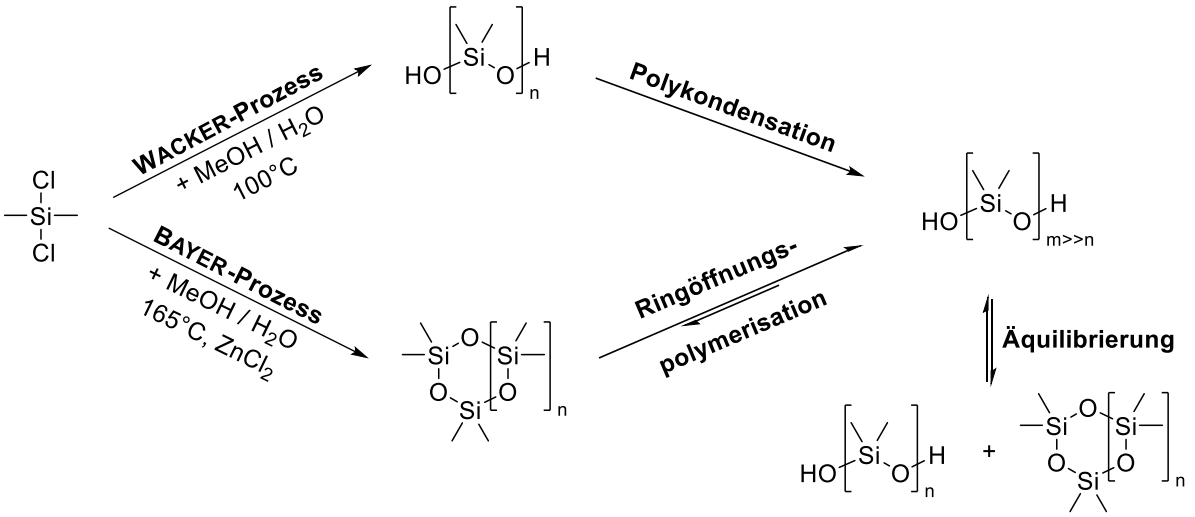

Schema 6. Verfahren für die Herstellung von Polysiloxanen.[2,11,29]

Neben der eingesetzten Polymerisationsart ist das entstehende Polysiloxan stark vom strukturellen Aufbau des verwendeten Chlorsilans abhängig. So können verschiedene Polymertypen mit unterschiedlichem Eigenschaftsprofil je nach Anzahl der Chlorgruppen am Silan erzeugt werden. Diese definieren den möglichen Vernetzungsgrad im Polysiloxan und spiegeln sich in dessen Nomenklatur wider (Schema 7).

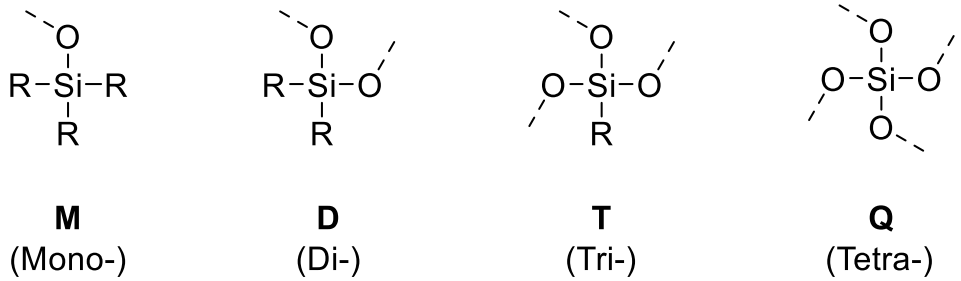

Schema 7. Nomenklatur der Siloxaneinheiten.

Monofunktionelle Einheiten dienen für den Kettenabschluss von Polysiloxanen. Durch difunktionelle Strukturen können lineare oder zyklische höhermolekulare Polysiloxane erzeugt werden, die häufig als Silikonöle für Schmier- und Hydraulikanwendungen,[32] als Entschäumungsmittel,[33] Dielektrika,[34] Trenn- und Imprägniermittel eingesetzt werden.[35] Trifunktionelle Einheiten bilden die Grundlage für Elastomere, welche durch

Vernetzung mit D-Einheiten erzeugt werden. Werden zusätzlich tetrafunktionelle Einheiten eingesetzt, kommt es zur Bildung von Silikat-analogen Gerüsten, welche Silikonharze als Produkte erzeugen. Insgesamt lässt sich dadurch eine vielfältige Anwendungspalette von Anstrichen und Beschichtungen,[4,36–38] Elektronik,[4,36,39,40] Fahrzeugteilen,[4,36] Gläsern,[26] Haushaltsgeräten[4,36] Keramik,[26] Konsumgütern,[4,36,37,39,40] Körperpflegeprodukten[4,36–43] mechanischen Flüssigkeiten,[4,36,38] medizinischen Anwendungen[4,36,37,39–42] und Textilien[4,36] erreichen, die unser alltägliches Leben ermöglichen.

[1] F. S. Kipping, L. L. Lloyd, *J. Chem. Soc., Trans.* **1901**, *79*, 449–459.

[2] T. Köhler, A. Gutacker, E. Mejía, *Org. Chem. Front.* **2020**, *7*, 4108–4120.

[3] F. S. Kipping, *Proc. R. Soc. London, Ser. A* **1937**, *159*, 139–148.

[4] D. Seyferth, *Organometallics* **2001**, *20*, 4978–4992.

[5] E. G. Rochow, *J. Am. Chem. Soc.* **1945**, *67*, 963–965.

[6] E. G. Rochow, *Sci. Am.* **1948**, *179*, 50–53.

[7] "Global Silicones Market: By Type: Elastomers, Fluids, Gels, Resins; By Application: Industrial Process, Construction Materials, Home and Personal Care, Transportation, Energy, Healthcare, Electronics; Regional Analysis; Historical Market and Forecast (2018-2028); Market Dynamics; Competitive Landscape; Industry Events and Developments", gefunden unter https://www.expertmarketresearch.com/reports/silicone-market-report (Aufgerufen am: 17.01.2023), **2022**.

[8] J. E. Mark, H. R. Allcock, R. West, *Inorganic polymers*, Oxford University Press, New York, **2005**.

[9] L. Pauling, *The nature of the chemical bond and the structure of molecules and crystals*. *An introduction to modern structural chemistry*, Cornell University Press, Ithaca, New York, **1960**.

[10] İ. Yilgör, J. E. McGrath *Polysiloxane containing copolymers: A survey of recent developments*. *Advances in Polymer Science, 86*. Advances in Polymer Science, Springer, Berlin, Heidelberg, **1988**.

[11] W. Noll, *Chemistry and Technology of Silicones*, Academic Press, London, **1968.**

[12] E. Yilgör, I. Yilgör, *Prog. Polym. Sci.* **2014**, *39*, 1165–1195.

[13] M. G. Voronkov, V. P. Miĺěskevĭc, J. A. Jŭzelevskij, *The siloxane bond*. *Physical properties and chemical transformations*, Springer US, New York, **1978**.

[14] J. E. Mark, *Acc. Chem. Res.* **2004**, *37*, 946–953.

[15] M. Butts, J. Cella, C. D. Wood, G. Gillette, R. Kerboua, J. Leman, L. Lewis, S. Rajaraman, S. Rubinsztajn, F. Schattenmann, J. Stein, J. Wengrovius, D. Wicht, *Silicones*, John Wiley & Sons, Ltd, **2003**.

[16] L. N. Lewis, F. J. Schattenmann, T. M. Jordan, J. C. Carnahan, W. P. Flanagan, R. J. Wroczynski, J. P. Lemmon, J. M. Anostario, M. A. Othon, *Inorg. Chem.* **2002**, *41*, 2608–2615.

[17] E. Suzuki, M. Akiyama, Y. Ono, *J. Chem. Soc., Chem. Commun.* **1992**, 136–137.

[18] Y. Ono, M. Akiyama, E. Suzuki, *Chem. Mater.* **1993**, *5*, 442–447.

[19] M. Akiyama, E. Suzuki, Y. Ono, *Inorg. Chim. Acta* **1993**, *207*, 259–261.

[20] A. Boudin, G. Cerveau, C. Chuit, R. J. P. Corriu, C. Reye, *Organometallics* **1988**, *7*, 1165–1171.

[21] A. Boudin, G. Cerveau, C. Chuit, R. J. P. Corriu, C. Reye, *Angew. Chem., Int. Ed.* **1986**, *25*, 473–474.

[22] A. Rosenheim, B. Raibmann, G. Schendel, *Z. anorg. allg. Chem.* **1931**, *196*, 160–176.

[23] K. Y. Blohowiak, D. R. Treadwell, B. L. Mueller, M. L. Hoppe, S. Jouppi, P. Kansal, K. W. Chew, C. L. S. Scotto, F. Babonneau, *Chem. Mater.* **1994**, *6*, 2177–2192.

[24] H. Cheng, R. Tamaki, R. M. Laine, F. Babonneau, Y. Chujo, D. R. Treadwell, *J. Am. Chem. Soc.* **2000**, *122*, 10063–10072.

[25] M. E. Kenney, G. B. Goodwin (Case Western Reserve University), US 4717773, **1988**.

[26] R. M. Laine, K. Y. Blohowiak, T. R. Robinson, M. L. Hoppe, P. Nardi, J. Kampf, J. Uhm, *Nature* **1991**, *353*, 642–644.

[27] A. F. Hollemann, E. Wiberg, *Lehrbuch der anorganischen Chemie*, Walter de Gruyter GmbH, Berlin, Boston, **1995**.

[28] a) J. Chojnowski, M. Cypryk in *Silicon-Containing Polymers*, Springer, Dordrecht, **2000**, pp. 3–41; b) H.-H. Moretto, M. Schulze, G. Wagner, *Ullmann's Encyclopedia of Industrial Chemistry*. *Silicones*, Wiley-VCH Verlag GmbH & Co. KGaA, **2000**.

[29] J. Ackermann, V. Damrath, *Chem. Unserer Zeit* **1989**, *23*, 86–99.

[30] R. Schliebs, J. Ackermann, *Chem. Unserer Zeit* **1987**, *21*, 121–127.

[31] D. W. Scott, *J. Am. Chem. Soc.* **1946**, *68*, 2294–2298.

[32] a) R. D. Blackledge, M. Vincenti, *J. Forensic Sci. Soc.* **1994**, *34*, 245–256; b) T. Coyle, N. Anwar, *Sci. Justice* **2009**, *49*, 32–40.

[33] V. Bergeron, P. Cooper, C. Fischer, J. Giermanska-Kahn, D. Langevin, A. Pouchelon, *Colloids Surf., A* **1997**, *122*, 103–120.

[34] P. K. Sharma, N. Gupta, P. I. Dankov, *IEEE Sens. J.* **2021**, *21*, 19492–19504.

[35] E. D. Goddard, *Principles of Polymer Science and Technology in Cosmetics and Personal Care*, Taylor & Francis Group, Milton, **1999**.

[36] E. Pouget, J. Tonnar, P. Lucas, P. Lacroix-Desmazes, F. Ganachaud, B. Boutevin, *Chem. Rev.* **2010**, *110*, 1233–1277.

[37] S. Varaprath, K. L. Salyers, K. P. Plotzke, S. Nanavati, *Anal. Biochem.* **1998**, *256*, 14–22.

[38] B. A. Kamino, T. P. Bender, *Chem. Soc. Rev.* **2013**, *42*, 5119–5130.

[39] Y. Horii, K. Kannan, *Arch. Environ. Contam. Toxicol.* **2008**, *55*, 701–710.

[40] R. Wang, R. P. Moody, D. Koniecki, J. Zhu, *Environ. Int.* **2009**, *35*, 900–904.

[41] W. Johnson, W. F. Bergfeld, D. V. Belsito, R. A. Hill, C. D. Klaassen, D. C. Liebler, J. G. Marks, R. C. Shank, T. J. Slaga, P. W. Snyder, F. A. Andersen, *Int. J. Toxicol.* **2011**, *30*, 149S-227S.

[42] P. C. Klykken, T. W. Galbraith, G. B. Kolesar, P. A. Jean, M. R. Woolhiser, M. R. Elwell, L. A. Burns-Naas, R. W. Mast, J. A. Mccay, K. L. White, A. E. Munson, *Drug Chem. Toxicol.* **1999**, *22*, 655–677.

[43] G. Zareba, R. Gelein, P. E. Morrow, M. J. Utell, *Skin Pharmacol. Appl. Skin Physiol.* **2002**, *15*, 184–194.

2 Aufgabenstellung

Ziel dieser Arbeit ist es, die Elektrifizierung wertschöpfender Syntheserouten für WACKER-relevante Produkte zu evaluieren. Dies beinhaltet besonders die Konversion von Chlor- und Hydrosilanen, wie auch den energieeffizienten Zugang zu Siloxanen, wobei der selektive Zugang zu ausgewählten Verbindungen im Vordergrund steht. Um mögliche Syntheserouten auch im industriellen Maßstab etablieren zu können, ist der Verzicht auf Opferanodenmaterialien, wie beispielsweise Mg oder Al, welche im Reaktionsverlauf das Metallchlorid erzeugen, was aufwändig entsorgt werden muss, unabdingbar. Auch auf den Einsatz von wahrscheinlich krebserregenden organischen Verbindungen, wie Hexamethylphosphorsäuretriamid (HMPT),[1] als komplexierende Additive ist zu verzichten. Mögliche Syntheserouten sollen im besten Fall für bestehende Kreislaufprozesse, wie beispielsweise für Chlorwasserstoff, welches in weiteren Reaktionsprozessen wiederverwendet werden kann, kompatibel sein. Diese Arbeit umspannt dabei insbesondere die kritische Prüfung von drei möglichen Einsatzgebieten für die elektrochemische Konversion:

- Die Dimerisierung von $SiCl_4$, bzw. $HSiCl_3$ soll untersucht werden, welche als kostengünstige Produkte in hoher Quantität bei der Erzeugung von Solar- und Reinstsilizium[2] vorliegen. Der mögliche Zugang zu dem, für die Halbleiterindustrie essentiellen, Produkt Si_2Cl_6 soll über anionische, kationische und radikalische Reaktionsführung beleuchtet werden (Schema 8, a).
- Die selektive Route zu industriell relevanten Produkten der Si-C-Bindung, besonders für die Darstellung von Allylsilanen, für die weitere Funktionalisierung zu Silikonelastomeren,[3] soll geprüft werden (Schema 8, b).
- Das elektrochemische Syntheseprotokoll zur direkten Konversion von SiO_2 zu Siloxanen, welches in der Vergangenheit durch eine zurückgezogene Publikation[4] und mehrere Patentanmeldungen[5] beschrieben wurde, soll kritisch evaluiert werden (Schema 8, c).

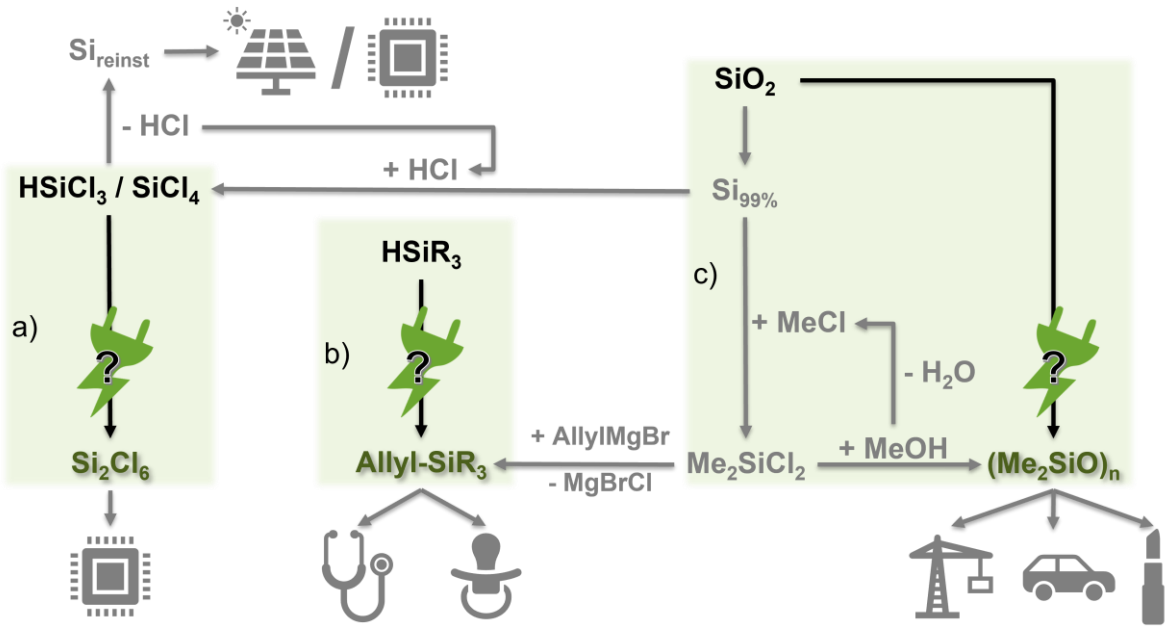

Schema 8. Prüfung der Elektrifizierung möglicher Syntheserouten und -zugänge für WACKER-relevante Produkte: a) Zugang zu Si_2Cl_6 ausgehend von $SiCl_4$ und $HSiCl_3$; b) Zugang zu Allylsilanen ausgehend von Hydrosilanen; c) Direkter Zugang zu Siloxanen ausgehend von SiO_2.

[1] W. Pflaumbaum, M. Steinhausen, "Liste der krebserzeugenden, keimzellmutagenen und reproduktionstoxischen Stoffe (KMR-Stoffe)", gefunden unter https://www.google.com/url?sa=t&rct=j&q=&esrc=s&source=web&cd=&ved=2ahUKEwi_5Oyax4r8AhWqi_0HHcuZAaYQFnoECA8QAQ&url=https%3A%2F%2Fpublikationen.dguv.de%2Fwidgets%2Fpdf%2Fdownload%2Farticle%2F3517&usg=AOvVaw1zTQafPdTe21fnnAXj1oAR (Aufgerufen am: 17.01.2023), **2022**.

[2] a) M. K. Nazeeruddin, *Nature* **2016**, *538*, 463–464; b) S. Yadav, K. Chattopadhyay, C. V. Singh, *Renewable Sustainable Energy Rev.* **2017**, *78*, 1288–1314; c) Z. Yang, T. Kang, Y. Ji, J. Li, Y. Zhu, H. Liu, X. Jiang, Z. Zhong, F. Su, *J. Colloid Interface Sci.* **2021**, *589*, 198–207.

[3] F. B. Madsen, I. Javakhishvili, R. E. Jensen, A. E. Daugaard, S. Hvilsted, A. L. Skov, *Polym. Chem.* **2014**, *5*, 7054–7061.

[4] J. E. Dick, D. Chong, *J. Am. Chem. Soc.* **2014**, *136*, 6776; Zurückgezogen aufgrund von Bedenken bezüglich der Rechte an geistigem Eigentum.

[5] a) C. Huajun, F. Hongcheng, H. Jinghui, L. Liguo (Zhejiang Hesheng Silicon Industry Co), CN 103924259 A, **2014**; b) J. Jianxiong, L. Zhifang, L. Mengxian, W. Chuan (Hangzhou Normal University), CN 104120442 A, **2014**; c) L. Kai (Luo Kai), CN 103952716 A, **2014**.

3 Ergebnisse und Diskussion

3.1 Elektrochemische Si-Si Bindungsknüpfung zu Si_2Cl_6

Zu diesem Kapitel wurde ein Manuskript veröffentlicht:
A. D. Beck, S. Haufe, J. Tillmann, S. R. Waldvogel*, *Challenges in the Electrochemical Synthesis of Si_2Cl_6 Starting from Tetrachlorosilane and Trichlorosilane*, *ChemElectroChem* **2022**, *9*, e202101374. [DOI: 10.1002/celc.202101374] *Korrespondenzautor
Erläuterung meines Beitrags: Alle experimentellen Untersuchungen und Auswertungen dieser Arbeit wurden von mir durchgeführt und die Rohfassung des Manuskripts wurde von mir verfasst. Die Finalisierung der Veröffentlichung wurde von mir unter Betreuung von Dr. Stefan Haufe, Dr. Jan Tillmann und Prof. Dr. Siegfried R. Waldvogel abgeschlossen.

Einleitung

Si_2Cl_6 ist ein vielversprechender, Silan-basierter Vorläufer für die Herstellung von Halbleiterbauelementen.[1] Es entspricht den hohen Anforderungen an die Erzeugung von isolierenden Dünnschichten, sodass Sub-7-nm-Technologiestandards ermöglicht werden. Durch atomic layer deposition (ALD) können die einzigartigen Eigenschaften der Si-Si-Bindung in Si_2Cl_6 für die Erzeugung der isolierenden Zwischenschichten im industriellen Prozess genutzt werden.[2] Dies geschieht im NH_3-Plasmaprozess bei niedrigeren Temperaturen und führt zur Abscheidung von SiN_x-Dünnschichten. Es wurden in der Vergangenheit diverse synthetische Ansätze zur Herstellung von Si_2Cl_6 beleuchtet,[3] sowohl durch direkte Chlorierung von Silizium[4] als auch durch chlorinduzierte oxidative Spaltung von Polychlorsilanen.[5] Elektrochemische Ansätze zur Dimerisierung von Chlorsilanen beschränken sich bisher jedoch auf die Umwandlung von monofunktionalisierten Substraten.[6] Synthesetechniken zur Konversion von perchlorierten Silanen zu Si_2Cl_6 wurden bisher nicht untersucht. Da $SiCl_4$ als Nebenprodukt bei der Herstellung von $HSiCl_3$[7] und $HSiCl_3$, welches in großen Mengen für die Silizium-Photovoltaik produziert wird,[8] reichlich zur Verfügung steht, wäre eine elektrochemische Synthese ausgehend von diesen perchlorierten Silanen vorteilhaft.

Zusammenfassung der Ergebnisse

Der reduktive Ansatz zur Bildung von Si_2Cl_6 ausgehend von $SiCl_4$ wurde durch CV untersucht. Es zeigt sich, dass $SiCl_4$ kathodisch reduziert werden kann. Die erhaltenen perchlorierten Di- und Oligosilane sind jedoch elektrochemisch leichter reduzierbar als das ursprüngliche Ausgangsmaterial. Dies führt zu einer Verschiebung des Reduktionspotentials in den weniger kathodischen Bereich und damit zu einer unkontrollierbaren Reduktion zu Polysilanen (Schema 9). Diese passivieren im Reaktionsverlauf die Kathodenoberfläche, wodurch sich die Reduktion selbst hemmt und schlussendlich zum Erliegen kommt.

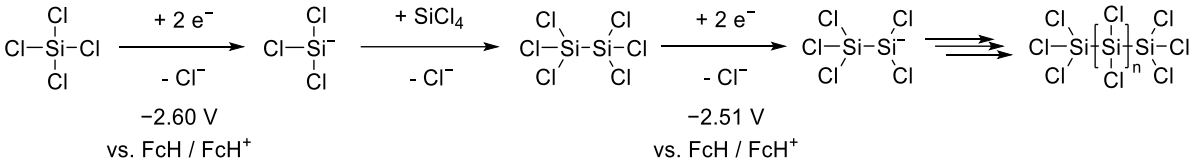

Schema 9. Postulierter Verlauf der Reduktion von $SiCl_4$ mit Si_2Cl_6 als potenzielles Zwischenprodukt und unkontrollierbarer Überreduktion zu Polysilanen (FcH/FcH⁺: Ferrocen/Ferrocenium).

Um die Reduktion zu steuern, wurde die selektive Bromierung zu $SiCl_3Br$ untersucht. Wie sich zeigt, führt die Anwesenheit von freien Halogeniden zu einer katalytischen Umwandlung des Zielprodukts Si_2Cl_6 zu längerkettigen Oligosilanen unter Abspaltung von $SiCl_4$. Um die Stabilität des Produkts zu gewährleisten, muss die Reaktion daher auf einen halogenidfreien Ansatz umgestellt werden.

Auf der Grundlage früherer Veröffentlichungen wurde die oxidative Umwandlung von Hydrosilanen untersucht. In einer Studie zur Dimerisierung von Me_2PhSiH, konnten KUNAI und Mitarbeiter zeigen, dass die Si-H-Bindung oxidativ gespalten werden kann.[9] Hierbei entstehen Protonen als Nebenprodukt, die zu Wasserstoff reduziert werden können, ohne die Stabilität von Si_2Cl_6 zu beeinflussen. Eigene Versuche haben gezeigt, dass der vermutete Mechanismus über ein Silylkation, welches anschließend kathodisch zum Silylanion reduziert wird, plausibel erscheint. Dies lässt sich durch die Si-Si-Bindung begründen, welche nur in einer ungeteilten Zelle mit Zugang zu Anode und Kathode erreicht werden kann. Die Umsetzung von $HSiCl_3$ mit Dimerisierung zu Si_2Cl_6 über den kathodischen Zugang führt jedoch, aufgrund des hohen Oxidationspotentials im Vergleich zum erreichbaren Reduktionspotential, ausschließlich zur Reduktion zu Polysilanen und zur Freisetzung von Chlorid, analog zur Reduktion von $SiCl_4$.

Es wurden daher verschiedene Konzepte für die Aktivierung der Si-H-Bindung von $HSiCl_3$ untersucht (Schema 10). Die Aktivierung der Si-H-Bindung durch Lewis-saure Borane wie $B(C_6F_5)_3$ konnte so an elektronenreichen Silanen wie Me_2PhSiH nachgewiesen werden. Eine Mediator-analoge Funktion reduziert die für das Zielprodukt erforderliche Ladungsmenge um mehr als die Hälfte. Dieses Konzept lässt sich jedoch nicht auf Lewis-saure Silane wie $HSiCl_3$ anwenden. Hier findet keine Si-H-Aktivierung statt, und das Boran wird zum Redox-Shuttle, wodurch der Gesamtumsatz sinkt. Die Zugabe von tertiären Aminen sollte analog zur Benkeser-Reaktion durch Protonenabstraktion Silylanionen erzeugen, die anschließend anodisch zum Dimer oxidiert werden. CV Studien zeigen eine leichtere Oxidierbarkeit der tertiären Amine im Vergleich zu den gebildeten Silylanionen. Zusätzlich ist das Zielprodukt Si_2Cl_6 gegenüber den entsprechenden Aminen nicht stabil und führt erneut unter katalytischer Transformation zu Oligosilanen. Der Einsatz von Wasserstoff-Atom-Transfer (HAT)-Mediatoren wurde untersucht, die in der Literatur bereits für die Umwandlung von Hydrosilanen zu dem entsprechenden Silylradikal verwendet wurden. Auch hier schließt die Stabilität des Produkts die Verwendung von *N*-Oxyl-Radikalen oder Aminen als HAT-Mediator aus, sodass eine radikalische Umwandlung nicht möglich ist.

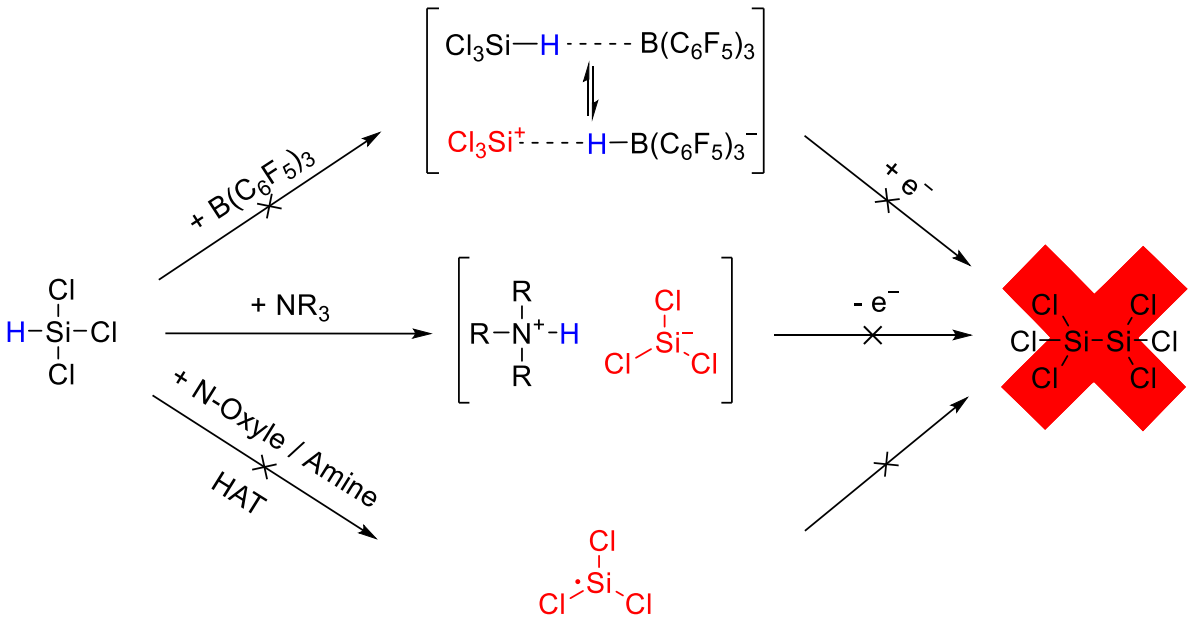

Schema 10. Untersuchte Konzepte für die elektrochemische Dimerisierung von $HSiCl_3$ zu Si_2Cl_6, durch Lewis-saure Aktivierung über ein kationisches Intermediat, Protonenabstraktion zum Silylanion und Wasserstoff-Atom-Transfer durch *N*-Oxyl-Radikale oder Amine.

Fazit

Die elektrochemische Synthese von Si_2Cl_6 ausgehend von Chlorsilanen ist sehr anfällig für eine Überreduktion, die zur Beschichtung der Kathode durch einen isolierenden Polysilan-Film führt. Die Freisetzung von Halogeniden in der reduktiven Umwandlung verhindert zusätzlich die Akkumulation von Si_2Cl_6 aufgrund von Instabilitätsproblemen. Das hohe Oxidationspotential von $HSiCl_3$ verhindert den direkten anodischen Zugang zu dem gewünschten Disilan. Verschiedene Techniken zur Aktivierung der Si-H-Bindung führen zu unerwünschten katalytischen Umwandlungen des Zielprodukts Si_2Cl_6 in Oligosilane. Obwohl ein dringender Bedarf an einem umweltfreundlichen Zugang zu Si_2Cl_6 besteht, sind mehrere Hürden zu überwinden.

[1] a) R. A. Ovanesyan, D. M. Hausmann, S. Agarwal, *ACS Appl. Mater. Interfaces* **2018**, *10*, 19153–19161; b) R. A. Ovanesyan, N. Leick, K. M. Kelchner, D. M. Hausmann, S. Agarwal, *Chem. Mater.* **2017**, *29*, 6269–6278; c) K. Park, W.-D. Yun, B.-J. Choi, H.-D. Kim, W.-J. Lee, S.-K. Rha, C. O. Park, *Thin Solid Films* **2009**, *517*, 3975–3978; d) R. C. Taylor, B. A. Scott, *J. Electrochem. Soc.* **1989**, *136*, 2382–2386.

[2] a) L. Du, W. Chu, H. Miao, D. Wang, C. Xu, Y. Ding, *Eur. J. Inorg. Chem.* **2015**, *2015*, 3205–3211; b) R. A. Ovanesyan, D. M. Hausmann, S. Agarwal, *ACS Appl. Mater. Interfaces* **2015**, *7*, 10806–10813; c) A. M. Wrobel, A. Walkiewicz-Pietrzykowska, I. Blaszczyk-Lezak, *Appl. Organomet. Chem.* **2010**, *24*, 201–207.

[3] a) G. Martin, *J. Chem. Soc., Trans.* **1914**, *105*, 2836–2860; b) A. Stock, A. Brandt, H. Fischer, *Ber. Dtsch. Chem. Ges. A/B* **1925**, *58*, 643–657; c) G. Urry, *J. Inorg. Nucl. Chem.* **1964**, *26*, 409–414.

[4] a) T. Hattori, M. Ito, Y. Miwa (Toagosei Chemical Industry Co., Ltd.), DE3623493 A1, **1986**; b) PSC Polysilane Chemicals GmbH (PSC Polysilane Chemicals GmbH), DE102014007767 A1, **2014**.

[5] a) N. Auner, C. Bauch, R. Deltschew, T. Gebel, S. Holl, G. Lippold, J. A. S. Mohsseni (REV Renewable Energy Ventures Inc.), DE102009056438 A1, **2010**; b) PSC Polysilane Chemicals GmbH (PSC Polysilane Chemicals GmbH), DE102014007685 A1, **2014**.

[6] a) C. Grogger, B. Loidl, H. Stueger, T. Kammel, B. Pachaly, *J. Organomet. Chem.* **2006**, *691*, 105–110; b) E. Hengge, H. Firgoi, *J. Organomet. Chem.* **1981**, *212*, 155–161; c) E. Hengge, G. Litscher, *Angew. Chem., Int. Ed.* **1976**, *15*, 370; *Angew. Chem.*, **1976**, *88*, 414; d) A. Kunai, T. Kawakami, E. Toyoda, M. Ishikawa, *Organometallics*

1991, *10*, 893–895; e) A. Kunai, T. Kawakami, E. Toyoda, M. Ishikawa, *Organometallics* **1991**, *10*, 2001–2003; f) J. Ohshita, K. Hino, T. Iwawaki, A. Kunai, *J. Organomet. Chem.* **2009**, *625*, 138–143.

[7] Z. Yang, T. Kang, Y. Ji, J. Li, Y. Zhu, H. Liu, X. Jiang, Z. Zhong, F. Su, *J. Colloid Interface Sci.* **2021**, *589*, 198–207.

[8] a) M. K. Nazeeruddin, *Nature* **2016**, *538*, 463–464; b) S. Yadav, K. Chattopadhyay, C. V. Singh, *Renewable Sustainable Energy Rev.* **2017**, *78*, 1288–1314.

[9] A. Kunai, T. Kawakami, E. Toyoda, T. Sakurai, M. Ishikawa, *Chem. Lett.* **1993**, *22*, 1945–1948.

ChemElectroChem

Research Article
doi.org/10.1002/celc.202101374

Chemistry Europe
European Chemical Societies Publishing

www.chemelectrochem.org

Special Collection

Challenges in the Electrochemical Synthesis of Si_2Cl_6 Starting from Tetrachlorosilane and Trichlorosilane

Alexander D. Beck,[a, b] Stefan Haufe,[a] Jan Tillmann,[a] and Siegfried R. Waldvogel*[b]

The strongly increasing demand for nano- and microelectronics calls for new and environmentally benign reaction pathways for the preparation of one of the most important substrates in the production of semiconductor materials: Si_2Cl_6. We present a comprehensive study of the opportunities and challenges for the selective electrochemical formation of higher halo-functionalized silanes to Si_2Cl_6 achieved by cyclic voltammetry measurements and electrochemical synthesis. Cathodic dehalo-dimerization reaction of $SiCl_4$ and the approach to halogen exchange for better substrate reduction are envisioned. An anodic halide-free dimerization pathway by dehydrogenation of $HSiCl_3$ is investigated, including Lewis acid activation of the Si–H bond. In addition, tertiary amine-driven, Benkeser-like in-situ formation of a $SiCl_3^-$ anion was tested as well. The target molecule Si_2Cl_6 is strongly promoted to direct electro-conversions making the anodic and cathodic electrosynthesis very challenging.

Introduction

The steady growth in the demand for nano- and microelectronics is leading to new challenges in processing semiconductor devices reaching sub-7-nm technology nodes.[1,2] The corresponding structure resolution requires selection of suitable precursor substrates in the production of insulating thin films by atomic layer deposition (ALD).[2] Si_2Cl_6 has shown to be a continuing promising silane-based precursor for the use in interlayer dielectrics.[3] Due to unique Si–Si construction features, Si_2Cl_6 met the strict requirements for desired SiN_x thin film deposition even in the industrial lower-temperature process with NH_3 plasma.[4] Since the first generation of Si_2Cl_6 150 years ago, various approaches to the synthesis of Si_2Cl_6 have been investigated,[5] including direct chlorination of silicon,[6] and oxidative cleavage of polychlorosilanes by chlorine.[7] While the synthesis of Si_2Cl_6 is hitherto challenging, chlorinated monosilanes like $SiCl_4$ are abundantly available. $SiCl_4$ is co-generated in large amounts as a by-product in the direct synthesis of $HSiCl_3$,[8] that itself is used as a primary feedstock in high volumes to produce silicon-based photovoltaics.[9]

The increasing demand for Si_2Cl_6 requires the investigation of new synthetic strategies, particularly in terms of low temperature, energy-efficient approaches starting from easily available chlorosilanes. This suggests the field of electrosynthesis that has experienced a renaissance, represents a green alternative to traditional synthesis protocols,[10] and evolves to a key discipline for future synthesis applications.[11] This methodology can easily pay off,[12] if highly value-added compounds are addressed.[13] The significant advantages of electrosynthesis are the avoidance of stoichiometric amounts of oxidizers or reducing agents.[14,15] Therefore, only little or no reagent waste is generated and due to the simple switch off, no thermal runaway reactions are possible making this method inherently safe.[16]

The first electrochemical synthesis of disilanes from halosilanes was reported by Hengge and Litscher (Scheme 1).[17] Instead of the hitherto known Wurtz-type pathway using alkali metals for the reductive coupling, mild reaction conditions applying electrons as reagents lead to the desired disilane formation in high current efficiency. With mono-functionalized substrates, a variety of disilanes have been obtained in the past decades by the reductive electrochemical route, mainly with metal anodes such as copper,[18] magnesium,[19] mercury,[17,20] and silver.[21] These metals form the corresponding chlorides as by-products. Alternative anode concepts have been tested,[22] refraining on sacrificial electrodes. While selective pathways for the dimerization of mono-functionalized substrates have been reported, difunctionalized halosilanes were reductively coupled to linear oligo- and polysilanes with varying chain length dependent on reaction conditions and substrate composition.[23] For higher halo substituted silanes there are only few reports in the literature with silicon deposition for appropriate reaction conditions and network polysilanes as sole products,[24–27] allowing the reduction of $SiCl_4$ to silicon nanoparticles.[28]

Besides the reductive pathway, an oxidative route to Si–Si bond formation of alkyl and allyl H-silanes is known in literature,[29] and a successful dimerization of Me_2PhSiH via cleavage of Si–H bond and cathodic proton reduction to H_2 has

[a] *A. D. Beck, Dr. S. Haufe, Dr. J. Tillmann*
Consortium für elektrochemische Industrie
Wacker Chemie AG
Zielstattstraße 20, 81379 München, Germany
[b] *A. D. Beck, Prof. Dr. S. R. Waldvogel*
Department Chemie
Johannes Gutenberg-Universität Mainz
Duesbergweg 10–14, 55128 Mainz, Germany
E-mail: waldvogel@uni-mainz.de
Homepage: https://www.aksw.uni-mainz.de

Supporting information for this article is available on the WWW under https://doi.org/10.1002/celc.202101374

Special Collection *An invited contribution to the Wolfgang Schuhmann Festschrift*

ChemElectroChem
Research Article
doi.org/10.1002/celc.202101374
Chemistry Europe
European Chemical Societies Publishing

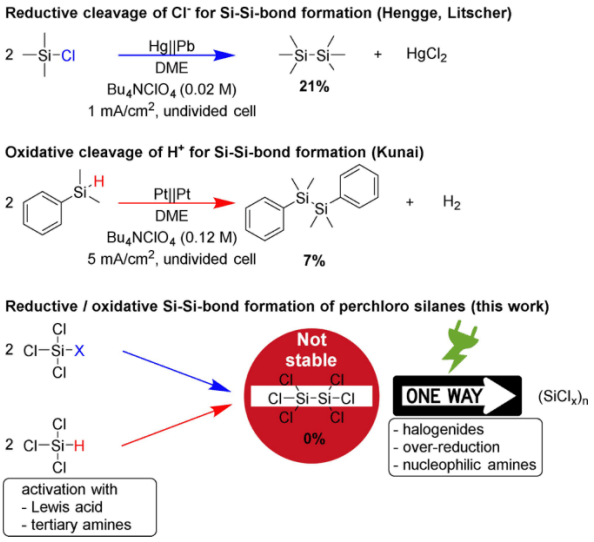

Scheme 1. Reported strategies for electrochemical Si–Si bond formation and attempts of this work.[17,30]

been described by Kunai and co-workers (Scheme 1).[30] This methodology provides a halide free pathway in the absence of otherwise often used sacrificial anodes. The route is discussed via a cationic intermediate stabilized by the perchlorate anion of the supporting electrolyte leading to reductive dimerization by successive cathodic conversion. To the best of our knowledge, neither the reductive nor the oxidative pathway was reported for selective dimerization of perchloro silanes. Here, a comprehensive study of the possibilities and challenges for a selective formation of higher halo functionalized silanes to Si_2Cl_6 is outlined.

Results and Discussion

The straightforward attempt to the formation of Si_2Cl_6 is the dehalo-dimerization of $SiCl_4$ under reductive displacement of chloride, as used for the Si–Si coupling of mono-functionalized halosilanes. This approach will indeed elongate the silicon backbone with Si_2Cl_6 as potential intermediate as Homma and co-workers reported.[26] However, Si_2Cl_6 could not be isolated. Depending on constant current or constant potential conditions, an orange polysilane $(SiCl_{0.7})_n$,[25] or deposits of elemental silicon at the surface of various cathodic materials are obtained.[26,27] This phenomenon is rationalized by a shift of the reduction potential towards less cathodic values, visible in cyclic voltammetry (CV) measurements at platinum electrodes with the elongation of the silicon backbone (Scheme 2).

The reduction of $SiCl_4$ shows two irreversible events, a wave at about −1.38 V vs. FcH/FcH$^+$ (Ferrocene/Ferrocenium) for the reduction of H^+ that is formed due to traces of water in the electrolyte and consequential formation of HCl with $SiCl_4$ and a second peak at −2.60 V vs. FcH/FcH$^+$ for the reduction of $SiCl_4$. This agrees with previously reported data by Bard and co-

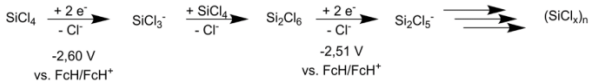

Scheme 2. Proposed pathway for the reductive coupling of $SiCl_4$ with Si_2Cl_6 as potential intermediate in consecutive elongation to polysilane with parameter x dependent on electrode material and reaction conditions (FcH/FcH$^+$: Ferrocene/Ferrocenium).

workers.[27] In comparison to $SiCl_4$, for Si_2Cl_6 a less cathodic reduction peak at −2.51 V vs. FcH/FcH$^+$ and a second one at −3.03 V vs. FcH/FcH$^+$ arises (Figure 1), that could be related to another silicon-chloride bond cleavage. The missing reduction wave of H^+ might be due to higher stability of Si_2Cl_6 towards protic media. For $SiCl_4$ and Si_2Cl_6 consecutive measurement cycles by CV show similar characteristics: the current density declines, the reduction wave vanishes and at the same time the onset reduction potential is shifted towards less cathodic values below −2.00 V vs. FcH/FcH$^+$. This trend is attributed to the possible generation of a surface layer of perchloro oligosilane species which is further reduced to deposit on the platinum cathode. The change in charge transfer properties of the electrode material due to this coating inhibits the hitherto occurring H^+ reduction and blocks the cathode, resulting in the decrease of current density also visible in electrochemical synthesis. The reduction potential declines for elongated perchlorinated silicon species, which further promotes the polymerization reaction starting from the oligosilanes instead of $SiCl_4$, favoring the polymerization and deposition over possible dimerization.

While the straightforward attempt is hindered by the preferential reduction of polysilanes, respective bromosilanes are easier reduced as shown by the difference of 170 mV for the reduction of $SiBr_4$ vs. $SiCl_4$ facilitating silicon-bromine bond cleavage (see Supporting Information). A pathway favoring dimerization over polymerization for a monobromo halosilanes is conceivable. The halogen exchange of chloro to bromo silanes has been reported by Schmidt and Russ for in-situ bromination of Me_3SiCl to Me_3SiBr in MeCN with group 1 and 2

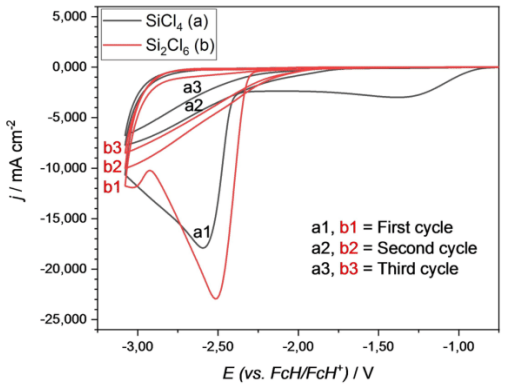

Figure 1. Cyclic voltammogram of (a) 15 mM $SiCl_4$ in 0.1 M Bu_4NCl / MeCN, (b) 15 mM Si_2Cl_6 in 0.1 M Bu_4NCl and 0.1 M Bu_4NClO_4 / MeCN showing identical results, respectively. W.E. Pt (A = 8.0 mm^2), sweep rate ν = 0.2 V/s.

ChemElectroChem
Research Article
doi.org/10.1002/celc.202101374
Chemistry Europe
European Chemical Societies Publishing

bromide salts.[31] This exchange reaction could be reproduced with yields of 3–20% depending on bromide source at room temperature. The reaction is in equilibrium with identical yields for one hour to 7 days reaction time, solely shifted by increasing solubility of the individual metal bromide ($NaBr < MgBr_2 < LiBr$). When the mild and easy halogen exchange method is applied to $SiCl_4$ using LiBr or $MgBr_2$ as bromide source, a monobromination to $SiCl_3Br$ with 9% and 5% yield occurs, respectively. No further bromide displacement to $SiCl_2Br_2$, $SiClBr_3$ or $SiBr_4$ was observed. This can be a useful concept for the selective reductive dimerization of further silane species. However, Si_2Cl_6 is not stable towards chloride as reported by Holthausen and co-workers.[32] Chloride catalytically participates in the formation of elongated oligosilane species with consecutive cleavage of $SiCl_4$. This effect is not limited to chloride ions, as comparable results with cleavage of $SiCl_4$ and precipitation of insoluble oligosilanes in the presence of bromide indicates, that cannot be suppressed by variation of temperature or concentration of the respective halide ion. For the desired product stability, a halide free reaction pathway to Si_2Cl_6 is required.

Besides the already mentioned reductive pathway, the oxidative route to Si–Si bond formation inspired by Kunai and co-workers is examined.[30] Corresponding yields are relatively low given with 7% disilane and 15% disiloxane which is probably formed by a decomposition reaction with the supporting electrolyte. Own experiments show that disilane is no longer detectable, but the yield of disiloxane increases to 20% when access to the cathode for the intermediate is prevented by using a divided cell. This indicates a necessary subsequent reduction step for disilane formation. Another reason for low disilane yield is the distinct less anodic potential for the Si–Si bond cleavage of the desired product in comparison to the Si–H bond cleavage of the educt with a difference of 0.91 V (see Supporting Information). Despite the addressed hurdles this pathway provides the possibility of halide-free dimerization and has hitherto not been described for halo functionalized silanes like $HSiCl_3$.

In a first step the stability of Si_2Cl_6 towards oxidative cleavage of the Si–Si bond is studied. By substitution of silicon-carbon bonds through electron withdrawing chlorine, the oxidation potential shifts to higher anodic region linearly with the amount of chlorine functionalization (Figure 2). The oxidation potential of Si_2Me_6 is at 1.51 V vs. FcH/FcH^+, raising the chlorine content to Si_2Me_5Cl and $Si_2Me_4Cl_2$ shifts the potential to 1.84 V vs. FcH/FcH^+ and 2.15 V vs. FcH/FcH^+, respectively. Following this trend of anodic stabilization of about 320 mV per substitution with chlorine, it is not surprising that the oxidation potential for the Si–Si bond cleavage of Si_2Cl_6 is not measurable before electrolyte decomposition.

A reduction potential for oxidizable silane compounds at about −0.16 V vs. FcH/FcH^+ occurs on platinum electrodes, that is identical for different disilanes and H-silanes (see Supporting Information). This is very likely linked to a desorption process of the respective silyl cationic species. Neither the oxidation of Si_2Cl_6 nor the reductive desorption can be observed confirming the oxidative stability.

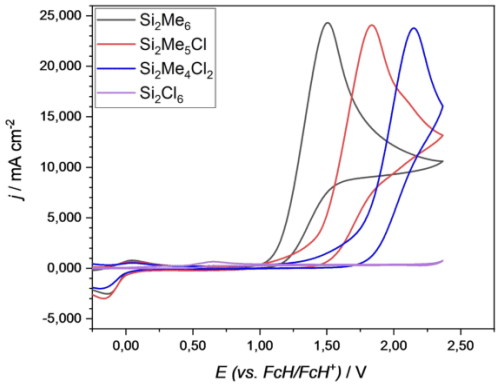

Figure 2. Cyclic voltammogram of 20 mM Si_2Me_6, Si_2Me_5Cl, $Si_2Me_5Cl_2$, Si_2Cl_6 in 0.1 M Bu_4NClO_4 and MeCN. W.E. Pt ($A = 8.0\ mm^2$), sweep rate $\nu = 0.2$ V/s, first cycle each.

Our experiments reveal that the electrolyte system based on 1,2-dimethoxyethane used for oxidative Si–Si bond formation[30] slowly dismutates $HSiCl_3$ to $SiCl_4$ and H_2SiCl_2 and does not provide the needed anodic stability. Anodic stable acetonitrile does not show this dismutation reaction and is used for further investigations. A pale yellow polysilane $(SiCl_{0.1})_n$, analogue to $SiCl_4$, is formed at the platinum cathode by the reductive polymerization of $HSiCl_3$ in an undivided cell. A divided H-type cell with diaphragm is used to prevent cathodic access of $HSiCl_3$. Electrode material and reaction parameters are screened (see Supporting Information for experimental details). The high anodic reaction conditions limit the choice for anode materials to (electro)chemical robust boron-doped diamond (BDD) and glassy carbon (GC).[15,33]

Diffusion of $HSiCl_3$ to the cathode is delayed but not inhibited by the diaphragm. The synthesis duration elongates with higher applied charge, increasing the amount of polysilane formed on the cathodic surface due to diffusive mass transport in the cathodic compartment. At the anode the desired oxidative cleavage of Si–H bonds seems to occur promoted by BDD, forming $SiCl_4$ and Si_2OCl_6 in the anodic cell compartment, increasing with rising applied charge (Table 1). In the cathodic compartment the products obtained are polymeric $(SiCl_{0.1})_n$, H_2SiCl_2 and traces of $SiCl_4$ due to diffusion. The low yield for the

Table 1. Oxidation of $HSiCl_3$ in a divided H-type cell at BDD anode.[a]

Applied Charge	$SiCl_4$ Yield[b] [%]	Si_2OCl_6 Yield[b] [%]	$(SiCl_{0.1})_n$ Yield[b] [%]	H_2SiCl_2 Yield[b] [%]
0.5 *F*	4%[c]	1%[c]	–	–
0.5 *F*	1%[d]	–	6%[d]	7%[d]
1.0 *F*	10%[c]	2%[c]	–	–
1.0 *F*	2%[d]	–	10%[d]	17%[d]
1.5 *F*	11%[c]	2%[c]	–	–
1.5 *F*	5%[d]	–	23%[d]	18%[d]

[a] Electrolysis with platinum cathode in 0.2 M TBAP in MeCN at 10 °C with 3.3 mA/cm². [b] Yield determined by NMR referenced to TMS. [c] Obtained from anodic compartment. [d] Obtained from cathodic compartment.

ChemElectroChem
Research Article
doi.org/10.1002/celc.202101374
Chemistry Europe
European Chemical Societies Publishing

applied charge of 0.5 *F* indicates that the dehydrogenation of $HSiCl_3$ is in concurrence with electrolyte decomposition.

Electrolyte decomposition can be diminished with lower current density, at the same time the diffusion of $HSiCl_3$ to the cathodic compartment rises with the elongating synthesis duration. The same applies for increasing the applied charge. Rising from 0.5 *F* to 1.0 *F*, the amount of anodic dehydrogenated $HSiCl_3$ as well as cathodic formed polysilane and H_2SiCl_2 increase due to elongated diffusion time. At 1.5 *F* the polysilane formation is the main reaction occurring with 23% yield and current density declines accordingly.

These results reveal that anodic and cathodic reactions, due to diffusion of $HSiCl_3$ are occurring. Anodic dehydrogenation of $HSiCl_3$, in which the intermediate formed is probably oxidized to the corresponding $SiCl_3^+$ shows two possible ways: recombination with reductively released chloride forming $SiCl_4$ or decomposing with the stabilizing perchlorate anion, analogue to the Me_2PhSiH system, leading to Si_2OCl_6 (Scheme 3). Simultaneously, after diffusion into the cathodic compartment, $HSiCl_3$ is reduced presumably to an anionic intermediate. Recombining with the anodic generated H^+ to H_2SiCl_2 or polymerizing to $(SiCl_{0.1})_n$ is possible under release of chloride that itself restricts stability of Si_2Cl_6 as discussed previously.

This consecutive reaction expresses the main difficulty towards the desired disilane Si_2Cl_6. A cationic intermediate needs cathodic access for the dimerization to Si–Si bond formation. At the same time the cathodic access reduces and polymerizes $HSiCl_3$ as cathodic coating further inhibiting H^+ reduction leading to a self-suppressing system and the subsequent release of chloride destabilizes the desired product. To overcome this hurdle two promising possibilities are discussed: activation of Si–H bond for easier oxidation and proton abstraction by additives to form the silyl anion in the anodic compartment, so the direct dimerization with the cationic species is available.

Facilitating the oxidation of $HSiCl_3$ by activation of Si–H bond could prevent its competing reduction. $B(C_6F_5)_3$ is known in literature as a strong enough Lewis acid for the Si–H bond activation by partial abstraction of hydride from electron-rich alkyl and allyl H-silanes.[34] The use in organic chemistry and its electrochemical properties have been investigated previously, surprisingly it has not been used in electrochemical synthesis for substrate activation so far.[34,35]

By CV measurements the evidence for an activation of Si–H bond in presence of perchlorate anion is not clear. Adduct formation without hydride abstraction by $B(C_6F_5)_3$ elongates the Si–H bond,[36] and should shift the oxidation potential to less anodic values due to decreasing activation barrier for Si–H cleavage. For the borohydride stabilized silyl cation an oxidation peak for $[HB(C_6F_5)_3]^-$ at about 0.88 V vs. FcH/FcH^+ was reported by Wildgoose and co-workers.[37] 5.0 mol% $B(C_6F_5)_3$ increases the oxidation current of Me_2PhSiH by 5-fold at GC with a shift of the oxidation potential of about 0.09 V to higher anodic values (Figure 3). This indicates that adduct formation with bond elongation is not the measured intermediate. This current gain is equal for further electron-rich H-silanes like Ph_3SiH (see Supporting Information). A very weak and ill-defined oxidation wave appears at about 0.88 V vs. FcH/FcH^+ prior to oxidation of Me_2PhSiH. This appearance is not conclusive enough to be related to $[HB(C_6F_5)_3]^-$, although it was reported to form only small amount at equilibrium in the absence of a substrate.[37]

Activation of Si–H bond with $B(C_6F_5)_3$ in electrochemical synthesis lowers the needed applied charge. In presence of 2.5 mol% $B(C_6F_5)_3$ 7% disilane and 15% disiloxane are already obtained at 2.0 *F* instead of 4.4 *F*. While the yield of disilane is not increased, the needed applied charge is less than half, indicating a mediator like functionality: formation of silyl cation stabilized borohydride enables direct reduction to the silyl anion with anodic regeneration of borohydride to the Lewis acid for consecutive activation of Si–H bond.

Applying this concept to the activation of $HSiCl_3$, CV measurements indicate that the activation of electron-poor H-silanes is hindered by the Lewis acidity of $HSiCl_3$ itself as has been mentioned in literature.[38] $B(C_6F_5)_3$ is oxidized with a peak potential at 2.26 V vs. FcH/FcH^+ at GC, an identical trend is obtained by $HSiCl_3$ with 5 mol% of $B(C_6F_5)_3$ (Figure 4). Neither the previously mentioned oxidation wave at 0.88 V vs. FcH/FcH^+ nor the increase of oxidation current at GC electrode is observed. This interpretation is further supported by data of synthesis in an undivided cell, due to the needed cationic

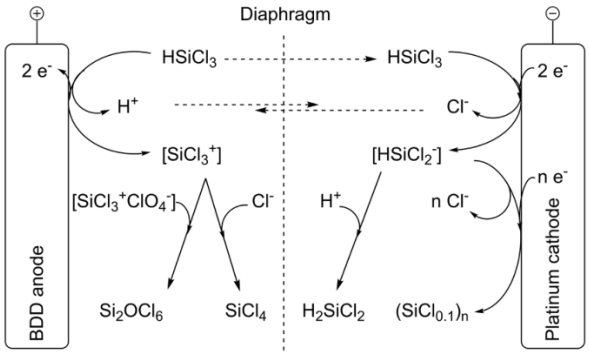

Scheme 3. Proposed mechanism for the dehydrogenative Si–H bond cleavage and reductive Si–Cl bond cleavage due to diffusion.

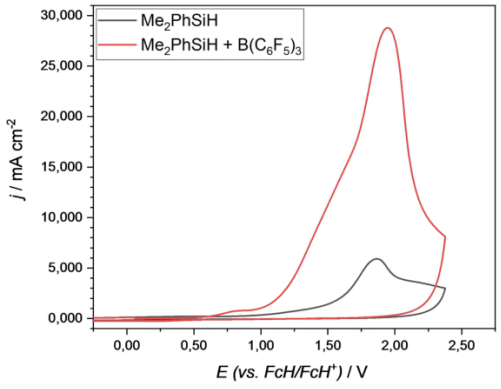

Figure 3. Cyclic voltammogram of 40 mM Me_2PhSiH in absence and presence of 2 mM $B(C_6F_5)_3$ in 0.1 M Bu_4NClO_4 and MeCN. W.E. GC (A = 8.0 mm^2), sweep rate ν = 0.2 V/s, first cycle each.

ChemElectroChem
Research Article
doi.org/10.1002/celc.202101374
Chemistry Europe
European Chemical Societies Publishing

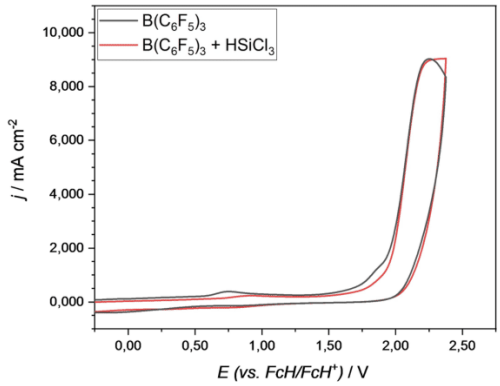

Figure 4. Cyclic voltammogram of 2 mM $B(C_6F_5)_3$ in absence and presence of 40 mM $HSiCl_3$ in 0.1 M Bu_4NClO_4 and MeCN. W.E. GC (A = 8.0 mm^2), sweep rate $\nu = 0.2$ V/s, first cycle each.

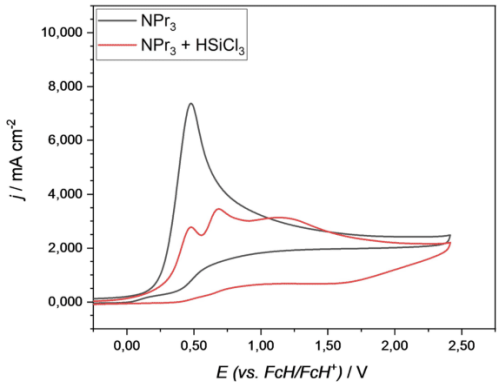

Figure 5. Cyclic voltammogram of 10 mM nPr_3N in absence and presence of 40 mM $HSiCl_3$ in 0.1 M Bu_4NClO_4 and MeCN. W.E. GC (A = 8.0 mm^2), sweep rate $\nu = 0.2$ V/s, first cycle each.

access for possible dimerization. With increasing amount of $B(C_6F_5)_3$ additive, the yield for the dehydrogenative oxidation as well as the reductive polymerization of $HSiCl_3$ decline over proportional (see Supporting Information). $B(C_6F_5)_3$ is reported to be reduced to the respective radical anion at −1.59 V vs. FcH/FcH^+ at GC at significant less cathodic potential than the respective reduction of $HSiCl_3$ with an onset potential of −2.23 V vs. FcH/FcH^+ at GC electrode.[37] This indicates the occurrence of a borane driven redox shuttle between radical anion and $B(C_6F_5)_3$ decreasing the current efficiency for oxidative and reductive $HSiCl_3$ conversion due to lacking formation of borohydride with $HSiCl_3$.

Another concept to prevent reductive polymerization is the proton abstraction by less sterically hindered tertiary amines like nPr_3N and nBu_3N as known in Benkeser systems in organic chemistry to provide the $SiCl_3^-$ anion.[39] In combination with a good leaving group this has already been reported for Si–Si coupling by trichlorosilylation of trimethylsilyltriflate,[40] but the Benkeser system has hitherto not been evaluated electrochemically. As ^1H NMR data reveals a 1:1 mixture of $HSiCl_3$ and nBu_3N deprotonates 50% of $HSiCl_3$ forming an equilibrium at room temperature with broadening of the nBu_3N-H^+ signal, indicating high proton mobility at the ammonium cation. The arising ^{29}Si NMR chemical shift of 29.6 ppm agrees with previously reported data for $SiCl_3^-$.[32,41] For the use as additive in electrochemical synthesis the anodic stability of the respective amine needs to exceed that of the $SiCl_3^-$ formed, to avoid amine overoxidation and shift of the equilibrium reaction off $SiCl_3^-$. CV measurements show oxidation of nPr_3N and nBu_3N with an irreversible oxidation peak at 0.48 V vs. FcH/FcH^+ in absence of $HSiCl_3$ at GC electrodes. By addition of $HSiCl_3$ the original oxidation current declines due to amine protonation and a second oxidation peak at 0.68 V vs. FcH/FcH^+ arises (Figure 5). This indicates the formation of oxidizable $SiCl_3^-$ accompanied by a broad oxidation wave at about 1.17 V vs. FcH/FcH^+ most likely correlating with further oxidation of the chlorosilane species. The amine oxidation is electrochemically favored compared to the oxidation of $SiCl_3^-$ anion. A shift of the oxidation potential of tertiary amines to higher anodic values does not occur for more sterically hindered species as nOc_3N, but for less basic ones like Ph_3N. CV measurement data agree with previously reported data,[42] yet the increasing oxidative stability does not suffice the oxidation potential of $SiCl_3^-$. Further, the low basicity prevents the proton abstraction as NMR and CV data reveal. Due to their high basicity, amines suitable for proton abstraction at $HSiCl_3$ disproportionate Si_2Cl_6 forming higher oligosilanes depending on reaction temperature under the release of $SiCl_4$, as already described in the literature,[43] even in the presence of a 10-fold excess of $HSiCl_3$.

Besides reductive and oxidative dimerization, the possibility of a mediated radical pathway is examined. Through hydrogen-atom-transfer (HAT) mediators a coupled one-electron one-proton abstraction of a substrate is possible, generating a radical intermediate.[44] N-Hydroxyphthalimide (NHPI) is known as electrochemical HAT mediator by oxidation to the phthalimide-N-oxyl (PINO) radical.[45] Recently, Liang and co-workers selectively oxidized electron-rich H-silanes to the respective silanols in aqueous MeCN by NHPI / PINO HAT mediator.[46] Their investigation indicates consecutive oxidation of the arising silyl radical intermediate to cationic SiR_3^+ and subsequent reaction with water to form the desired silanol. Own results showing no increase of disilane by radical dimerization in a water-free NHPI mediated system, support the suggested cationic pathway. By exchanging the H-silane substrate to $HSiCl_3$, cathodic polymerization with similar product distribution to the unmediated anodic dehydrogenation occurs in synthesis. This indicates a favored reduction of $HSiCl_3$ compared to oxidation of NHPI. Further the high oxophilicity precludes the N-oxyl radical mediated pathway for chlorosilane compounds to Si_2Cl_6 as NMR measurements show. Pietschnig and co-workers reported the respective ^{29}Si NMR chemical shift arising by Si–O bond formation of TEMPO and $SiCl_4$ to the respective TEMPO-$SiCl_3$ to be −30.6 ppm.[47] Results obtained for Si_2Cl_6 agree and feature preferential TEMPO-$SiCl_3$ formation in presence of N-oxyl radical. Additional HAT mediators as bicyclic tertiary amines like quinuclidine and DABCO disproportionate

ChemElectroChem
Research Article
doi.org/10.1002/celc.202101374
Chemistry Europe
European Chemical Societies Publishing

Si_2Cl_6 with cleavage of $SiCl_4$ analog to the reaction with tertiary amines of Benkeser systems. The high oxophilicity and reactivity with Lewis bases of Si_2Cl_6 and the very likely cationic pathway due to the easy oxidizability of a resulting radical represent the hurdles for the mediated pathway to the desired dimerization.

Conclusion

As outlined, the electrochemical route to Si_2Cl_6 shows significant challenges that need to be overcome. For the reductive pathway an elongated silicon backbone lowers the reduction potential. Thus, a Si–Si bond formation does not stop at Si_2Cl_6 but generates a polymeric coating at the cathode. Furthermore, Si_2Cl_6 is not stable against the released halogenide ions. The oxidative pathway requires harsh conditions, due to high anodic stability of $HSiCl_3$. While all experimental data suggest a cationic pathway with the need of cathodic access for $SiCl_3^+$ to Si–Si bond formation, the cathodic access leads to over-reduction of $HSiCl_3$ to a polymeric coating at the cathode with blockage of the targeted H^+ reduction. High Lewis acidity of $HSiCl_3$, low stability of Si_2Cl_6 towards Lewis basic amines and easier oxidation of amines than $SiCl_3^-$ prevent the described methods for Si–H bond activation.

In conclusion, the electrochemical synthesis of Si_2Cl_6 starting from chlorosilanes is very prone to over-reduction. Consecutive release of halogenides prevents the accumulation of Si_2Cl_6 due to oligomerization. In addition, the anodic oxidation of the Si–H bond in silanes by various strategies also does not lead to the desired disilane. While there is an urgent need for an environmentally benign access to Si_2Cl_6, several challenges need to be overcome. The most promising option might be a halide-free dimerization pathway with Si–H bond activation.

Experimental Section

Detailed information on general procedures, electrochemical conversions, cyclic voltammetry measurements and product characterization can be found in the Supporting Information.

Acknowledgements

Open Access funding enabled and organized by Projekt DEAL.

Conflict of Interest

The authors declare no conflict of interest.

Keywords: Dehalogenation · Dimerization · Oxidation · Reductive coupling · Silicon

[1] C. Martin, *Nat. Nanotechnol.* **2016**, *11*, 112.
[2] R. A. Ovanesyan, E. A. Filatova, S. D. Elliott, D. M. Hausmann, D. C. Smith, S. Agarwal, *J. Vac. Sci. Technol. A* **2019**, *37*, 60904.
[3] a) R. A. Ovanesyan, D. M. Hausmann, S. Agarwal, *ACS Appl. Mater. Interfaces* **2018**, *10*, 19153–19161; b) R. A. Ovanesyan, N. Leick, K. M. Kelchner, D. M. Hausmann, S. Agarwal, *Chem. Mater.* **2017**, *29*, 6269–6278; c) K. Park, W.-D. Yun, B.-J. Choi, H.-D. Kim, W.-J. Lee, S.-K. Rha, C. O. Park, *Thin Solid Films* **2009**, *517*, 3975–3978; d) R. C. Taylor, B. A. Scott, *J. Electrochem. Soc.* **1989**, *136*, 2382–2386.
[4] a) L. Du, W. Chu, H. Miao, D. Wang, C. Xu, Y. Ding, *Eur. J. Inorg. Chem.* **2015**, *2015*, 3205–3211; b) R. A. Ovanesyan, D. M. Hausmann, S. Agarwal, *ACS Appl. Mater. Interfaces* **2015**, *7*, 10806–10813; c) A. M. Wrobel, A. Walkiewicz-Pietrzykowska, I. Blaszczyk-Lezak, *Appl. Organomet. Chem.* **2010**, *24*, 201–207.
[5] a) G. Martin, *J. Chem. Soc. Trans.* **1914**, *105*, 2836–2860; b) A. Stock, A. Brandt, H. Fischer, *Ber. Dtsch. Chem. Ges. A* **1925**, *58*, 643–657; c) G. Urry, *J. Inorg. Nucl. Chem.* **1964**, *26*, 409–414.
[6] a) T. Hattori, M. Ito, Y. Miwa (Toagosei Chemical Industry Co., Ltd.), DE3623493 A1, **1986**; b) PSC Polysilane Chemicals GmbH (PSC Polysilane Chemicals GmbH), DE102014007767 A1, **2014**.
[7] a) N. Auner, C. Bauch, R. Deltschew, T. Gebel, S. Holl, G. Lippold, J. A. S. Mohsseni (REV Renewable Energy Ventures Inc.), DE102009056438 A1, **2010**; b) PSC Polysilane Chemicals GmbH (PSC Polysilane Chemicals GmbH), DE102014007685 A1, **2014**.
[8] Z. Yang, T. Kang, Y. Ji, J. Li, Y. Zhu, H. Liu, X. Jiang, Z. Zhong, F. Su, *J. Colloid Interface Sci.* **2021**, *589*, 198–207.
[9] a) M. K. Nazeeruddin, *Nature* **2016**, *538*, 463–464; b) S. Yadav, K. Chattopadhyay, C. V. Singh, *Renewable Sustainable Energy Rev.* **2017**, *78*, 1288–1314.
[10] a) P. Anastas, N. Eghbali, *Chem. Soc. Rev.* **2010**, *39*, 301–312; b) S. R. Waldvogel, B. Janza, *Angew. Chem. Int. Ed.* **2014**, *53*, 7122–7123; *Angew. Chem.* **2014**, *126*, 7248–7249; c) Y. Yuan, A. Lei, *Nat. Commun.* **2020**, *11*, 802.
[11] D. Pollok, S. R. Waldvogel, *Chem. Sci.* **2020**, *11*, 12386–12400.
[12] J. Seidler, J. Strugatchi, T. Gärtner, S. R. Waldvogel, *MRS Energy Sustainability* **2020**, *7*, E42.
[13] S. Möhle, M. Zirbes, E. Rodrigo, T. Gieshoff, A. Wiebe, S. R. Waldvogel, *Angew. Chem. Int. Ed.* **2018**, *57*, 6018–6041; *Angew. Chem.* **2018**, *130*, 6124–6149.
[14] a) M. D. Kärkäs, *Chem. Soc. Rev.* **2018**, *47*, 5786–5865; b) R. D. Little, K. D. Moeller, *Chem. Rev.* **2018**, *118*, 4483–4484; c) S. R. Waldvogel, S. Lips, M. Selt, B. Riehl, C. J. Kampf, *Chem. Rev.* **2018**, *118*, 6706–6765; d) A. Wiebe, T. Gieshoff, S. Möhle, E. Rodrigo, M. Zirbes, S. R. Waldvogel, *Angew. Chem. Int. Ed.* **2018**, *57*, 5594–5619; *Angew. Chem.* **2018**, *130*, 5694–5721; e) M. Yan, Y. Kawamata, P. S. Baran, *Chem. Rev.* **2017**, *117*, 13230–13319.
[15] J. L. Röckl, D. Pollok, R. Franke, S. R. Waldvogel, *Acc. Chem. Res.* **2020**, *53*, 45–61.
[16] E. J. Horn, B. R. Rosen, P. S. Baran, *ACS Cent. Sci.* **2016**, *2*, 302–308.
[17] E. Hengge, G. Litscher, *Angew. Chem. Int. Ed.* **1976**, *15*, 370; *Angew. Chem.* **1976**, *88*, 414.
[18] a) A. Kunai, T. Kawakami, E. Toyoda, M. Ishikawa, *Organometallics* **1991**, *10*, 2001–2003; b) J. Ohshita, K. Hino, T. Iwawaki, A. Kunai, *J. Organomet. Chem.* **2009**, *625*, 138–143.
[19] C. Grogger, B. Loidl, H. Stueger, T. Kammel, B. Pachaly, *J. Organomet. Chem.* **2006**, *691*, 105–110.
[20] E. Hengge, H. Firgoi, *J. Organomet. Chem.* **1981**, *212*, 155–161.
[21] A. Kunai, T. Kawakami, E. Toyoda, M. Ishikawa, *Organometallics* **1991**, *10*, 893–895.
[22] C. Jammegg, S. Graschy, E. Hengge, *Organometallics* **1994**, *13*, 2397–2400.
[23] a) M. Bordeau, C. Biran, M.-P. Léger-Lambert, J. Dunoguès, *J. Chem. Soc. Chem. Commun.* **1991**, 1476–1477; b) M. Elangovan, A. Muthukumaran, M. Anbu Kulandainathan, *Eur. Polym. J.* **2005**, *41*, 2450–2460; c) M. Ishifune, S. Kashimura, Y. Kogai, Y. Fukuhara, T. Kato, H.-B. Bu, N. Yamashita, Y. Murai, H. Murase, R. Nishida, *J. Organomet. Chem.* **2000**, *611*, 26–31; d) A. Kunai, E. Toyoda, T. Kawakami, M. Ishikawa, *Organometallics* **1992**, *11*, 2899–2903; e) M. Umezawa, H. Ichikawa, T. Ishikawa, T. Nonaka, *Denki Kagaku (1961–1998)* **1991**, *59*, 421–426; f) M. Umezawa, M. Takeda, H. Ichikawa, T. Ishikawa, T. Koizumi, T. Fuchigami, T. Nonaka, *Electrochim. Acta* **1990**, *35*, 1867–1872; g) M. Umezawa, M. Takeda, H. Ichikawa, T. Ishikawa, T. Koizumi, T. Nonaka, *Electrochim. Acta* **1991**, *36*, 621–624.
[24] a) M. Okano, H. Fukai, M. Arakawa, H. Hamano, *Electrochem. Commun.* **1999**, *1*, 223–226; b) M. Okano, K. Nakamura, K. Yamada, N. Hosoda, M. Wasaka, *Electrochemistry* **2006**, *74*, 956–958; c) A. Watanabe, T. Komatsu-

ChemElectroChem
Research Article
doi.org/10.1002/celc.202101374
Chemistry Europe
European Chemical Societies Publishing

bara, M. Matsuda, Y. Yoshida, S. Tagawa, *J. Photopolym. Sci. Technol.* **1992**, *5*, 545–546.
[25] E. Hengge, G. Litscher, *Monatsh. Chem.* **1978**, *109*, 1217–1225.
[26] Y. Tsuyuki, T. Fujimura, M. Kunimoto, Y. Fukunaka, P. Pianetta, T. Homma, *J. Electrochem. Soc.* **2017**, *164*, D994–D998.
[27] T. Munisamy, A. J. Bard, *Electrochim. Acta* **2010**, *55*, 3797–3803.
[28] S. Aihara, R. Ishii, M. Fukuhara, N. Kamata, D. Terunuma, Y. Hirano, N. Saito, M. Aramata, S. Kashimura, *J. Non-Cryst. Solids* **2001**, *296*, 135–138.
[29] a) Y. Kimata, H. Suzuki, S. Satoh, A. Kuriyama, *Organometallics* **1995**, *14*, 2506–2511; b) Y. Kimata, H. Suzuki, S. Satoh, A. Kuriyama, *Chem. Lett.* **1994**, *23*, 1163–1164.
[30] A. Kunai, T. Kawakami, E. Toyoda, T. Sakurai, M. Ishikawa, *Chem. Lett.* **1993**, *22*, 1945–1948.
[31] A. H. Schmidt, M. Russ, *Chem. Ber.* **1981**, *114*, 1099–1110.
[32] J. Tillmann, L. Meyer, J. I. Schweizer, M. Bolte, H.-W. Lerner, M. Wagner, M. C. Holthausen, *Chem. Eur. J.* **2014**, *20*, 9234–9239.
[33] a) S. Lips, S. R. Waldvogel, *ChemElectroChem* **2019**, *6*, 1649–1660; b) N. Yang, S. Yu, J. V. Macpherson, Y. Einaga, H. Zhao, G. Zhao, G. M. Swain, X. Jiang, *Chem. Soc. Rev.* **2019**, *48*, 157–204; c) S. R. Waldvogel, S. Mentizi, A. Kirste in *Radicals in Synthesis III*; (Eds. M. Heinrich, A. Gansäuer), Springer Berlin Heidelberg, Berlin, Heidelberg, **2012**, pp. 1–31.
[34] a) Parks, Blackwell, Piers, *J. Org. Chem.* **2000**, *65*, 3090–3098; b) W. E. Piers, A. J. V. Marwitz, L. G. Mercier, *Inorg. Chem.* **2011**, *50*, 12252–12262.
[35] a) E. J. Lawrence, R. J. Blagg, D. L. Hughes, A. E. Ashley, G. G. Wildgoose, *Chem. Eur. J.* **2015**, *21*, 900–906; b) Y. M. Lee, J. E. Seo, N.-S. Choi, J.-K. Park, *Electrochim. Acta* **2005**, *50*, 2843–2848.
[36] T. Hackel, N. A. McGrath, *Molecules* **2019**, *24*, 432.
[37] E. J. Lawrence, V. S. Oganesyan, D. L. Hughes, A. E. Ashley, G. G. Wildgoose, *J. Am. Chem. Soc.* **2014**, *136*, 6031–6036.
[38] A. Šimarek, M. Lamač, M. Horáček, J. Pinkas, *Appl. Organomet. Chem.* **2018**, *32*, e4442.
[39] a) R. A. Benkeser, *Pure Appl. Chem.* **1966**, *13*, 133–140; b) R. A. Benkeser, *Acc. Chem. Res.* **1971**, *4*, 94–100; c) R. A. Benkeser, K. M. Foley, J. M. Gaul, G. S. H. Li, W. E. Smith, *J. Am. Chem. Soc.* **1969**, *91*, 4578–4579; d) R. A. Benkeser, J. M. Gaul, W. E. Smith, *J. Am. Chem. Soc.* **1969**, *91*, 3666–3667; e) S. C. Bernstein, *J. Am. Chem. Soc.* **1970**, *92*, 699–700; f) H. Schmidbaur, J. Ebenhöch, *Z. Naturforsch. B* **1986**, *41*, 1527–1534.
[40] W. Uhlig, A. Tzschach, *Z. Chem.* **1989**, *29*, 335–336.
[41] S. B. Choi, B. K. Kim, P. Boudjouk, D. G. Grier, *J. Am. Chem. Soc.* **2001**, *123*, 8117–8118.
[42] E. T. Seo, R. F. Nelson, J. M. Fritsch, L. S. Marcoux, D. W. Leedy, R. N. Adams, *J. Am. Chem. Soc.* **1966**, *88*, 3498–3503.
[43] a) A. Kaczmarczyk, M. Millard, J. W. Nuss, G. Urry, *J. Inorg. Nucl. Chem.* **1964**, *26*, 421–425; b) A. Kaczmarczyk, G. Urry, *J. Inorg. Nucl. Chem.* **1964**, *26*, 415–420; c) A. Kaczmarczyk, G. Urry, *J. Am. Chem. Soc.* **1960**, *82*, 751–752; d) G. Urry, *Acc. Chem. Res.* **1970**, *3*, 306–312.
[44] F. Wang, S. S. Stahl, *Acc. Chem. Res.* **2020**, *53*, 561–574.
[45] M. Masui, T. Ueshima, S. Ozaki, *J. Chem. Soc. Chem. Commun.* **1983**, 479–480.
[46] H. Liang, L.-J. Wang, Y.-X. Ji, H. Wang, B. Zhang, *Angew. Chem. Int. Ed.* **2021**, *60*, 1839–1844; *Angew. Chem.* **2021**, *133*, 1867–1872.
[47] S. Stefan, F. Belaj, T. Madl, R. Pietschnig, *Eur. J. Inorg. Chem.* **2010**, *2010*, 289–297.

Manuscript received: October 11, 2021
Revised manuscript received: November 10, 2021
Accepted manuscript online: November 23, 2021

ChemElectroChem

Supporting Information

Challenges in the Electrochemical Synthesis of Si_2Cl_6 Starting from Tetrachlorosilane and Trichlorosilane

Alexander D. Beck, Stefan Haufe, Jan Tillmann, and Siegfried R. Waldvogel*

Contents

General Information

All reagents were of analytical grade and obtained from commercial suppliers such as Aldrich, VWR, and Acros. Solvents were obtained in anhydrous quality and water content was checked by Karl-Fischer titration. Electrochemical reactions were carried out at boron-doped diamond (BDD), glassy carbon (GC), platinum (Pt) and dimension stabile anodes (DSA) with ruthenium-/ iridiumoxide electrodes on tantal as support. BDD electrodes were obtained as DIACHEM™ quality (CONDIAS GmbH, Itzehoe, Germany). BDD (10 µm diamond layer) was used on silicon as support. GC and Pt electrodes were obtained from IKA (IKA-Werke GmbH & Co. KG, Staufen, Germany). The dimensions of all used electrode materials were 7 cm x 1 cm x 0.3 cm.

Gas chromatography was performed on an Agilent GC-A6890N (Agilent, Santa Clara, California, USA) using a RTX200 column (Agilent Technologies, Santa Clara, California, USA), length: 60 m + 30 m, inner diameter: 2 x 0.32 mm, film: 0.25 µm, carrier gas: helium. **GC-MS** measurements were carried out on an Agilent GC-A6890N using a HP-5 column (Agilent Technologies, Santa Clara, California), length: 30 m, inner diameter: 0.25 mm, film: 0.25 µm, carrier gas: helium. The chromatograph was coupled to a mass spectrometer Agilent MSD 5975 C (Agilent, Santa Clara, California, USA).

NMR Spectroscopy of ^{1}H, ^{13}C and ^{29}Si spectra were recorded at 25 °C, using a Bruker Avance 500 (500 MHz, Analytische Messtechnik, Karlsruhe, Germany). Chemical shifts (δ) are reported in parts per million (ppm). Traces of CH_2Cl_2 in the corresponding deuterated solvent, or tetramethylsilane for ^{29}Si spectra were used as internal standard for calibration.

Cyclic voltammetry was performed under inert gas in a 20 mL glass vial (SVC-3 voltammetry cell, ALS Co., Ltd., Tokyo, Japan) equipped with an SP-300 potentiostat (Bio-Logic Science Instruments, Seyssinet-Pariset, France) *WE*: GC / Pt electrode tip, 1.6 mm diameter; *CE*: platinum wire; *RE*: Ag/Ag^+ in 0.01 M $AgNO_3$ / 0.1 M Bu_4NClO_4. Solvent: MeCN. v = 200 mV/s, T = 25 °C, supporting electrolyte: $n$$Bu_4NClO_4$, c ($n$$Bu_4NClO_4$) = 0.1 M.

Energy-dispersive X-ray Spectroscopy (EDX) was carried out with an Oxford X-Max 80N (Oxford Instruments, Abingdon, United Kingdom). Compound composition was analyzed by testing several particles and stochastic evaluation.

1 Set-up and general protocols for electrochemical synthesis

GP1: Undivided Cell

For screening experiments undivided (5mL) PTFE cells for electrolysis with reaction block, stirrer, power supply were obtained as IKA Screening System (IKA-Werke GmbH & Co. KG, Staufen, Germany). The active surface of the respective used electrode was 1.3 cm^2, anode and cathode surface were apart by 0.5 cm. The software used was IKA Labworldsoft 6.0

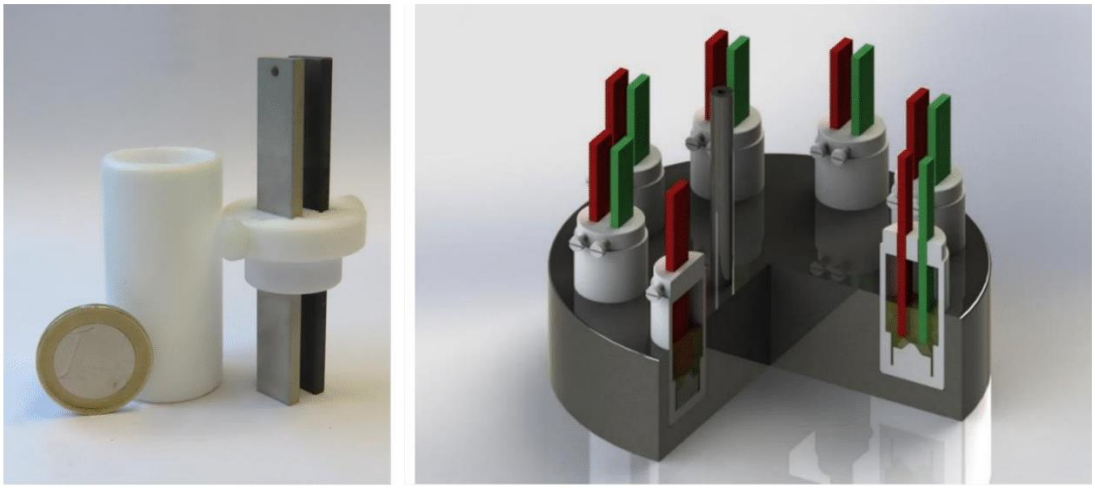

Figure 1: 5 mL PTFE cell; left: with 1 Euro coin for size comparison; right: schematic visualization of 5 mL PTFE cells in a screening block.

GP2: Divided Cell

For screening experiments divided (8mL for anolyte and catholyte compartment, respectively) cells for electrolysis were used. Anolyte and catholyte were separated by a porous glass frit sealed by an EPDM ring. Additionally, reaction block, stirrer, power supply was obtained as IKA Screening System (IKA-Werke GmbH & Co. KG, Staufen, Germany). The active surface of the respective used electrode was 3.0 cm^2, anode and cathode surface were separated by 2.0 cm, including the glass frit separator. The software used was IKA Labworldsoft 6.0

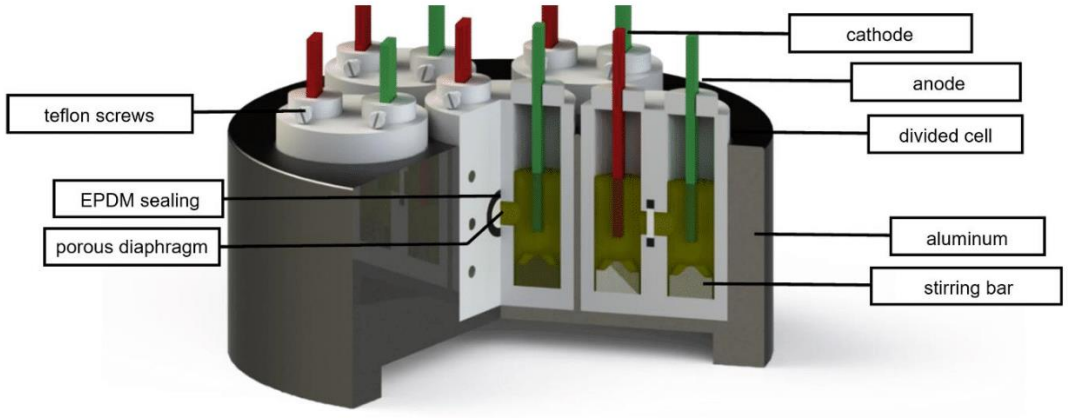

Figure 2: Screening system with 6 divided electrolysis cells fitting on a common magnetic stirrer; electrode gap: 2 cm; active surface of each planar electrode: 3.0 cm^2; dimensions of electrodes: (7.0 x 1.0 x 0.3) cm.

The general procedure for temperature controlled chlorosilane syntheses was cooling the reaction block with cells by a stainless-steel cooling plate, inserted between reaction block and magnetic stirrer, with a cryostat (Julabo Presto LH85, JULABO GmbH, Seelbach, Germany) until the reaction block reached the desired temperature for 15 min and then to place the electrolyte in the respective PTFE cell unit. The appropriate chlorosilane was added to the cooled reaction solution and electrolysis was started. After application of the desired charge quantity the reaction was stopped.
Product distribution was determined by direct ^{1}H and ^{29}Si NMR spectroscopy of samples of 300 µL of the reaction solution with a reference of 50 µL tetramethylsilane (TMS). For ^{29}Si NMR spectroscopy an additive of 8 mg $Cr(acac)_3$ as paramagnetic reagent for enhanced longitudinal relaxation was used.
The general workup protocol consisted of stripping off volatile compounds, filtration with pentane as eluent and vacuum distillation of the products. Polysilane compounds in the residue were washed with acetonitrile to remove the supporting electrolyte and dried under vacuum.

2 General cyclic voltammetry protocol

The complete set-up was used in a glovebox under argon as inert atmosphere (<0.1 ppm O_2 and <0.1 ppm H_2O content), so no further degassing of the solvent was necessary. Acetonitrile (water content <10 ppm, checked by Karl-Fischer titration) containing 0.1 M Bu_4NClO_4 or 0.1 M Bu_4NCl as supporting electrolyte was placed in a 20 mL glass vial. Cyclic voltammetry was performed with a sweep rate of 0.2 V/s otherwise noted, using glassy carbon or platinum working electrode (tip, 1.6 mm diameter, each), a platinum wire as counter electrode and an Ag/Ag^+ reference electrode in 0.01 M $AgNO_3$ / 0.1 M Bu_4NClO_4 acetonitrile solution. Ferrocene/Ferrocenium (FcH/FcH^+) was used as internal reference (half-wave potential 0.09 V vs. Ag/Ag^+).

3 Results for the electrochemical screening reactions

The electrochemical screening reactions of chlorosilanes were carried out via GP2 in divided cells. Screening experiments of Me_2PhSiH was performed in undivided cells (GP1). Conversion was evaluated relative to TMS based on ^{29}Si NMR integrals.

3.1 Anode material for $HSiCl_3$ oxidation

For the anodic dehydrogenative oxidation under constant current conditions, $HSiCl_3$ (1.69 g, 12.5 mmol) is used as substrate and dissolved in 7.0 mL electrolyte, consisting of a solution of acetonitrile with 0.2 M Bu_4NClO_4, in the anolyte cell unit. 8.0 mL electrolyte is used in the cathodic cell compartment and a platinum electrode is used as cathode material. The reaction is performed at 10 °C. A charge quantity of 1.0 *F* was passed with a charge density of 5.0 mA/cm^2, unless otherwise noted.

Table S1. Screening of anode materials for dehydrogenative oxidation of $HSiCl_3$.

Entry	Anode material	*Q* [*F*]	Yield of $SiCl_4$[a]	Yield of Si_2OCl_6[a]	Anode alteration
1	BDD	1.0	9%	2%	-
2	Glassy carbon	1.0	7%	-	-
3	Platinum	1.0	10%	-	Corrosion
4	DSA	0.2[b]	-	-	Corrosion

Constant current electrolysis of $HSiCl_3$ in divided PTFE cells. [a] Quantification of the yield of anolyte compartment was performed by ^{29}Si NMR relative to tetramethylsilane as internal standard. [b] After 0.2 *F* current density declines and electrolysis is stopped. *Q*: charge quantity.

3.2 Electrolyte composition for $HSiCl_3$ oxidation

For the anodic dehydrogenative oxidation under constant current conditions, $HSiCl_3$ (1.69 g, 12.5 mmol) is used as substrate, platinum as cathode and BDD as anode material. 0.2 M solution of supporting electrolyte is used at 10°C. A charge quantity of 1.0 *F* was passed with a charge density of 5.0 mA/cm^2, unless otherwise noted.

Table S2. Screening of electrolyte composition for dehydrogenative oxidation of $HSiCl_3$.

Entry	Solvent	Supporting Electrolyte	*j* [mA cm^{-2}]	Yield of $SiCl_4$[a]	Yield of Si_2OCl_6[a]
1	MeCN	Bu_4NClO_4	5.0	9%	2%
2	DCM[b]	Bu_4NClO_4	3.0[c]	11%	1%
3	MeCN	$MeEt_3NMeSO_4$	5.0	3%[d]	-
4	DME	Bu_4NClO_4	1.0[c]	5%[d]	-

Constant current electrolysis of $HSiCl_3$ in divided PTFE cells. [a] Quantification of the yield within anolyte compartment was performed by ^{29}Si NMR relative to tetramethylsilane as internal standard. [b] DCM used for anolyte compartment, MeCN used for catholyte compartment. [c] Limited by conductivity due to power supply instrument maximum. [d] Formation due to disproportionation of $HSiCl_3$. *j*: current density.

3.3 Charge quantity, current density, and $B(C_6F_5)_3$ concentration for $HSiCl_3$ oxidation

For the anodic dehydrogenative oxidation under constant current conditions, $HSiCl_3$ (1.69 g, 12.5 mmol) is used as substrate, platinum as cathode and BDD as anode material. A 0.2 M solution of acetonitrile with Bu_4NClO_4 as supporting electrolyte at 10 °C. The amount of additional $B(C_6F_5)_3$ was varied.

Table S3. Screening of charge quantity, current density, and $B(C_6F_5)_3$ concentration for dehydrogenative oxidation of $HSiCl_3$.

Entry	*Q* [*F*]	*j* [mA cm^{-2}]	$B(C_6F_5)_3$ [mol%]	Yield of $SiCl_4$[a]	Yield of Si_2OCl_6[a]
1[b]	1.0	15[d]	-	7%	1%
2[b]	1.0	10	-	11%	2%
3[b]	1.0	6.7	-	9%	2%
4[b]	1.0	5.0	-	9%	2%
5[b]	0.5	3.3	-	4%	1%
6[b]	1.0	3.3	-	10%	2%
7[b]	1.5	3.3	-	11%	2%
8[c]	1.0	10	5%	6%	2%
9[c]	1.0	10	10%	3%	1%

Constant current electrolysis of $HSiCl_3$ in divided PTFE cells. [a] Quantification of the yield of anolyte compartment was performed by ^{29}Si NMR relative to tetramethylsilane as internal standard. [b] Divided cell compartments (GP2). [c] Undivided cell compartments (GP1). [d] Limited by conductivity due to power supply instrument maximum. *Q*: charge quantity. *j*: current density.

3.4 Charge quantity, current density, and $B(C_6F_5)_3$ concentration for Me_2PhSiH oxidation

As model system, the anodic dehydrogenative oxidation of Me_2PhSiH under constant current conditions was used. Me_2PhSiH (2.1 mmol) was used as substrate, platinum as cathode and platinum or glassy carbon as anode material. A 0.12 M solution of 1,2-dimethoxyethan with Bu_4NClO_4 as supporting electrolyte was used at room temperature. The amount of additional $B(C_6F_5)_3$ was varied. Undivided cells were used (GP1).

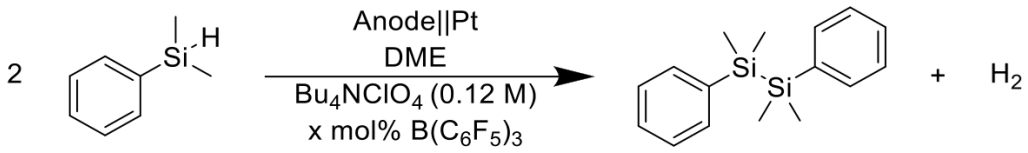

Scheme 1: Oxidative Si-Si-bond formation for Me_2PhSiH.

Table S4. Screening of charge quantity, current density, and $B(C_6F_5)_3$ concentration for dehydrogenative oxidation of Me_2PhSiH.

Entry	*Q* [*F*]	*j* [mA cm^{-2}]	$B(C_6F_5)_3$ [mol%]	Anode	Yield of Si-Si[a]	Yield of Si-O-Si[a]
1	1.5	5.0	2.5	GC	3%	12%
2	1.5	5.0	5.0	GC	1%	21%
3	1.5	5.0	7.5	GC	1%	28%
4	1.5	2.5	2.5	GC	6%	11%
5	1.5	7.5	2.5	GC	1%	13%
6	1.5	10	2.5	GC	-	11%
7	1.5	5.0	2.5	Pt	3%	14%
8	1.5	5.0	5.0	Pt	2%	20%
9	1.5	5.0	7.5	Pt	2%	25%
10	1.5	2.5	2.5	Pt	2%	13%
11	1.5	7.5	2.5	Pt	2%	10%
13	1.5	10	2.5	Pt	4%	14%
14	1.8	10	2.5	Pt	6%	14%
15	2.0	10	2.5	Pt	7%	15%

Constant current electrolysis of $HSiCl_3$ in divided PTFE cells. [a] Quantification was performed by ^{29}Si NMR relative to tetramethylsilane as internal standard. *Q*: charge quantity. *j*: current density.

4 Cyclic voltammetry data

4.1 Reduction of $SiBr_4$ in comparison to $SiCl_4$

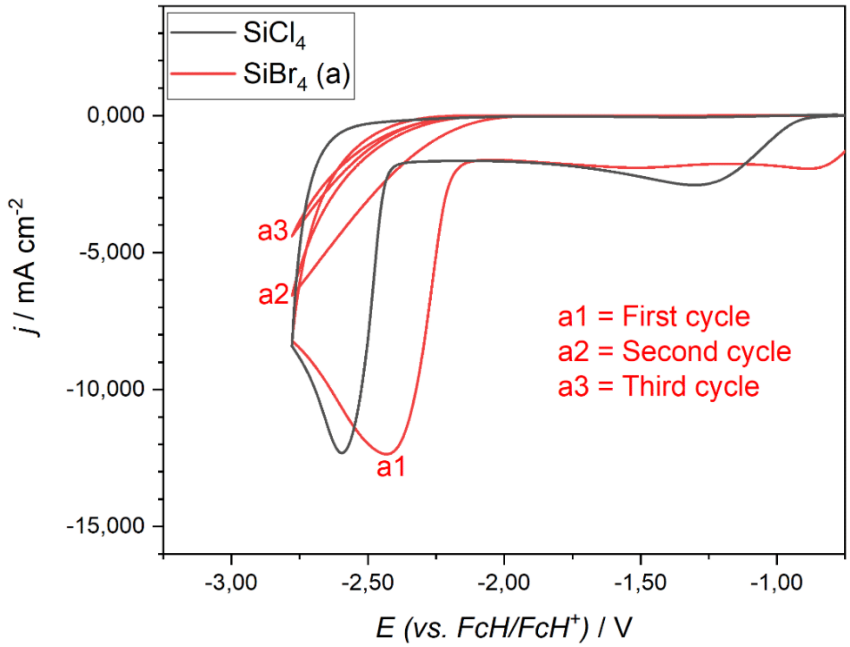

Figure 3: Cyclic voltammogram of 20 mM $SiCl_4$ in 0.1 M Bu_4NCl and MeCN in comparison to 20 mM $SiBr_4$ in 0.1 M Bu_4NBr and MeCN. W.E. Pt (A = 8.0 mm²), *v* = 0.1 V/s, $SiCl_4$: first cycle. Peak potential of $SiCl_4$: −1.38 V vs. FcH/FcH⁺ (wave) and −2.60 V vs. FcH/FcH⁺. Peak potential of $SiBr_4$: −2.43 V vs. FcH/FcH⁺.

4.2 Oxidation of H-Silanes

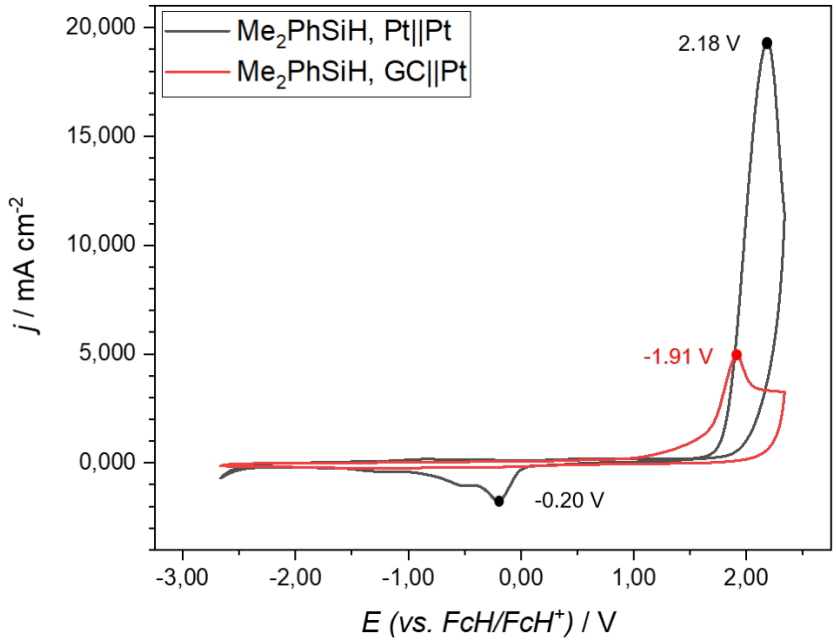

Figure 4: Cyclic voltammogram of 20 mM Me_2PhSiH in 0.1 M Bu_4NClO_4 and MeCN. W.E. Pt (A = 8.0 mm²) or GC (A = 8.0 mm²), v = 0.2 V/s, first cycle each. Peak potential at Pt electrode: 2.18 V vs. FcH/FcH⁺ and −0.20 V vs. FcH/FcH⁺. Peak potential at GC electrode: 1.91 V vs. FcH/FcH⁺.

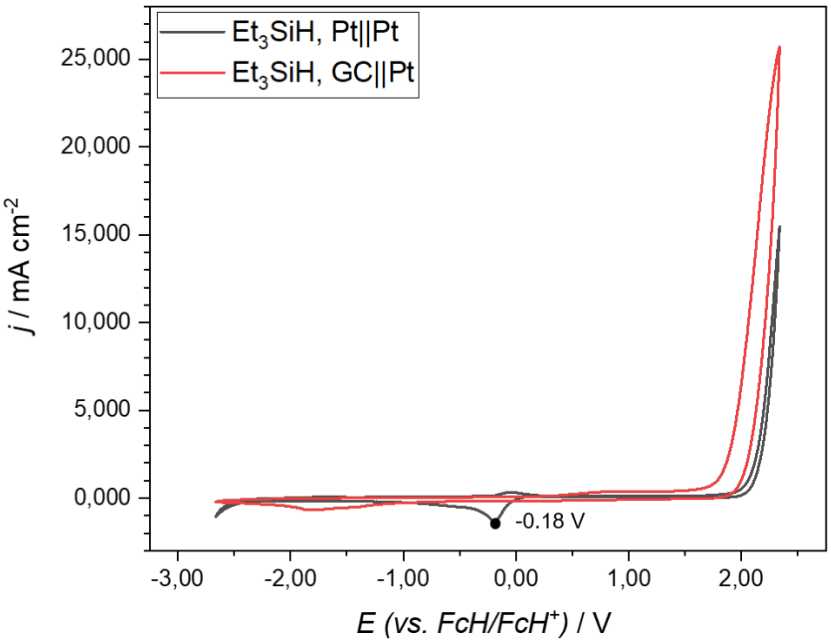

Figure 5: Cyclic voltammogram of 20 mM Et_3SiH in 0.1 M Bu_4NClO_4 and MeCN. W.E. Pt (A = 8.0 mm²) or GC (A = 8.0 mm²), *v* = 0.2 V/s, first cycle each. Peak potential at Pt electrode: –0.18 V vs. FcH/FcH⁺.

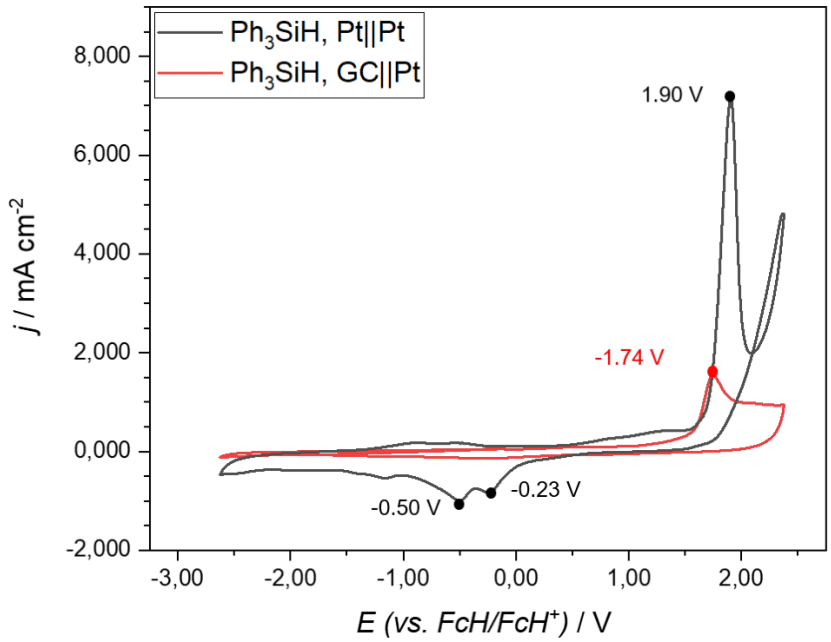

Figure 6: Cyclic voltammogram of 20 mM Ph_3SiH in 0.1 M Bu_4NClO_4 and MeCN. W.E. Pt (A = 8.0 mm²) or GC (A = 8.0 mm²), *v* = 0.2 V/s, first cycle each. Peak potential at Pt electrode: 1.90 V vs. FcH/FcH⁺ and –0.23 V vs. FcH/FcH⁺ and –0.50 V vs. FcH/FcH⁺. Peak potential at GC electrode: 1.74 V vs. FcH/FcH⁺.

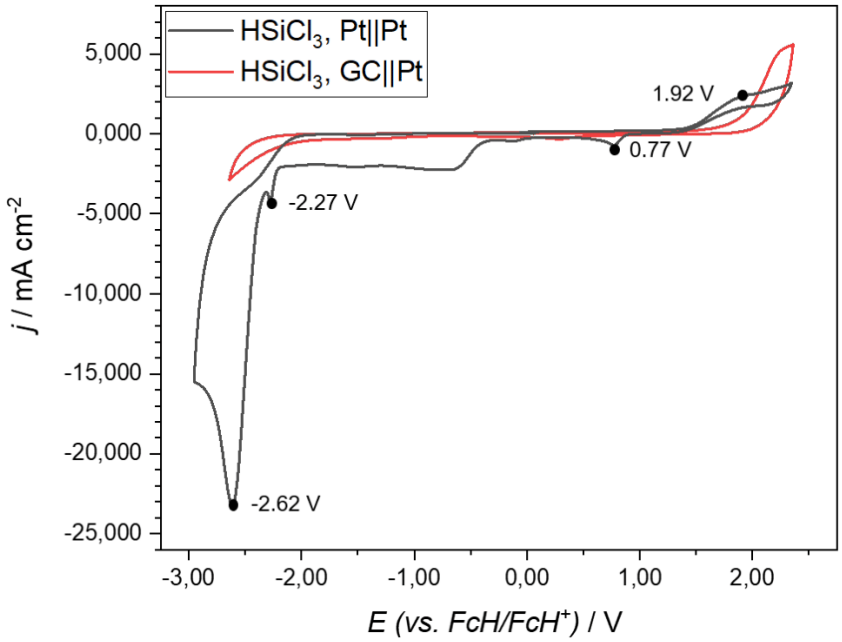

Figure 7: Cyclic voltammogram of 20 mM $HSiCl_3$ in 0.1 M Bu_4NClO_4 and MeCN. W.E. Pt (A = 8.0 mm²) or GC (A = 8.0 mm²), *v* = 0.2 V/s, first cycle each. Peak potential at Pt electrode: 1.92 V vs. FcH/FcH⁺ (wave) and 0.77 V vs. FcH/FcH⁺ and −2.27 V vs. FcH/FcH⁺ and −2.62 V vs. FcH/FcH⁺.

4.3 Oxidative cleavage of Si-Si-bond

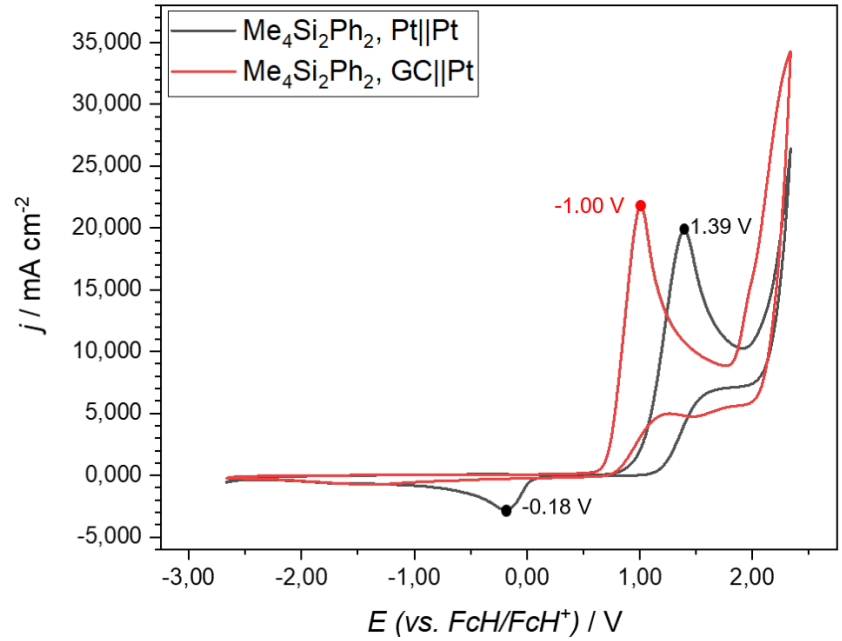

Figure 8: Cyclic voltammogram of 20 mM $Me_4Si_2Ph_2$ in 0.1 M Bu_4NClO_4 and MeCN. W.E. Pt (A = 8.0 mm²) or GC (A = 8.0 mm²), *v* = 0.2 V/s, first cycle each. Peak potential at Pt electrode: 1.39 V vs. FcH/FcH⁺ and −0.18 V vs. FcH/FcH⁺. Peak potential at GC electrode: 1.00 V vs. FcH/FcH⁺.

4.4 Si-H activation by Lewis acid $B(C_6F_5)_3$

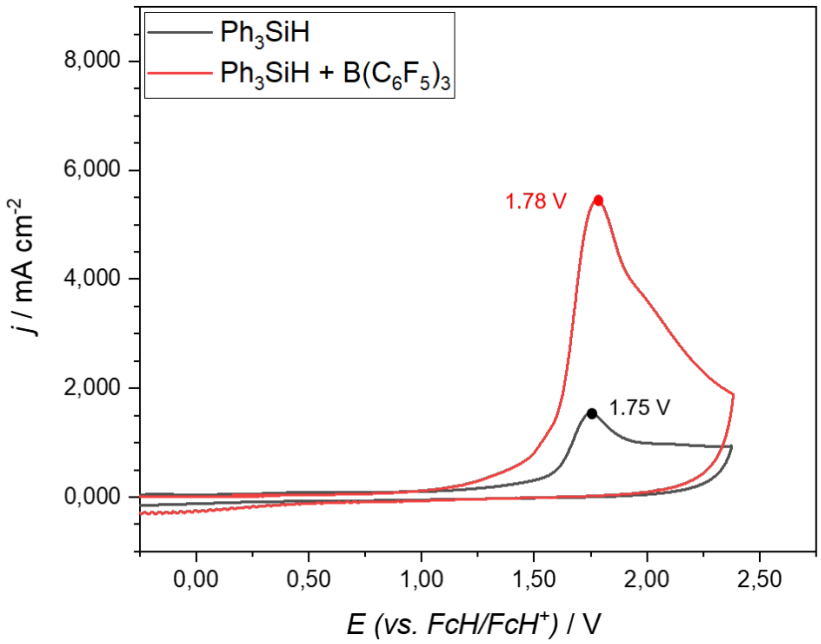

Figure 9: Cyclic voltammogram of 40 mM Ph_3SiH in absence and presence of 2 mM $B(C_6F_5)_3$ in 0.1 M Bu_4NClO_4 and MeCN. W.E. GC (A = 8.0 mm²), *v* = 0.2 V/s, first cycle each. Peak potential in absence of $B(C_6F_5)_3$: 1.75 V vs. FcH/FcH⁺. Peak potential in presence of $B(C_6F_5)_3$: 1.78 V vs. FcH/FcH⁺.

4.5 Si-H activation by Benkeser system $HSiCl_3$ + NR_3

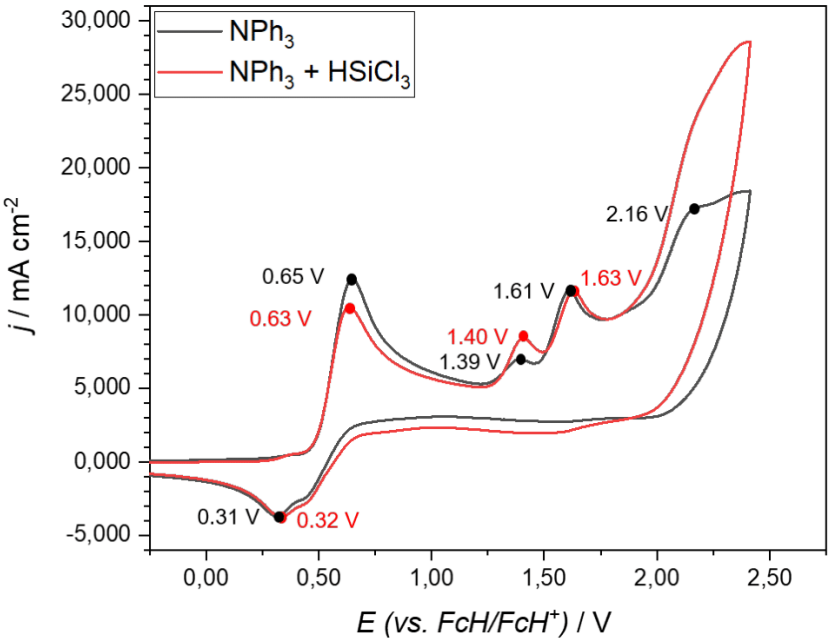

Figure 10: Cyclic voltammogram of 10 mM NPh_3 in absence and presence of 40 mM $HSiCl_3$ in 0.1 M Bu_4NClO_4 and MeCN. W.E. GC (A = 8.0 mm²), *v* = 0.2 V/s, first cycle each. Peak potential in absence of $HSiCl_3$: 0.65 V vs. FcH/FcH⁺ and 1.39 V vs. FcH/FcH⁺ and 1.61 V vs. FcH/FcH⁺ and 2.16 V vs. FcH/FcH⁺ (wave) and 0.31 V vs. FcH/FcH⁺. Peak potential in presence of $HSiCl_3$: 0.63 V vs. FcH/FcH⁺ and 1.40 V vs. FcH/FcH⁺ and 1.63 V vs. FcH/FcH⁺ and 0.32 V vs. FcH/FcH⁺.

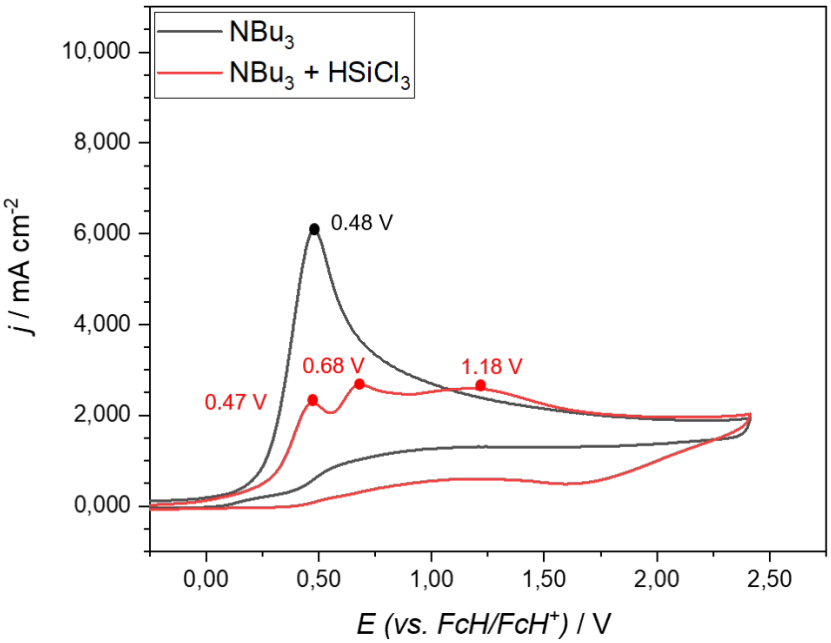

Figure 11: Cyclic voltammogram of 10 mM NBu_3 in absence and presence of 40 mM $HSiCl_3$ in 0.1 M Bu_4NClO_4 and MeCN. W.E. GC (A = 8.0 mm²), *v* = 0.2 V/s, first cycle each. Peak potential in absence of $HSiCl_3$: 0.48 V vs. FcH/FcH⁺. Peak potential in presence of $HSiCl_3$: 0.47 V vs. FcH/FcH⁺ and 0.68 V vs. FcH/FcH⁺ and 1.18 V vs. FcH/FcH⁺ (wave).

5 Characterization of products

$SiCl_4$:
The product was analyzed from the reaction solution and referenced by authentic samples.
^{29}Si NMR (100 MHz, CD_2Cl_2): δ [ppm] = -18.80.
Data are in agreement with literature.[1]

$SiCl_3Br$:
The product was analyzed from the reaction solution.
^{29}Si NMR (100 MHz, CD_2Cl_2): δ [ppm] = -32.43.
Data are in agreement with literature.[2]

H_2SiCl_2:
The product was analyzed from the reaction solution and referenced by authentic samples.
^{1}H NMR (500 MHz, CD_2Cl_2): δ [ppm] = 5,33.
^{29}Si NMR (100 MHz, CD_2Cl_2): δ [ppm] = -11.05.
Data are in agreement with literature.[1,3]

Si_2OCl_6:
The product was analyzed from the reaction solution and referenced by authentic samples.
^{29}Si NMR (100 MHz, CD_2Cl_2): δ [ppm] = -45.90.
Data are in agreement with literature.[4]

$(SiCl_{0.1})_n$:
The product was insoluble in organic solvents.
Elemental analysis: Si: 90,3% Cl: 9,7%

$Me_4Ph_2Si_2$:
Colorless oil
^{1}H NMR (500 MHz, CD_2Cl_2): δ [ppm] = 7.42-7.47 (m, 4H), 7.31-7.37 (m, 6H), 0.38 (s, 12H).
^{13}C NMR (125 MHz, CD_2Cl_2): δ [ppm] = 139.4 (C_q), 134.2 (CH), 128.7 (CH), 128.0 (CH), -3.8 (CH_3).
^{29}Si NMR (100 MHz, CD_2Cl_2): δ [ppm] = -21.79.
MS m/z = 270 $[M]^+$
Data are in agreement with literature.[5]

$Me_4Ph_2Si_2O$:
Colorless oil
^{1}H NMR (500 MHz, CD_2Cl_2): δ [ppm] = 7.73-7.75 (m, 4H), 7.50-7.52 (m, 6H), 0.53 (s, 12H).
^{13}C NMR (125 MHz, CD_2Cl_2): δ [ppm] = 133.38 (CH), 129.61 (CH), 128.05 (CH), 0.91 (CH_3).
^{29}Si NMR (100 MHz, CD_2Cl_2): δ [ppm] = -1.23.
MS m/z = 286 $[M]^+$
Data are in agreement with literature.[6]

TEMPO-$SiCl_3$:
The product was analyzed from the reaction solution.
^{29}Si NMR (100 MHz, CD_2Cl_2): δ [ppm] = -31,16.
Data are in agreement with literature.[7]

6 NMR Spectra

6.1 Halogen exchange of $SiCl_4$ to $SiCl_3Br$

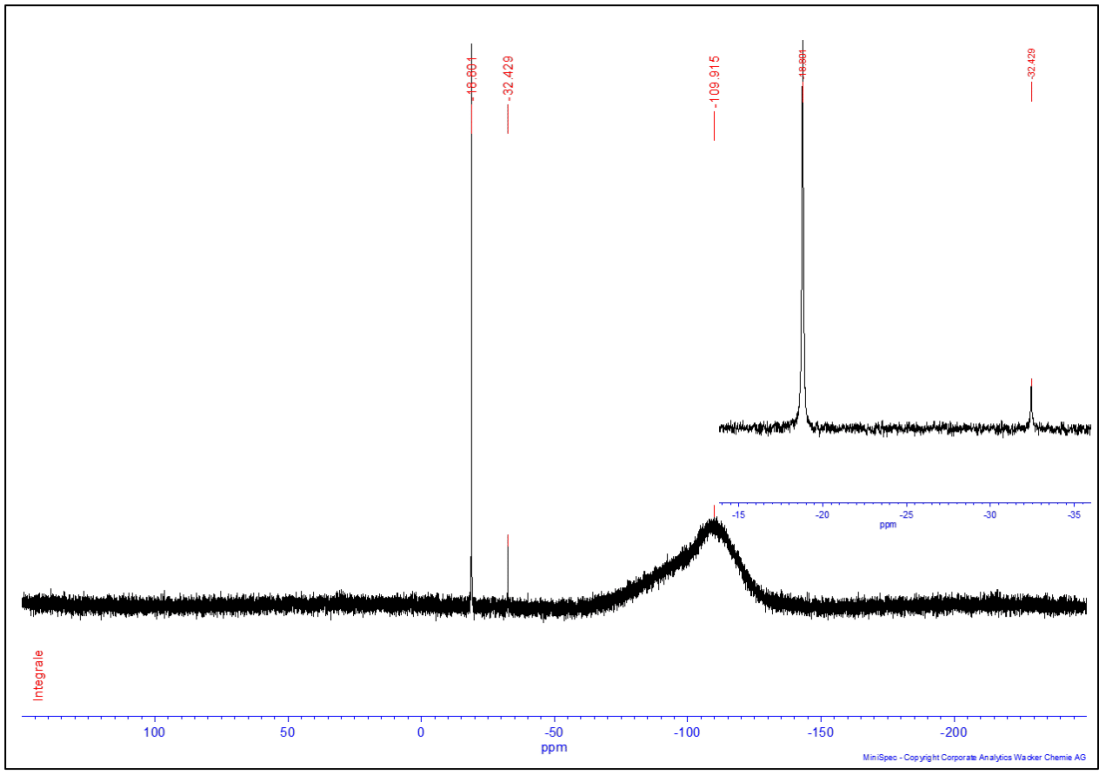

Figure 12: Halogen exchange of $SiCl_4$ in saturated LiBr / acetonitrile solution, stirred at room temperature for 60 min.

6.2 Reaction of Si_2Cl_6 with Amines

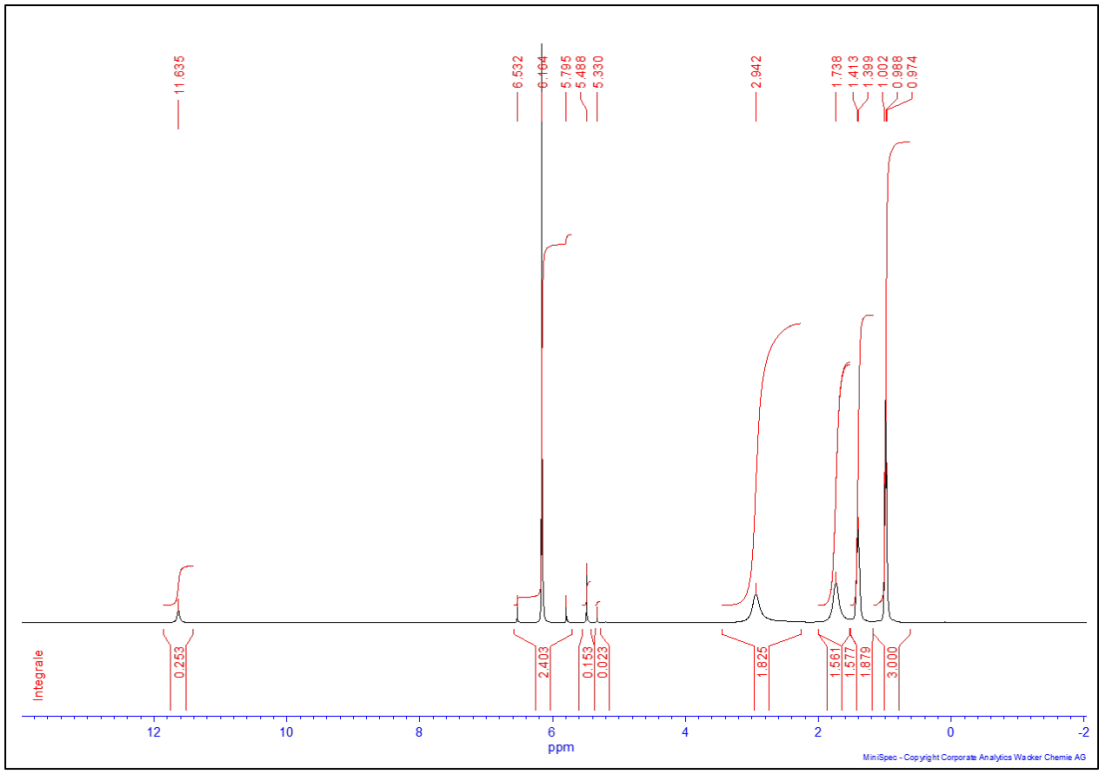

Figure 13: ^{1}H NMR Data of the reaction of Si_2Cl_6 with nBu$_3$ (HSiCl$_3$: Si_2Cl_6 : nBu$_3$ = 10 : 1 : 1) for 24h at room temperature, in CD_2Cl_2.

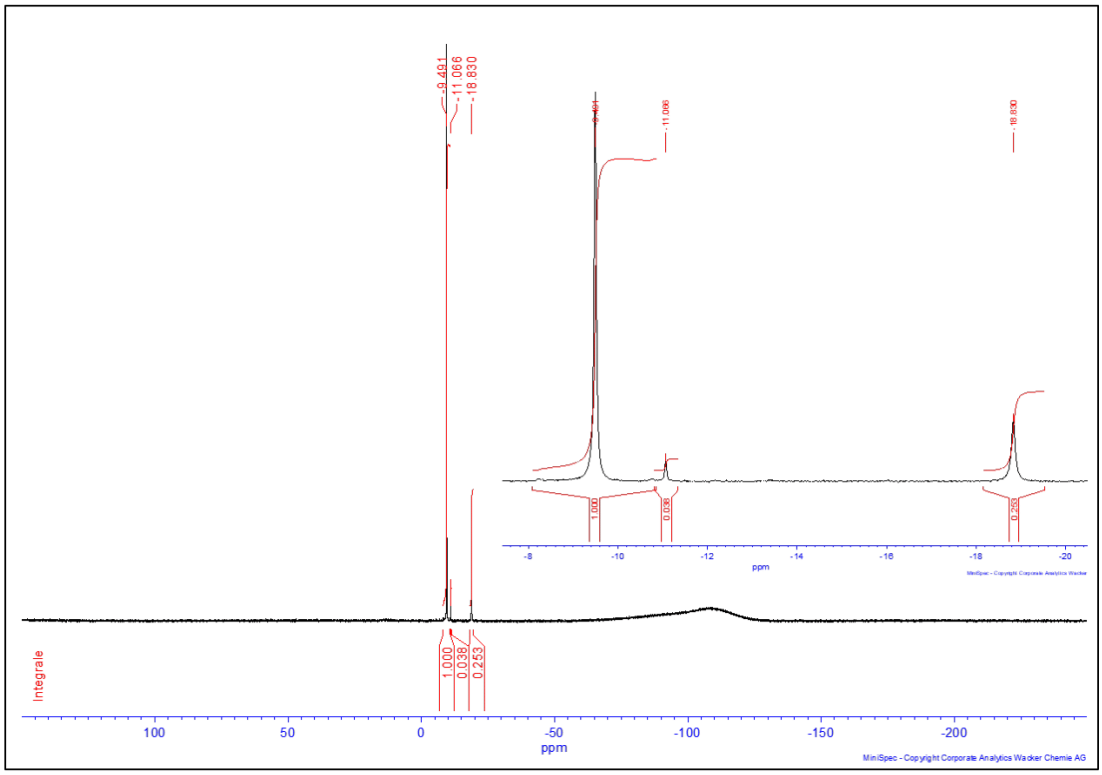

Figure 14: ^{29}Si NMR Data of the reaction of Si_2Cl_6 with nBu$_3$ (HSiCl$_3$: Si_2Cl_6 : nBu$_3$ = 10 : 1 : 1) for 24h at room temperature, in CD_2Cl_2.

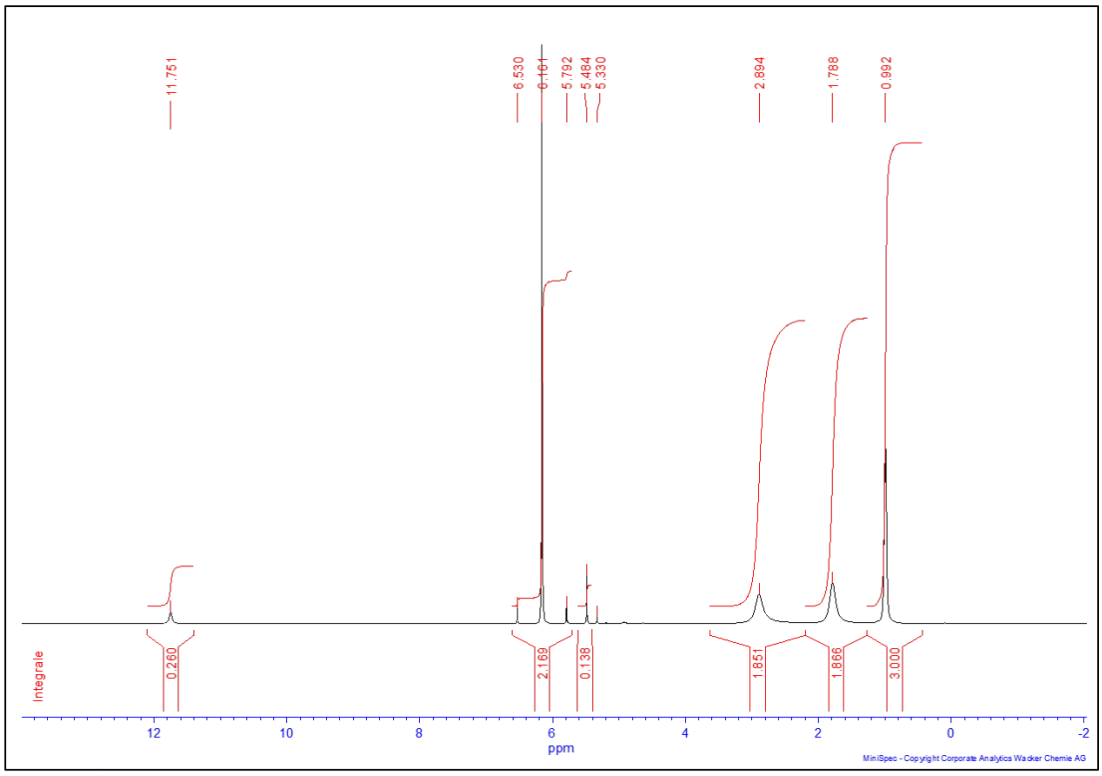

Figure 15: ^{1}H NMR Data of the reaction of Si_2Cl_6 with *n*Pr_3 ($HSiCl_3$: Si_2Cl_6 : *n*Pr_3 = 10 : 1 : 1) for 24h at room temperature, in CD_2Cl_2.

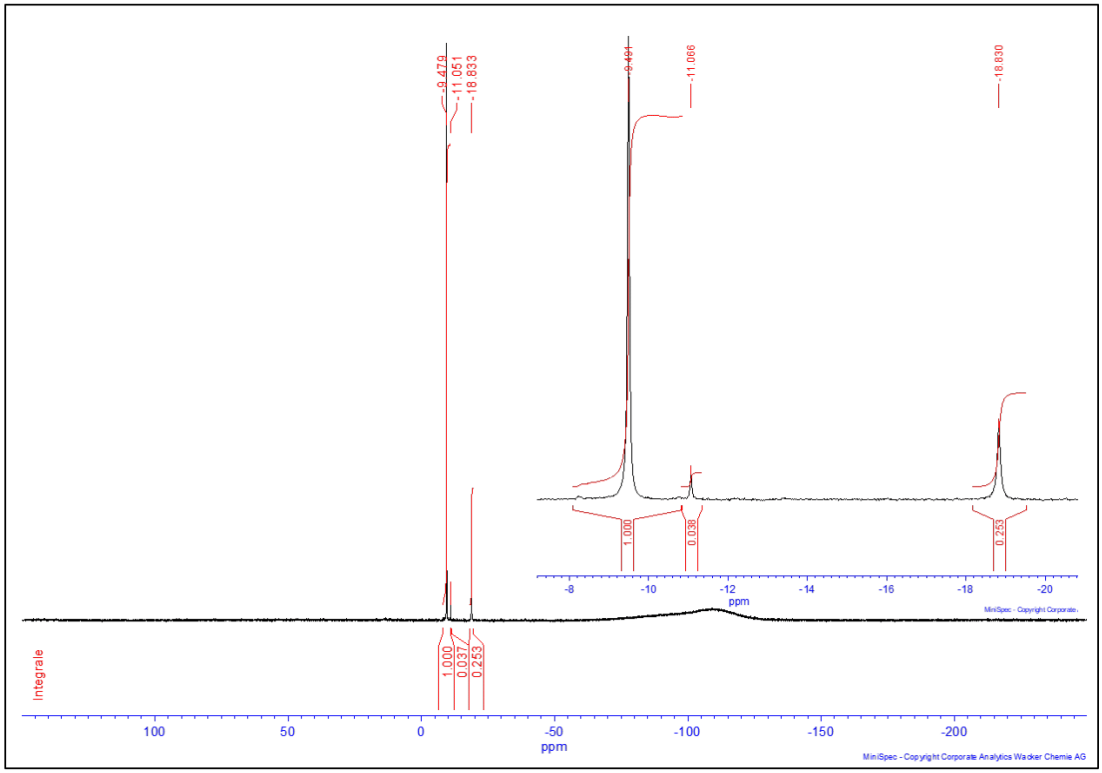

Figure 16: ^{29}Si NMR Data of the reaction of Si_2Cl_6 with *n*Pr_3 ($HSiCl_3$: Si_2Cl_6 : *n*Pr_3 = 10 : 1 : 1) for 24h at room temperature, in CD_2Cl_2.

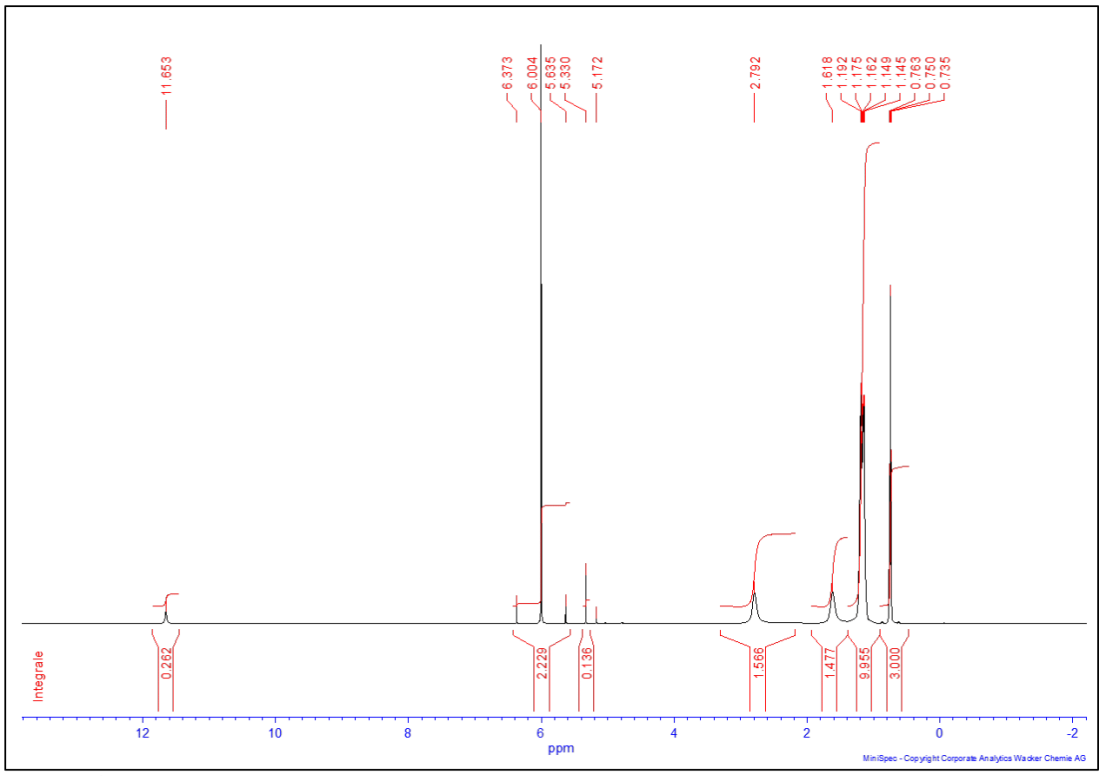

Figure 17: ^{1}H NMR Data of the reaction of Si_2Cl_6 with *n*Oc_3 ($HSiCl_3$: Si_2Cl_6 : *n*Oc_3 = 10 : 1 : 1) for 24h at room temperature, in CD_2Cl_2.

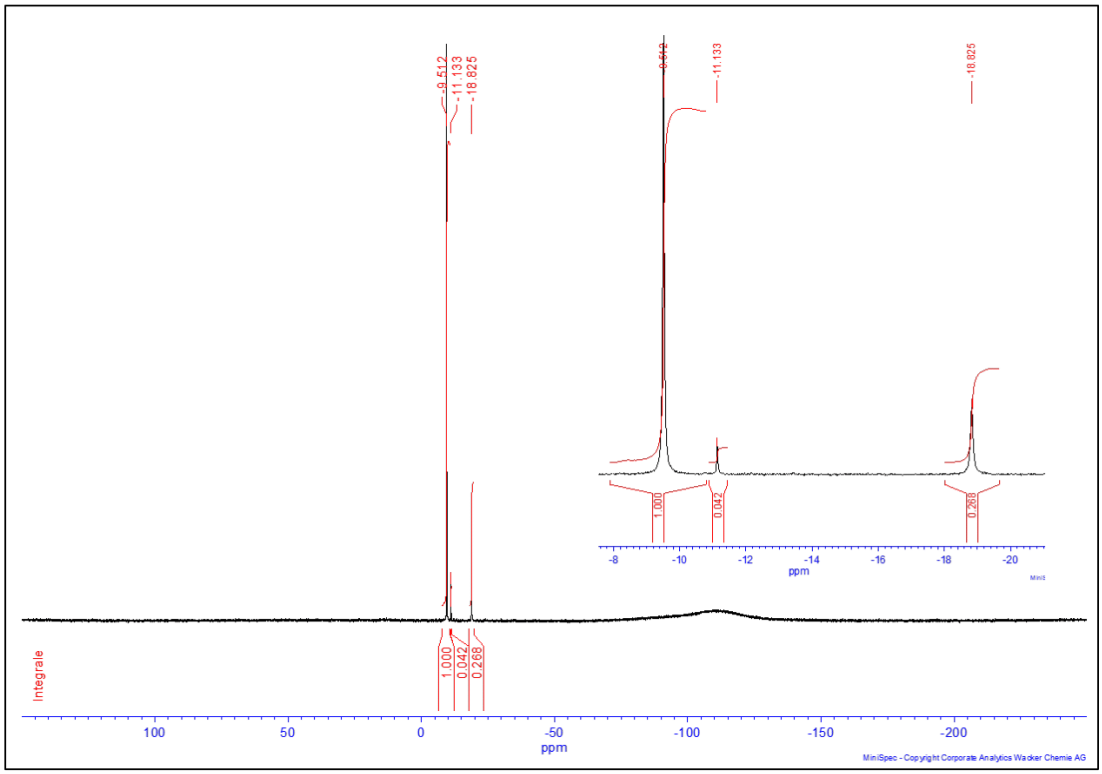

Figure 18: ^{29}Si NMR Data of the reaction of Si_2Cl_6 with *n*Oc_3 ($HSiCl_3$: Si_2Cl_6 : *n*Oc_3 = 10 : 1 : 1) for 24h at room temperature, in CD_2Cl_2.

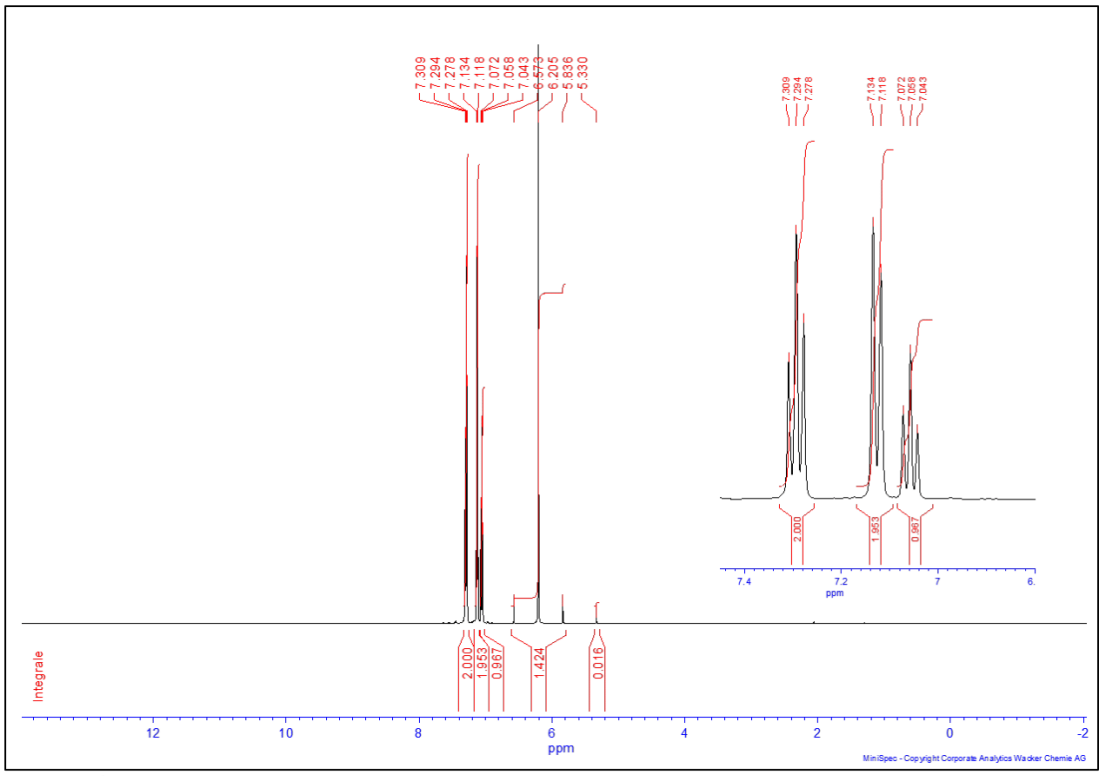

Figure 19: ^{1}H NMR Data of the reaction of Si_2Cl_6 with *n*Ph_3 ($HSiCl_3$: Si_2Cl_6 : *n*Ph_3 = 10 : 1 : 1) for 24h at room temperature, in CD_2Cl_2.

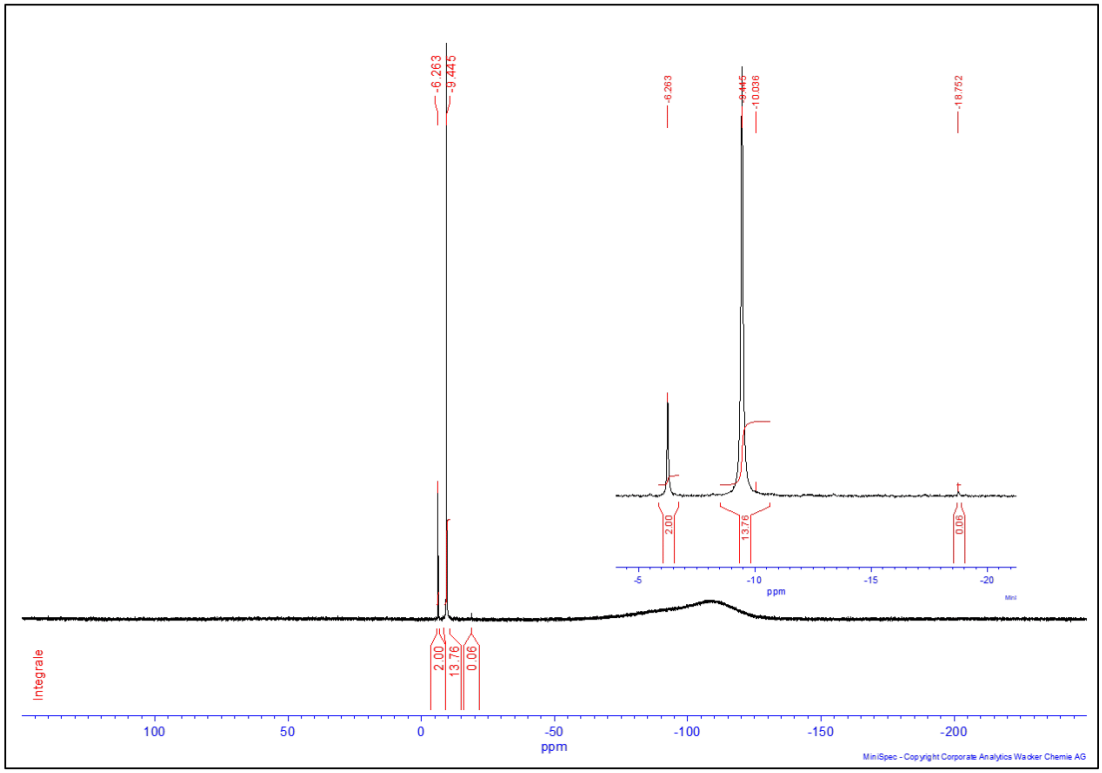

Figure 20: ^{29}Si NMR Data of the reaction of Si_2Cl_6 with *n*Ph_3 ($HSiCl_3$: Si_2Cl_6 : *n*Ph_3 = 10 : 1 : 1) for 24h at room temperature, in CD_2Cl_2.

6.3 Reaction of Si_2Cl_6 and with TEMPO

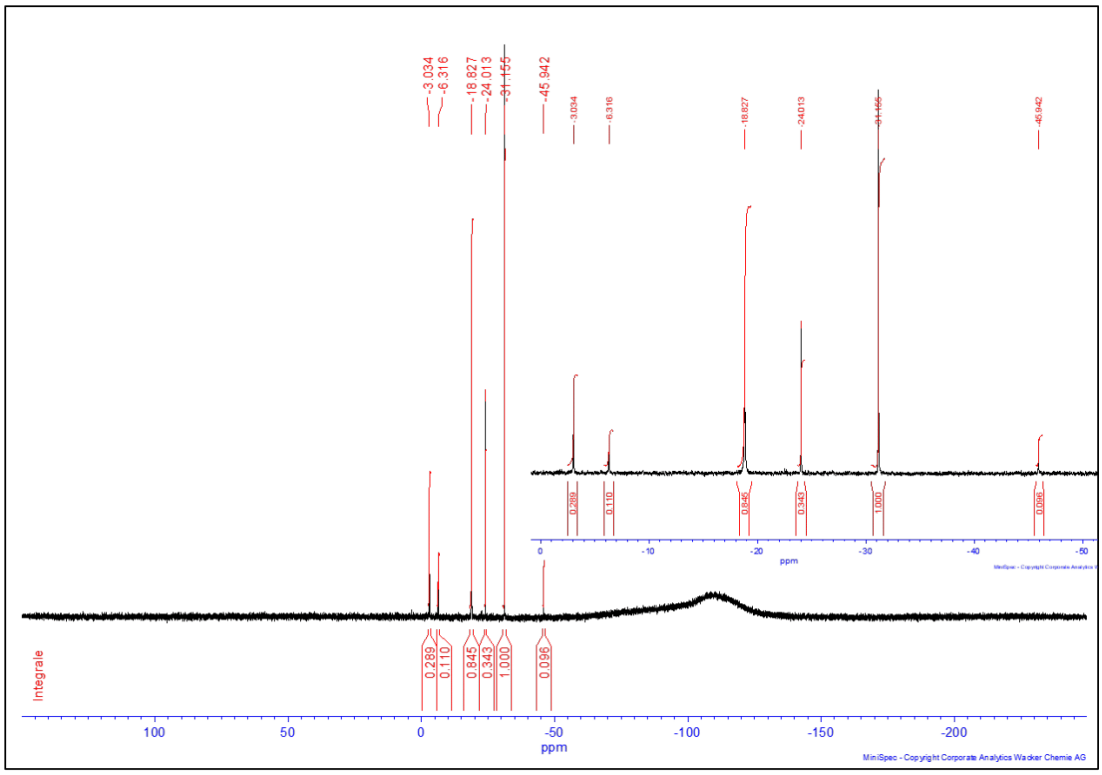

Figure 21: ^{29}Si NMR Data of the reaction of Si_2Cl_6 with TEMPO (Si_2Cl_6 : TEMPO = 1 : 1) for 24h at room temperature, in CD_2Cl_2.

7 References

[1] K. Thorshaug, O. Swang, I. M. Dahl, A. Olafsen, *J. Phys. Chem. A* **2006**, *110*, 9801–9804.
[2] U. Niemann, H. C. Marsmann, *Z. Naturforsch., B* **1975**, *30*, 202–206.
[3] R. Löwer, M. Vongehr, H. C. Marsmann, *Chem.-Ztg.* **1975**, *99*, 33.
[4] H. C. Marsmann, E. Meyer, M. Vongehr, E. F. Weber, *Makromol. Chem.* **1983**, *184*, 1817–1822.
[5] A. Lesbani, H. Kondo, J.-I. Sato, Y. Yamanoi, H. Nishihara, *Chem. Commun.* **2010**, *46*, 7784–7786.
[6] B. T. Gregg, A. R. Cutler, *J. Am. Chem. Soc.* **1996**, *118*, 10069–10084.
[7] S. Stefan, F. Belaj, T. Madl, R. Pietschnig, *Eur. J. Inorg. Chem.* **2010**, *2010*, 289–297.

3.2 Elektrochemische Si-C-Bindungsknüpfung ausgehend von Hydrosilanen

Zu diesem Kapitel wurde ein Manuskript veröffentlicht:
A. D. Beck, S. Haufe, S. R. Waldvogel*, *Boron-Catalyzed Electrochemical Si–C Bond Formation for Safe and Controllable Benzylation and Allylation of Hydrosilanes, ChemElectroChem* **2022**, *9*, e202200840. [DOI: 10.1002/celc.202200840] *Korrespondenzautor
Erläuterung meines Beitrags: Alle experimentellen Untersuchungen und Auswertungen dieser Arbeit wurden von mir durchgeführt und die Rohfassung des Manuskripts wurde von mir verfasst. Die Finalisierung der Veröffentlichung wurde von mir unter Betreuung von Dr. Stefan Haufe und Prof. Dr. Siegfried R. Waldvogel abgeschlossen.

Einleitung

Allyl- und Benzylsilane sind in der (elektro-)organischen Synthese von Interesse,[1] da sie sowohl für die anschließende Funktionalisierung[2] als auch für die synthetische Herstellung pharmazeutisch aktiver Verbindungen[3] verwendet werden können. In der Literatur sind organische Synthesestrategien bekannt, die eine Konversion von Chlorsilanen nach GRIGNARD-analogen Bedingungen[4] sowie die Pd-katalysierte Transformation von Disilanen[5] und Silylboronaten[6] beinhalten. Der elektrochemische Zugang zu Allyl- und Benzylsilanen wurde in der Vergangenheit durch die Reduktion der entsprechenden organischen Halogenide in Gegenwart von Chlorsilanen erreicht.[7] Allerdings ist die Verwendung des Opferelektrolyten *N*,*N*-Dimethylformamid, der die freigesetzten Halogenidionen durch anodische Halogenierung abfängt, der einzige beschriebene Weg. Dies lässt den ökologischen Vorteil der elektrochemischen Konversion für diese Produktmoleküle zweifelhaft erscheinen.

Zusammenfassung der Ergebnisse

Um die bisherige Herausforderung einer geeigneten anodischen Reaktion in Gegenwart freigesetzter Halogenide zu überwinden, wurde die parallele Umsetzung von Hydrosilanen an der Anode und organischen Halogeniden an der Kathode untersucht. Ausgehend von Untersuchungen von KUNAI und Mitarbeitern (Schema 11, a),[8] die die Bildung von Si-Si-Bindungen ausgehend von einem Chlorsilan und einem Hydrosilan

beschreiben, wurde dieses Konzept auf die Bildung von Si-C-Bindungen übertragen. Hierbei soll im Verlauf der Reaktion Chlorwasserstoff gebildet werden, welcher aus der Reaktionslösung entweichen kann und eine weitere Nutzung durch einen Stoffverbund denkbar gestaltet. Die Benzylierung von Me_2PhSiH konnte mit einer Ausbeute von 12% erreicht werden (Schema 11, b), wobei die Halogenierung des Lösungsmittels und die C-H-Bindungsbildung die dominierenden Reaktionen darstellen. Analog zu der vorherigen Si-Si-Bindungsstudie zu Si_2Cl_6 wurde das Lewis-saure Boran $B(C_6F_5)_3$ zur Aktivierung der Si-H-Bindung zugegeben (Schema 11, c).

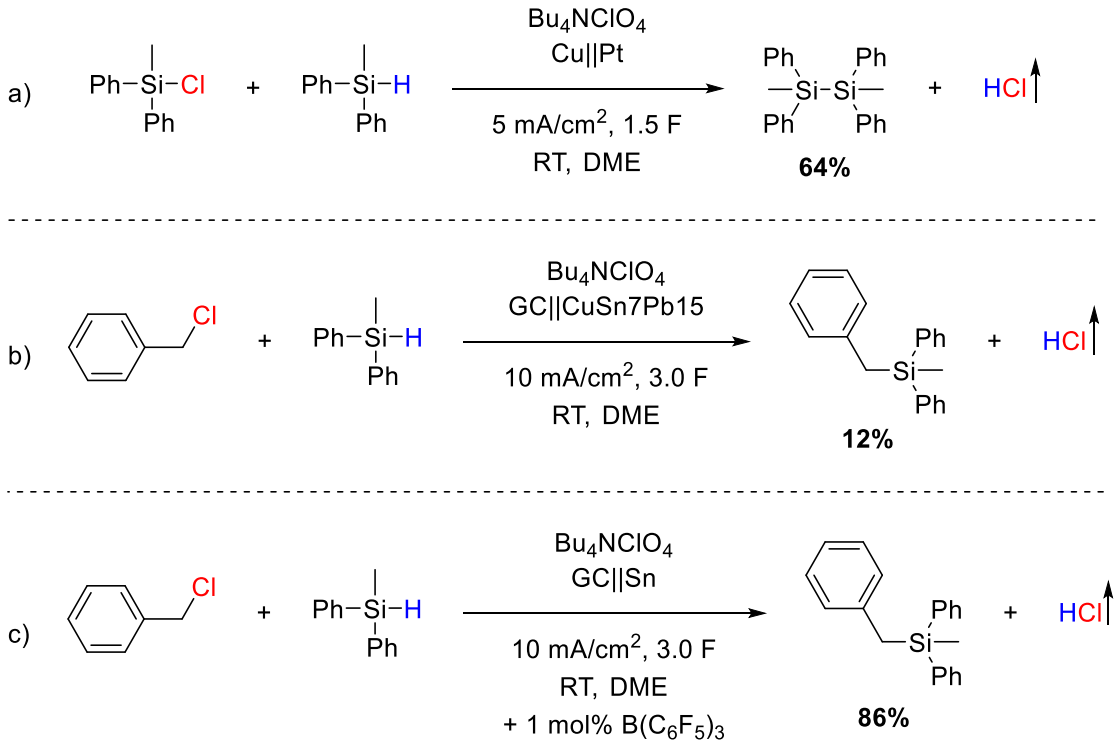

Schema 11. Elektrochemische Konversion von Hydrosilanen: a) Umsetzung von Hydro- und Chlorsilan nach KUNAI[8] als Domino-Reaktion mit Freisetzung von Chlorwasserstoff als Nebenprodukt; b) Benzylierung von Me_2PhSiH führt hauptsächlich zur Chlorierung des Lösemittels mit geringer Ausbeute des Benzylsilans; c) Optimierte Reaktionsbedingungen unter Einsatz von 1 Mol% $B(C_6F_5)_3$ als Mediator.

Entgegen der Erwartung, welche in der Literatur vorherrscht,[9] führt das Perchlorat-Leitsalz-Anion nicht zu einer irreversiblen Deaktivierung des Borans aufgrund von schwach koordinierenden Eigenschaften. Im Gegenteil, ein schwach koordinierendes Leitsalz-Anion wie Perchlorat oder Tetrafluoroborat ist obligatorisch, um die katalytische Reaktion des aktivierten Hydrosilans mit dem Lösungsmittel 1,2-Dimethoxyethan zu verhindern. In Abwesenheit von Leitsalz kommt es anderenfalls zu einer spontanen Reaktion mit dem Lösungsmittel und einer quantitativen Bildung des Silylethers (Schema 12).

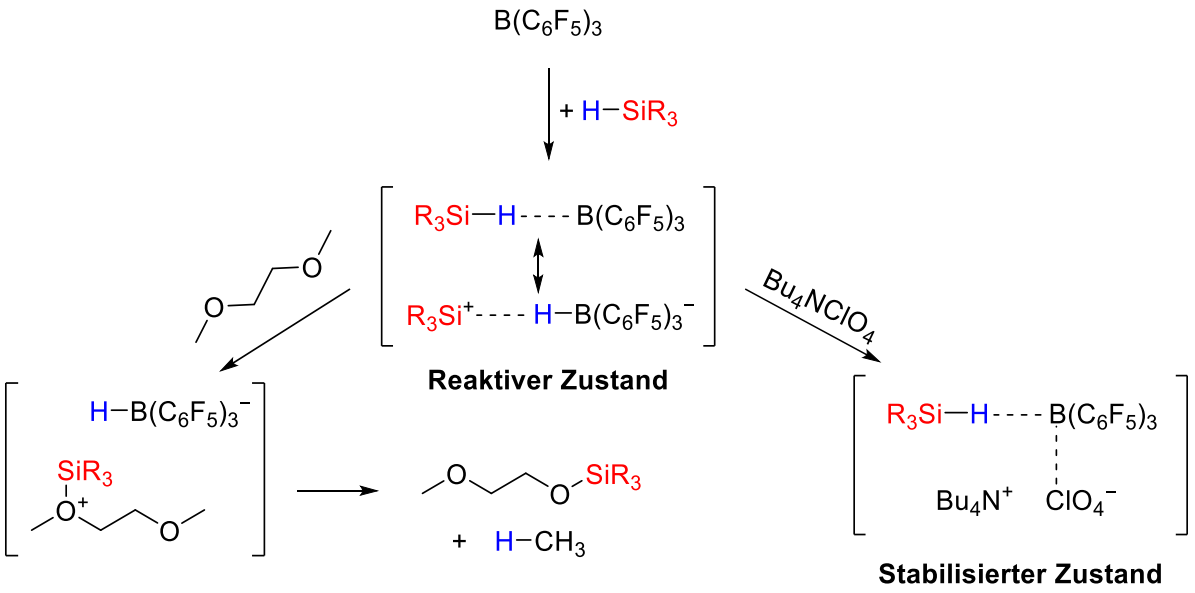

Schema 12. Reaktionswege für das reaktive, aktivierte Hydrosilan: Bildung eines Silylethers mit dem verwendeten Lösemittel 1,2-Dimethoxyethan (links), oder Stabilisierung durch ein schwach koordinierendes Leitsalz-Anion, wie ClO_4^- (rechts).

Die Ausbeute der Benzylierung von Me_2PhSiH führt durch katalytische Mengen an Boran von 1Mol-% zu einer Steigerung von 12% auf 67%. Optimierung der Reaktionsbedingungen und der Elektrodenmaterialien erhöht die maximale Ausbeute des Benzylsilans auf 86% (Schema 11, c). Es zeigte sich, dass Bleibronzen besonders geeignete Kathodenmaterialien sind und im Gegensatz zu Zinn und Blei keine Kontamination des Elektrolyten verursachen. Untersuchungen des Reaktionsverlaufs zeigten, dass das Benzylsilan auch nach vollständiger Umsetzung des Hydrosilans weiterhin gebildet wird. Als Nebenreaktion der Konvertierung des Hydrosilans wird das entsprechende Chlorsilan gebildet, welches für eine kathodische Umwandlung zur Verfügung steht. Die Verwendung des Chlorsilans in Abwesenheit des Hydrosilans zeigte jedoch, dass das Chlorsilan kein wesentliches Intermediat für die gewünschte Si-C-Bindungsbildung ist. Die Reaktion kann auf weitere Hydrosilane übertragen werden, wobei mit zunehmenden sterischen Anforderungen der organischen Gruppen die Ausbeute an Benzylsilanen geringer wird.

Das Syntheseprotokoll kann auf die Reduktion von Allylchlorid angewendet werden. Hier erfüllt das Boran zusätzlich die Funktion des Überoxidationsschutzes durch die Si-H-Aktivierung. Das Allylsilan-Zielprodukt kann leichter oxidativ umgesetzt werden als das Hydrosilan-Ausgangsmaterial. Daher ist das Zielprodukt in Abwesenheit des Borans nicht zugänglich. Bei Verwendung des Borans verschiebt sich das

Oxidationspotential des Reaktanten um 880 mV in den weniger anodischen Bereich und schützt das Produkt so vor weiterer Oxidation. Durch diese Aktivierung kann das entsprechende Allylsilan mit einer Ausbeute von bis zu 35% dargestellt werden. Im Gegensatz zur Synthese von Benzylsilanen ist das Allylsilan nicht durch Reduktion des Chlorsilan-Nebenprodukts zugänglich. Sobald das Hydrosilan als Ausgangsmaterial verbraucht ist, wird das Allylsilan an der Anode oxidiert, wodurch im Folgeprozess Disiloxan und Chlorsilan entstehen. Das Chlorsilan wird erst umgesetzt, wenn das Allylsilan vollständig umgewandelt ist, was die Bildung des Allylsilans auf diesem Weg verhindert. Auch bei der Synthese von Allylsilanen nehmen Bleibronzen eine Sonderstellung ein, die zu den höchsten Ausbeuten ohne Kontamination des Elektrolyten führen. Analog zur Benzylierung ist der sterische Anspruch des Hydrosilans entscheidend für die Ausbeute der Allylierung und nimmt mit zunehmender Sterik der Substituenten ab.

Fazit

Diese Methode stellt das erste elektrochemische Syntheseprotokoll für die Bildung von Si-C-Bindungen zu Allyl- und Benzylsilanen ohne den Einsatz einer Opferanode oder eines Opferelektrolyten dar. Chlorwasserstoff kann leicht als Nebenprodukt aus der Reaktion entweichen und könnte als Reaktant in weiteren Prozessen verwendet werden. Weder die aufwändige Entsorgung der sonst anfallenden Metallchloride noch die stöchiometrische Chlorierung des Elektrolyten führen zu ökologischen Bedenken. Die Verwendung eines Lewis-sauren Borans, insbesondere $B(C_6F_5)_3$, zur Aktivierung der Si-H-Bindung erhöht die Ausbeute der Zielprodukte erheblich. Ein schwach koordinierendes Leitsalz-Anion ist für die Stabilisierung des reaktiven Intermediats unerlässlich. Darüber hinaus erfüllt das Boran die Funktion des Oxidationsschutzes des Zielmoleküls. Die Methode ist bisher stark von der Stabilisierung des erzeugten Carbanions abhängig und wurde an 6 verschiedenen Produkten mit Ausbeuten von bis zu 86% demonstriert.

[1] M. A. Brook, *Silicon in organic, organometallic, and polymer chemistry*, Wiley, New York, Weinheim, **2000**.

[2] a) A. Hosomi, *Acc. Chem. Res.* **1988**, *21*, 200–206; b) H. Sakurai, *Pure Appl. Chem.* **1982**, *54*, 1–22.

[3] A. Ramirez, K. A. Woerpel, *Org. Lett.* **2005**, *7*, 4617–4620.

[4] a) Z. Li, X. Cao, G. Lai, J. Liu, Y. Ni, J. Wu, H. Qiu, *J. Organomet. Chem.* **2006**, *691*, 4740–4746; b) G. Martin, F. S. Kipping, *J. Chem. Soc., Trans.* **1909**, *95*, 302–314; c) R. Robison, F. S. Kipping, *J. Chem. Soc., Trans.* **1908**, *93*, 439–456.

[5] R. E. Grote, E. R. Jarvo, *Org. Lett.* **2009**, *11*, 485–488.

[6] Z.-D. Huang, R. Ding, P. Wang, Y.-H. Xu, T.-P. Loh, *Chem. Commun.* **2016**, *52*, 5609–5612.

[7] a) T. Shono, Y. Matsumura, S. Katoh, N. Kise, *Chem. Lett.* **1985**, *14*, 463–466; b) J. Yoshida, K. Muraki, H. Funahashi, N. Kawabata, *J. Organomet. Chem.* **1985**, *284*, C33-C35; c) J. Yoshida, K. Muraki, H. Funahashi, N. Kawabata, *J. Org. Chem.* **1986**, *51*, 3996–4000.

[8] A. Kunai, T. Kawakami, E. Toyoda, T. Sakurai, M. Ishikawa, *Chem. Lett.* **1993**, *22*, 1945–1948.

[9] a) C.-C. Chang, T.-K. Chen, *J. Power Sources* **2009**, *193*, 834–840; b) C.-C. Chang, T.-K. Chen, L.-J. Her, G. T.-K. Fey, *J. Electrochem. Soc.* **2009**, *156*, A828-A832; c) G.-B. Han, J.-N. Lee, J. W. Choi, J.-K. Park, *Electrochim. Acta* **2011**, *56*, 8997–9003; d) E. J. Lawrence, V. S. Oganesyan, G. G. Wildgoose, A. E. Ashley, *Dalton Trans.* **2013**, *42*, 782–789; e) Y. M. Lee, J. E. Seo, N.-S. Choi, J.-K. Park, *Electrochim. Acta* **2005**, *50*, 2843–2848.

ChemElectroChem

Research Article
doi.org/10.1002/celc.202200840

Chemistry Europe
European Chemical Societies Publishing

www.chemelectrochem.org

Boron-Catalyzed Electrochemical Si–C Bond Formation for Safe and Controllable Benzylation and Allylation of Hydrosilanes

Alexander D. Beck,[a, b] Stefan Haufe,[a] and Siegfried R. Waldvogel*[b]

The range of possible applications of $B(C_6F_5)_3$ extends into many areas of organic and inorganic chemistry. However, electrochemical synthesis with hydrosilanes using $B(C_6F_5)_3$ to increase yield or scope has not yet been achieved. A comprehensive study on the use of Lewis acidic boron species, especially $B(C_6F_5)_3$, for the activation of hydrosilanes in presence of commercially available supporting electrolyte for Si–C bond formation was presented. The benzylation and allylation of hydrosilane species was successfully conducted in presence of catalytic amounts of $B(C_6F_5)_3$ in yields up to 86%. Screening of electrode materials revealed leaded bronzes as superior for cathodic conversion without contamination of the electrolyte by heavy metals. Supported by cyclic voltammetry studies, $B(C_6F_5)_3$ activated the hydrosilane for easier nucleophilic access, leading to significant increase in yield and enrichment of the target product in the reaction mixture.

Introduction

Tris(pentafluorophenyl)borane, $B(C_6F_5)_3$, has been subject to numerous applications in organic[1,2] and inorganic chemistry[3] since its discovery in 1963.[4] It is a powerful Lewis acid comparable to BF_3 or BCl_3,[5] but unlike these boron halides, it is an easy-to-handle, and a quite thermally stable solid. Due to its high steric demand, $B(C_6F_5)_3$ is incapable to form dative bonds in acid-base adducts despite its high Lewis acidity.[6] This feature has been associated with the term "frustrated Lewis pair" (FLP) chemistry,[6] which opens up new reaction pathways and possibilities, as demonstrated by the activation of small molecules like H_2,[6,7,8,9] CO,[6,7,9,10] CO_2[6,7,9,11] etc.

In addition, the activation of Si–H bonds with $B(C_6F_5)_3$ is possible. In contrast to common Lewis acid activation of carbonyl moieties, $B(C_6F_5)_3$ does not coordinate the carbonyl oxygen, which polarizes the double bond and generates a highly electrophilic carbon. The electron withdrawing $B(C_6F_5)_3$ **I** rather forms an adduct **II** with the hydrosilane,[12] and may partially abstract the hydride (Scheme 1).[13–15] By nucleophilic attack of a carbonyl oxygen at the silicon center, the activated hydrosilane forms a borohydride stabilized ion pair **III**, that releases $B(C_6F_5)_3$ to close the catalytic cycle by hydride transfer to accomplish the silyl ether species.

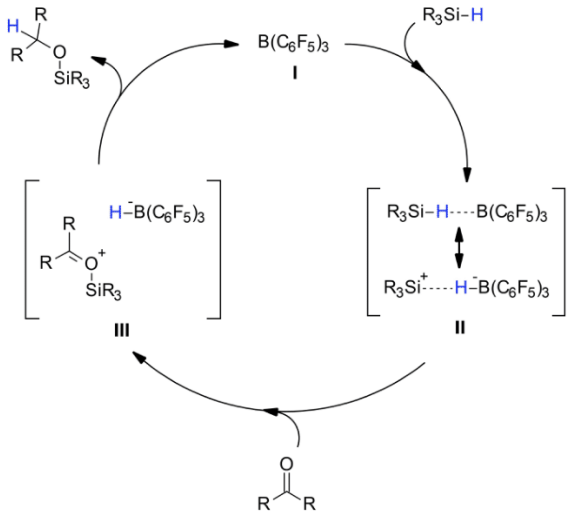

Scheme 1. Activation of hydrosilane by $B(C_6F_5)_3$ and subsequent hydrosilylation of carbonyl compounds with regeneration of $B(C_6F_5)_3$.[12,13,15–17]

This key discovery of a metal-free hydrosilane activation by $B(C_6F_5)_3$ has been of significant interest within the past 20 years. The range of application for $B(C_6F_5)_3$ has greatly expanded and several catalytic silane-based transformations e.g. silylation of alcohols,[18] hydrosilylation of aldehydes,[19] alkenes,[20,21] alkynes,[21] enols,[22] esters,[19] imines,[14,17,23] and ketones,[17,19,24] the chlorination of hydrosilanes to respective chlorosilanes[25] and deoxygenation of alcohols[1,26] and carbonyl compounds.[26] have been reported so far.

Recently, this unique boron compound has expanded into the field of electrochemistry. Studies on the reduction potential of $B(C_6F_5)_3$,[27,28] as well as electrosynthetic aspects, especially

[a] *A. D. Beck, Dr. S. Haufe*
Consortium für elektrochemische Industrie
Wacker Chemie AG
Zielstattstraße 20, 81379 München (Germany)
[b] *A. D. Beck, Prof. Dr. S. R. Waldvogel*
Department Chemie
Johannes Gutenberg-Universität Mainz
Duesbergweg 10–14, 55128 Mainz (Germany)
E-mail: waldvogel@uni-mainz.de
Homepage: https://www.aksw.uni-mainz.de/

Supporting information for this article is available on the WWW under https://doi.org/10.1002/celc.202200840

ChemElectroChem | Research Article
doi.org/10.1002/celc.202200840
Chemistry Europe
European Chemical Societies Publishing

with respect to the activation of hydrogen,[29,30] have been the focus of such research. Previous studies indicate that $B(C_6F_5)_3$ is deactivated in electrolytes containing coordinating anions such as perchlorate.[28,31] This phenomenon is exploited by the use of $B(C_6F_5)_3$ as anion receptor in lithium-ion batteries to stabilize the solid-electrolyte-interphase (SEI),[32] and to inhibit the electrolyte decomposition by anion complexation.[33]

Notwithstanding, we have recently shown that anion receptor function of $B(C_6F_5)_3$ does not appear to be an irreversible, deactivating type of complexation in the presence of perchlorate.[34] This has led to the case of a $B(C_6F_5)_3$ mediated silicon based organic electrochemistry. As our results revealed, a catalytic activity of $B(C_6F_5)_3$ is detectable in presence of perchlorate anion, indicating a mediator role. In this case, the amount of applied charge required for intended oxidative Si–Si bond formation decreases by more than half in the presence of 2.5 mol% $B(C_6F_5)_3$. This suggests an alternative reaction pathway. However, to the best of our knowledge, $B(C_6F_5)_3$ has not yet been applied to increase yield or scope for the electrochemical Si bond formation. Here, we present the first study to successfully apply $B(C_6F_5)_3$ as mediator in electrochemical silane-based synthesis regarding Si–C bond formation, increasing yield and substrate scope for an exemplary benzylation and allylation of hydrosilane species.

Allylation of silanes has been an interest of (electro) organic synthesis for many years, due to easy subsequent functionalization,[35] and synthetic application in production of pharmaceutically active compounds.[36] Over this period, various approaches to the corresponding allylsilanes have been established: Grignard related Sm-mediated systems,[37] the Pd-catalyzed cleavage of disilanes and reaction with trifluoroacetate,[38] as well as the electrochemical reduction of the corresponding organic halides in presence of chlorosilanes (Scheme 2, top).[39–41]

The benzylation of silanes by Grignard reagents reacting with chlorosilanes to form the respective Si–C bond is known for over 100 years.[42] It has further gained attraction in the electrochemical,[39] as well as in the Pd-catalyzed field of organic chemistry (Scheme 2, bottom).[43] Benzylsilanes are used as organosilicon fragments in organic synthesis.[44] While conventional synthetic protocols need stoichiometric or even larger amounts of oxidizers or reducing agents, electrochemistry provides a green alternative.[45] In particular, reagent waste is avoided and if renewable electricity is applied such processes become very sustainable.[46] In addition, the reaction occurs close to the electrode and the simple switch-off for the electric power prevent thermal runaway reactions and makes this technology inherently safe.[47]

However, the reduction of chlorosilanes and organic halides in aprotic media leads to electrolyte halogenation in the absence of a halide scavenger, which does not allow the reaction to be defined as sustainable. Due to this circumstance, we may report an electrochemical reaction pathway with $B(C_6F_5)_3$ mediator, allowing the oxidation of hydrosilanes to the corresponding allyl- or benzylsilanes and suppressing solvent chlorination.

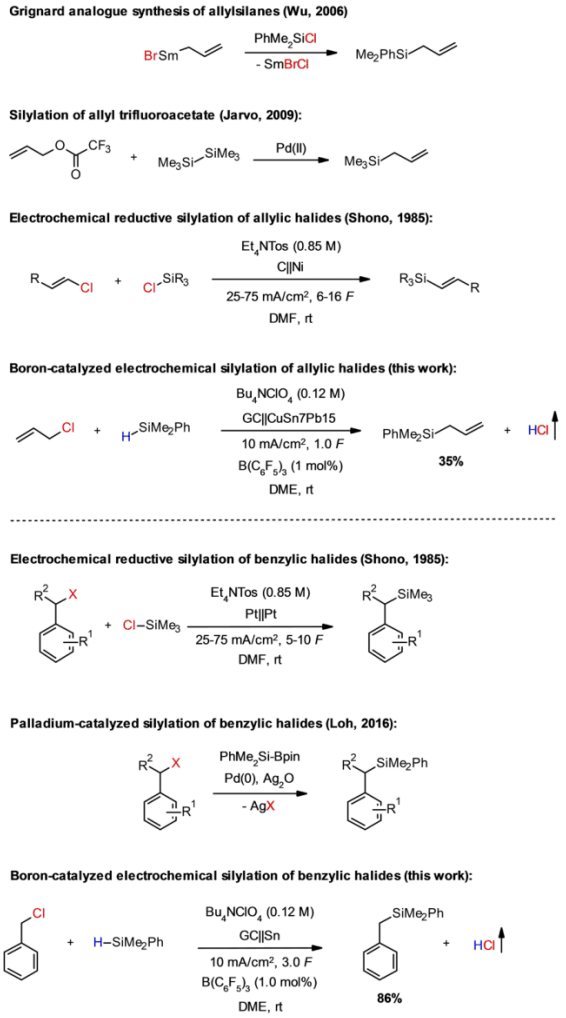

Scheme 2. Strategies for the synthesis of allylsilanes;[37–41] (top) and benzylsilanes,[39,43] (bottom) Tos = *p*-toluenesulfonate, DMF = *N*,*N*-dimethylformamide, GC = glassy carbon, DME = 1,2-dimethoxyethane, Bpin = 4,4,5,5-tetramethyl-1,3,2-dioxaborolane.

Results and Discussion

Electrochemical reduction of halosilanes and organic halides involves cleavage of free halides, which must be removed from the reaction process to prevent halogenation of the aprotic solvent. In the past, this was often achieved by the use of sacrificial metal anodes, such as magnesium,[48] copper[49] or mercury,[50] which form the corresponding insoluble metal halides. Alternatively, non-sacrificial anode materials have been tested.[51] The use of proton releasing species for halogen scavenging to generate hydrogen chloride, which can be removed during the reaction, is scarce in silicon based electrochemistry. One option for oxidative proton generation is anodic conversion of hydrosilanes. This represents an environmentally friendlier alternative without the formation of metal chlorides. Inspired by this oxidative electrochemical transformation of

ChemElectroChem
Research Article
doi.org/10.1002/celc.202200840
Chemistry Europe
European Chemical Societies Publishing

hydrosilanes, as reported by Kunai *et al.* for the Si–Si bond formation in presence of chlorosilanes to form the respective disilanes (Scheme 3, top),[52] we utilized this combined electrochemical transformation to generate Si–C bonds under the release of hydrogen chloride. In analogy we used the hydrosilane dimethylphenylsilane (Me_2PhSi–H, **1**) for an oxidative cleavage of the Si–H bond to form the respective silyl cation. At the same time, reduction of an organic halide allows for the Si–C bond formation (Scheme 3, bottom).

Screening of solvent, electrode materials and stoichiometry of starting materials revealed, that the reaction suffers from a lack of selectivity and thus forms chlorodimethylphenylsilane (Me_2PhSi–Cl, **2**) and tetramethyldiphenyldisiloxane (Me_2PhSi–O–$SiMe_2Ph$, **3**) as by-products (see Supporting Information). The depicted reaction conditions show a maximum yield of 10% for the benzylation of hydrosilane to benzyldimethylphenylsilane (Me_2PhSi–Bn, **4**). Conversion of starting material is low, especially in the case of benzyl chloride. In addition to the desired benzylsilane **4**, C–H bond formation and chlorination of the solvent occur, indicating an anodic competition of chloride ions to the oxidation of hydrosilane,

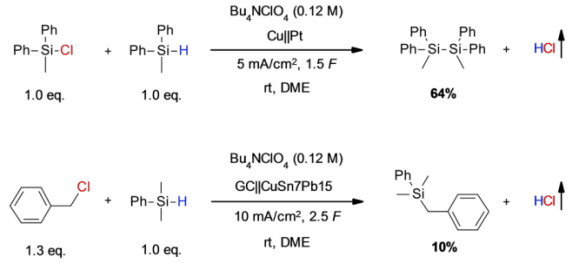

Scheme 3. Direct Si–Si bond formation via oxidation of hydrosilane (top),[52] analogue oxidative coupling for Si–C bond formation of this work (bottom), DME = 1,2-dimethoxyethane, GC = glassy carbon.

Table 1. Product yield for the catalyzed and non-catalyzed oxidative Si–C bond formation.

Entry	Lewis acid	Mol%	Si–C, **4** Yield[b]	Si–Cl, **2** Yield[b]	Si–O, **3** Yield[b]	Conversion[a]
1[c]	None	0.0	10%	6%	2%	22%
2[c]	$B(C_6F_5)_3$	1.0	51%	39%	6%	100%
3[c]	$B(C_6F_5)_3$	2.5	49%	36%	14%	100%
4[c]	$B(C_6F_5)_3$	5.0	46%	34%	20%	100%
5[d]	$B(C_6F_5)_3$	1.0	0%	0%	1%	1%
6[d]	$B(C_6F_5)_3$	2.5	0%	0%	4%	4%
7[d]	$B(C_6F_5)_3$	5.0	0%	0%	7%	7%
8[e]	$B(C_6F_5)_3$	1.0	67%	21%	8%	100%
9[e]	BCl_3	1.0	25%	25%	4%	56%
10[e]	BEt_3	1.0	58%	36%	3%	100%
11[e]	$AlCl_3$	1.0	2%	6%	5%	13%
12[e]	None	0.0	12%	7%	3%	23%

[a] Reaction conditions: 1,2-dimethoxyethane as solvent with 0.12 M Bu_4NClO_4 supporting electrolyte, anode material is glassy carbon, cathode material is CuSn7Pb15, Me_2PhSiH (0.50 M, 2.5 mmol) and benzyl chloride (0.69 M, 3.43 mmol), at room temperature. [b] Yield determined by NMR referenced to TMS; Si–C, 4 = benzyldimethylphenylsilane; Si–Cl, 2 = chlorodimethylphenylsilane; Si–O, 3 = tetramethyldiphenyldisiloxane. [c] Current density of 10 mA/cm², applied charge of 1.0 *F*. [d] Without electric current. [e] Current density of 10 mA/cm², applied charge of 3.0 *F*.

due to a peak potential of hydrosilane **1** of 2.07 V vs. FcH/FcH^+ (Ferrocene / Ferrocenium) (*vide infra*). Comparable results are obtained by using alkyl halides, such as 1-chlorooctane, and aryl halides, like chlorobenzene. The yield of Si–C bond formation increases with increasing stabilization of the corresponding carbanion intermediate, showing benzylsilane **4** as the product of highest yield with 10% to be obtained so far (Table 1, entry 1).

As we have recently shown,[34] $B(C_6F_5)_3$ represents a possibility for Si–H bond activation even in the presence of perchlorate. Based on these studies, we have investigated the use of $B(C_6F_5)_3$ for oxidative Si–C bond formation. By addition of a catalytic amount of 1.0 mol% $B(C_6F_5)_3$ to the reaction mixture, 100% conversion and an increase in yield of benzylsilane **4** to 51% is achieved (Table 1, entry 2). With increasing amount of $B(C_6F_5)_3$, the product distribution is shifted to disiloxane **3** (Table 1, entries 2–4), probably due to the high reactivity of the activated hydrosilane in presence of the perchlorate species. Nucleophilic access and decomposition of perchlorate leads to subsequent formation of disiloxane **3**. In a current-less state, no Si–C bond formation is obtained and regardless of reaction time, only a minor amount of hydrosilane **1** is converted to form disiloxane **3**, the yield of which increases with the amount of $B(C_6F_5)_3$ used (Table 1, entries 5–7).

We extended the hydrosilane activation for electrochemical Si–C bond formation to additional borane species and Lewis acids. Besides $B(C_6F_5)_3$, BCl_3 and BEt_3 allow for a successful catalytic activation of Si–H bonds in presence of perchlorate although $B(C_6F_5)_3$ provides the highest yield of benzylsilane **4** for an applied charge of 3.0 *F* (Table 1, entry 8). Conversion and yield for BCl_3 are significantly diminished (Table 1, entry 9), due to complexation of chloride ions by the high Lewis acidic and relatively minor steric demanding BCl_3. Still, an increase in yield of more than two-fold compared to the non-catalyzed reaction pathway shows its potential for Si–H bond activation in presence of perchlorate. BEt_3 generates almost comparable results to $B(C_6F_5)_3$, yielding 58% of benzylsilane **4** with full conversion of the hydrosilane species (Table 1, entry 10). BEt_3 is known as a radical initiator for the hydrosilylation of electron-rich alkenes,[53] indicating an aspect for a possible one-electron process of the activated Si–C bond formation. Leaving the field of borane chemistry and entering aluminum related Lewis acids, $AlCl_3$ does not only show missing ability for Si–H bond activation (Table 1, entry 11). Moreover, the yield and conversion decrease compared to the product distribution of the non-activated route. A redox shuttle functionality of $AlCl_3$ is supposed, with charge amount being consumed by alternating oxidation and reduction of the aluminum species without conversion of the desired silyl species. In absence of the Lewis acid, reduction of benzyl chloride with subsequent oxidation of released chloride occurs. Due to the high oxidation potential of hydrosilane **1**, solvent chlorination is the main reaction, leading to low hydrosilane conversion (Table 1, entry 12).

The presence of a coordinating anion such as perchlorate is mandatory to stabilize the reactive, activated silyl species, otherwise a quantitative catalytic reaction of hydrosilane **1** with the solvent 1,2-dimethoxyethane occurs at room temperature.

ChemElectroChem
Research Article
doi.org/10.1002/celc.202200840
Chemistry Europe
European Chemical Societies Publishing

The solvent is converted to the corresponding silyl ether (2-methoxyethoxy)dimethylphenylsilane ($Me_2PhSi–OCH_2CH_2OMe$, **5**) in 96% yield under elimination of methane (Scheme 4, path **I**). Various perchlorate and tetrafluoroborate supporting electrolytes prevent this catalytic process with only minor conversion of hydrosilane **1** to the corresponding disiloxane **3** for perchlorate or fluorosilane in case of tetrafluoroborate supporting electrolyte (see Supporting Information). Is the boron activated hydrosilane in a stabilized state due to the coordinating anion (Scheme 4, path **II**), access for nucleophilic attack at the silicon center is facilitated. A carbanion generated via cathodic reduction can easily form the respective Si–C bond. A competing reaction of the released chloride ion leads to the formation of a chlorosilane compound. By consecutive oxidation, the Lewis acidic boron species is regenerated to be ready for further hydrosilane activation under the release of protons. The mediator, in addition to the role of activating the hydrosilane species for nucleophilic attack, further fulfills the function of oxidative protection of the supporting electrolyte. As indicated by cyclic voltammetry measurements (*vide infra*) the oxidation potential of the intermediate is shifted to the less anodic values, thus preventing oxidation of chloride and subsequent solvent halogenation. Anodic hydrogen evolution could not be detected in course of reaction, indicating the formation of hydrogen chloride, dissolved in the supporting electrolyte.

To gain deeper insight into the reaction process and conversion, we analyzed the reaction mixture with increasing applied charge by GC and NMR. An interesting picture emerges, which can be divided into two sections (Figure 1): In the first section, up to 1.0 *F*, the reaction is driven by the activated hydrosilane **1**. Conversion leads to benzylsilane **4** as main product and the corresponding chlorosilane **2** as by-product. A small initial amount of disiloxane **3** is formed, probably due to decomposition of the activated silyl species with the supporting electrolyte, that does not further increase as the reaction proceeds. Formation of disiloxane **3** is not electrochemical induced for the benzylation of hydrosilanes.

At 1.0 *F* hydrosilane **1** is completely consumed, marking the transition to the second process section: Benzylsilane **4** continues to be formed, since the benzyl chloride concentration is at about 50% of its initial amount and available for further reduction. In this case, however, the organic halide reacts with chlorosilane **2** instead of hydrosilane **1**, diminishing the amount of chlorosilane in the course of reaction and increasing the yield of benzylsilane **4** up to 67%. Beyond 3.0 *F*, solvent chlorination occurs, and the reaction is discontinued.

Analysis of the product distribution with increasing applied charge leads to two observations: the investigated borane-activated electrochemical conversion indicates a single-electron process, allowing for the complete conversion of hydrosilane **1** after 1.0 *F*. Second, these results show a possible formation of benzylsilane **4** by reductive conversion of benzyl chloride and chlorosilane **2**. Using identical reaction conditions with chlorosilane **2** instead of hydrosilane **1**, the reductive coupling yielded 19% of benzylsilane **4** with subsequent chlorination of solvent. While the reductive route is a possible pathway to the benzylsilane, higher yields without solvent chlorination can only be achieved via the oxidative synthesis route, indicating the chlorosilane species not to be an essential intermediate.

We further investigated the influence of current density and electrode material, confirming the optimal conditions at 10 mA/cm^2 (see Supporting Information). Leaded bronze combines the advantages of high overpotential for hydrogen evolution, as

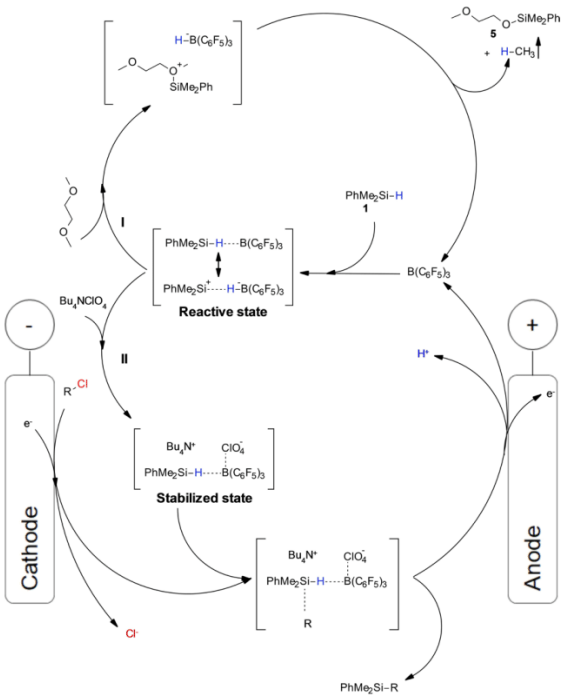

Scheme 4. Proposed mechanism for the anion stabilized and non-stabilized reaction pathway for the activated hydrosilane.

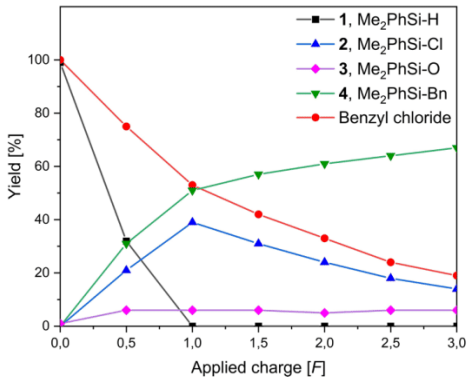

Figure 1. Distribution of components for the $B(C_6F_5)_3$-catalyzed benzylation of Me_2PhSiH in the course of electrolysis with **1**, $Me_2PhSi–H$ (black), **2**, $Me_2PhSi–Cl$ (blue), **3**, $Me_2PhSi–O–SiMe_2Ph$ (magenta), **4**, $Me_2PhSi–Bn$ (green) and benzyl chloride (red). Reaction conditions: current density of 10 mA/cm^2, 1,2-dimethoxyethane as solvent with 0.12 M Bu_4NClO_4 supporting electrolyte, anode material is glassy carbon, cathode material is CuSn7Pb15, Me_2PhSiH (0.50 M, 2.5 mmol) and benzyl chloride (0.69 M, 3.43 mmol), 1 mol% $B(C_6F_5)_3$ catalyst, at room temperature.

ChemElectroChem
Research Article
doi.org/10.1002/celc.202200840
Chemistry Europe
European Chemical Societies Publishing

well as outstanding chemical and mechanical stability, that diminishes contamination of the product mixture by heavy metals at a low cost of 6–12 €/kg.[54] Furthermore, leaded bronzes have demonstrated to be more stable towards cathodic corrosion.[55] In addition to the hitherto used CuSn7Pb15 composition, we have investigated different variations of leaded bronzes, as well as their neat components as cathode materials (Table 2). Lead as cathode material suffers from corrosion, contaminating the supporting electrolyte with 600 ppm lead in course of reaction while shifting the product distribution to chlorosilane **2** as main product with 56% (Table 2, entry 1). Copper, as alloy matrix of leaded bronze, is corrosion resistant under these reaction conditions and yields benzylsilane **4** close to the amount for leaded bronzes with a shifted ratio favoring chlorosilane **2** (Table 2, entry 2). Interestingly, with rising amount of tin in the composition of leaded bronzes, the yield of Si–C bond formation increases with a maximum yield of 71% for CuSn10Pb10 (Table 2, entries 4–6). This can be even raised using a tin cathode, generating 86% of benzylsilane **4** and rendering the formation of chlorosilane **2** a minor side reaction (Table 2, entry 3). It should be noted, that while no visible corrosion of the tin electrode occurs, contamination of the supporting electrolyte with tin (16 ppm) is detectable after conversion. For the leaded bronze compositions, no contamination of the electrolyte by heavy metals was detectable.

Table 2. Product yield for the variation of cathode material for the activated oxidative Si–C bond formation with benzyl chloride.

Entry	Cathode material	Si–C, **4** Yield[b]	Si–Cl, **2** Yield[b]	Si–O, **3** Yield[b]	Conversion[a]
1[c]	Pb	28%	56%	9%	100%
2	Cu	60%	33%	4%	100%
3[d]	Sn	86%	8%	6%	100%
4	CuSn5Pb20	65%	27%	7%	100%
5	CuSn7Pb15	67%	21%	8%	100%
6	CuSn10Pb10	71%	23%	4%	100%

[a] Reaction conditions: current density of 10 mA/cm², applied charge of 3.0 *F*, 1,2-dimethoxyethane as solvent with 0.12 M Bu_4NClO_4 supporting electrolyte, anode material is glassy carbon, Me_2PhSiH (0.50 M, 2.5 mmol) and benzyl chloride (0.69 M, 3.43 mmol), 1 mol% $B(C_6F_5)_3$ catalyst, at room temperature. [b] Yield determined by NMR referenced to TMS; Si–C, 4 = benzyldimethylphenylsilane; Si–Cl, 2 = chlorodimethylphenylsilane; Si–O, 3 = tetramethyldiphenyldisiloxane. [c] 600 ppm Pb detectable in the electrolyte after conversion. [d] 16 ppm Sn detectable in the electrolyte after conversion.

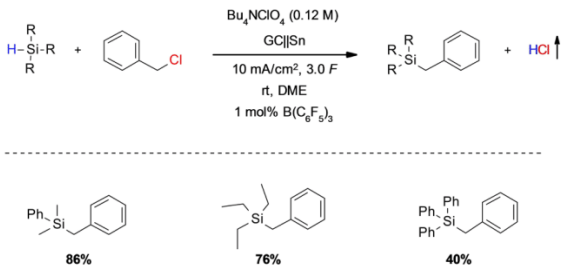

Scheme 5. Scope of electrochemical hydrosilane benzylation, yield determined by NMR referenced to TMS, GC = glassy carbon, DME = 1,2-dimethoxyethane.

The concept of boron-catalyzed electrochemical oxidative Si–C bond formation can be extended to alkylated and arylated hydrosilanes (Scheme 5). With increasing steric demand, the yield of Si–C bond formation diminishes, whereas the amount of chlorosilane rises.

Aside from the hitherto shown benzylation of hydrosilanes we further studied the allylation reaction. In this case, formation of the Si–C bond is made possible by the use of $B(C_6F_5)_3$, as underlined by cyclic voltammetry measurements (Figure 2). Hydrosilane **1** is oxidized in an irreversible process with a peak potential of 2.07 V vs. FcH/FcH^+. In comparison the product allyldimethylphenylsilane (Me_2PhSi-Allyl, **6**) is already oxidized at a peak potential of 1.49 V vs. FcH/FcH^+. In synthesis, the allylsilane can thus only be detected in traces. Preferential oxidation of the product compared to the starting material does not allow product accumulation. By oxidation of the allyl moiety, increasing amounts of disiloxane **3** and chlorosilane **2** are formed in course of reaction by electrolyte decomposition.

In presence of 1 mol% $B(C_6F_5)_3$, two additional oxidation potentials arise, shifting the onset potential by 880 mV, leading to oxidation potentials of 1.19 V vs. FcH/FcH^+ and 1.40 V vs. FcH/FcH^+. The oxidation potential of $[HB(C_6F_5)_3]^-$ is reported to be at 0.88 V vs. FcH/FcH^+,[29] differing from the obtained data by 310 mV. This indicates that complete hydride abstraction and availability of free $[HB(C_6F_5)_3]^-$ might not be the case in a perchlorate containing electrolyte. As discussed previously,[34] elongation of the Si–H bond without hydride abstraction should shift the oxidation potential of the formed adduct to less positive potentials due to decreasing activation barrier for Si–H cleavage. Here, it appears to correspond to an elongation of the Si–H bond without abstraction of hydride, since the reactivity of $B(C_6F_5)_3$ is decreased by the anion of the supporting electrolyte. Investigation of substrate stoichiometry indicated that an excess of 1.5 to 1.0 of hydrosilane **1** to allyl chloride allows for the highest yields for allylation reaction (see Supporting Information). For deeper insight into the reaction process and conversion, the reaction mixture was analyzed with

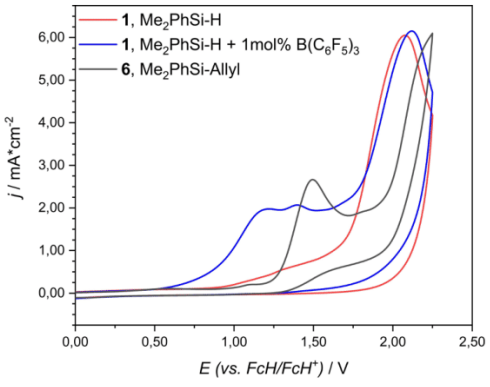

Figure 2. Cyclic voltammogram of 40 mM **1**, Me_2PhSiH (red), **1**, Me_2PhSiH with 1 mol% $B(C_6F_5)_3$ (blue) and **6**, Me_2PhSi-Allyl (black) in 0.1 M Bu_4NClO_4 and γ-butyrolactone. W.E. glassy carbon (A = 8.0 mm²), sweep rate ν = 0.2 V/s.

ChemElectroChem
Research Article
doi.org/10.1002/celc.202200840
Chemistry Europe
European Chemical Societies Publishing

increasing applied charge by GC and NMR. The emerging distribution can be divided into three parts (Figure 3).

In the first part of the reaction progress, until 1.0 *F* of applied charge is transferred, hydrosilane **1** is oxidatively consumed to form chlorosilane **2** as main product as well as allylsilane **6** as byproduct. Disiloxane **3** is generated by initial decomposition with the supporting electrolyte and yield does barely increase until 1.0 *F* applied charge is exceeded. At 1.0 *F* the maximum yield of allylsilane **6** is reached with 35% and hydrosilane **1** is completely consumed.

For the second part, due to the absence of a hydrosilane, allylsilane **6** is now the oxidatively consumed species, diminishing its yield and generating chlorosilane **2** as well as disiloxane **3**. Between 2.0 and 2.5 *F* allylsilane **6** is completely consumed and the yield of chlorosilane **2** reaches its maximum with 65%. The third part is initialized and due to missing alternative species, anodic halogenation of supporting electrolyte occurs

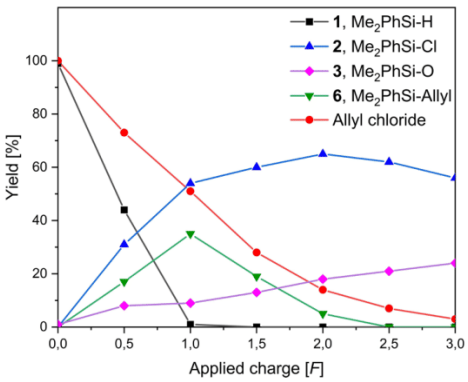

Figure 3. Distribution of components for the $B(C_6F_5)_3$-catalyzed allylation of Me_2PhSiH in the course of electrolysis with **1**, Me_2PhSi–H (black), **2**, Me_2PhSi–Cl (blue), **3**, Me_2PhSi–O–$SiMe_2Ph$ (magenta), **6**, Me_2PhSi-Allyl (green) and allyl chloride (red). Reaction conditions: current density of 10 mA/cm², 1,2-dimethoxyethane as solvent with 0.12 M Bu_4NClO_4 supporting electrolyte, anode material is glassy carbon, cathode material is CuSn7Pb15, Me_2PhSiH (0.50 M, 2.50 mmol) and allyl chloride (0.33 M, 1.67 mmol), 1 mol% $B(C_6F_5)_3$ catalyst, at room temperature.

Table 3. Product yield for the variation of cathode material for the activated oxidative Si–C bond formation with allyl chloride.

Entry	Cathode material	Si–C, **6** Yield[b]	Si–Cl, **2** Yield[b]	Si–O, **3** Yield[b]	Conversion[a]
1[c]	Pb	34%	54%	9%	100%
2	Cu	31%	57%	7%	100%
3[d]	Sn	8%	77%	8%	100%
4	CuSn5Pb20	30%	60%	9%	100%
5	CuSn7Pb15	35%	54%	9%	100%
6	CuSn10Pb10	29%	57%	9%	100%

[a] Reaction conditions: current density of 10 mA/cm², applied charge of 1.0 *F*, 1,2-dimethoxyethane as solvent with 0.12 M Bu_4NClO_4 supporting electrolyte, anode material is glassy carbon, Me_2PhSiH (0.50 M, 2.50 mmol) and allyl chloride (0.33 M, 1.67 mmol), 1 mol% $B(C_6F_5)_3$ catalyst, at room temperature. [b] Yield determined by NMR referenced to TMS; Si–C, 6 = allyldimethylphenylsilane; Si–Cl, 2 = chlorodimethylphenylsilane; Si–O, 3 = tetramethyldiphenyldisiloxane. [c] 400 ppm Pb detectable in the electrolyte after conversion. [d] 14 ppm Sn detectable in the electrolyte after conversion.

while chlorosilane **2** is reduced by cathodic reduction with consecutive formation of disiloxane **3** as thermodynamic sink. It should be noted that no further generation of allylsilane by reductive coupling of allyl chloride with chlorosilane **2** is detectable.

These observations support the suggestion that for borane-activated electrochemical Si–C bond formation, a one-electron process could occur for the conversion of intermediate. Furthermore, since the product is prone to oxidation, the maximum yield cannot be increased after complete conversion of the starting hydrosilane.

Analogue to materials chosen for the benzylation reaction, a screening of electrode material was conducted. For the allylation reaction lead and the leaded bronze CuSn7Pb15 generate the highest yield of allylsilane **6** with 35% (Table 3, entries 1 and 5). For lead, visible corrosion of the electrode material occurs and contamination of the supporting electrolyte by lead (400 ppm) is detectable after conversion. Tin as the most promising material for the benzylation of hydrosilanes is not suitable for the allylation reaction, diminishing the yield for allylsilane **6** to 8% and favoring the Si–Cl bond formation towards chlorosilane **2** (Table 3, entry 3). Furthermore, contamination of the supporting electrolyte by 14 ppm tin is determined. The leaded bronze alloys CuSn5Pb20 and CuSn10Pb10 show comparable results to the copper cathode, with formation of allylsilane **6** in the range of 29–31%, as well as yields determined for chlorosilane **2** and disiloxane **3** (Table 3, entries 2, 4 and 6). Increase of lead content to a maximum amount of 20% for CuSn5Pb20 does not increase the yield compared to CuSn7Pb15, rendering CuSn7Pb15 as preferred cathode material for the allylation of hydrosilanes without contamination of the supporting electrolyte by heavy metals.

Like the benzylation of hydrosilanes, this concept can be extended to alkylated and arylated hydrosilanes (Scheme 6). Again, increasing steric demand diminishes the yield of Si–C bond formation and raises the amount of chlorosilane.

Product distribution for the allylation reaction shows, that chlorination of the reactive silyl intermediate is one major side reaction, leading to the respective chlorosilanes. Hydrogen chloride released in course of reaction might be mainly responsible for the generation of chlorosilane species, diminishing the preferred Si–C bond formation. We therefore tried

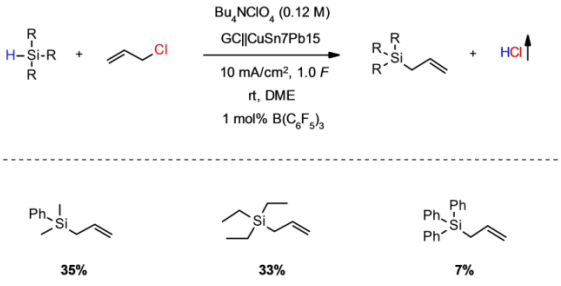

Scheme 6. Product scope of hydrosilane allylation, yield determined by NMR referenced to TMS, GC = glassy carbon, DME = 1,2-dimethoxyethane.

ChemElectroChem
Research Article
doi.org/10.1002/celc.202200840
Chemistry Europe
European Chemical Societies Publishing

various approaches to eliminate the released hydrogen chloride from the reaction mixture and to increase the amount of Si–C bond formation. Different scavenging strategies like precipitation of insoluble chloride salts, ion exchange as well as addition reactions involving epoxides were used (see Supporting Information). While the amount of chlorosilane **2** could be diminished, the yield of allylsilane **6** and the conversion of hydrosilane **1** was reduced as well, indicating anodic competition reactions and inactivation of $B(C_6F_5)_3$.

The electrochemical reaction of hydrosilanes with organic halides under borane-catalyzed conditions can be well demonstrated by the systems of benzyl and allyl species. These exhibit high stabilization of the anionic intermediate and show relatively low reduction potentials. However, extension of the scope quickly shows limits if reduction potential or stabilization of the intermediate are not sufficient. Using halo benzenes, the respective Si–C bond formation and complete conversion of hydrosilane can be achieved, yet the yield of the desired phenylsilane is rather low and cannot be increased by the use of $B(C_6F_5)_3$. Changing the halide species from chlorobenzene to bromo and iodobenzene does not change the yield in relation to the decreasing reduction potential. If the stabilization of the anion is increased by electron-withdrawing substituents, such as cyano groups, there is also no increase in yield. 4-Chloro- and 4-bromobenzonitrile show relatively low reduction potentials, cathodic access is thus possible and the conversion of the hydrosilane is 100% (see Supporting Information). However, stabilization of negative charge by resonance remains crucial for successful conversion so far.

Conclusion

The first boron-catalyzed electrochemical Si–C bond formation was established. By application of only catalytic amounts in the range of 1 mol% of Lewis acidic boranes such as $B(C_6F_5)_3$, benzylation and allylation of hydrosilanes were achieved in yields up to 86%. Cyclic voltammetry studies demonstrated that $B(C_6F_5)_3$ could be assigned the role to activate the hydrosilane for easier oxidation in presence of supporting electrolyte, resulting in significant increase in yield and the enrichment of the target product. Subsequent oxidation of product could be successfully suppressed by the shift of oxidation potential achieved by activation of hydrosilane with the Lewis acidic borane. The conversion was not only safe and easily controllable, but also cost-effective due to the use of glassy carbon and leaded bronze as electrode materials. Leaded bronze as cathode materials showed superior properties for this application and prevented contamination of the electrolyte with heavy metals. The scope of substrates has thus far been successfully applied only to benzyl and allyl chloride. However, we are convinced that further suitable substrates will be found in the near future to enrich the opportunity of electrochemical borane-catalyzed Si–C bond formation.

Experimental Section

Synthesis of material

For screening experiments undivided (5 mL) PTFE cells for electrolysis with reaction block, stirrer, power supply were obtained as IKA Screening System (IKA-Werke GmbH & Co. KG, Staufen, Germany). The active surface of the respective used electrode was 1.3 cm^2, anode and cathode surface were separated by 0.5 cm. The software used was IKA Labworldsoft 6.0.

Electrochemical benzylation of hydrosilanes

The undivided cell compartment was charged with $B(C_6F_5)_3$ (12.8 mg, $2.5\cdot10^{-2}$ mmol, $1.0\cdot10^{-2}$ eq.), DME (5.0 mL) and Bu_4NClO_4 (205 mg, 0.12 M). Me_2PhSiH (383.2 µL, 2.5 mmol, 1.0 eq.) and benzyl chloride (394.7 µL, 3.4 mmol, 1.3 eq.) were added under stirring (500 rpm). The electrodes were connected to the IKA power supply, and the reaction was conducted at room temperature ($j = 10$ mA/cm^2, 3.0 *F*). The general workup procedure consisted of stripping off volatile compounds. Chlorosilanes were distilled under inert gas atmosphere. Organosilanes were further purified by washing of the organic layer with distilled water (3×25 mL) and back-washing with n-pentane (3×25 mL). The combined organic fractions were dried over Na_2SO_4 and filtered. Volatile compounds were stripped off and the crude product was purified by column chromatography.

Electrochemical allylation of hydrosilanes

The undivided cell compartment was charged with $B(C_6F_5)_3$ (12.8 mg, $2.5\cdot10^{-2}$ mmol, $1.0\cdot10^{-2}$ eq.), DME (5.0 mL) and Bu_4NClO_4 (205 mg, 0.12 M). Me_2PhSiH (383.2 µL, 2.5 mmol, 1.0 eq.) and allyl chloride (135.7 µL, 1.7 mmol, 0.7 eq.) were added under stirring (500 rpm). The electrodes were connected to the IKA power supply, and the reaction was conducted at room temperature ($j = 10$ mA/cm^2, 1.0 *F*). The workup procedure was analogue to the synthesis of benzylsilanes.

Characterization

NMR Spectroscopy of ^1H, ^{13}C and ^{29}Si spectra were recorded at 25 °C, using a Bruker Avance 500 (500 MHz, Analytische Messtechnik, Karlsruhe, Germany). Chemical shifts (δ) are reported in parts per million (ppm). Traces of CH_2Cl_2 in the corresponding deuterated solvent, or tetramethylsilane for ^{29}Si spectra were used as internal standard for calibration. GC-MS measurements were carried out on an Agilent GC-A6890 N using a HP-5 column (Agilent Technologies, Santa Clara, California), length: 30 m, inner diameter: 0.25 mm, film: 0.25 µm, carrier gas: helium. The chromatograph was coupled to a mass spectrometer Agilent MSD 5975 C (Agilent, Santa Clara, California, USA).

Allyldimethylphenylsilane: ^1H NMR (500 MHz, CD_2Cl_2): δ [ppm] = 7.68–7.72 (m, 5H), 5.87–5.99 (m, 1H), 4.95–5.04 (m, 2H), 1.91 (d, J = 8.0 Hz, 2H), 0.43 (s, 6H). ^{13}C NMR (125 MHz, CD_2Cl_2): δ [ppm] = 140.1, 135.0, 133.9, 129. 6, 128.0, 113.5, 23.9, −3.4. ^{29}Si NMR (100 MHz, CD_2Cl_2): δ [ppm] = −4.72. MS m/z = 176 $[M]^+$.

Allyltriethylsilane: ^1H NMR (500 MHz, CD_2Cl_2): δ [ppm] = 6.03–6.22 (m, 1H), 5.56–5.74 (m, 2H), 1.86 (d, J = 8.0 Hz, 2H), 0.99 (t, J = 7.8 Hz, 9H), 0.43–0.65 (m, 6H). ^{13}C NMR (125 MHz, CD_2Cl_2): δ [ppm] = 127.6, 112.5, 18.5, 7.4, 3.1. ^{29}Si NMR (100 MHz, CD_2Cl_2): δ [ppm] = 5.74. MS m/z = 156 $[M]^+$.

Allyltriphenylsilane: ^1H NMR (500 MHz, CD_2Cl_2): δ [ppm] = 7.52–7.58 (m, 6H), 7.36–7.48 (m, 9H), 5.85–5.95 (m, 1H), 4.88–5.00 (m, 2H), 2.45

ChemElectroChem
Research Article
doi.org/10.1002/celc.202200840
Chemistry Europe
European Chemical Societies Publishing

(d, J = 8.0 Hz, 2H). ^{13}C NMR (125 MHz, CD_2Cl_2): δ [ppm] = 135.7, 134.6, 133.9, 129.6, 127.8, 114.8, 21.0. ^{29}Si NMR (100 MHz, CD_2Cl_2): δ [ppm] = −13.73. MS m/z = 301 $[M]^+$.

Benzyldimethylphenylsilane: ^{1}H NMR (500 MHz, CD_2Cl_2): δ [ppm] = 7.58–7.68 (m, 2H), 7.40–7.50 (m, 3H), 7.31 (t, J = 7.6 Hz, 2H), 7.20 (t, J = 7.4 Hz, 1H), 7.10 (d, J = 7.6 Hz, 2H), 2.47 (s, 2H), 0.41 (s, 6H). ^{13}C NMR (125 MHz, CD_2Cl_2): δ [ppm] = 139.9, 138.6, 133.9, 129.1, 128.4, 128.2, 127.8, 124.2, 26.1, −3.5. ^{29}Si NMR (100 MHz, CD_2Cl_2): δ [ppm] = −3.76. MS m/z = 226 $[M]^+$.

Benzyltriethylsilane: ^{1}H NMR (500 MHz, CD_2Cl_2): δ [ppm] = 7.22–7.27 (m, 2H), 7.06–7.11 (m, 3H), 2.18 (s, 2H), 0.99 (t, J = 8.0 Hz, 9H), 0.51 (q, J = 8.0 Hz, 6H). ^{13}C NMR (125 MHz, CD_2Cl_2): δ [ppm] = 141.2, 129.0, 128.5, 124.2, 21.9, 7.5, 3.4. ^{29}Si NMR (100 MHz, CD_2Cl_2): δ [ppm] = 6.41. MS m/z = 206 $[M]^+$.

Benzyltriphenylsilane: ^{1}H NMR (500 MHz, CD_2Cl_2): δ [ppm] = 7.53–7.59 (m, 6H), 7.42–7.47 (m, 9H), 7.12–7.22 (m, 2H), 6.99–7.03 (m, 3H), 3.10 (s, 2H). ^{13}C NMR (125 MHz, CD_2Cl_2): δ [ppm] = 138.5, 136.0, 134.4, 129.3, 129.1, 128.2, 127.9, 124.7, 23.3. ^{29}Si NMR (100 MHz, CD_2Cl_2): δ [ppm] = −12.26. MS m/z = 350 $[M]^+$.

Chlorodimethylphenylsilane: ^{1}H NMR (500 MHz, CD_2Cl_2): δ [ppm] = 7.71–7.74 (m, 2H), 7.46–7.54 (m, 3H), 0.77 (s, 6H). ^{13}C NMR (125 MHz, CD_2Cl_2): δ [ppm] = 136.7, 133.5, 130.8, 128.5, 2.2. ^{29}Si NMR (100 MHz, CD_2Cl_2): δ [ppm] = 20.49. MS m/z = 170 $[M]^+$.

Dimethyloctylphenylsilane: ^{1}H NMR (500 MHz, CD_2Cl_2): δ [ppm] = 7.46–7.55 (m, 2H), 7.29–7.37 (m, 3H), 1.18–1.40 (m, 12H), 0.85 (t, J = 6.9 Hz, 3H), 0.72–0.78 (m, 2H), 0.22 (s, 6H). ^{13}C NMR (125 MHz, CD_2Cl_2): δ [ppm] = 139.8, 133.7, 128.8, 127.8, 33.8, 32.1, 29.4, 24.0, 22.8, 15.9, 14.3, −2.8. ^{29}Si NMR (100 MHz, CD_2Cl_2): δ [ppm] = −2.41. MS m/z = 248 $[M]^+$.

Dimethyldiphenylsilane: ^{1}H NMR (500 MHz, CD_2Cl_2): δ [ppm] = 7.50–7.59 (m, 4H), 7.29–7.44 (m, 6H), 0.48 (s, 6H). ^{13}C NMR (125 MHz, CD_2Cl_2): δ [ppm] = 137.9, 134.0, 128.7, 127.3, −3.0. ^{29}Si NMR (100 MHz, CD_2Cl_2): δ [ppm] = −8.17. MS m/z = 212 $[M]^+$.

4-(Dimethylphenylsilyl)benzonitrile: ^{1}H NMR (500 MHz, CD_2Cl_2): δ [ppm] = 7.62–7.69 (m, 4H), 7.51–7.56 (m, 2H), 7.31–7.40 (m, 3H), 0.43 (s, 6H). ^{13}C NMR (125 MHz, CD_2Cl_2): δ [ppm] = 145.2, 136.6, 134.8, 134.3, 131.2, 129.8, 128.3, 119.1, 112.9, −2.5. ^{29}Si NMR (100 MHz, CD_2Cl_2): δ [ppm] = −7.12. MS m/z = 237 $[M]^+$.

1,1,3,3-tetramethyl-1,3-diphenyldisiloxane: ^{1}H NMR (500 MHz, CD_2Cl_2): δ [ppm] = 7.58–7.63 (m, 4H), 7.36–7.44 (m, 6H), 0.40 (s, 12H). ^{13}C NMR (125 MHz, CD_2Cl_2): δ [ppm] = 140.2, 133.4, 129.6, 128.0, 0.9. ^{29}Si NMR (100 MHz, CD_2Cl_2): δ [ppm] = −1.08. MS m/z = 286 $[M]^+$.

(2-Methoxyethoxy)dimethylphenylsilane: ^{1}H NMR (500 MHz, CD_2Cl_2): δ [ppm] = 7.60–7.67 (m, 2H), 7.38–7.47 (m, 3H), 3.80 (t, J = 5.0 Hz, 2H), 3.52 (t, J = 5.0 Hz, 2H), 3.39 (s, 3H), 0.45 (s, 6H). ^{13}C NMR (125 MHz, CD_2Cl_2): δ [ppm] = 138.3, 133.8, 129.9, 128.1, 74.6, 62.6, 59.3, −1.7. ^{29}Si NMR (100 MHz, CD_2Cl_2): δ [ppm] = 7.72. MS m/z = 195 $[M–CH_3]^+$.

Further detailed information on general procedures, electrochemical conversions, cyclic voltammetry measurements and product characterization can be found in the Supporting Information.

Acknowledgements

Open Access funding enabled and organized by Projekt DEAL.

Conflict of Interest

The authors declare no conflict of interest.

Data Availability Statement

The data that support the findings of this study are available in the supplementary material of this article.

Keywords: Boron · Electrolysis · Lewis acid activation · Oxidative coupling · Silicon

[1] V. Gevorgyan, M. Rubin, S. Benson, J.-X. Liu, Y. Yamamoto, *J. Org. Chem.* **2000**, *65*, 6179–6186.
[2] a) V. Gevorgyan, J.-X. Liu, Y. Yamamoto, *Chem. Commun.* **1998**, 37–38; b) R. L. Melen, *Chem. Commun.* **2014**, *50*, 1161–1174; c) D. J. Morrison, J. M. Blackwell, W. E. Piers, *Pure Appl. Chem.* **2004**, *76*, 615–623; d) D. J. Morrison, W. E. Piers, *Org. Lett.* **2003**, *5*, 2857–2860.
[3] a) A. Bernsdorf, H. Brand, R. Hellmann, M. Köckerling, A. Schulz, A. Villinger, K. Voss, *J. Am. Chem. Soc.* **2009**, *131*, 8958–8970; b) I. Krossing, I. Raabe, *Angew. Chem. Int. Ed.* **2004**, *43*, 2066–2090; *Angew. Chem.* **2004**, *116*, 2116–2142; c) S. J. Lancaster, A. Rodriguez, A. Lara-Sanchez, M. D. Hannant, D. A. Walker, D. H. Hughes, M. Bochmann, *Organometallics* **2002**, *21*, 451–453; d) R. E. LaPointe, G. R. Roof, K. A. Abboud, J. Klosin, *J. Am. Chem. Soc.* **2000**, *122*, 9560–9561; e) X. Yang, C. L. Stern, T. J. Marks, *J. Am. Chem. Soc.* **1994**, *116*, 10015–10031.
[4] a) A. G. Massey, A. J. Park, *J. Organomet. Chem.* **1964**, *2*, 245–250; b) A. G. Massey, A. J. Park, *J. Organomet. Chem.* **1966**, *5*, 218–225; c) A. G. Massey, A. J. Park, F. G. A. Stone, *Proc. Chem. Soc.* **1963**, *212*.
[5] a) M. A. Beckett, D. S. Brassington, S. J. Coles, M. B. Hursthouse, *Inorg. Chem. Commun.* **2000**, *3*, 530–533; b) H. Jacobsen, H. Berke, S. Döring, G. Kehr, G. Erker, R. Fröhlich, O. Meyer, *Organometallics* **1999**, *18*, 1724–1735.
[6] D. W. Stephan, G. Erker, *Angew. Chem. Int. Ed.* **2015**, *54*, 6400–6441; *Angew. Chem.* **2015**, *127*, 6498–6541.
[7] D. W. Stephan, *Science* **2016**, *354*, aaf7229.
[8] a) L. Greb, P. Oña-Burgos, B. Schirmer, S. Grimme, D. W. Stephan, J. Paradies, *Angew. Chem. Int. Ed.* **2012**, *51*, 10164–10168; *Angew. Chem.* **2012**, *124*, 10311–10315; b) D. W. Stephan, G. Erker, *Angew. Chem. Int. Ed.* **2010**, *49*, 46–76; *Angew. Chem.* **2010**, *122*, 50–81; c) G. C. Welch, D. W. Stephan, *J. Am. Chem. Soc.* **2007**, *129*, 1880–1881.
[9] D. W. Stephan, G. Erker, *Chem. Sci.* **2014**, *5*, 2625–2641.
[10] R. Dobrovetsky, D. W. Stephan, *J. Am. Chem. Soc.* **2013**, *135*, 4974–4977.
[11] C. M. Mömming, E. Otten, G. Kehr, R. Fröhlich, S. Grimme, D. W. Stephan, G. Erker, *Angew. Chem. Int. Ed.* **2009**, *48*, 6643–6646; *Angew. Chem.* **2009**, *121*, 6770–6773.
[12] A. Y. Houghton, J. Hurmalainen, A. Mansikkamäki, W. E. Piers, H. M. Tuononen, *Nat. Chem.* **2014**, *6*, 983–988.
[13] D. J. Parks, J. M. Blackwell, W. E. Piers, *J. Org. Chem.* **2000**, *65*, 3090–3098.
[14] J. M. Blackwell, E. R. Sonmor, T. Scoccitti, W. E. Piers, *Org. Lett.* **2000**, *2*, 3921–3923.
[15] W. E. Piers, A. J. V. Marwitz, L. G. Mercier, *Inorg. Chem.* **2011**, *50*, 12252–12262.
[16] T. Hackel, N. A. McGrath, *Molecules* **2019**, *24*, 432.
[17] D. T. Hog, M. Oestreich, *Eur. J. Org. Chem.* **2009**, *2009*, 5047–5056.
[18] J. M. Blackwell, K. L. Foster, V. H. Beck, W. E. Piers, *J. Org. Chem.* **1999**, *64*, 4887–4892.
[19] D. J. Parks, W. E. Piers, *J. Am. Chem. Soc.* **1996**, *118*, 9440–9441.
[20] M. Rubin, T. Schwier, V. Gevorgyan, *J. Org. Chem.* **2002**, *67*, 1936–1940.
[21] W. Yuan, P. Smirnov, M. Oestreich, *Chem* **2018**, *4*, 1443–1450.
[22] J. M. Blackwell, D. J. Morrison, W. E. Piers, *Tetrahedron* **2002**, *58*, 8247–8254.
[23] a) J. Hermeke, M. Mewald, M. Oestreich, *J. Am. Chem. Soc.* **2013**, *135*, 17537–17546; b) K. Müther, J. Mohr, M. Oestreich, *Organometallics* **2013**, *32*, 6643–6646.
[24] S. Rendler, M. Oestreich, *Angew. Chem. Int. Ed.* **2008**, *47*, 5997–6000; *Angew. Chem.* **2008**, *120*, 6086–6089.

ChemElectroChem
Research Article
doi.org/10.1002/celc.202200840
Chemistry Europe
European Chemical Societies Publishing

[25] K. Chulsky, R. Dobrovetsky, *Angew. Chem. Int. Ed.* **2017**, *56*, 4744–4748; *Angew. Chem.* **2017**, *129*, 4822–4826.
[26] W. Yang, L. Gao, J. Lu, Z. Song, *Chem. Commun.* **2018**, *54*, 4834–4837.
[27] S. A. Cummings, M. Iimura, C. J. Harlan, R. J. Kwaan, I. V. Trieu, J. R. Norton, B. M. Bridgewater, F. Jäkle, A. Sundararaman, M. Tilset, *Organometallics* **2006**, *25*, 1565–1568.
[28] E. J. Lawrence, V. S. Oganesyan, G. G. Wildgoose, A. E. Ashley, *Dalton Trans.* **2013**, *42*, 782–789.
[29] E. J. Lawrence, V. S. Oganesyan, D. L. Hughes, A. E. Ashley, G. G. Wildgoose, *J. Am. Chem. Soc.* **2014**, *136*, 6031–6036.
[30] E. J. Lawrence, T. J. Herrington, A. E. Ashley, G. G. Wildgoose, *Angew. Chem. Int. Ed.* **2014**, *53*, 9922–9925; *Angew. Chem.* **2014**, *126*, 10080–10083.
[31] Y. M. Lee, J. E. Seo, N.-S. Choi, J.-K. Park, *Electrochim. Acta* **2005**, *50*, 2843–2848.
[32] G.-B. Han, J.-N. Lee, J. W. Choi, J.-K. Park, *Electrochim. Acta* **2011**, *56*, 8997–9003.
[33] a) C.-C. Chang, T.-K. Chen, *J. Power Sources* **2009**, *193*, 834–840; b) C.-C. Chang, T.-K. Chen, L.-J. Her, G. T.-K. Fey, *J. Electrochem. Soc.* **2009**, *156*, A828-A832.
[34] A. D. Beck, S. Haufe, J. Tillmann, S. R. Waldvogel, *ChemElectroChem* **2022**, *9*, e202101374.
[35] a) A. Hosomi, *Acc. Chem. Res.* **1988**, *21*, 200–206; b) H. Sakurai, *Pure Appl. Chem.* **1982**, *54*, 1–22.
[36] A. Ramirez, K. A. Woerpel, *Org. Lett.* **2005**, *7*, 4617–4620.
[37] Z. Li, X. Cao, G. Lai, J. Liu, Y. Ni, J. Wu, H. Qiu, *J. Organomet. Chem.* **2006**, *691*, 4740–4746.
[38] R. E. Grote, E. R. Jarvo, *Org. Lett.* **2009**, *11*, 485–488.
[39] T. Shono, Y. Matsumura, S. Katoh, N. Kise, *Chem. Lett.* **1985**, *14*, 463–466.
[40] J. Yoshida, K. Muraki, H. Funahashi, N. Kawabata, *J. Org. Chem.* **1986**, *51*, 3996–4000.
[41] J. Yoshida, K. Muraki, H. Funahashi, N. Kawabata, *J. Organomet. Chem.* **1985**, *284*, C33-C35.
[42] a) G. Martin, F. S. Kipping, *J. Chem. Soc. Trans.* **1909**, *95*, 302–314; b) R. Robison, F. S. Kipping, *J. Chem. Soc. Trans.* **1908**, *93*, 439–456.
[43] Z.-D. Huang, R. Ding, P. Wang, Y.-H. Xu, T.-P. Loh, *Chem. Commun.* **2016**, *52*, 5609–5612.
[44] M. A. Brook, *Silicon in organic, organometallic, and polymer chemistry*, Wiley, New York, Weinheim, **2000**.
[45] a) D. Cantillo, *Chem. Commun.* **2022**, *58*, 619–628; b) C. Kingston, M. D. Palkowitz, Y. Takahira, J. C. Vantourout, B. K. Peters, Y. Kawamata, P. S. Baran, *Acc. Chem. Res.* **2020**, *53*, 72–83; c) M. C. Leech, K. Lam, *Nat. Chem. Rev.* **2022**, *6*, 275–286; d) R. D. Little, K. D. Moeller, *Chem. Rev.* **2018**, *118*, 4483–4484; e) S. Möhle, M. Zirbes, E. Rodrigo, T. Gieshoff, A. Wiebe, S. R. Waldvogel, *Angew. Chem. Int. Ed.* **2018**, *57*, 6018–6041; *Angew. Chem.* **2018**, *130*, 6124–6149; f) A. Shatskiy, H. Lundberg, M. D. Kärkäs, *ChemElectroChem* **2019**, *6*, 4067–4092; g) A. Wiebe, T. Gieshoff, S. Möhle, E. Rodrigo, M. Zirbes, S. R. Waldvogel, *Angew. Chem. Int. Ed.* **2018**, *57*, 5594–5619; *Angew. Chem.* **2018**, *130*, 5694–5721; h) M. Yan, Y. Kawamata, P. S. Baran, *Chem. Rev.* **2017**, *117*, 13230–13319.
[46] a) B. A. Frontana-Uribe, R. D. Little, J. G. Ibanez, A. Palma and R. Vasquez-Medrano, *Green Chem.* **2010**, *12*, 2099; b) D. Pollok, S. R. Waldvogel, *Chem. Sci.* **2020**, *11*, 12386–12400; c) J. Seidler, J. Strugatchi, T. Gärtner, S. R. Waldvogel, *MRS Energy Sustainability* **2020**, *7*, E42.
[47] a) J. L. Röckl, D. Pollok, R. Franke, S. R. Waldvogel, *Acc. Chem. Res.* **2020**, *53*, 45–61; b) S. R. Waldvogel, S. Lips, M. Selt, B. Riehl, C. J. Kampf, *Chem. Rev.* **2018**, *118*, 6706–6765.
[48] C. Grogger, B. Loidl, H. Stueger, T. Kammel, B. Pachaly, *J. Organomet. Chem.* **2006**, *691*, 105–110.
[49] a) A. Kunai, T. Kawakami, E. Toyoda, M. Ishikawa, *Organometallics* **1991**, *10*, 2001–2003; b) J. Ohshita, K. Hino, T. Iwawaki, A. Kunai, *J. Organomet. Chem.* **2009**, *625*, 138–143.
[50] a) E. Hengge, H. Firgoi, *J. Organomet. Chem.* **1981**, *212*, 155–161; b) E. Hengge, G. Litscher, *Angew. Chem. Int. Ed.* **1976**, *15*, 370; *Angew. Chem.* **1976**, *88*, 414.
[51] C. Jammegg, S. Graschy, E. Hengge, *Organometallics* **1994**, *13*, 2397–2400.
[52] A. Kunai, T. Kawakami, E. Toyoda, T. Sakurai, M. Ishikawa, *Chem. Lett.* **1993**, *22*, 1945–1948.
[53] M. Palframan, A. Parsons, P. Johnson, *Synlett* **2011**, *2011*, 2811–2814.
[54] a) C. Gütz, V. Grimaudo, M. Holtkamp, M. Hartmer, J. Werra, L. Frensemeier, A. Kehl, U. Karst, P. Broekmann, S. R. Waldvogel, *ChemElectroChem* **2018**, *5*, 247–252; b) C. Gütz, M. Selt, M. Bänziger, C. Bucher, C. Römelt, N. Hecken, F. Gallou, T. R. Galvão, S. R. Waldvogel, *Chem. Eur. J.* **2015**, *21*, 13878–13882.
[55] a) C. Gütz, M. Bänziger, C. Bucher, T. R. Galvão, S. R. Waldvogel, *Org. Process Res. Dev.* **2015**, *19*, 1428–1433; b) T. Wirtanen, T. Prenzel, J.-P. Tessonnier, S. R. Waldvogel, *Chem. Rev.* **2021**, *121*, 10241–10270; c) T. Wirtanen, E. Rodrigo, S. R. Waldvogel, *Chem. Eur. J.* **2020**, *26*, 5592–5597.

Manuscript received: August 9, 2022
Revised manuscript received: August 12, 2022
Accepted manuscript online: August 12, 2022

ChemElectroChem

Supporting Information

Boron-Catalyzed Electrochemical Si–C Bond Formation for Safe and Controllable Benzylation and Allylation of Hydrosilanes

Alexander D. Beck, Stefan Haufe, and Siegfried R. Waldvogel*

Supporting Information

Contents

1 General Information

All reagents were of analytical grade and obtained from commercial suppliers such as Aldrich, VWR, and Acros. Solvents were obtained in anhydrous quality and water content was checked by Karl-Fischer analysis. Electrochemical reactions were carried out at boron-doped diamond (BDD), glassy carbon (GC), platinum (Pt), copper (Cu), leaded bronze (CuSn7Pb15), graphite (C) and silver (Ag). BDD electrodes were obtained as DIACHEM™ quality (CONDIAS GmbH, Itzehoe, Germany). BDD (10 µm diamond layer) was used on silicon as support. GC, Pt, Cu, leaded bronze, C and Ag electrodes were obtained from IKA (IKA-Werke GmbH & Co. KG, Staufen, Germany). The dimensions of all used electrode materials were 7 cm x 1 cm x 0.3 cm.

Gas chromatography was performed on an Agilent GC-A6890N (Agilent, Santa Clara, California, USA) using a RTX200 column (Agilent Technologies, Santa Clara, California, USA), length: 60 m + 30 m, inner diameter: 2 x 0.32 mm, film: 0.25 µm, carrier gas: helium. **GC-MS** measurements were carried out on an Agilent GC-A6890N using a HP-5 column (Agilent Technologies, Santa Clara, California), length: 30 m, inner diameter: 0.25 mm, film: 0.25 µm, carrier gas: helium. The chromatograph was coupled to a mass spectrometer Agilent MSD 5975 C (Agilent, Santa Clara, California, USA).

NMR Spectroscopy of ^{1}H, ^{13}C and ^{29}Si spectra were recorded at 25 °C, using a Bruker Avance 500 (500 MHz, Analytische Messtechnik, Karlsruhe, Germany). Chemical shifts (δ) are reported in parts per million (ppm). Traces of CH_2Cl_2 in the corresponding deuterated solvent, or tetramethylsilane for ^{29}Si spectra were used as internal standard for calibration.

Cyclic voltammetry was performed under inert gas in a 20 mL glass vial (SVC-3 voltammetry cell, ALS Co., Ltd., Tokyo, Japan) equipped with an SP-300 potentiostat (Bio-Logic Science Instruments, Seyssinet-Pariset, France) *WE*: GC / Pt / Ag electrode tip, 1.6 mm diameter; *CE*: platinum wire; *RE*: Ag/Ag^+ in 0.01 M $AgNO_3$ / 0.1 M Bu_4NClO_4. Solvent: γ-butyrolactone. v = 200 mV/s, T = 25 °C, supporting electrolyte: $n Bu_4NClO_4$, c ($n Bu_4NClO_4$) = 0.1 M.

2 Set-up and general protocols for electrochemical synthesis

Undivided Cell:
For screening experiments undivided (5 mL) PTFE cells for electrolysis with reaction block, stirrer, power supply were obtained as IKA Screening System (IKA-Werke GmbH & Co. KG, Staufen, Germany). The active surface of the respective used electrode was 1.3 cm^2, anode and cathode surface were separated by 0.5 cm. The software used was IKA Labworldsoft 6.0.

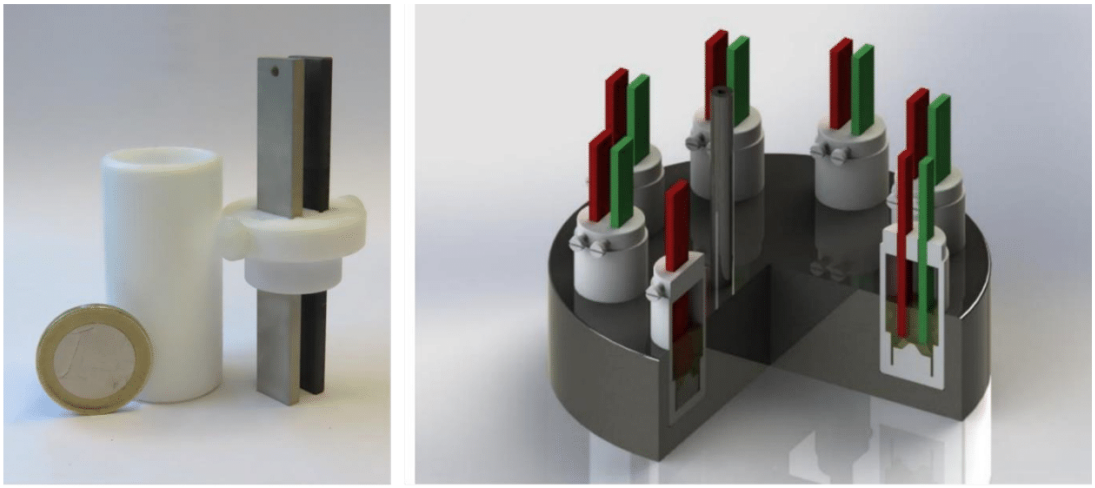

Figure 1: 5 mL PTFE cell; left: with 1 Euro coin for size comparison; right: schematic visualization of 5 mL PTFE cells in a screening block.

General procedure for optimization reactions (GP1):
The undivided cell compartment was charged with DME (5.0 mL) and Bu_4NClO_4 (205 mg, 0.12 M). Me_2PhSiH (383.2 µL, 2.5 mmol, 1.0 eq.) and chlorobenzene (253.5 µL, 2.5 mmol, 1.0 eq.) were added under stirring (500 rpm). The electrodes were connected to the IKA power supply, and the reaction was conducted at room temperature. After termination of the electrolysis (j = 10 mA/cm^2, 2.5 F), the product distribution was determined by direct ^1H and ^{29}Si NMR spectroscopy of samples of 300 µL of the reaction solution with a reference of 50 µL tetramethylsilane (TMS). For ^{29}Si NMR spectroscopy an additive of 8 mg $Cr(acac)_3$ as paramagnetic reagent for enhanced longitudinal relaxation was used.
The general workup procedure consisted of stripping off volatile compounds. Chlorosilanes were distilled under inert gas atmosphere. Organosilanes were further purified by washing of the organic layer with distilled water (3x25 mL) and back-washing with n-pentane (3x25 mL). The combined organic fractions were dried over Na_2SO_4 and filtered. Volatile compounds were stripped off and the crude product was purified by column chromatography.

General procedure for optimization reactions (GP2):
The undivided cell compartment was charged with $B(C_6F_5)_3$ (12.8 mg, $2.5 \cdot 10^{-2}$ mmol, $1.0 \cdot 10^{-2}$ eq.), DME (5.0 mL) and Bu_4NClO_4 (205 mg, 0.12 M). Me_2PhSiH (383.2 µL, 2.5 mmol, 1.0 eq.) and benzyl chloride (394.7 µL, 3.4 mmol, 1.3 eq.) were added under stirring (500 rpm). The electrodes were connected to the IKA power supply, and the reaction was conducted at room temperature. After termination of the electrolysis (j = 10 mA/cm^2, 3.0 F), the product distribution was determined by direct ^1H and ^{29}Si NMR spectroscopy of samples of 300 µL of the reaction solution with a reference of 50 µL tetramethylsilane (TMS). For ^{29}Si NMR spectroscopy an additive of 8 mg $Cr(acac)_3$ as paramagnetic reagent for enhanced longitudinal relaxation was used. The workup procedure was analogue to GP1.

General procedure for optimization reactions (GP3):

The undivided cell compartment was charged with $B(C_6F_5)_3$ (12.8 mg, $2.5 \cdot 10^{-2}$ mmol, $1.0 \cdot 10^{-2}$ eq.), DME (5.0 mL) and Bu_4NClO_4 (205 mg, 0.12 M). Me_2PhSiH (383.2 µL, 2.5 mmol, 1.0 eq.) and allyl chloride (135.7 µL, 1.7 mmol, 0.7 eq.) were added under stirring (500 rpm). The electrodes were connected to the IKA power supply, and the reaction was conducted at room temperature. After termination of the electrolysis (j = 10 mA/cm^2, 1.0 F), the product distribution was determined by direct ^{1}H and ^{29}Si NMR spectroscopy of samples of 300 µL of the reaction solution with a reference of 50 µL tetramethylsilane (TMS). For ^{29}Si NMR spectroscopy an additive of 8 mg $Cr(acac)_3$ as paramagnetic reagent for enhanced longitudinal relaxation was used. The workup procedure was analogue to GP1.

3 General cyclic voltammetry protocol

The complete set-up was used in a Glovebox under argon inert gas atmosphere (<0.1 ppm O_2 and <0.1 ppm H_2O content), so no further degassing of the solvent was necessary. As supporting electrolyte γ-butyrolactone (water content <10 ppm, checked by Karl-Fischer analysis) containing 0.1 M Bu_4NClO_4 was placed in a 20 mL glass vial. Cyclic voltammetry was performed with a scan rate of 0.2 V/s otherwise noted, using glassy carbon, platinum or silver working electrode (tip, 1.6 mm diameter, each), a platinum wire as counter electrode and an Ag/Ag^+ reference electrode in 0.01 M $AgNO_3$ / 0.1 M Bu_4NClO_4 acetonitrile solution. Ferrocene/Ferrocenium (FcH/FcH^+) was used as internal reference (half-wave potential 0.09 V vs. Ag/Ag^+).

4 Results for the electrochemical screening reactions

The electrochemical screening reactions were carried out in undivided cells. Conversion was evaluated relative to TMS based on ^{29}Si NMR integrals.

4.1 Screening of electrolyte solvent

For the oxidative Si-C bond formation, the supporting electrolyte solvent was screened (Table 1) according to GP1 with a silver cathode and a glassy carbon anode (Scheme 1). Bu_4NClO_4 was used as supporting electrolyte for all experiments.

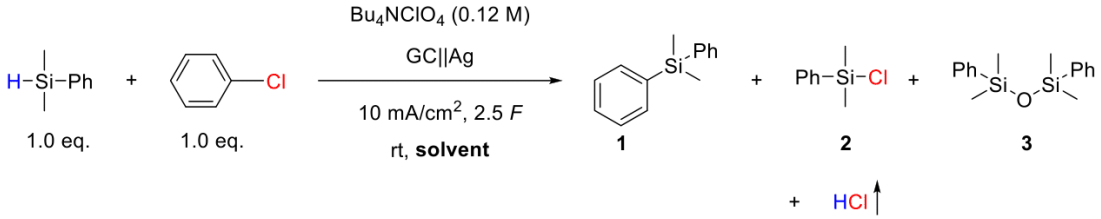

Scheme 1. Solvent Screening for oxidative Si-C bond formation.

Table 1. Screening of electrolyte solvent for oxidative Si-C bond formation.[a]

Entry	Solvent	Yield of Si-C, 1[b]	Yield of Si-Cl, 2[b]	Yield of Si-O, 3[b]	Conversion
1	Dimethoxyethane	5%	17%	14%	44%
2	Tetrahydrofuran	3%	17%	19%	52%
3	Acetonitrile	0%	19%	39%	80%
4[c]	1,3-Dimethyl-imidazolidin-2-one	3%	6%	8%	21%
5	γ-butyrolactone	0%	0%	19%	24%
6[c]	*N,N*-Dimethylformamide	0%	0%	7%	8%
7	Propylene carbonate	0%	0%	61%	69%

[a] Conditions for electrolysis and product range are depicted in Scheme 1. [b] Quantification of the yield was performed by ^{29}Si NMR relative to tetramethylsilane as internal standard. [c] Decomposition of electrolyte occurs.

4.2 Screening of electrode material

For the oxidative Si-C bond formation, the electrode material was screened (Table 2) according to GP1 with DME / Bu_4NClO_4 supporting electrolyte (Scheme 2).

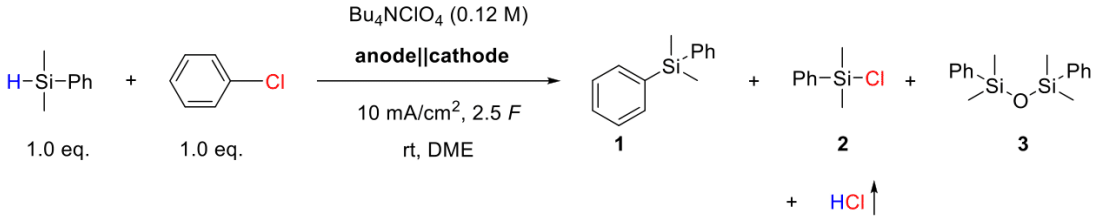

Scheme 2. Electrode material screening for oxidative Si-C bond formation.

Table 2. Screening of electrode material for oxidative Si-C bond formation.[a]

Entry	Anode[b]	Cathode[b]	Yield of Si-C, 1[c]	Yield of Si-Cl, 2[c]	Yield of Si-O, 3[c]	Conversion
1	GC	Ag	5%	17%	14%	44%
2	C	Ag	4%	18%	15%	41%
3	BDD	Ag	1%	11%	8%	23%
4[d]	Cu	Ag	2%	9%	7%	22%
5	GC	BDD	0%	12%	7%	20%
6	GC	C	1%	6%	7%	15%
7	GC	GC	2%	10%	2%	17%
8	GC	CuSn7Pb15	6%	22%	9%	46%
9	GC	Pt	3%	15%	18%	42%

[a] Conditions for electrolysis and product range are depicted in Scheme 2. [b] Ag = silver; GC = glassy carbon; BDD = boron-doped diamond; Cu = copper; C = graphite, CuSn7Pb15 = leaded bronze with 7w% tin and 15w% lead; Pt = platinum. [c] Quantification of the yield was performed by ^{29}Si NMR relative to tetramethylsilane as internal standard. [d] Corrosion of the copper anode occurs.

4.3 Screening of educt stoichiometry

For the oxidative Si-C bond formation, the educt stoichiometry was screened (Table 3) according to GP1 with DME / Bu_4NClO_4 supporting electrolyte and CuSn7Pb15 cathode and glassy carbon anode (Scheme 3).

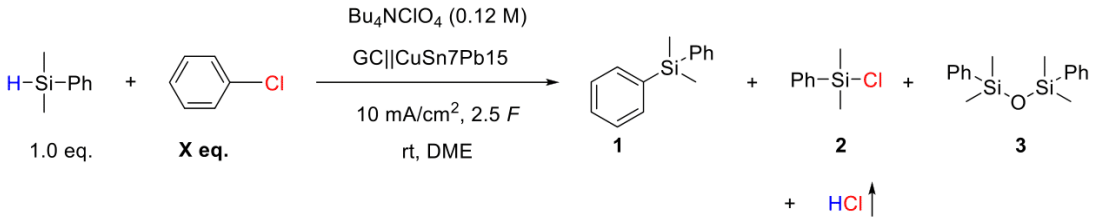

Scheme 3. Educt stoichiometry screening for oxidative Si-C bond formation by phenylation of hydrosilane.

Table 3. Screening of educt stoichiometry for oxidative Si-C bond formation by phenylation of hydrosilane.[a]

Entry	Eq. of chlorobenzene	Yield of Si-C, 1[b]	Yield of Si-Cl, 2[b]	Yield of Si-O, 3[b]	Conversion
1	0.7	4%	14%	7%	31%
2	1.0	6%	22%	9%	46%
3	1.3	9%	27%	10%	57%
4	1.5	6%	23%	9%	51%
5	2.0	3%	13%	8%	25%
6	3.0	1%	9%	5%	18%

[a] Conditions for electrolysis and product range are depicted in Scheme 3. [b] Quantification of the yield was performed by ^{29}Si NMR relative to tetramethylsilane as internal standard.

4.4 Screening of organic halides

For the oxidative Si-C bond formation, the organic halide was screened (Table 4) according to GP1 with DME / Bu_4NClO_4 supporting electrolyte and CuSn7Pb15 cathode and glassy carbon anode with a stoichiometry of 1.0 : 1.3 of hydrosilane in comparison to organic halide (Scheme 4).

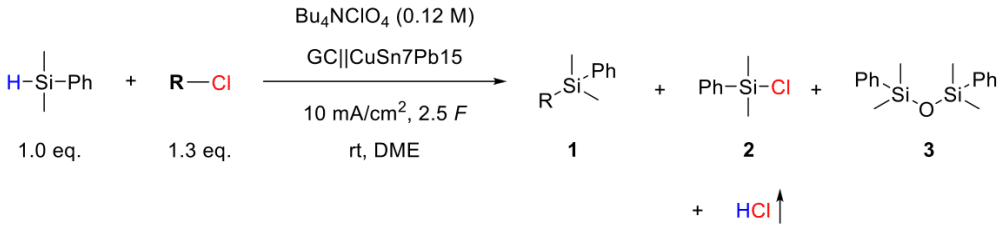

Scheme 4. Organic halide screening for oxidative Si-C bond formation.

Table 4. Screening of the organic halide for oxidative Si-C bond formation.[a]

Entry	Organic halide	Yield of Si-C, 1[b]	Yield of Si-Cl, 2[b]	Yield of Si-O, 3[b]	Conversion
1	Chlorobenzene	9%	27%	10%	57%
2	1-Chlorooctane	4%	16%	7%	53%
3	Benzyl chloride	10%	6%	2%	23%

[a] Conditions for electrolysis and product range are depicted in Scheme 4. [b] Quantification of the yield was performed by ^{29}Si NMR relative to tetramethylsilane as internal standard.

4.5 Screening of supporting electrolyte for the stabilization of activated hydrosilane

For the oxidative Si-C bond formation, the influence of different supporting electrolytes for the stabilization of activated hydrosilane was investigated (Table 5) according to GP2 with 2.5 mol% of $B(C_6F_5)_3$, in presence of an organic halide, that does not take part in course of the reaction. DME was used as solvent with varying supporting electrolyte (each 0.12 M) in a current-less state (Scheme 5). A stoichiometry of 1.0 : 1.3 of hydrosilane in comparison to organic halide was applied.

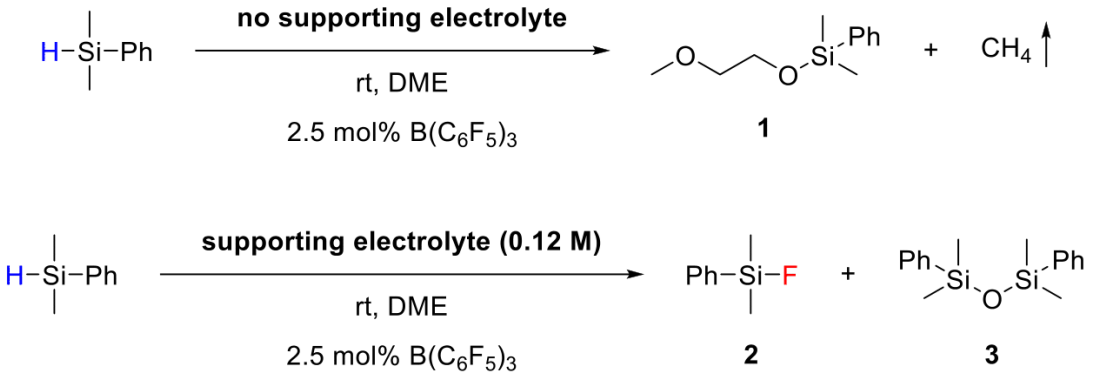

Scheme 5. Influence of the supporting electrolyte on the reactivity for oxidative Si-C bond formation.

Table 5. Stabilization of activated hydrosilane based on different supporting electrolytes.[a]

Entry	Supporting electrolyte	Yield of Si-O, 1[b]	Yield of Si-F, 2[b]	Yield of Si-O, 3[b]	Conversion
1[c]	None	96%	0%	3%	100%
2	Bu_4NClO_4	0%	0%	4%	4%
3	$LiClO_4$	0%	0%	4%	4%
4	Bu_4NBF_4	0%	5%	0%	5%

[a] Conditions for electrolysis and product range are depicted in Scheme 5. [b] Quantification of the yield was performed by ^{29}Si NMR relative to tetramethylsilane as internal standard. [c] The reaction occurred spontaneously and vigorously with release of methane gas and heating by the addition of hydrosilane.

4.6 Screening of charge density

For the oxidative Si-C bond formation, the charge density was screened (Table 6) according to GP2 with DME / Bu_4NClO_4 supporting electrolyte and CuSn7Pb15 cathode and glassy carbon anode with a stoichiometry of 1.0 : 1.3 of hydrosilane in comparison to organic halide (Scheme 6).

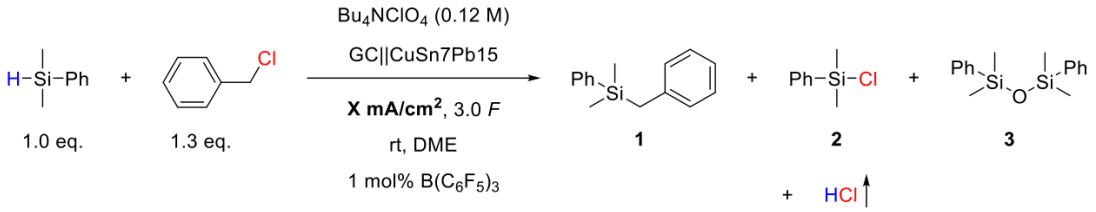

Scheme 6. Charge density screening for oxidative Si-C bond formation.

Table 6. Screening of charge density for oxidative Si-C bond formation.[a]

Entry	Charge density [mA/cm²]	Yield of Si-C, 1[b]	Yield of Si-Cl, 2[b]	Yield of Si-O, 3[b]	Conversion
1	7	50%	33%	14%	100%
2	10	67%	21%	8%	100%
3	13	60%	28%	9%	100%

[a] Conditions for electrolysis and product range are depicted in Scheme 6. [b] Quantification of the yield was performed by ^{29}Si NMR relative to tetramethylsilane as internal standard.

4.7 Screening of educt stoichiometry for allylation of hydrosilanes

For the oxidative Si-C bond formation, the educt stoichiometry was screened (Table 7) according to GP3 with DME / Bu_4NClO_4 supporting electrolyte and CuSn7Pb15 cathode and glassy carbon anode (Scheme 7).

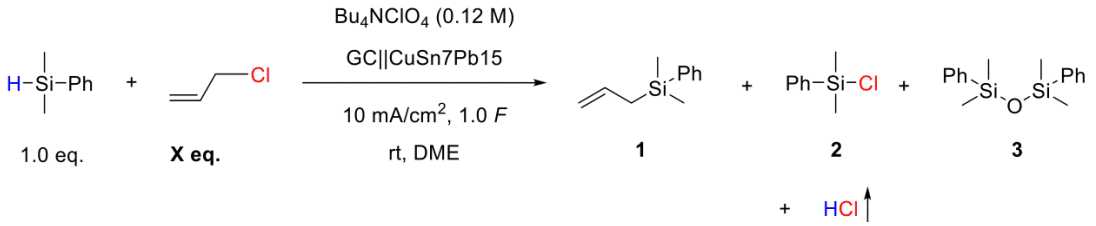

Scheme 7. Educt stoichiometry screening for oxidative Si-C bond formation by allylation of hydrosilane.

Table 7. Screening of educt stoichiometry for oxidative Si-C bond formation by allylation of hydrosilane.[a]

Entry	Eq. of allyl chloride	Yield of Si-C, **1**[b]	Yield of Si-Cl, **2**[b]	Yield of Si-O, **3**[b]	Conversion
1	1.3	16%	75%	5%	100%
2	1.0	24%	68%	8%	100%
3	0.8	32%	60%	7%	100%
4	0.7	35%	54%	9%	100%
5	0.5	24%	56%	4%	100%

[a] Conditions for electrolysis and product range are depicted in Scheme 7. [b] Quantification of the yield was performed by ^{29}Si NMR relative to tetramethylsilane as internal standard.

4.8 Screening of HCl scavenger for benzylation of hydrosilanes

Different scavenging strategies like precipitation of insoluble chloride salts, ion exchange as well as addition reactions involving epoxides were used. While the amount of chlorosilane **2** could be diminished, the yield of benzylsilane **1** and the conversion of the starting hydrosilane was reduced as well, indicating anodic competition reactions and inactivation of $B(C_6F_5)_3$. One strategy is to scavenge hydrogen chloride by precipitation as insoluble chloride salts with K_2CO_3 as KCl, $AgNO_3$ or $AgClO_4$ as AgCl, pyridine as pyridinium chloride and the non-nucleophilic base 2,6-di-*tert*-butylpyridine as alternative to pyridine with increased steric demand. The carbonate shifts the amount of chlorosilane **2** and benzylsilane **1** to disiloxane **3** (Table 8, entry 2). In presence of Ag(I) salts, disiloxane **3** is the sole product obtained after conversion (Table 8, entries 8-9). The high activity of the silyl intermediate limits the use of HCl scavengers and precludes the use of carbonate anions as well as Ag(I) salts for further studies. Pyridine forms polymeric by-products by anodic oxidation in a competition reaction to the hydrosilane oxidation, despite its high oxidative stability (Table 8, entry 4). No oxidation potential can be determined by CV in the range of electrolyte stability, whereas upon addition of $B(C_6F_5)_3$ an ill-defined oxidation wave at 1.57 V vs. FcH/FcH^+ arises (see chapter 5.3). Thereby the original oxidation potential of the activated as well as the non-activated hydrosilane is suppressed and oxidation favors pyridine. This leads to coating of the anode material by polymeric oxidation products and barely conversion of hydrosilane. Increasing the steric demand by the use of 2,6-di-*tert*-butylpyridine, anodic coating can be suppressed and conversion of hydrosilane is almost complete (Table 8, entry 5). At the same time, yield of Si-C bond formation is slightly diminished to 31% while the generation of chlorosilane **2** is not suppressed. This indicates no scavenging of hydrogen chloride in the used supporting electrolyte probably due to solubility of 2,6-di-*tert*-butylpyridinium chloride, causing availability of halide ions to the silyl intermediate species. Polyethylenimine (PEI) with the function as acid trapping material as well as 1,2-epoxybutane, an epoxide capable of hydrogen halide scavenging by addition reaction under ring opening, alter the activity of $B(C_6F_5)_3$. As CV measurements reveal, the presence of PEI or 1,2-epoxybutane completely suppresses the activation of the starting hydrosilane by $B(C_6F_5)_3$ (see chapter 5.3). This is probably due to complexation of $B(C_6F_5)_3$ by PEI or 1,2-epoxybutane which removes $B(C_6F_5)_3$ from reaction equilibrium and thus prevents the activation of the Si-H bond (Table 8, entries 3 and 7). Comparable results were achieved for the allylation reaction (see chapter 4.9).

For the oxidative Si-C bond formation, the use of HCl-scavenger was screened (Table 8) according to GP2 with DME / Bu_4NClO_4 supporting electrolyte and CuSn7Pb15 cathode and glassy carbon anode (Scheme 8). The amount of HCl-scavenger was 1.0 eq. relative to the organic halide.

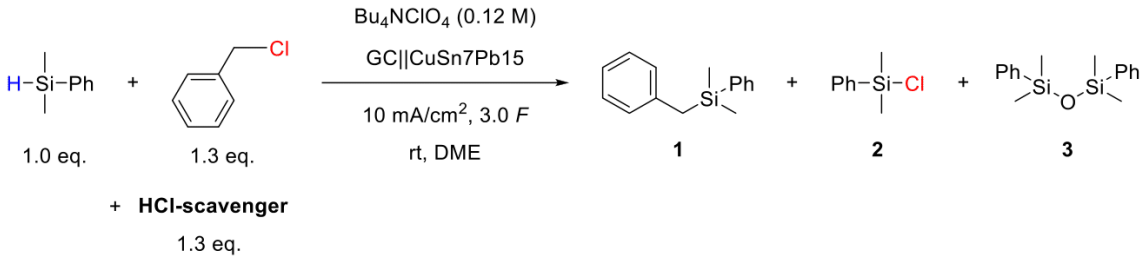

Scheme 8. HCl-scavenger screening for oxidative Si-C bond formation by benzylation of hydrosilane.

Table 8. Screening of HCl-scavenger for oxidative Si-C bond formation by benzylation of hydrosilane.[a]

Entry	HCl-scavenger	Yield of Si-C, **1**[b]	Yield of Si-Cl, **2**[b]	Yield of Si-O, **3**[b]	Conversion
1	None	67%	21%	8%	100%
2	K_2CO_3	53%	8%	36%	100%
3	1,2-Epoxybutane	0%	0%	3%	4%
4[c]	Pyridine	0%	0%	2%	4%
5	2,6-Di-*tert*-butylpyridine	63%	23%	7%	94%
6[c]	DABCO	3%	0%	4%	9%
7[d]	Polyethyleneimine on silica gel	0%	0%	25%	25%
8	$AgClO_4$	0%	6%	91%	100%
9	$AgNO_3$	0%	9%	85%	100%

[a] Conditions for electrolysis and product range are depicted in Scheme 8. [b] Quantification of the yield was performed by ^{29}Si NMR relative to tetramethylsilane as internal standard. [c] Polymer formation at the anode. [d] 20-60 mesh.

4.9 Screening of HCl scavenger for allylation of hydrosilanes

For the oxidative Si-C bond formation, the use of HCl-scavenger was screened (Table 9), analogue to the benzylation reaction (see chapter 4.8) according to GP3 with DME / Bu_4NClO_4 supporting electrolyte and CuSn7Pb15 cathode and glassy carbon anode (Scheme 9). The amount of HCl-scavenger was 1.0 eq. relative to the organic halide.

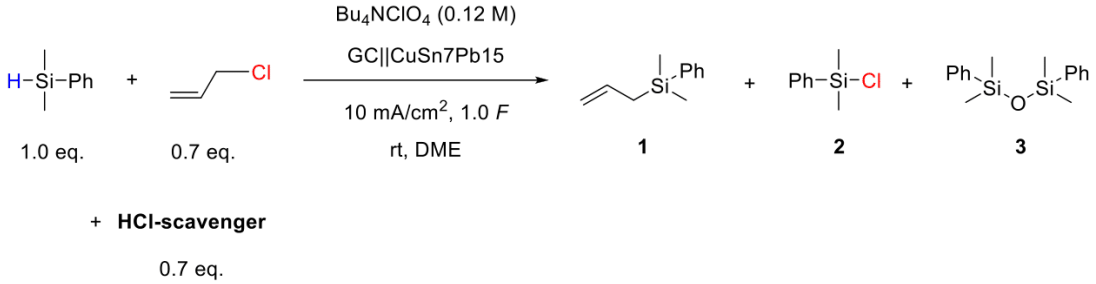

Scheme 9. HCl-scavenger screening for oxidative Si-C bond formation by allylation of hydrosilane.

Table 9. Screening of HCl-scavenger for oxidative Si-C bond formation by allylation of hydrosilane.[a]

Entry	HCl-scavenger	Yield of Si-C, 1[b]	Yield of Si-Cl, 2[b]	Yield of Si-O, 3[b]	Conversion
1	None	35%	54%	9%	100%
2	K_2CO_3	10%	46%	22%	100%
3	1,2-Epoxybutane	0%	3%	9%	12%
4[c]	Pyridine	0%	0%	5%	5%
5	2,6-Di-*tert*-butylpyridine	31%	56%	5%	95%
6[c]	DABCO	4%	0%	2%	7%
7[d]	Polyethylenimine on silica gel	0%	0%	26%	26%
8	$AgClO_4$	0%	0%	100%	100%
9	$AgNO_3$	0%	0%	100%	100%

[a] Conditions for electrolysis and product range are depicted in Scheme 9. [b] Quantification of the yield was performed by ^{29}Si NMR relative to tetramethylsilane as internal standard. [c] Polymer formation at the anode. [d] 20-60 mesh.

4.10 Screening of organic halides for Si-C bond formation with hydrosilanes

For the oxidative Si-C bond formation, the use of further organic halides was screened (Table 10) according to GP2 with DME / Bu_4NClO_4 supporting electrolyte and CuSn7Pb15 cathode and glassy carbon anode (Scheme 10).

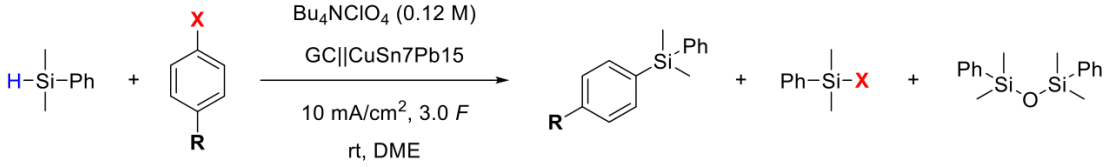

Scheme 10. Organic halide screening for oxidative Si-C bond formation with action of hydrosilane.

Table 10. Screening of organic halide for activated oxidative Si-C bond formation with hydrosilane.[a]

Entry	X	R	Yield of Si-C, 1[b]	Yield of Si-X, 2[b]	Yield of Si-O, 3[b]	Conversion
1	-Cl	-H	4%	18%	70%	100%
2	-Br	-H	15%	0%	78%	100%
3	-I	-H	7%	0%	85%	100%
4	-Cl	-CN	8%	57%	24%	100%
5	-Br	-CN	15%	0%	80%	100%

[a] Conditions for electrolysis and product range are depicted in Scheme 10. [b] Quantification of the yield was performed by ^{29}Si NMR relative to tetramethylsilane as internal standard.

5 Cyclic voltammetry data

5.1 Reduction potential of organic halides

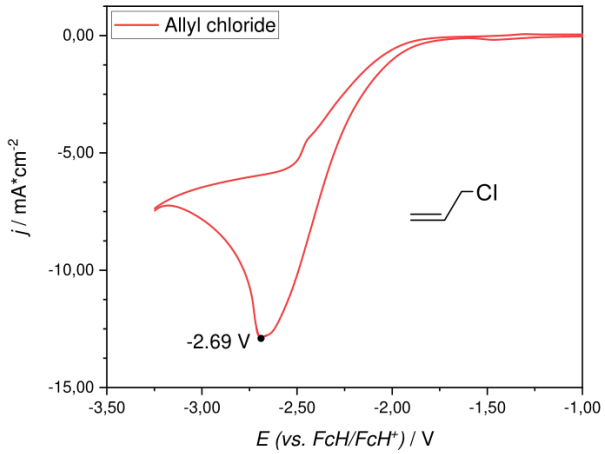

Figure 2. Cyclic voltammogram of 40 mM allyl chloride in 0.1 M Bu_4NClO_4 and γ-butyrolactone. W.E. Ag (A = 8.0 mm²), *v* = 0.2 V/s. Peak potential of allyl chloride: −2.69 V vs. FcH/FcH⁺.

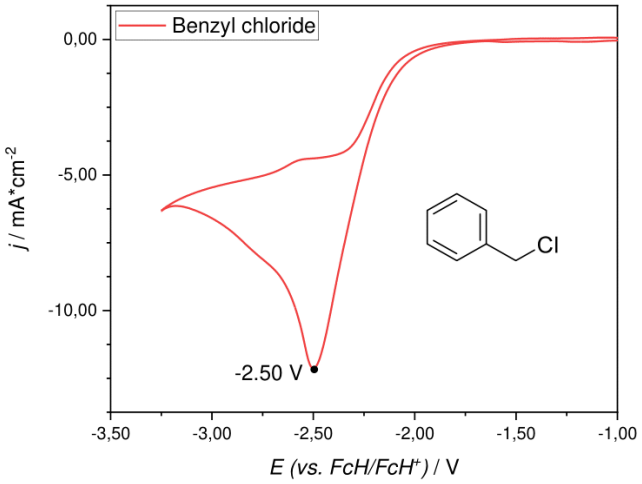

Figure 3. Cyclic voltammogram of 40 mM benzyl chloride in 0.1 M Bu_4NClO_4 and γ-butyrolactone. W.E. Ag (A = 8.0 mm²), *v* = 0.2 V/s. Peak potential of benzyl chloride: −2.50 V vs. FcH/FcH⁺.

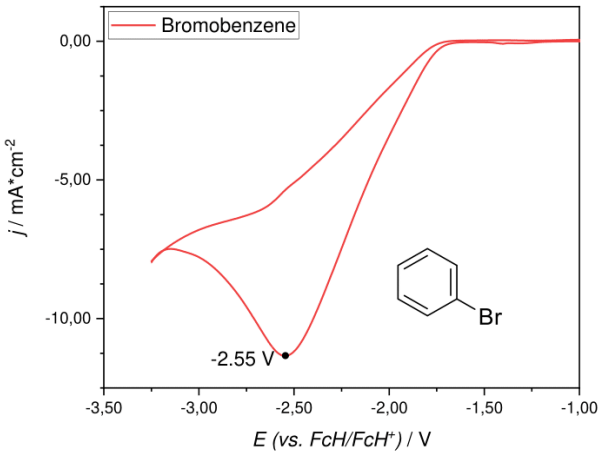

Figure 4. Cyclic voltammogram of 40 mM bromobenzene in 0.1 M Bu_4NClO_4 and γ-butyrolactone. W.E. Ag (A = 8.0 mm²), *v* = 0.2 V/s. Peak potential of bromobenzene: −2.55 V vs. FcH/FcH⁺.

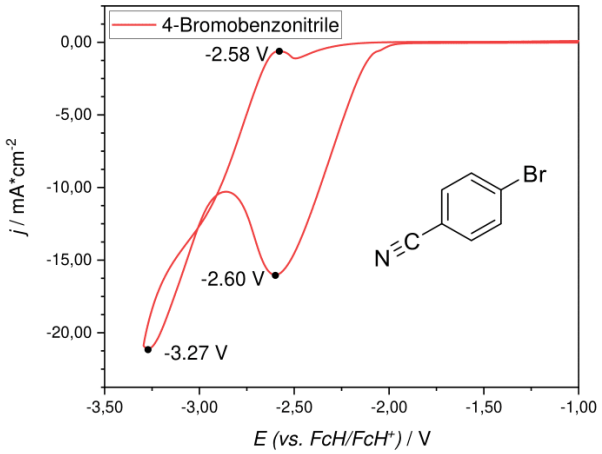

Figure 5. Cyclic voltammogram of 40 mM 4-bromobenzonitrile in 0.1 M Bu_4NClO_4 and γ-butyrolactone. W.E. Ag (A = 8.0 mm²), *v* = 0.2 V/s. Peak potentials of 4-bromobenzonitrile: −2.58 V vs. FcH/FcH⁺, −2.60 V vs. FcH/FcH⁺ and −3.27 V vs. FcH/FcH⁺.

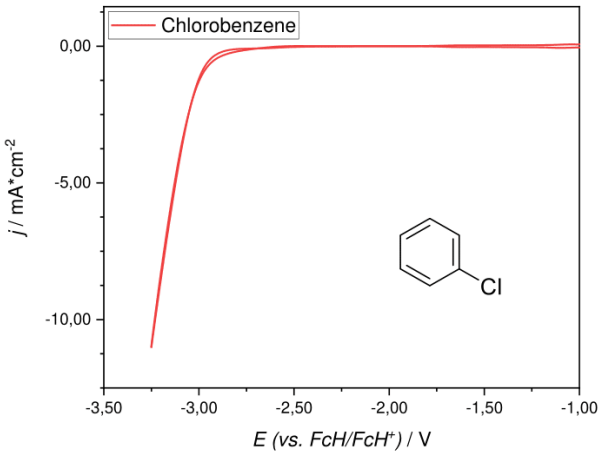

Figure 6. Cyclic voltammogram of 40 mM chlorobenzene in 0.1 M Bu_4NClO_4 and γ-butyrolactone. W.E. Ag (A = 8.0 mm²), *v* = 0.2 V/s. No peak potential of chlorobenzene in the range of cathodic reduction.

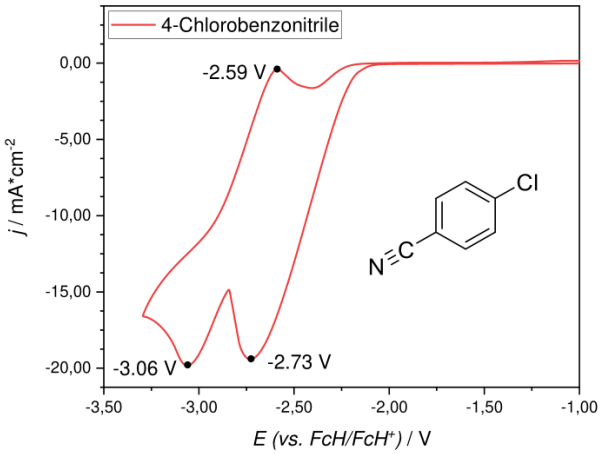

Figure 7. Cyclic voltammogram of 40 mM 4-chlorobenzonitrile in 0.1 M Bu_4NClO_4 and γ-butyrolactone. W.E. Ag (A = 8.0 mm²), *v* = 0.2 V/s. Peak potentials of 4-chlorobenzonitrile: −2.59 V vs. FcH/FcH^+, −2.73 V vs. FcH/FcH^+ and −3.06 V vs. FcH/FcH^+.

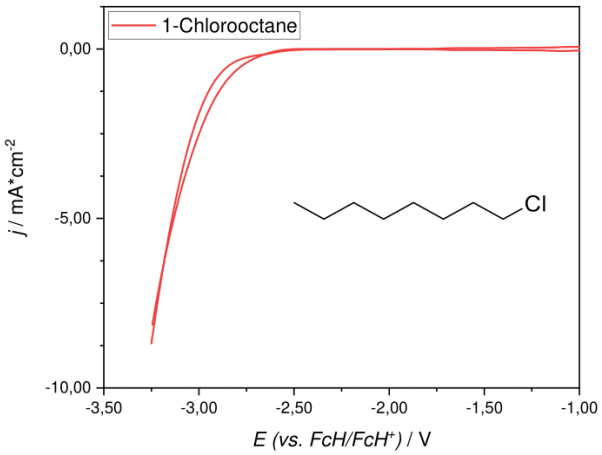

Figure 8. Cyclic voltammogram of 40 mM 1-chlorooctane in 0.1 M Bu_4NClO_4 and γ-butyrolactone. W.E. Ag (A = 8.0 mm²), *v* = 0.2 V/s. No peak potential of 1-chlorooctane in the range of cathodic reduction.

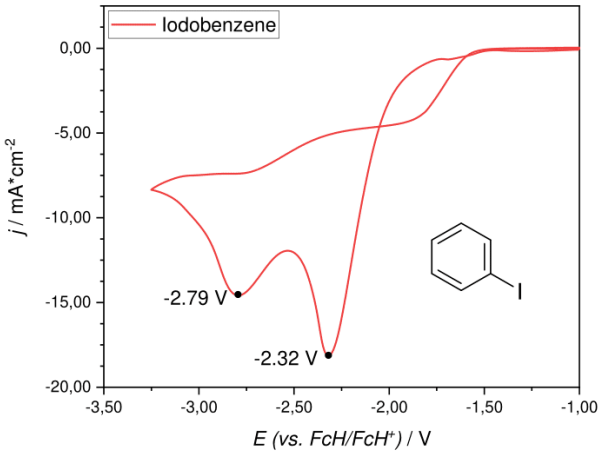

Figure 9. Cyclic voltammogram of 40 mM iodobenzene in 0.1 M Bu_4NClO_4 and γ-butyrolactone. W.E. Ag (A = 8.0 mm²), *v* = 0.2 V/s. Peak potentials of iodobenzene: −2.32 V vs. FcH/FcH^+ and −2.79 V vs. FcH/FcH^+.

5.2 Reduction potential of chlorosilanes

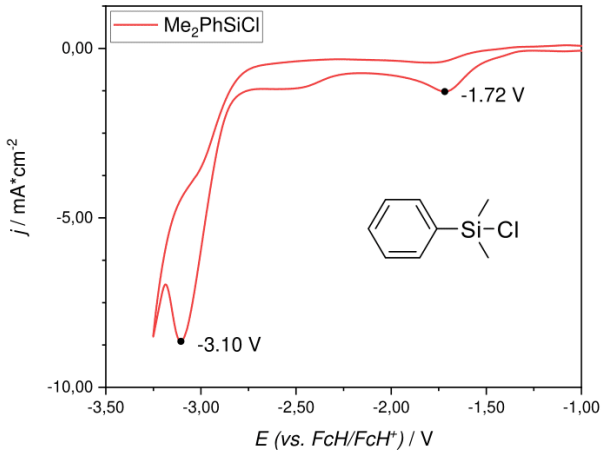

Figure 10. Cyclic voltammogram of 40 mM $Me_2PhSiCl$ in 0.1 M Bu_4NClO_4 and γ-butyrolactone. W.E. Ag (A = 8.0 mm^2), *v* = 0.2 V/s. Peak potentials of $Me_2PhSiCl$: −1.72 V vs. FcH/FcH^+ and −3.10 V vs. FcH/FcH^+.

5.3 Oxidation potential of activated hydrosilane in presence hydrogen chloride scavengers

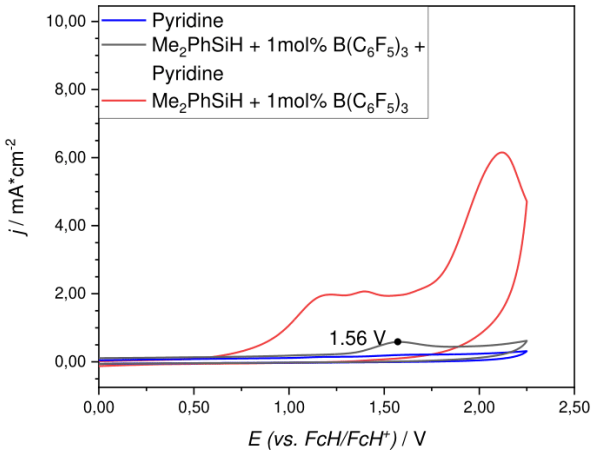

Figure 11. Cyclic voltammogram of 40 mM pyridine (blue), 40 mM Me_2PhSiH + 0.4 mM $B(C_6F_5)_3$ + 40 mM pyridine (black) and 40 mM Me_2PhSiH + 0.4 mM $B(C_6F_5)_3$ (red, for comparison) in 0.1 M Bu_4NClO_4 and γ-butyrolactone. W.E. Ag (A = 8.0 mm²), *v* = 0.2 V/s. Peak potential of 40 mM Me_2PhSiH + 0.4 mM $B(C_6F_5)_3$ + 40 mM pyridine: 1.56 V vs. FcH/FcH⁺.

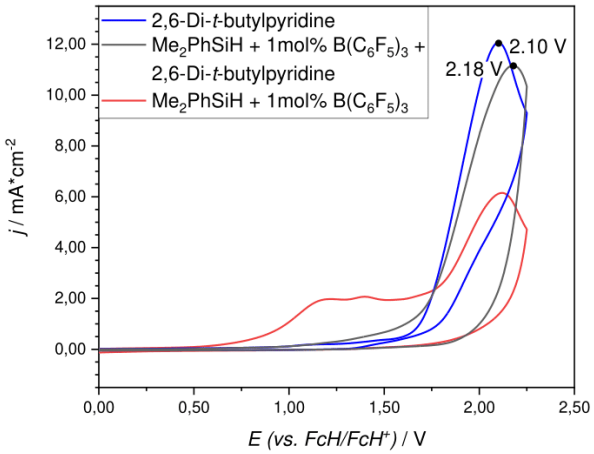

Figure 12. Cyclic voltammogram of 40 mM 2,6-di-*tert*-butylpyridine (blue), 40 mM Me_2PhSiH + 0.4 mM $B(C_6F_5)_3$ + 40 mM 2,6-di-*tert*-butylpyridine (black) and 40 mM Me_2PhSiH + 0.4 mM $B(C_6F_5)_3$ (red, for comparison) in 0.1 M Bu_4NClO_4 and γ-butyrolactone. W.E. Ag (A = 8.0 mm²), *v* = 0.2 V/s. Peak potential of 40 mM 2,6-di-*tert*-butylpyridine: 2.10 V vs. FcH/FcH⁺; and 40 mM Me_2PhSiH + 0.4 mM $B(C_6F_5)_3$ + 40 mM 2,6-di-*tert*-butylpyridine: 2.18 V vs. FcH/FcH⁺.

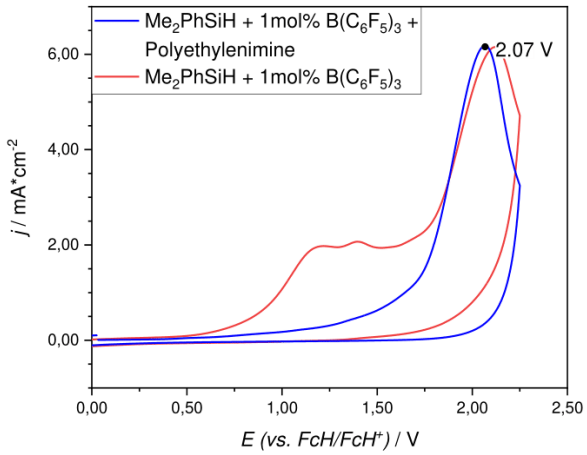

Figure 13. Cyclic voltammogram of 40 mM Me_2PhSiH + 0.4 mM $B(C_6F_5)_3$ + 40 mg polyethylenimine on silica (blue) and 40 mM Me_2PhSiH + 0.4 mM $B(C_6F_5)_3$ (red, for comparison) in 0.1 M Bu_4NClO_4 and γ-butyrolactone. W.E. Ag (A = 8.0 mm²), *v* = 0.2 V/s. Peak potential of 40 mM Me_2PhSiH + 0.4 mM $B(C_6F_5)_3$ + 40 mg polyethylenimine on silica: 2.07 V vs. FcH/FcH⁺.

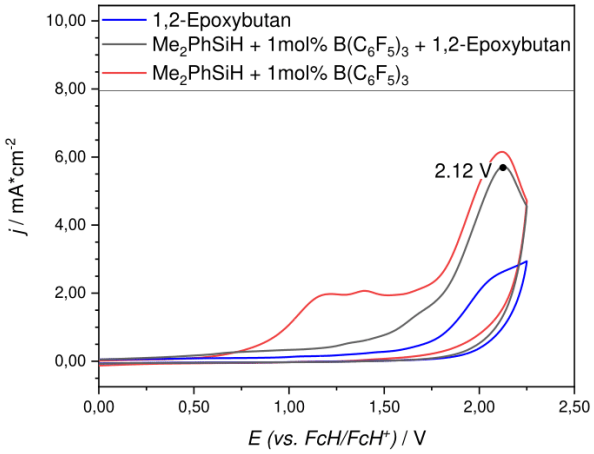

Figure 14. Cyclic voltammogram of 40 mM 1,2-epoxybutane (blue), 40 mM Me_2PhSiH + 0.4 mM $B(C_6F_5)_3$ + 40 mM 1,2-epoxybutane (black) and 40 mM Me_2PhSiH + 0.4 mM $B(C_6F_5)_3$ (red, for comparison) in 0.1 M Bu_4NClO_4 and γ-butyrolactone. W.E. Ag (A = 8.0 mm²), *v* = 0.2 V/s. Peak potential of 40 mM Me_2PhSiH + 0.4 mM $B(C_6F_5)_3$ + 40 mM 1,2-epoxybutane: 2.12 V vs. FcH/FcH⁺.

6 Product Characterization

6.1 Allyldimethylphenylsilane (1)

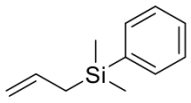

1

^{1}H NMR (500 MHz, CD_2Cl_2): δ [ppm] = 7.68–7.72 (m, 5H), 5.87–5.99 (m, 1H), 4.95–5.04 (m, 2H), 1.91 (d, *J* = 8.0 Hz, 2H), 0.43 (s, 6H).
^{13}C NMR (125 MHz, CD_2Cl_2): δ [ppm] = 140.1, 135.0, 133.9, 129. 6, 128.0, 113.5, 23.9, −3.4.
^{29}Si NMR (100 MHz, CD_2Cl_2): δ [ppm] = −4.72.
MS m/z = 176 $[M]^+$
Data are in agreement with literature.[1]

6.2 Allyltriethylsilane (2)

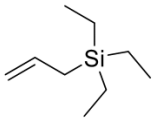

2

^{1}H NMR (500 MHz, CD_2Cl_2): δ [ppm] = 6.03–6.22 (m, 1H), 5.56–5.74 (m, 2H), 1.86 (d, *J* = 8.0 Hz, 2H), 0.99 (t, *J* = 7.8 Hz, 9H), 0.43–0.65 (m, 6H).
^{13}C NMR (125 MHz, CD_2Cl_2): δ [ppm] = 127.6, 112.5, 18.5, 7.4, 3.1.
^{29}Si NMR (100 MHz, CD_2Cl_2): δ [ppm] = 5.74.
MS m/z = 156 $[M]^+$
Data are in agreement with literature.[2]

6.3 Allyltriphenylsilane (3)

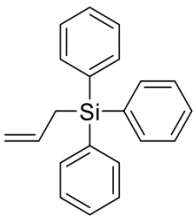

3

^{1}H NMR (500 MHz, CD_2Cl_2): δ [ppm] = 7.52–7.58 (m, 6H), 7.36–7.48 (m, 9H), 5.85–5.95 (m, 1H), 4.88–5.00 (m, 2H), 2.45 (d, *J* = 8.0 Hz, 2H).
^{13}C NMR (125 MHz, CD_2Cl_2): δ [ppm] = 135.7, 134.6, 133.9, 129.6, 127.8, 114.8, 21.0.
^{29}Si NMR (100 MHz, CD_2Cl_2): δ [ppm] = −13.73.
MS m/z = 301 $[M]^+$
Data are in agreement with literature.[1]

6.4 Benzyldimethylphenylsilane (4)

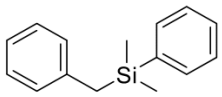

4

^{1}H NMR (500 MHz, CD_2Cl_2): δ [ppm] = 7.58–7.68 (m, 2H), 7.40–7.50 (m, 3H), 7.31 (t, *J* = 7.6 Hz, 2H), 7.20 (t, *J* = 7.4 Hz, 1H), 7.10 (d, *J* = 7.6 Hz, 2H), 2.47 (s, 2H), 0.41 (s, 6H).
^{13}C NMR (125 MHz, CD_2Cl_2): δ [ppm] = 139.9, 138.6, 133.9, 129.1, 128.4, 128.2, 127.8, 124.2, 26.1, −3.5.
^{29}Si NMR (100 MHz, CD_2Cl_2): δ [ppm] = −3.76.
MS m/z = 226 $[M]^+$
Data are in agreement with literature.[3]

6.5 Benzyltriethylsilane (5)

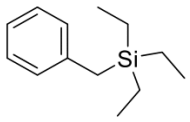

5

^{1}H NMR (500 MHz, CD_2Cl_2): δ [ppm] = 7.22–7.27 (m, 2H), 7.06–7.11 (m, 3H), 2.18 (s, 2H), 0.99 (t, *J* = 8.0 Hz, 9H), 0.51 (q, *J* = 8.0 Hz, 6H).
^{13}C NMR (125 MHz, CD_2Cl_2): δ [ppm] = 141.2, 129.0, 128.5, 124.2, 21.9, 7.5, 3.4.
^{29}Si NMR (100 MHz, CD_2Cl_2): δ [ppm] = 6.41.
MS m/z = 206 $[M]^+$
Data are in agreement with literature.[4]

6.6 Benzyltriphenylsilane (6)

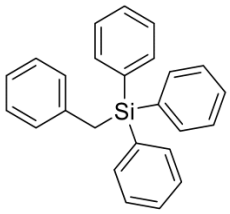

6

^{1}H NMR (500 MHz, CD_2Cl_2): δ [ppm] = 7.53–7.59 (m, 6H), 7.42–7.47 (m, 9H), 7.12–7.22 (m, 2H), 6.99–7.03 (m, 3H), 3.10 (s, 2H).
^{13}C NMR (125 MHz, CD_2Cl_2): δ [ppm] = 138.5, 136.0, 134.4, 129.3, 129.1, 128.2, 127.9, 124.7, 23.3.
^{29}Si NMR (100 MHz, CD_2Cl_2): δ [ppm] = −12.26.
MS m/z = 350 $[M]^+$
Data are in agreement with literature.[5]

6.7 Chlorodimethylphenylsilane (7)

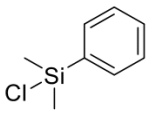

7

^{1}H NMR (500 MHz, CD_2Cl_2): δ [ppm] = 7.71–7.74 (m, 2H), 7.46–7.54 (m, 3H), 0.77 (s, 6H).
^{13}C NMR (125 MHz, CD_2Cl_2): δ [ppm] = 136.7, 133.5, 130.8, 128.5, 2.2.
^{29}Si NMR (100 MHz, CD_2Cl_2): δ [ppm] = 20.49.
MS m/z = 170 $[M]^+$
Data are in agreement with literature.[6]

6.8 Dimethyloctylphenylsilane (8)

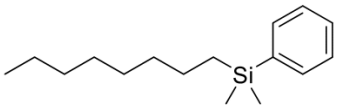

8

^{1}H NMR (500 MHz, CD_2Cl_2): δ [ppm] = 7.46–7.55 (m, 2H), 7.29–7.37 (m, 3H), 1.18–1.40 (m, 12H), 0.85 (t, *J* = 6.9 Hz, 3H), 0.72–0.78 (m, 2H), 0.22 (s, 6H).
^{13}C NMR (125 MHz, CD_2Cl_2): δ [ppm] = 139.8, 133.7, 128.8, 127.8, 33.8, 32.1, 29.4, 24.0, 22.8, 15.9, 14.3, −2.8.
^{29}Si NMR (100 MHz, CD_2Cl_2): δ [ppm] = −2.41.
MS m/z = 248 $[M]^+$
Data are in agreement with literature.[7]

6.9 Dimethyldiphenylsilane (9)

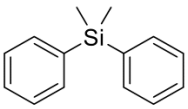

9

^{1}H NMR (500 MHz, CD_2Cl_2): δ [ppm] = 7.50–7.59 (m, 4H), 7.29–7.44 (m, 6H), 0.48 (s, 6H).
^{13}C NMR (125 MHz, CD_2Cl_2): δ [ppm] = 137.9, 134.0, 128.7, 127.3, -3.0.
^{29}Si NMR (100 MHz, CD_2Cl_2): δ [ppm] = −8.17.
MS m/z = 212 $[M]^+$
Data are in agreement with literature.[8]

6.10 4-(Dimethylphenylsilyl)benzonitrile (10)

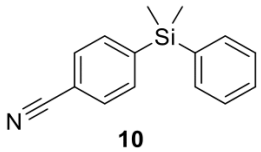

10

^{1}H NMR (500 MHz, CD_2Cl_2): δ [ppm] = 7.62–7.69 (m, 4H), 7.51–7.56 (m, 2H), 7.31–7.40 (m, 3H), 0.43 (s, 6H).
^{13}C NMR (125 MHz, CD_2Cl_2): δ [ppm] = 145.2, 136.6, 134.8, 134.3, 131.2, 129.8, 128.3, 119.1, 112.9, −2.5.
^{29}Si NMR (100 MHz, CD_2Cl_2): δ [ppm] = −7.12.
MS m/z = 237 $[M]^+$
Data are in agreement with literature.[9]

6.11 1,1,3,3-tetramethyl-1,3-diphenyldisiloxane (11)

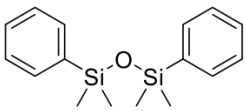

11

^{1}H NMR (500 MHz, CD_2Cl_2): δ [ppm] = 7.58–7.63 (m, 4H), 7.36–7.44 (m, 6H), 0.40 (s, 12H).
^{13}C NMR (125 MHz, CD_2Cl_2): δ [ppm] = 140.2, 133.4, 129.6, 128.0, 0.9.
^{29}Si NMR (100 MHz, CD_2Cl_2): δ [ppm] = −1.08.
MS m/z = 286 $[M]^+$
Data are in agreement with literature.[10]

6.12 (2-Methoxyethoxy)dimethylphenylsilane (12)

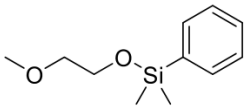

12

^{1}H NMR (500 MHz, CD_2Cl_2): δ [ppm] = 7.60–7.67 (m, 2H), 7.38–7.47 (m, 3H), 3.80 (t, *J* = 5.0 Hz, 2H), 3.52 (t, *J* = 5.0 Hz, 2H), 3.39 (s, 3H), 0.45 (s, 6H).
^{13}C NMR (125 MHz, CD_2Cl_2): δ [ppm] = 138.3, 133.8, 129.9, 128.1, 74.6, 62.6, 59.3, −1.7.
^{29}Si NMR (100 MHz, CD_2Cl_2): δ [ppm] = 7.72.
MS m/z = 195 $[M - CH_3]^+$
Data are in agreement with literature.[11]

7 NMR Spectra of all isolated compounds

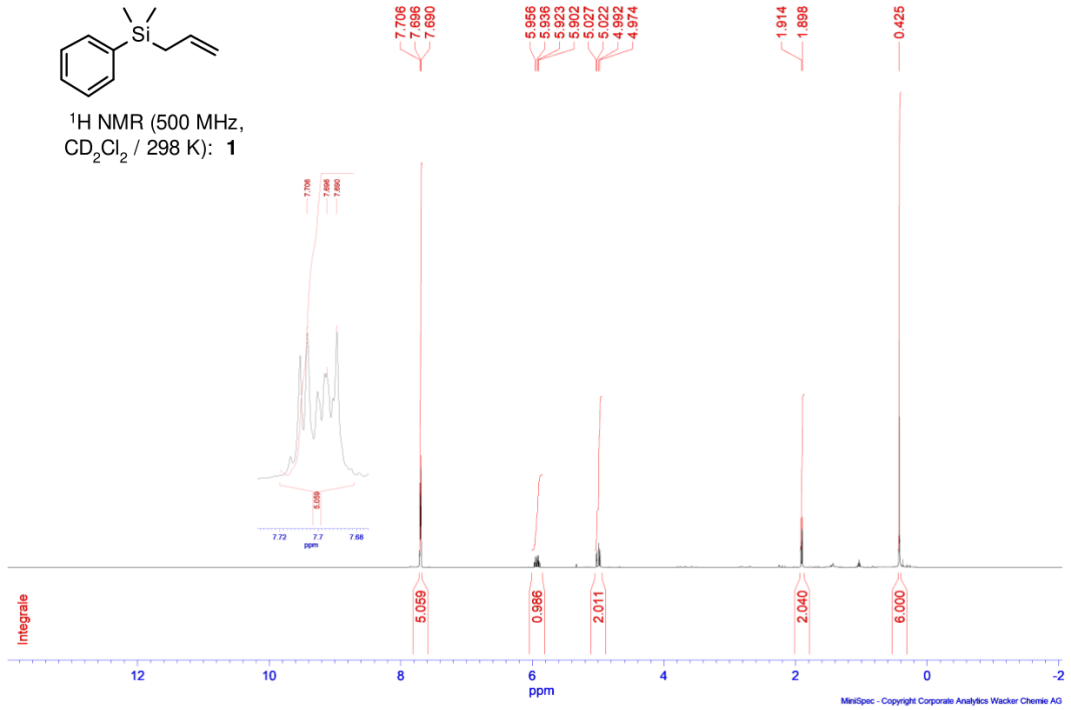

^{1}H NMR (500 MHz, CD_2Cl_2 / 298 K): **1**

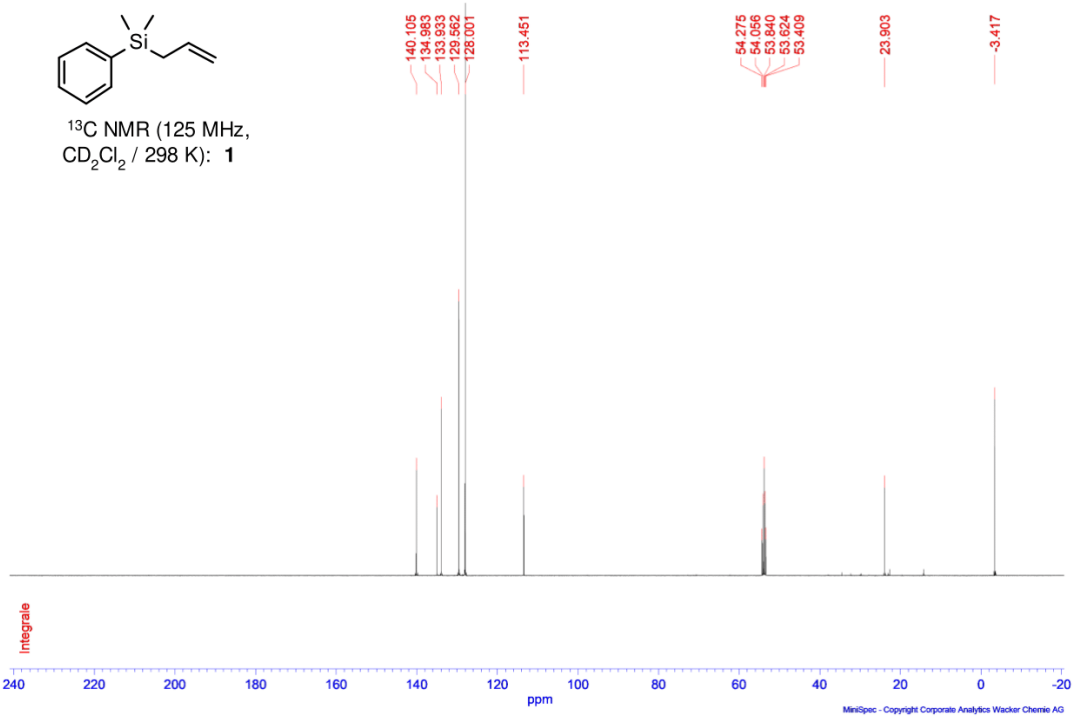

^{13}C NMR (125 MHz, CD_2Cl_2 / 298 K): **1**

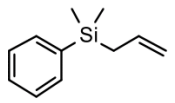

^{29}Si NMR (100 MHz, CD_2Cl_2 / 298 K): **1**

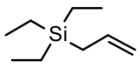

^{1}H NMR (500 MHz, CD_2Cl_2 / 298 K): **2**

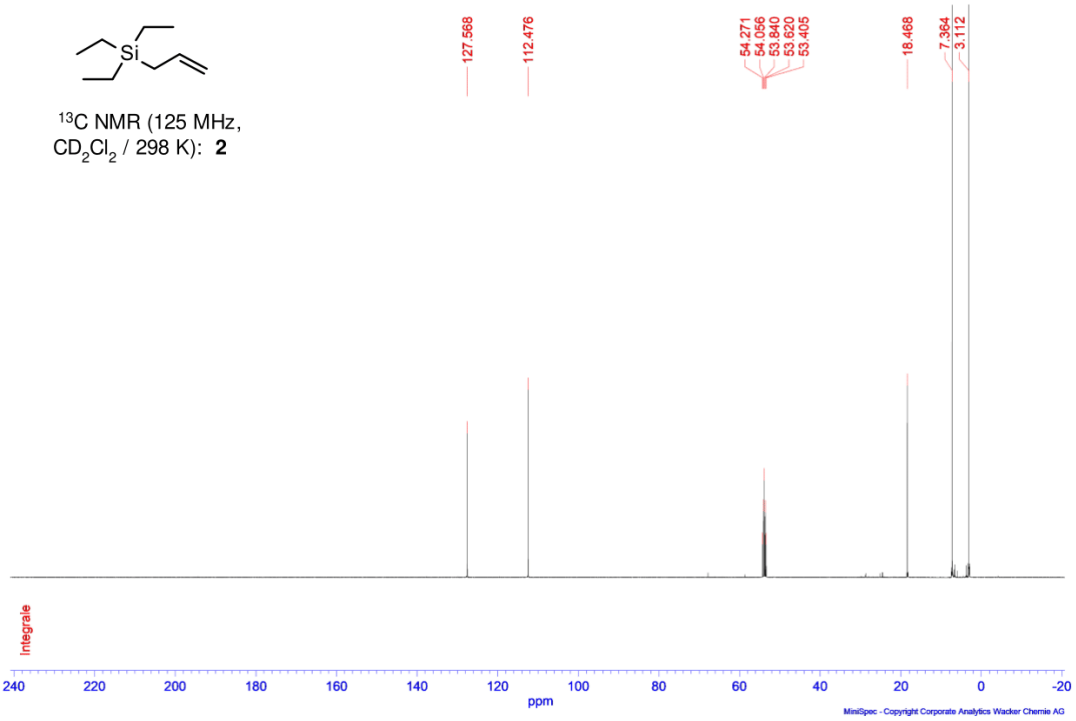
Si
^{13}C NMR (125 MHz,
CD_2Cl_2 / 298 K): **2**
127.568
112.476
54.271
54.056
53.840
53.620
53.405
18.468
7.364
3.112
Integrale
240
220
200
180
160
140
120
100
80
60
40
20
0
-20
ppm
MiniSpec - Copyright Corporate Analytics Wacker Chemie AG

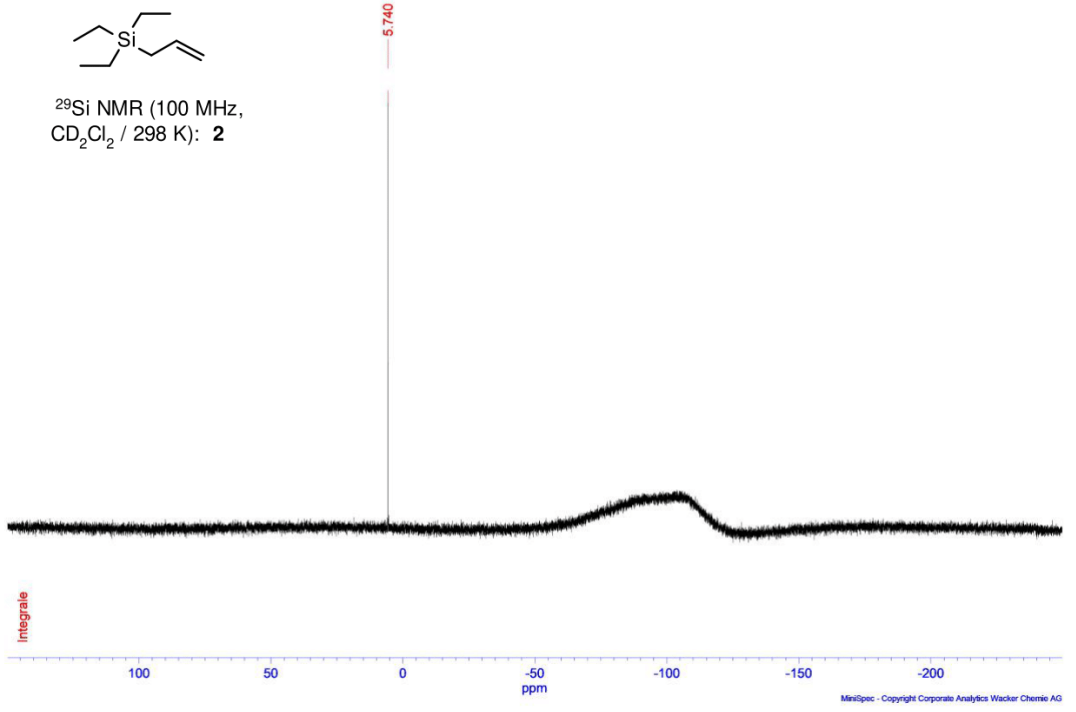
Si
^{29}Si NMR (100 MHz,
CD_2Cl_2 / 298 K): **2**
5.740
Integrale
100
50
0
-50
-100
-150
-200
ppm
MiniSpec - Copyright Corporate Analytics Wacker Chemie AG

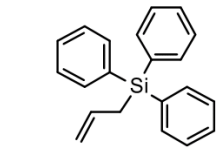

^{1}H NMR (500 MHz, CD_2Cl_2 / 298 K): **3**

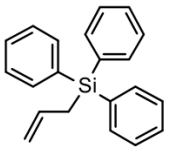

^{13}C NMR (125 MHz, CD_2Cl_2 / 298 K): **3**

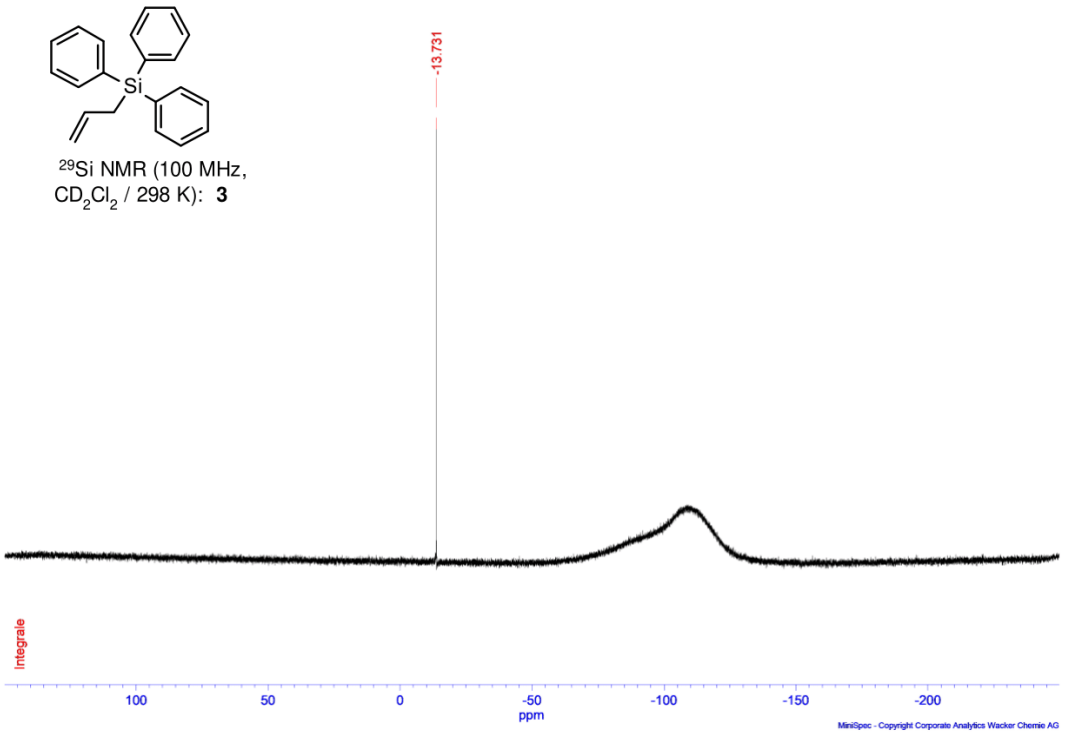

^{29}Si NMR (100 MHz, CD_2Cl_2 / 298 K): **3**

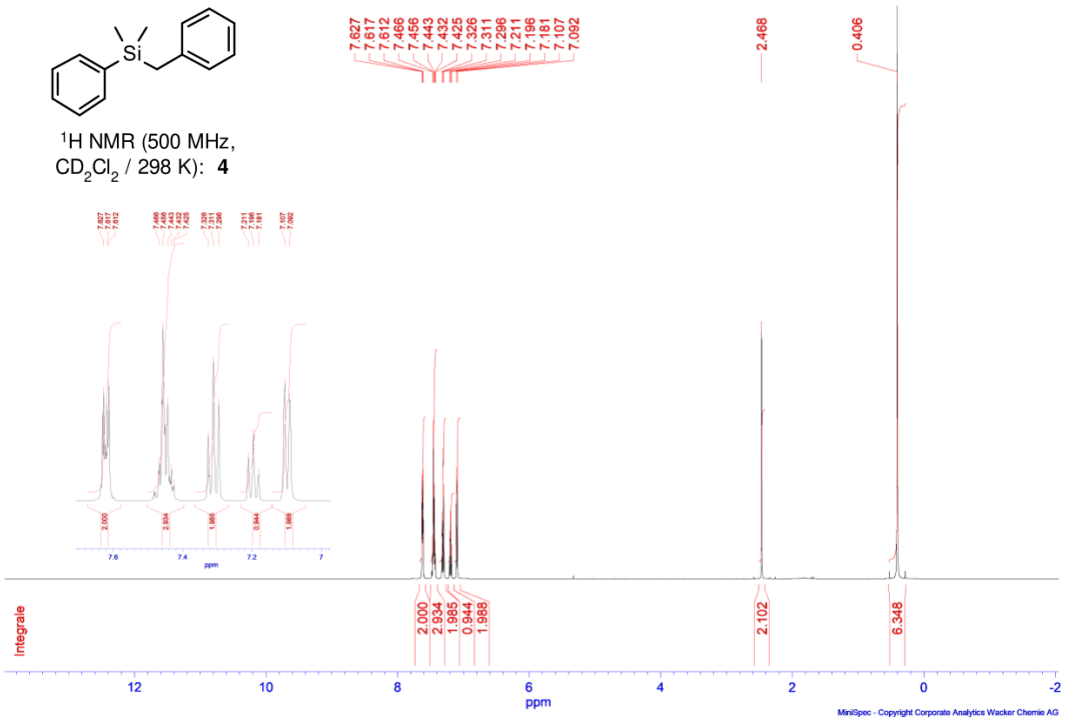

^{1}H NMR (500 MHz, CD_2Cl_2 / 298 K): **4**

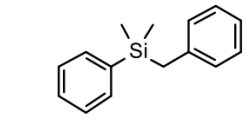

^{13}C NMR (125 MHz, CD_2Cl_2 / 298 K): **4**

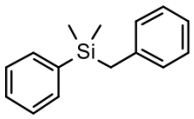

^{29}Si NMR (100 MHz, CD_2Cl_2 / 298 K): **4**

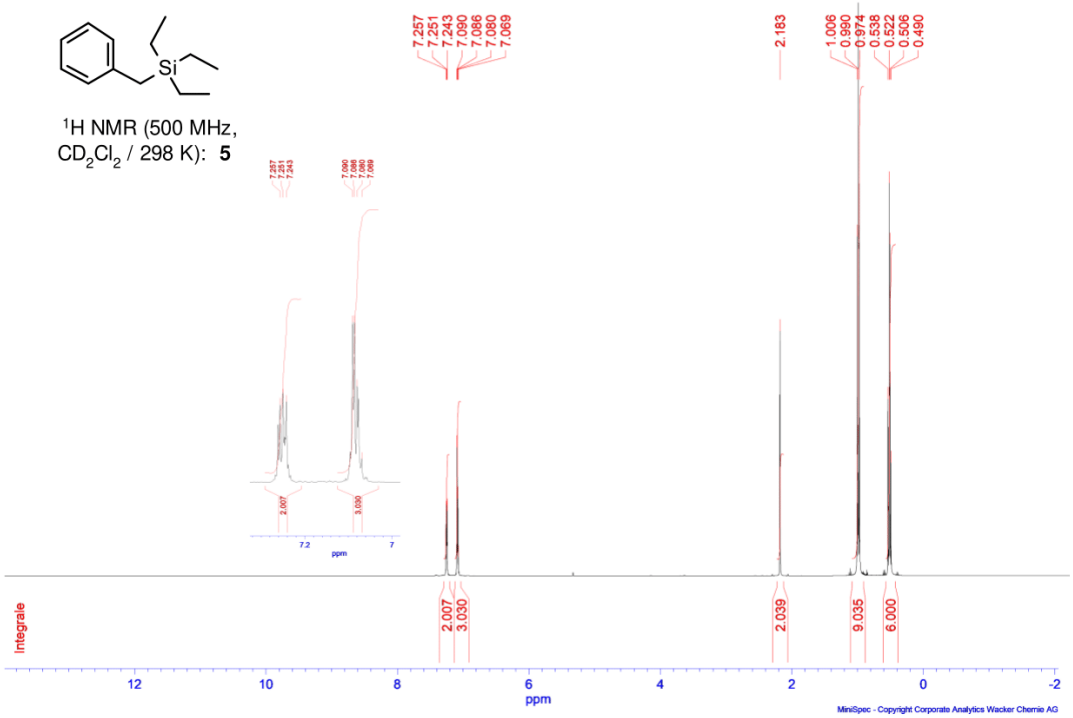

^{1}H NMR (500 MHz, CD_2Cl_2 / 298 K): **5**

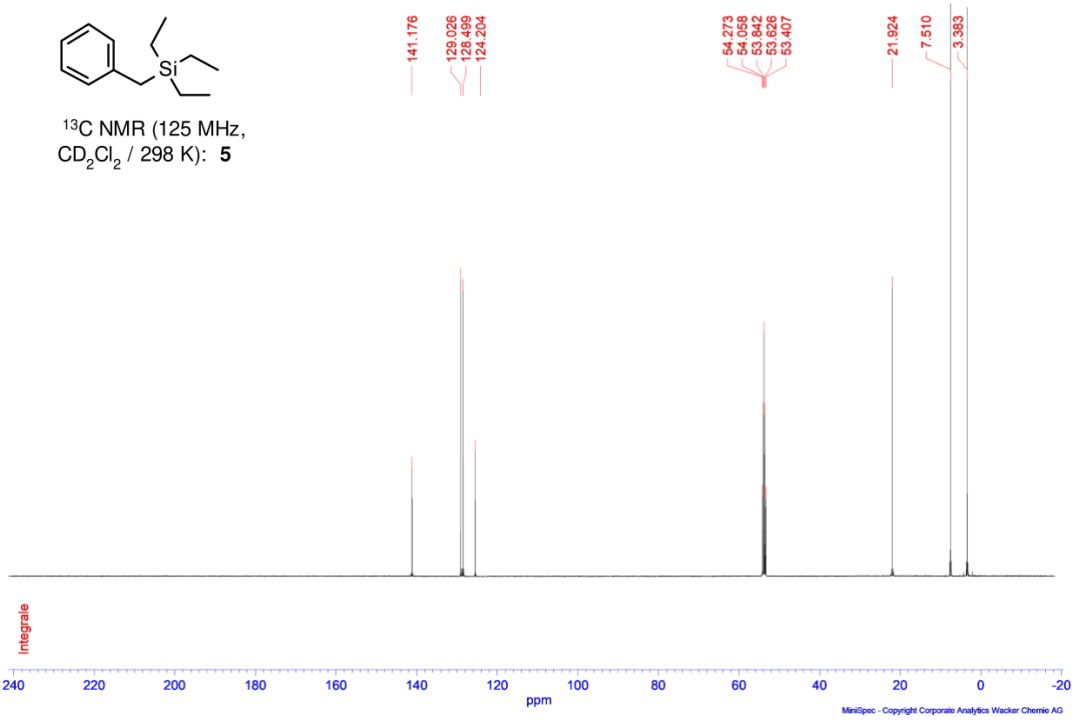

^{13}C NMR (125 MHz, CD_2Cl_2 / 298 K): **5**

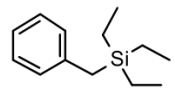

^{29}Si NMR (100 MHz, CD_2Cl_2 / 298 K): **5**

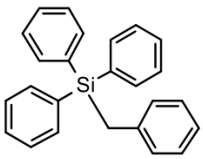

^{1}H NMR (500 MHz, CD_2Cl_2 / 298 K): **6**

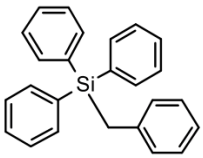

^{13}C NMR (125 MHz, CD_2Cl_2 / 298 K): **6**

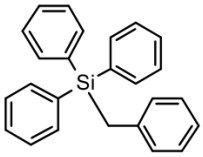

^{29}Si NMR (100 MHz, CD_2Cl_2 / 298 K): **6**

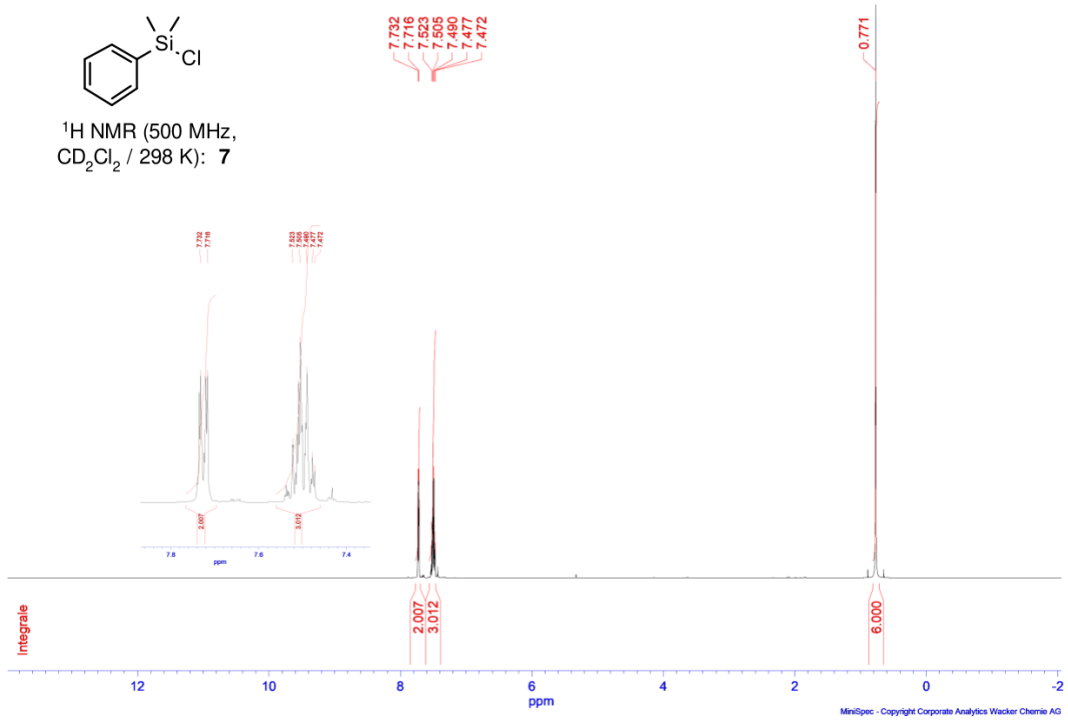
Si
Cl
^{1}H NMR (500 MHz,
CD_2Cl_2 / 298 K): **7**
7.732
7.716
7.523
7.505
7.490
7.477
7.472
0.771
2.007
3.012
6.000
Integrale
12
10
8
6
4
2
0
-2
ppm
MiniSpec - Copyright Corporate Analytics Wacker Chemie AG

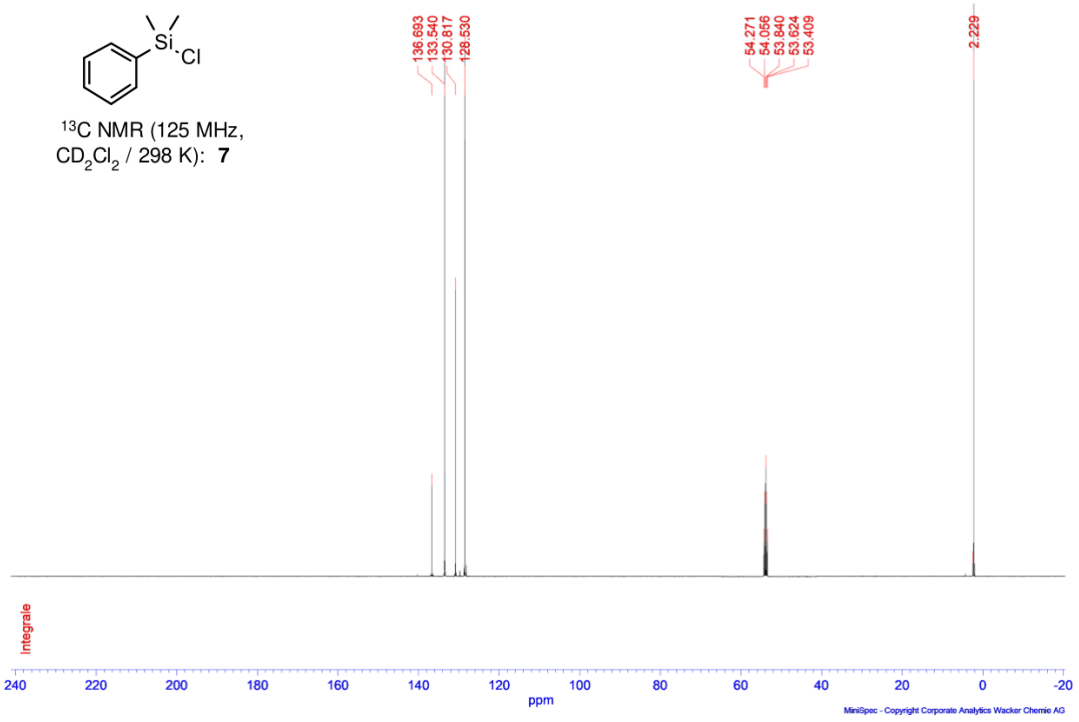
Si
Cl
^{13}C NMR (125 MHz,
CD_2Cl_2 / 298 K): **7**
136.693
133.540
130.817
128.530
54.271
54.056
53.840
53.624
53.409
2.229
Integrale
240
220
200
180
160
140
120
100
80
60
40
20
0
-20
ppm
MiniSpec - Copyright Corporate Analytics Wacker Chemie AG

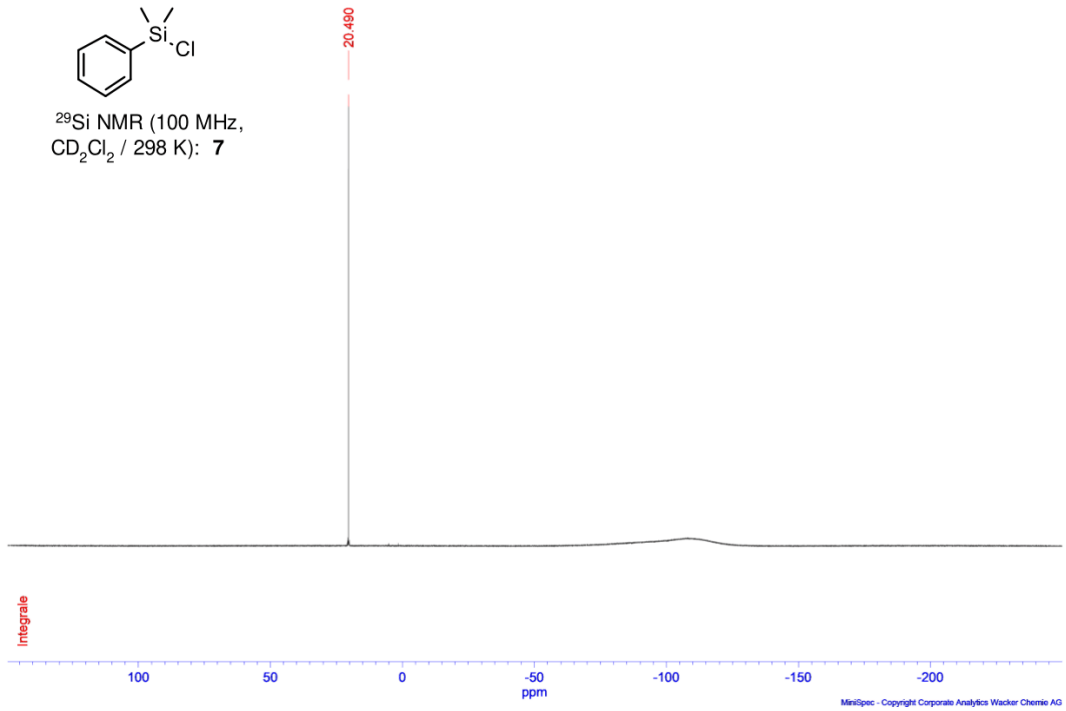

^{29}Si NMR (100 MHz, CD_2Cl_2 / 298 K): **7**

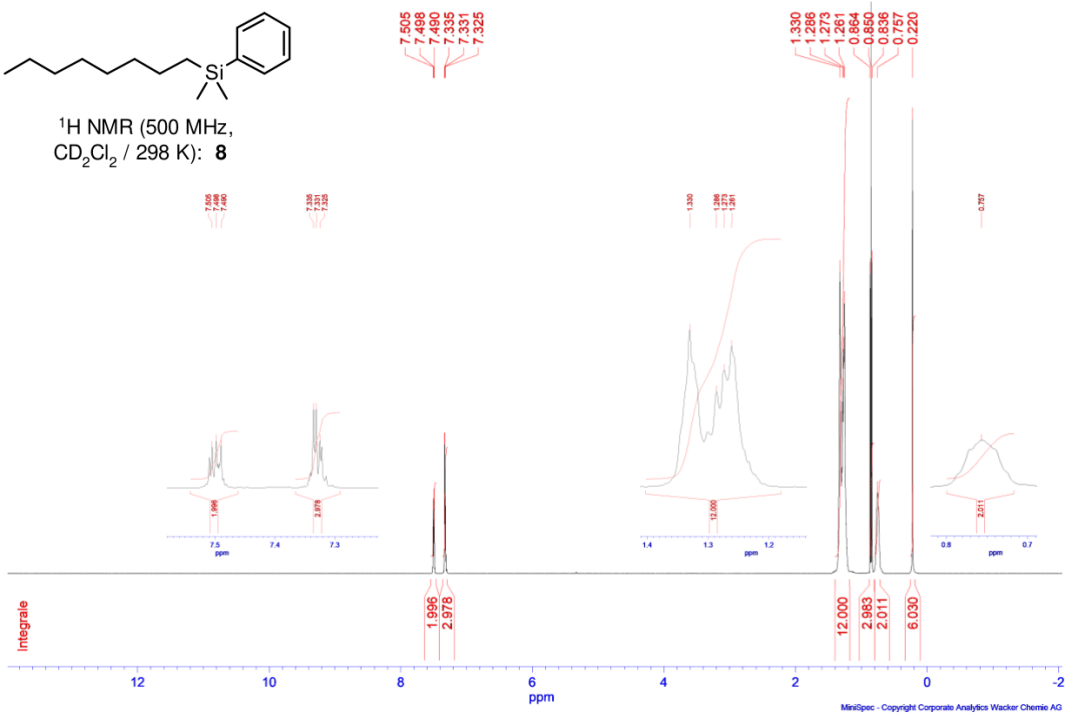

^{1}H NMR (500 MHz, CD_2Cl_2 / 298 K): **8**

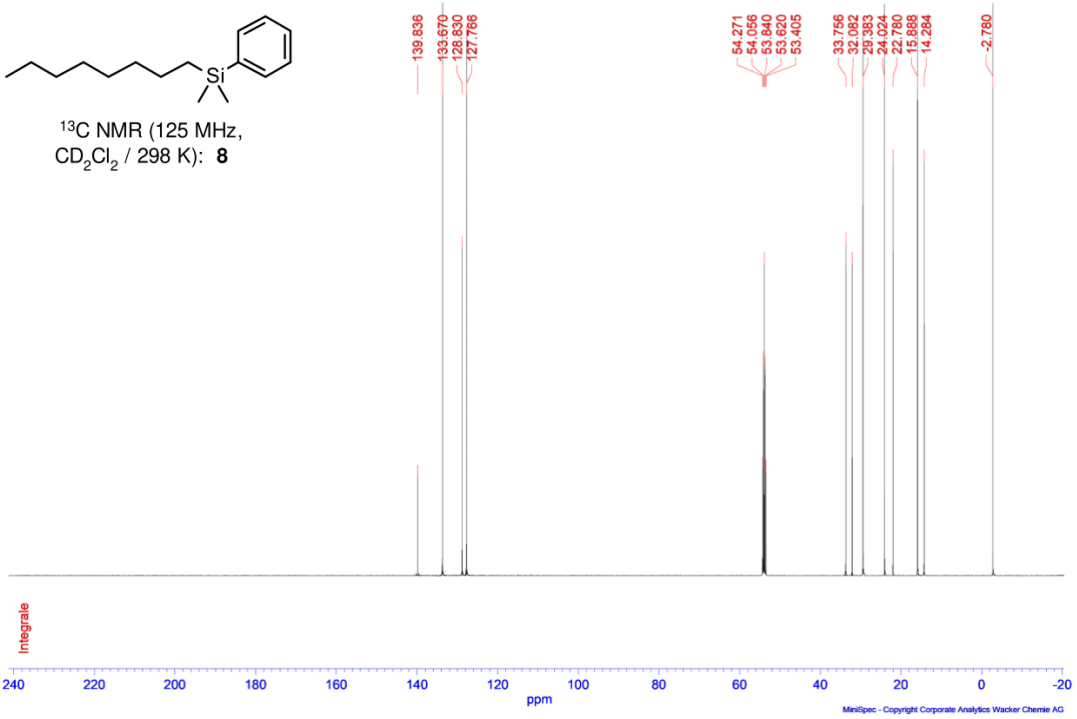

^{13}C NMR (125 MHz, CD_2Cl_2 / 298 K): **8**

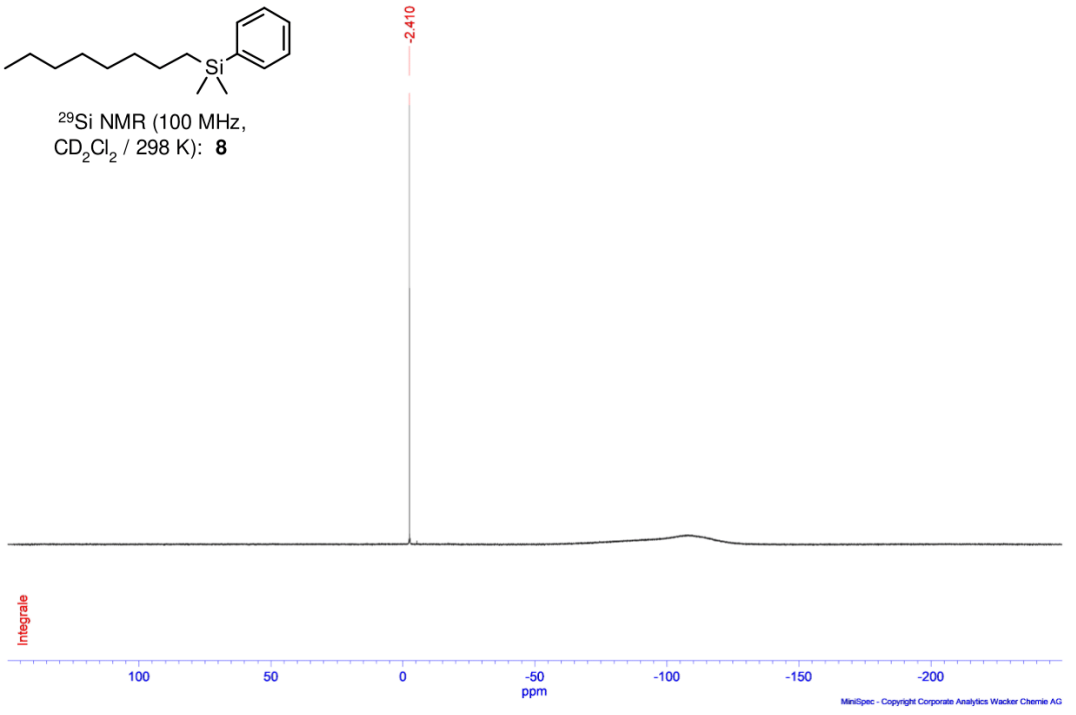

^{29}Si NMR (100 MHz, CD_2Cl_2 / 298 K): **8**

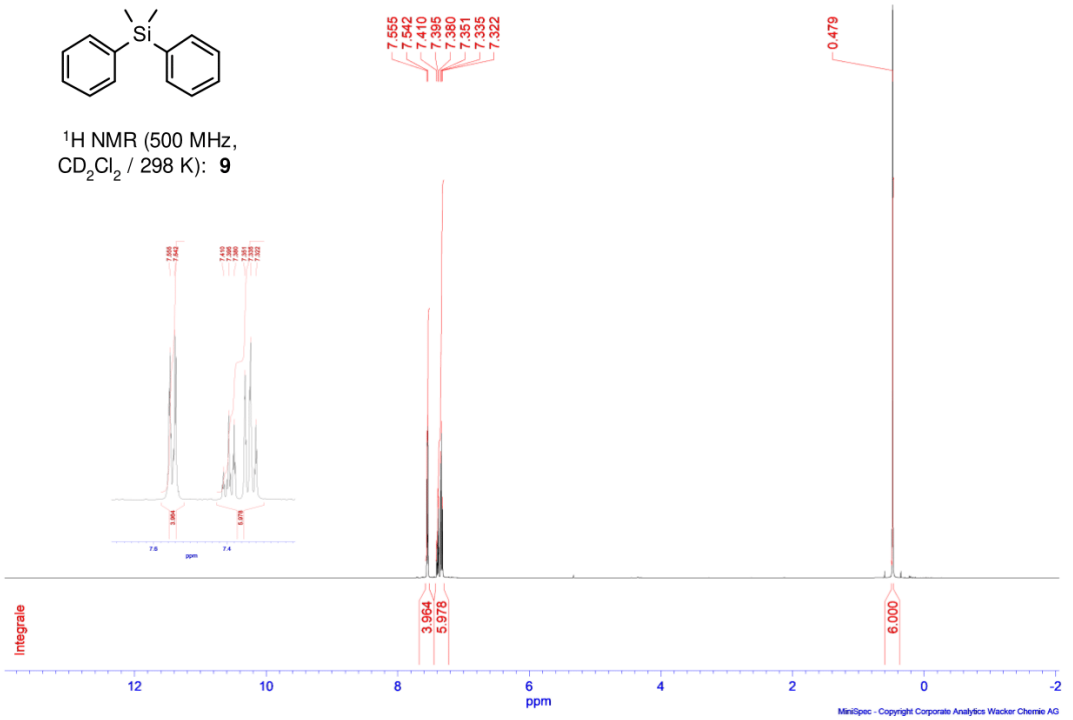
Si
^{1}H NMR (500 MHz,
CD_2Cl_2 / 298 K): **9**
7.555
7.542
7.410
7.395
7.380
7.351
7.335
7.322
0.479
3.964
5.978
6.000
Integrale
12
10
8
6
4
2
0
-2
ppm
MiniSpec - Copyright Corporate Analytics Wacker Chemie AG

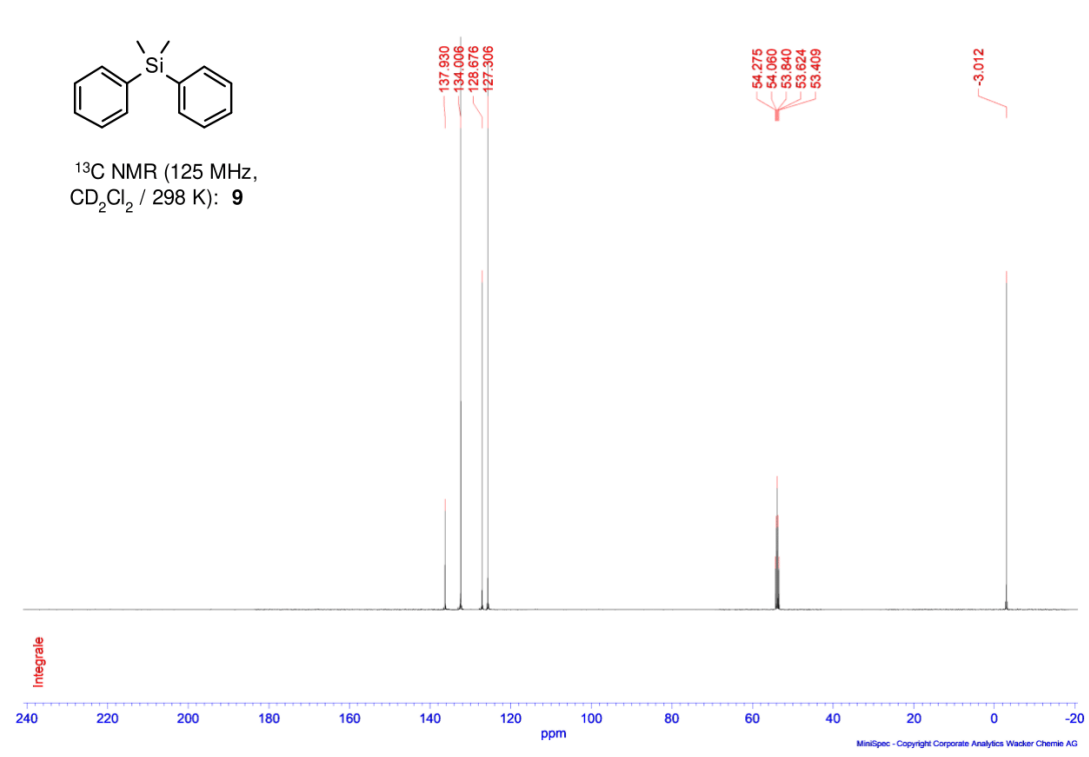
Si
^{13}C NMR (125 MHz,
CD_2Cl_2 / 298 K): **9**
137.930
134.006
128.676
127.306
54.275
54.060
53.840
53.624
53.409
-3.012
Integrale
240
220
200
180
160
140
120
100
80
60
40
20
0
-20
ppm
MiniSpec - Copyright Corporate Analytics Wacker Chemie AG

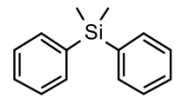

^{29}Si NMR (100 MHz, CD_2Cl_2 / 298 K): **9**

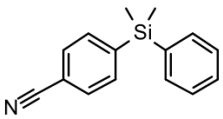

^{1}H NMR (500 MHz, CD_2Cl_2 / 298 K): **10**

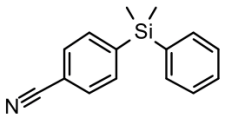

^{13}C NMR (125 MHz, CD_2Cl_2 / 298 K): **10**

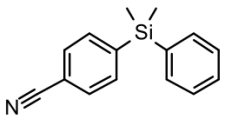

^{29}Si NMR (100 MHz, CD_2Cl_2 / 298 K): **10**

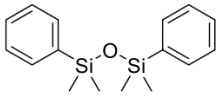

^{1}H NMR (500 MHz, CD_2Cl_2 / 298 K): **11**

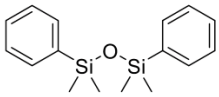

^{13}C NMR (125 MHz, CD_2Cl_2 / 298 K): **11**

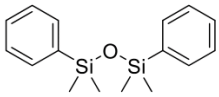

^{29}Si NMR (100 MHz, CD_2Cl_2 / 298 K): **11**

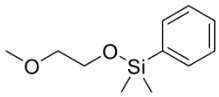

^{1}H NMR (500 MHz, CD_2Cl_2 / 298 K): **12**

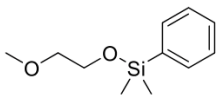

^{13}C NMR (125 MHz, CD_2Cl_2 / 298 K): **12**

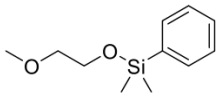

^{29}Si NMR (100 MHz, CD_2Cl_2 / 298 K): **12**

8 References

[1] Z. Li, X. Cao, G. Lai, J. Liu, Y. Ni, J. Wu, H. Qiu, *J. Organomet. Chem.* **2006**, *691*, 4740–4746.
[2] L. N. Lewis, *J. Am. Chem. Soc.* **1990**, *112*, 5998–6004.
[3] Z.-D. Huang, R. Ding, P. Wang, Y.-H. Xu, T.-P. Loh, *Chem. Commun.* **2016**, *52*, 5609–5612.
[4] C. Eaborn, A. R. Hancock, W. A. Stańczyk, *J. Organomet. Chem.* **1981**, *218*, 147–154.
[5] N. Hirone, H. Sanjiki, R. Tanaka, T. Hata, H. Urabe, *Angew. Chem., Int. Ed.* **2010**, *49*, 7762–7764.
[6] G. A. Olah, R. J. Hunadi, *J. Am. Chem. Soc.* **1980**, *102*, 6989–6992.
[7] a) A. D. Ibrahim, S. W. Entsminger, L. Zhu, A. R. Fout, *ACS Catal.* **2016**, *6*, 3589–3593; b) T. Mitsudome, S. Fujita, M. Sheng, J. Yamasaki, K. Kobayashi, T. Yoshida, Z. Maeno, T. Mizugaki, K. Jitsukawa, K. Kaneda, *Green Chem.* **2019**, *21*, 4566–4570; c) M. Rivero-Crespo, J. Oliver-Meseguer, K. Kapłońska, P. Kuśtrowski, E. Pardo, J. P. Cerón-Carrasco, A. Leyva-Pérez, *Chem. Sci.* **2020**, *11*, 8113–8124.
[8] M. Uchiyama, Y. Kobayashi, T. Furuyama, S. Nakamura, Y. Kajihara, T. Miyoshi, T. Sakamoto, Y. Kondo, K. Morokuma, *J. Am. Chem. Soc.* **2008**, *130*, 472–480.
[9] a) M. Iizuka, Y. Kondo, *Eur. J. Org. Chem.* **2008**, *2008*, 1161–1163; b) C. A. van Walree, X. Y. Lauteslager, A. M. van Wageningen, J. W. Zwikker, L. W. Jenneskens, *J. Organomet. Chem.* **1995**, *496*, 117–125.
[10] B. T. Gregg, A. R. Cutler, *J. Am. Chem. Soc.* **1996**, *118*, 10069–10084.
[11] D. Gao, C. Cui, *Chem. - Eur. J.* **2013**, *19*, 11143–11147.

3.3 Elektrochemische Konversion von SiO_2 zu Silikonen

Zu diesem Kapitel wurde ein Manuskript veröffentlicht:

A. D. Beck, L. Schäffer, S. Haufe, S. R. Waldvogel*, *Assessment of the Electrochemical Synthesis Route to Silicones Starting from Silica as Feedstock*, *Eur. J. Org. Chem.* **2022**, *e202201253*.
[DOI: 10.1002/ejoc.202201253]
*Korrespondenzautor

Erläuterung meines Beitrags:

Die Messungen im vertikalen Elektrodenaufbau, unterstützende Messungen zur Untersuchung geeigneter Elektrolytkombinationen sowie der Äquilibrierungsreaktion der zyklischen Siloxane wurden von Lukas Schäffer durchgeführt. Alle weiteren experimentellen Untersuchungen und Auswertungen dieser Arbeit wurden von mir durchgeführt, und die Rohfassung des Manuskripts wurde von mir verfasst. Die Finalisierung der Veröffentlichung wurde von mir unter Betreuung von Dr. Stefan Haufe und Prof. Dr. Siegfried R. Waldvogel abgeschlossen.

Einleitung

Silikone spielen in der heutigen Gesellschaft eine entscheidende Rolle und sind in einer Vielzahl von Anwendungen zu finden, die von Haushaltsgeräten[1,2] und Fahrzeugteilen[1,2] bis hin zu Farben[1,2] und Textilien[1,2,3] reichen, wobei Polydimethylsiloxan den wichtigsten Vertreter darstellt.[4] Es sind verschiedene Routen zur Synthese von Polysiloxanen ausgehend von SiO_2 bekannt, wie durch thermische Zersetzung von Kohlensäureestern[5,6] sowie über die Umwandlung in hexakoordinierte Siliziumkomplexe durch Brenzcatechin.[7] Dennoch bleibt die carbothermische Route der einzige industriell genutzte Prozess zur Herstellung von Silikonen.[4] Hierbei wird SiO_2 bei 1500–3000 °C zu elementarem Silizium unter Freisetzung von CO_2 und CO reduziert und anschließend mit Chlormethan zu einer komplexen Mischung von Chlorsilanen chloriert.[2,4,5] Durch Hydrolyse werden Polysiloxane gebildet, jedoch ist der Prozess ausgehend von SiO_2 sehr energieintensiv und setzt umweltschädliche Gase frei. Im Jahr 2014 beschrieben CHONG und Mitarbeiter[8] einen elektrochemischen Weg über Methanolreduktion und radikalische Umwandlung zu den zyklischen Siloxanen D_3, D_4 und D_5 (Schema 13). Die Publikation wurde jedoch aufgrund von Bedenken hinsichtlich der Rechte an geistigem Eigentum zurückgezogen und mehrere Patentanmeldungen wurden im selben Jahr veröffentlicht,[9] Fragen zu diesem Thema blieben bisher jedoch ungelöst.

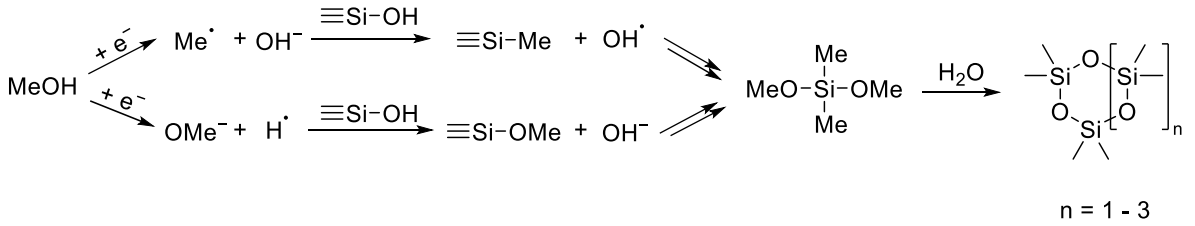

Schema 13. Direkte elektrochemische Reduktion ausgehend von Methanol mit SiO_2 als Rohstoff zu den zyklischen Methylsiloxanen D_3 – D_5, über Methylierung oder Methoxylierung zu Dimethyldimethoxysilan als zentrales Intermediat, nach CHONG (≡Si-OH = Oberfläche des SiO_2 Substrats).[8]

Zusammenfassung der Ergebnisse

Es konnte gezeigt werden, dass die gewünschte Umwandlung von SiO_2 in zyklische Siloxane grundsätzlich möglich ist. Allerdings tragen viele Parameter entscheidend zum Gelingen der Umsetzung bei. Der Abstand zwischen Kathode und SiO_2-Substrat spielt eine wesentliche Rolle für die Reproduzierbarkeit der Reaktion. Frühere Untersuchungen wurden durch Umwickeln einer Quarzküvette mit Platindraht durchgeführt. Dabei variiert der Abstand zwischen Kathode und Substrat wie auch der Abstand zwischen Kathode und Anode. Durch eine Änderung des Zellaufbaus hin zu einer Anschwemm-Elektrode, bei dem die spiralförmige Kathode vom SiO_2-Substrat bedeckt und die Gitteranode darüber parallel angeordnet ist, konnten reproduzierbare Ergebnisse erzielt werden. Hierbei spielen sowohl der Elektrolyt als auch die Stromdichte eine weitere tragende Rolle. Es werden sehr hohe Stromdichten benötigt, wobei das Optimum bei 6.6 A/cm² liegt, um die gewünschte Umwandlung zu erreichen. Ein Screening der Elektrolytkomponenten zeigt, dass Tetrahydrofuran (THF) als Lösungsmittel mit Bu_4OTf als einzige Kombination zu zyklischen Siloxanen führt.

In der Arbeit von CHONG[8] wird Methanol als Substrat für die Bildung von Methylradikalen beschrieben, das zu zyklischen Siloxanen durch Methylierung der SiO_2-Oberfläche führt. In eigenen Untersuchungen führt Methanol ausschließlich zur Methoxylierung des Lösungsmittels THF. Wird die Konzentration von Methanol verringert, steigt die Ausbeute an Siloxanen bis zu einem Maximum in Abwesenheit von Methanol. Die Verwendung von Ethanol und deuteriertem Methanol führt zu identischen Ausbeuten und Substratverteilungen, vergleichbar zu Methanol. Das zeigt, dass Methanol nicht die Quelle der Methylradikale darstellt. Die Verwendung von deuteriertem THF führt ebenfalls zu identischen Ausbeuten und schließt die Beteiligung des Lösungsmittels als Zwischenprodukt in der Reaktion aus. Wenn die Konzentration des Leitsalzes erhöht wird, steigt die Ausbeute der erhaltenen Siloxane bis zu einem Maximum bei 0.4 M Bu_4NOTf. Bei der Untersuchung des Leitsalzes mittels multipler

NMR-Techniken wurde eine Verunreinigung durch 4.3% Bu_3MeN^+ festgestellt. Bu_3MeN^+ dient als Methylquelle für die reduktive Konversion hin zu Methylradikalen (Schema 14). Die Verwendung von zusätzlichen OTf^- oder Methylammoniumsalzen führt zu einer Verringerung der Ausbeute, da die Methylradikale hohe stabilisierende Eigenschaften des Elektrolyten erfordern.

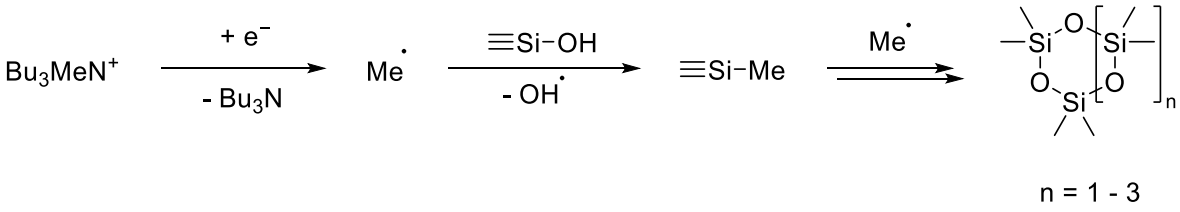

Schema 14. Elektrochemische Reduktion des Leitsalz-Kation Bu_3MeN^+ zu Methylradikalen und Konversion von SiO_2 zu den zyklischen Methylsiloxanen D_3 – D_5, (≡Si-OH = Oberfläche des SiO_2 Substrats).

Die Umsetzung durch die literaturbekannte chemische Erzeugung von Methylradikalen[10] über ein FENTON-analoges System mit DMSO / H_2O_2 / Fe(II) sowie weiteren wasserfreien Peroxiden, führte zu geringen Ausbeuten an zyklischen Siloxanen, die mit der elektrochemischen Umsetzung vergleichbar sind.

Über diesen Reaktionsweg kann sowohl der Methylradikal-getriebene Reaktionsweg belegt, als auch die bisherige Annahme einer stattfindenden Hydrolyse von Dimethyldimethoxysilan (DMDMS) zu den zyklischen Siloxanen widerlegt werden. Auch die selektive Hydrolyse von DMDMS durch Zugabe von Wasser führt unabhängig von der Wasserkonzentration nicht zur Bildung der zyklischen Siloxane. Der Mechanismus läuft vermutlich über eine direkte Methylierung an der SiO_2-Oberfläche ab, wobei die Ringstabilität die Produktverteilung bestimmt. Weiterhin konnte die elektrochemische Äquilibrierungsreaktion der zyklischen Siloxane gezeigt werden. Je nach Elektrolyt ist der Zugang zu D_6 ausgehend von D_3 möglich.

Fazit

Diese kritische Untersuchung zeigt, dass ein elektrochemischer Zugang zu zyklischen Siloxanen ausgehend von SiO_2 prinzipiell möglich ist. Entgegen den ursprünglichen Annahmen ist Methanol nicht die Quelle für die Methylradikale im Reaktionsprozess. Methylammoniumsalze erzeugen im Verlauf der Reaktion Methylradikale und führen über eine direkte Methylierung der SiO_2-Oberfläche zu den zyklischen Siloxanen. Zusätzlich ist DMDMS kein Zwischenprodukt für den Reaktionsverlauf. Die Ausbeuten

sind sehr gering und im Verlauf der Reaktion kommt es zwangsläufig zur Zersetzung des Leitsalzes an Anode und Kathode. Während offene Fragen zum Reaktionsablauf geklärt werden konnten, ist die industrielle Umsetzung über diesen Weg weder ökologisch noch ökonomisch realisierbar.

[1] E. Pouget, J. Tonnar, P. Lucas, P. Lacroix-Desmazes, F. Ganachaud, B. Boutevin, *Chem. Rev.* **2010**, *110*, 1233–1277.

[2] D. Seyferth, *Organometallics* **2001**, *20*, 4978–4992.

[3] a) B. A. Kamino, T. P. Bender, *Chem. Soc. Rev.* **2013**, *42*, 5119–5130; b) S. Varaprath, K. L. Salyers, K. P. Plotzke, S. Nanavati, *Anal. Biochem.* **1998**, *256*, 14–22.

[4] K. Y. Blohowiak, D. R. Treadwell, B. L. Mueller, M. L. Hoppe, S. Jouppi, P. Kansal, K. W. Chew, C. L. S. Scotto, F. Babonneau, *Chem. Mater.* **1994**, *6*, 2177–2192.

[5] L. N. Lewis, F. J. Schattenmann, T. M. Jordan, J. C. Carnahan, W. P. Flanagan, R. J. Wroczynski, J. P. Lemmon, J. M. Anostario, M. A. Othon, *Inorg. Chem.* **2002**, *41*, 2608–2615.

[6] a) Y. Ono, M. Akiyama, E. Suzuki, *Chem. Mater.* **1993**, *5*, 442–447; b) E. Suzuki, M. Akiyama, Y. Ono, *J. Chem. Soc., Chem. Commun.* **1992**, 136–137.

[7] a) A. Boudin, G. Cerveau, C. Chuit, R. J. P. Corriu, C. Reye, *Angew. Chem., Int. Ed.* **1986**, *25*, 473–474; b) A. Boudin, G. Cerveau, C. Chuit, R. J. P. Corriu, C. Reye, *Organometallics* **1988**, *7*, 1165–1171; c) A. Rosenheim, B. Raibmann, G. Schendel, *Z. anorg. allg. Chem.* **1931**, *196*, 160–176.

[8] J. E. Dick, D. Chong, *J. Am. Chem. Soc.* **2014**, *136*, 6776; Zurückgezogen aufgrund von Bedenken bezüglich der Rechte an geistigem Eigentum.

[9] a) C. Huajun, F. Hongcheng, H. Jinghui, L. Liguo (Zhejiang Hesheng Silicon Industry Co), CN 103924259 A, **2014**; b) J. Jianxiong, L. Zhifang, L. Mengxian, W. Chuan (Hangzhou Normal University), CN 104120442 A, **2014**; c) L. Kai (Luo Kai), CN 103952716 A, **2014**.

[10] a) Z. Li, X. Cui, L. Niu, Y. Ren, M. Bian, X. Yang, B. Yang, Q. Yan, J. Zhao, *Adv. Synth. Catal.* **2017**, *359*, 246–249; b) R. Zhang, X. Shi, Q. Yan, Z. Li, Z. Wang, H. Yu, X. Wang, J. Qi, M. Jiang, *RSC Adv.* **2017**, *7*, 38830–38833.

EurJOC
European Journal of Organic Chemistry

Research Article
doi.org/10.1002/ejoc.202201253

Chemistry Europe
European Chemical Societies Publishing

www.eurjoc.org

VIP *Very Important Paper*

Special Collection

Assessment of the Electrochemical Synthesis Route to Silicones Starting from Silica as Feedstock

Alexander D. Beck,[a, b] Lukas Schäffer,[b] Stefan Haufe,[a] and Siegfried R. Waldvogel*[b]

We successfully achieved methylation of various SiO_2 sources to cyclic methylsiloxanes via electroreduction reaction. Contrary to previous assumptions, the reaction does not start from methanol as methyl radical source, that results in methoxylation of the electrolyte solvent. Methylammonium cations were found to enable the direct conversion, strongly dependent on the radical intermediate stabilization by the electrolyte. THF/$Bu_4NCF_3SO_3$ is the sole applicable system with yields below 14% referred to the methylammonium cations for the highest amount of product obtained so far. Mechanistic insights show that methylation does not occur via the supposed hydrolysis of dimethoxydimethylsilane intermediate, but via a direct conversion reaction, as comparative studies of a Fenton-type procedure clearly indicate. Further, cyclic methylsiloxane products are prone to subsequent electrochemical equilibration, strongly directed by the electrolyte solvent.

Introduction

Today's society is highly dependent on an important class of materials in numerous areas ranging from common household materials to industrial applications: Silicones. They enable our everyday life and can be found in a wide variety of fields, including appliances,[1,2] automotives and transport,[1,2] ceramics,[3] consumer goods,[1,2,4–6] electronics,[1,2,4,6] glass,[3] mechanical fluids,[1,2,7] medical solutions,[1,2,4–6,8,9] paints and coatings,[1,2,5,7] personal care products,[1,2,4–10] proceeding aids,[1,2,7] and textiles.[1,2] Currently, silicones, with polydimethylsiloxane as one of the most important compounds, are prepared exclusively via a highly energy-intensive route (Scheme 1, a).[11] In this process, SiO_2 is converted to elemental silicon by carbothermal reduction at 1500–3000 °C with the subsequent release of CO_2 and CO.[2,11,12] The metallurgical grade silicon is then reoxidized in the Rochow process with chloromethane under copper catalysis at about 300 °C to a mixture of methylchlorosilanes, mainly dimethyldichlorosilane.[2,3,11–15] Due to the low boiling temperature differences, elaborate distillation over several steps is required.[12] Finally, hydrolysis leads to the desired polysiloxanes. The use of silica raw material (SiO_2) remains an excellent direct source of silicone feedstock chemicals, due to its high availability and extremely low cost. Yet, the high binding energy of Si–O bonds of 535 kJ/mol requires intense efforts to activate and convert SiO_2.[11]

To circumvent these high bonding strengths and to find a less energy-intense way, different approaches to activate SiO_2

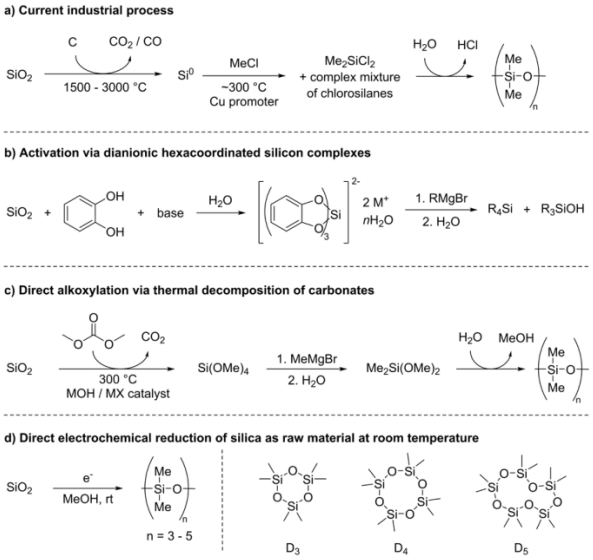

Scheme 1. Synthetic strategies for polydimethylsiloxane starting from silica as raw material: a) current industrial process via carbothermic reduction of SiO_2,[2,11,12] followed by Rochow's direct synthesis of methylchlorosilanes and hydrolysis to silicone materials,[2,3,11–15] b) activation of SiO_2 in alkaline environment by catechol to form the respective dianionic hexacoordinated silicon complexes (with M as alkaline earth metal) and subsequent Grignard alkylation and hydrolysis to form silanols for further condensation to silicone materials,[16–18] c) direct alkoxylation of SiO_2 by a thermal carbonate route (with M as alkaline earth metal, X as halogenide) with subsequent Grignard alkylation followed by hydrolysis and condensation to form the respective silicone materials,[12,20–22] d) direct electrochemical reduction of silica as raw material to cyclic methylsiloxanes (D_3–D_5).[15,26–28]

[a] *A. D. Beck, Dr. S. Haufe*
Consortium für elektrochemische Industrie
Wacker Chemie AG
Zielstattstraße 20, 81379 München (Germany)
[b] *A. D. Beck, L. Schäffer, Prof. Dr. S. R. Waldvogel*
Department Chemie
Johannes Gutenberg-Universität Mainz
Duesbergweg 10–14, 55128 Mainz (Germany)
E-mail: waldvogel@uni-mainz.de
https://www.aksw.uni-mainz.de/>

Supporting information for this article is available on the WWW under https://doi.org/10.1002/ejoc.202201253

Part of the "Board Member" Virtual Special Collection

EurJOC
European Journal of Organic Chemistry

Research Article
doi.org/10.1002/ejoc.202201253

Chemistry Europe
European Chemical Societies Publishing

have been pursued. The preparation of organosilanes via the transformation of SiO_2 with catechol to dianionic hexacoordinated,[16–18] or ethylene glycol to anionic pentacoordinated silicon complexes,[11,19] was explored (Scheme 1, b). Subsequent alkylation via Grignard routes to silanes and silanols with further condensation led to the respective siloxanes. However, access to industrially relevant mono- and disubstituted silanes remains difficult.[11] Direct alkoxylation of SiO_2 by thermal conversion of carbonates catalyzed with alkali halides or hydroxides at 300 °C under the stoichiometric release of CO_2 has also been reported (Scheme 1, c).[12,20–22] Further, acid induced alkoxylation of silicate starting materials has been demonstrated.[14] While these synthetic protocols need stoichiometric amounts of oxidizers or reducing agents and elevated temperatures, electrochemistry provides an environmentally benign alternative.[23] Reagent waste and stoichiometric CO_2 emission are avoided and by the use of regenerative electricity as a green alternative, this key discipline for future synthesis applications becomes very sustainable.[24] Furthermore, due to simple switch-off, thermal runaway reactions can be prevented, making this technology inherently safe.[25] Using these principles, Chong and co-workers described an electrochemical pathway using methanol and SiO_2 under reductive conditions to afford hexamethylcyclotrisiloxane (D_3), octamethylcyclotetrasiloxane (D_4), and decamethylcyclopentasiloxane (D_5) (Scheme 1, d).[15] However, this publication was retracted due to intellectual property rights concerns, and several patent applications were published about this subject in the same year.[26–28] Since cyclosiloxanes can be further used for the synthesis of linear polydimethylsiloxanes,[5,12] applications and a need are already established. However, the carbothermic reduction and subsequent Rochow process is still the sole utilized industrial access to silicones. Therefore, in this comprehensive study, the crucial reaction conditions, mechanistic aspects, and challenges of the direct electrochemical process are described in more detail to add new insights to the previous concept of the route.

Results and Discussion

The electrochemical direct access to cyclic methylsiloxanes starting from silica as raw materials as described by Chong and co-workers is claimed to proceed via the reductive transformation of methanol (Scheme 2).[15] By a one-electron reduction, methanol is converted to a methyl radical or methoxide species **I**. These highly reactive intermediates lead to methylation or methoxylation of the SiO_2 raw material silica surface **II**. In consecutive steps dimethoxydimethylsilane (DMDMS) **III** as a stable intermediate is formed, which could be detected as a byproduct. Hydrolysis of DMDMS with water formed in situ via esterification of the silica surface or by deprotonation of methanol by the electrochemically generated hydroxide finally leads to the cyclic methylsiloxanes (D_3–D_5) **IV**.

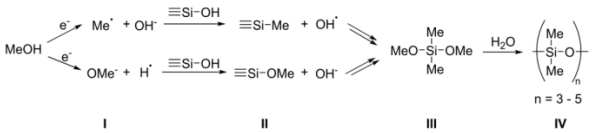

Scheme 2. The postulated mechanism by Chong and co-workers through the reduction of methanol via methyl radical or via methoxide species, consecutive reaction with silica surface (≡Si–OH) and subsequent reaction to form dimethoxydimethylsilane (DMDMS) as stable intermediate to further hydrolyze with water formed in situ to the respective cyclic methylsiloxanes (D_3–D_5).[15]

Using a supporting electrolyte consisting of MeCN or THF with Bu_4NOTf, suitable electrode materials Pt, Ni–Cr, Ni or graphite were listed, and the silica as raw material is a quartz glass cuvette or quartz sand. Reproduction of the corresponding results has proven to be difficult independent of potentiostatic or galvanostatic reaction conditions, a problem discussed in the literature.[29] Especially, wrapping of the quartz cuvette allows for considerable tolerance of the distance between cathode and SiO_2 substrate, which seems to be crucial for the desired conversion. We therefore decided to change the original electrode arrangement from a vertical to a horizontal design and cover the cathode material with silica sand to achieve the closest possible distance allowing high reproducibility. Furthermore, insoluble materials as quartz sand, fumed silica and quartz wool could be used as SiO_2 source. An aliquot of pre- and post-electrolysis samples of every experiment was analyzed to ensure the influence of electrolysis. The concentrations of the products were calculated based on a GC-MS calibration curve. The yield was calculated based on the number of electrons used for the respective cyclic methylsiloxanes with the assumption of one electron per methyl moiety, due to the previously postulated radical conversion (see Supporting Information).[15]

Screening of electrode materials, inter-electrode gap, type of SiO_2 source, applied current as well as possible supporting electrolyte combinations by galvanostatic conditions revealed, that cyclic methylsiloxanes (D_3 - D_5) can be accessed by the direct electrochemical route especially by very high current densities (see Supporting Information). Non-stabilized THF needs to be used, due to the radical scavenging properties of butylated hydroxytoluene (as stabilizing component in the stabilized THF). In addition, butylated hydroxytoluene is easier to reduce electrochemically compared to MeOH.

The stabilization of radical species as vital intermediate combined with high cathodic stability, due to the irreversible reduction of methanol at −2.71 V vs. FcH/FcH^+ (Ferrocene/Ferrocenium) at a platinum electrode, show some of the faced requirements to the supporting electrolyte. Yet, calculated yields of the desired products are low and DMDMS could not be detected. The previously postulated supporting electrolyte THF/Bu_4NOTf ($OTf = CF_3SO_3^-$) is so far the sole combination leading to a successful formation of 1.9% yield of cyclic methylsiloxanes exclusively obtained via electrical current. Deviant solvents including the originally described MeCN as well as further cyclic and linear ethers like 1,4-dioxane or 1,2-dimethoxyethane do not yield cyclic methylsiloxanes. THF may be attributed a special role for the desired conversion, among others due to its excellent solubilization properties.[5] In

EurJOC
European Journal of Organic Chemistry

Research Article
doi.org/10.1002/ejoc.202201253

Chemistry Europe
European Chemical Societies Publishing

addition, the combination with Bu_4NOTf is vital for a successful transformation. Further supporting electrolytes were investigated, such as Bu_4NClO_4, Bu_3MeNSO_4Me, Bu_4NBF_4 and $Bu_3MeNNTf_2$ ($NTf_2 = [(CF_3SO_2)_2N]^-$), which are electrochemically stable and exhibit weak to noncoordinating properties. However, in these cases, the formation of cyclic siloxanes could not be observed. High cathodic stability of the solvent in combination with low coordination of the anion seem to be only some of the requirements for the desired conversion. The stabilization of the reactive intermediate by hydrogen bonding via THF/OTf^- as well as a suitable anodic process in the course of the reaction are needed.

To gain deeper insights into the reaction mechanism and the species involved, we screened different methyl sources for the desired conversion referring to the patent applications.[26–28] Dimethyl carbonate, trimethoxymethane and dimethyl sulfoxide show high cathodic stability, exceeding the range of potential electrochemical stability of the used supporting electrolyte (see Supporting Information). Methyl trifluoromethanesulfonate is prone to hydrolysis with subsequent acidic catalyzed polymerization of the THF electrolyte, leading to exclusion even in strictly anhydrous supporting electrolytes. In presence of iodomethane (Table 1, entry 1) as well as trimethylsulfonium iodide (Table 1, entry 2) the cyclic methylsiloxanes could be detected although the yield is comparable to the results for methanol (Table 1, entry 3). This observation is surprising because the use of deuterated methanol did not lead to deuterated cyclic methylsiloxanes as one would expect (Table 1, entry 4). In fact, the product quantity, distribution, and species were identical to the use of non-deuterated methanol (Table 1, entry 3). The same results were achieved by application of further linear alcohols like ethanol. Instead of the formation of cyclic ethylsiloxanes, that should be accessible using the described direct pathway, cyclic methylsiloxanes were obtained (Table 1, entry 5). As the methanol content was reduced, the yield of cyclic methylsiloxanes increased to a maximum of 9.2% yield in the absence of methanol (Table 1, entry 6). With the reasonable assumption that methanol does not serve as source of methyl for the desired product formation as initially claimed, also solvent decomposition was ruled out as a source of intermediates (Table 1, entry 7). Again, no deuterated cyclic methylsiloxanes were detected, which inevitably focuses attention on the supporting electrolyte. In fact, the amount of cyclic methylsiloxanes increases with higher concentration of the supporting electrolyte. This can be raised to a maximum of 0.4 M Bu_4NOTf, resulting in a yield of 13.7% with D_4 as the main product (Table 1, entry 8).

In the presence of methanol, a comparable trend is obtained, yet the increase of D_3 - D_5 is considerably reduced, reaching 3.1% yield for 0.4 M Bu_4NOTf. Methanol, instead of being the source of methyl radical for cyclic methylsiloxanes,[30] leads to the methoxylation of solvent, as the side reaction to 2-methoxytetrahydrofuran shows. Although methanol should be more easily reduced than the supporting electrolyte, due to the low selectivity of this process, Bu_4NOTf is still one of the main substrates reductively converted. So, by electrochemical reduction of Bu_4NOTf in THF-d_8 in the presence of 0.2 M methanol, Bu_3N with 24% yield is obtained after application of 0.5 *F*. In the absence of methanol the yield of Bu_3N is raised to 30%. Subsequent formation of butane and octane can be detected, indicating a butyl radical species to dimerize or abstract hydrogen (Scheme 3). Cyclic butylsiloxanes could not be traced, due to the increased steric requirements and lower stabilization by THF compared to methyl radicals. However, the dimerization reveals the access to radical species via the reduction of the supporting electrolyte. The formation of methyl radicals as essential intermediates result in the activation of the SiO_2 surface and subsequent conversion (see below), as can be implemented by the reductive conversion (Scheme 3). Analytical investigation of the supporting electrolyte Bu_4NOTf by multiple NMR techniques revealed contamination by a methylated ammonium cation. Bu_3MeN^+ appears to act as the methyl source for the electrochemical methylation with 4.3%. The use of further ammonium triflate supporting electrolytes (R_4N^+ OTf^-), did not lead to the desired cyclosiloxanes, clearly indicating the necessity of methylated ammonium cations. However, attempts to increase the yield of cyclic methylsiloxanes using different methylated ammonium supporting electrolytes failed, due to the high requirements for the supporting electrolyte anions (see Supporting Information).

Table 1. Screening of methyl sources for the direct electrochemical conversion of silica raw material to cyclic methylsiloxanes.

Entry	Conditions[a]	Methyl source[b]	Yield in [%] and [µmol] of D_3[c]	D_4[c]	D_5[c]
1	Standard	MeI	0.0 (0.0)	0.6 (0.0)	0.5 (0.0)
2	Standard	Me_3S^+ I^-	0.8 (0.1)	1.7 (0.1)	1.4 (0.1)
3	Standard	MeOH	0.8 (0.1)	0.6 (0.0)	0.5 (0.0)
4	Standard	MeOH-d_3	0.8 (0.1)	0.6 (0.0)	0.5 (0.0)
5	Standard	EtOH	0.8 (0.1)	0.6 (0.0)	0.5 (0.0)
6	Standard	–	0.8 (0.1)	4.7 (0.3)	3.7 (0.2)
7	THF-d_8	–	0.8 (0.1)	4.7 (0.3)	3.7 (0.2)
8	Standard[d]	Bu_4NOTf (0.4 M)	2.9 (0.8)	6.3 (1.4)	4.5 (0.8)

[a] Reaction conditions: tetrahydrofuran as solvent with 0.1 M Bu_4NOTf supporting electrolyte, the anode is a platinum gauze, the cathode is a platinum wire emerged in 1.0 g quartz sand at room temperature, the inter-electrode gap is 2 mm, without stirring, current density of 6.6 A/cm^2, applied charge of 0.5 *F*, under argon inert gas atmosphere. [b] Concentration of substrates: 0.2 M, except otherwise noted. [c] Yield calculated based on the number of electrons used for the respective cyclic methylsiloxanes with the assumption of one electron per methyl moiety with Bu_3MeN^+ as methyl source, referenced to a GC-MS calibration curve. [d] The amount of supporting electrolyte differs from standard conditions, due to the application as methyl source, with an applied charge of 0.3 *F*.

EurJOC
European Journal of Organic Chemistry

Research Article
doi.org/10.1002/ejoc.202201253

Chemistry Europe
European Chemical Societies Publishing

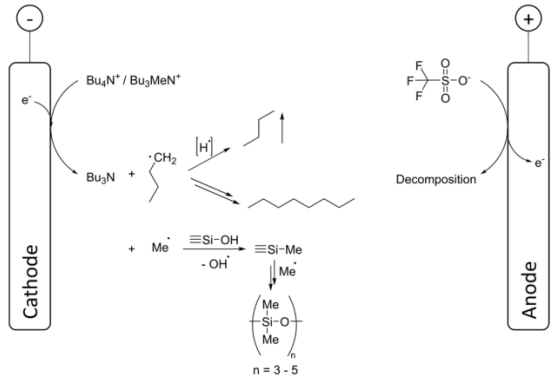

Scheme 3. Proposed mechanism for the methylation of SiO_2 raw material via the reduction of the supporting electrolyte cation (Bu_4N^+/Bu_3MeN^+) to a radical species and subsequent formation of butane and octane or methylation of the SiO_2 surface with following conversion to cyclic methylsiloxanes and simultaneous anodic decomposition of the supporting electrolyte anion.

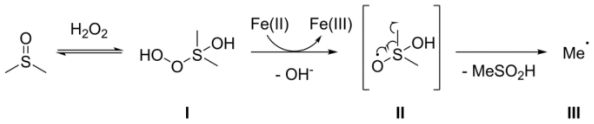

Scheme 4. Mechanism for the formation of free methyl radicals by the Fenton-type oxidation of DMSO by H_2O_2/Fe(II).[34,35]

Especially halide ions show a disturbing effect on the desired conversion by slight oxidation and scavenging effects.[31] However, the low availability of the actual methyl source and the radical side reactions as observed for butyl radicals could be the reason for the poor yield of target substrates as well as an explanation for an optimal amount of applied charge in catalytic amounts. Chong and co-workers mentioned an ideal amount of applied charge well below 1.0 *F*, based on a presumably electrochemically initiated, subsequently catalyzed reaction.[15] Screening of the applied charge indicated 0.3 *F* as ideal for the desired conversion, which is consistent with the findings of Chong and co-workers, here due to the limited access of a suitable methyl source combined with the radical side reactions. It should be noted, that in the absence of methanol instead of the formation of 2-methoxytetrahydrofuran, anodic decomposition of the supporting electrolyte anion to a sulfur and fluorine containing brown solid occurs. Hence, reusability of the electrolyte for further investigations is prevented, rendering the ecological advantage of the desired process doubtful.

Analogue to the electrochemical conversion, we investigated possibilities to initiate the generation of free methyl radicals via chemical routes. The corresponding activation and conversion of SiO_2 raw materials should achieve conversion to cyclic methylsiloxanes comparable to the electrochemical route. Using Fenton-type reaction conditions, the generation of free methyl radicals via the oxidation of dimethyl sulfoxide (DMSO) by a H_2O_2/Fe(II) system has been reported.[32–35] It is supposed that in the course of the reaction DMSO is oxidized by H_2O_2 to the peroxo intermediate **I**, subsequently reduced by Fe(II) with elimination of hydroxide to the respective radical species **II**, to yield the free methyl radical species **III** (Scheme 4).

Using analogue reaction conditions to previous studies,[34,35] we were able to convert quartz sand as silica source to the desired cyclic methylsiloxanes at room temperature via the formation of free methyl radicals. However, Fe(II) and a concentrated H_2O_2 solution (30%) were mandatory as well as the SiO_2 source for the favored activation and conversion, yielding the cyclic methylsiloxanes (Table 2, entries 1–4). The yield could be increased by using fumed silica, due to the very high surface area of 130–170 m^2/g and the hydrophobic properties enabling easier access for methyl radicals. As has been mentioned in literature, the surface of SiO_2 is a key aspect to stabilize methyl radicals,[36] simplifying the consecutive reaction to cyclic methylsiloxanes. Since the surface of the used fumed silica is modified by dimethylsiloxy groups, an additional positive influence through "pre-methylation" is conceivable. Yet, the yield remains low with 1.2% D_3–D_5 (Table 2, entry 5).

Table 2. Chemical conversion of SiO_2 via the free methyl radical pathway using the DMSO/peroxide/Fe(II) system.

Entry	Conditions[a]	Peroxide[b]	Yield in [%] and [µmol] of D_3[c]	D_4[c]	D_5[c]
1	No Fe(II)	H_2O_2	0.0 (0.0)	0.0 (0.0)	0.0 (0.0)
2	No SiO_2	H_2O_2	0.0 (0.0)	0.0 (0.0)	0.0 (0.0)
3	Standard	None	0.0 (0.0)	0.0 (0.0)	0.0 (0.0)
4	Standard	H_2O_2	0.1 (0.9)	0.3 (2.1)	0.1 (0.5)
5	Standard[d]	H_2O_2	0.2 (1.8)	0.8 (5.3)	0.2 (1.1)
6	Standard	$K_2S_2O_8$	0.1 (0.9)	0.2 (1.4)	0.1 (0.5)
7	Standard[d]	$K_2S_2O_8$	0.1 (0.9)	0.4 (2.7)	0.2 (1.1)
8	Standard	*t*BuOOH	0.1 (0.9)	0.1 (0.7)	0.1 (0.5)
9	Standard[d]	*t*BuOOH	0.1 (0.9)	0.2 (1.4)	0.1 (0.5)
10	Standard[e]	H_2O_2	0.0 (0.0)	0.0 (0.0)	0.0 (0.0)

[a] Reaction conditions: anhydrous $FeCl_2$ (0.5 mmol, 63 mg, 0.5 equiv.) and quartz sand (1.0 g) in 3 mL anhydrous DMSO under argon inert gas atmosphere, peroxide is added under stirring and extraction of cyclic methylsiloxanes with n-pentane after 24 h at room temperature. [b] Addition of H_2O_2 (30%, 5 mmol, 511 µL, 5 equiv.), $K_2S_2O_8$ (anhydrous, 5 mmol, 1352 mg, 5 equiv.) or *t*BuOOH = *tert*-butyl hydroperoxide (anhydrous in decane, 5 mmol, 250 µL, 5 equiv.). [c] Yield calculated based the amount of peroxide referenced to a GC-MS calibration curve. [d] Fumed silica (Wacker HDK H-15) was used instead of quartz sand. [e] TEMPO = (2,2,6,6-Tetramethylpiperidin-1-yl)oxyl (5 mmol, 781 mg, 5 equiv.) is applied.

EurJOC
European Journal of Organic Chemistry

Research Article
doi.org/10.1002/ejoc.202201253

Chemistry Europe
European Chemical Societies Publishing

Side reactions to the favored generation of cyclic methylsiloxanes could be detected. Due to the locally high radical concentration, dimerization of methyl radicals occurred at the beginning of the reaction as well as subsequent oxidation of DMSO to the stable dimethyl sulfone. In addition to the H_2O_2 approach in aqueous media, anhydrous systems could be used by the implementation of appropriate peroxides. Potassium persulfate and *tert*-butyl hydroperoxide, as anhydrous solution in decane, resulted cyclic methylsiloxanes, although the yield of the H_2O_2 system remains the highest so far (Table 2, entries 6, 8). Again, the use of fumed silica leads to a slightly increased yield compared to quartz sand as the SiO_2 source (Table 2, entries 7, 9). The product distribution indicates the formation of D_4 as the main product, independent of the used peroxide and the source of SiO_2. This is explained by the lower ring tension of the formed cyclic system and the higher Si–O bond energy in comparison to D_3,[37] which is in agreement with previous electrochemical experiments. There,[32,34,35] the use of TEMPO for scavenging of free methyl radicals leads to disruption of the desired reaction pathway (Table 2, entry 10) confirming the free radical pathway.

These investigations clearly support the hypothesis of a free methyl radical reaction pathway. However, DMDMS could not be detected, neither in the course of the electrochemical synthesis, nor by the chemically initiated radical methylation. In the preparation of cyclic siloxanes via the DMSO route in anhydrous conditions, the hydrolysis of DMDMS can be excluded, yet cyclic methylsiloxanes are obtained. To further support this theory, we added different concentrations of water to DMDMS as a substrate in the electrolyte at room temperature. Regardless of the water concentration, no cyclic siloxanes could be detected that should form due to the hydrolysis reactions (see Supporting Information). Therefore, the process involves direct methylation of the SiO_2 surface and conversion toward cyclic methylsiloxanes (Scheme 3), the thermodynamic optimum of which determining the ring size.

As mentioned before the cyclic methylsiloxanes D_4 and D_5 represent the thermodynamic optimum of this product class, due to the low ring tension and the high Si–O bond energy (see above).[37] However, in the course of our investigations, we discovered that the cyclic systems, especially D_3 can be electrochemically equilibrated to elongated ring structures. The catalytic effects of electrolyte, platinum surfaces and temperature, could be excluded by boiling D_3, D_4 and D_5 in the electrolyte under current-less conditions. The equilibration occurred only via electrochemical conversion. A cathodic process could be observed by using divided cells, although the reductive stability of cyclic methylsiloxanes exceeds that of the supporting electrolyte (see Supporting Information). Furthermore, the amount of applied charge needed for the respective equilibration is in the range of 0.2–1.0 *F*, indicating catalytic activity and an influence on the reaction by the supporting electrolyte. As expected D_4 and D_5, as the most stable substrates, show only minor conversion (Table 3, entries 1, 2). D_3 is converted to D_4–D_6 (Table 3, entry 3). While the equilibration to D_4 and D_5 is anticipated, D_6 is the main product starting from D_3, contra intuitive to its stability, due to the ring tension. This finding might involve a radical process of the cyclic methylsiloxane further dimerizing to D_6. This trend can be similarly observed with further supporting electrolytes, generating D_6 as the main product. A direct influence by intermediate species generated via the decomposition of the supporting electrolyte anion can be ruled out (Table 3, entries 4, 5). However, the role of the solvent used for the electrochemical conversion is vital for the stabilization of the intermediates. Using MeCN as solvent, similarly to the direct methylation of SiO_2 raw materials, the stabilization of radical species is significantly reduced, shifting D_6 to a side product and favoring the formation of D_4 (Table 3, entries 6–8).

Conclusion

We critically investigated the direct electrochemical conversion of silica as raw materials to silicones regarding reaction conditions, mechanistic aspects, and challenges. The direct methylation of SiO_2 materials has been achieved via electrochemical conversion, however, the desired pathway demands specific requirements of the used supporting electrolyte. High electrochemical stability, good stabilization of methyl radical species and low coordination by the supporting electrolyte anion are crucial. Methanol does not result in the release of methyl radicals during conversion as claimed by previous studies, but in the methoxylation of THF electrolyte solvent.

Table 3. Equilibration of the cyclic methylsiloxanes D_3–D_5 via the electrochemical conversion.[a]

Entry	Educt	Electrolyte	Yield in [%] and [mmol] of D_3[b]	D_4[b]	D_5[b]	D_6[b]
1	D_5	THF, Bu_4NOTf	0 (0.0)	7 (0.1)	93 (1.9)	0 (0.0)
2	D_4	THF, Bu_4NOTf	0 (0.0)	98 (2.0)	2 (0.0)	0 (0.0)
3	D_3	THF, Bu_4NOTf	46 (0.9)	15 (0.3)	8 (0.2)	31 (0.6)
4	D_3	THF, Bu_4NClO_4	34 (0.7)	14 (0.3)	15 (0.3)	37 (0.7)
5	D_3	THF, Bu_4NBF_4	57 (1.1)	13 (0.3)	6 (0.1)	24 (0.5)
6	D_3	MeCN, Bu_4NOTf	0 (0.0)	66 (1.3)	24 (0.5)	10 (0.2)
7	D_3	MeCN, Bu_4NClO_4	47 (0.9)	30 (0.6)	8 (0.2)	15 (0.3)
8	D_3	MeCN, Bu_4NBF_4	61 (1.2)	21 (0.4)	5 (0.1)	13 (0.3)

[a] Reaction conditions: 5 mL of anhydrous solvent with 0.1 M supporting electrolyte, cyclic methylsiloxanes (2 mmol, 0.4 M, 1.0 equiv.), anode and cathode are platinum, at room temperature, inter-electrode gap is 5 mm, without stirring, current density of 10 mA/cm^2, applied charge of 0.2 *F*, under argon inert gas atmosphere. [b] Yield determined by NMR referenced to TMS.

EurJOC
European Journal of Organic Chemistry

Research Article
doi.org/10.1002/ejoc.202201253

Chemistry Europe
European Chemical Societies Publishing

Contrary, methylated ammonium cations can be used as a methyl source for the methylation of SiO_2 via cathodic transformation. Similarly, the methylation of SiO_2 is achieved by the direct chemical access via Fenton-type conditions using a DMSO/Fe(II)/peroxide mixture to obtain cyclic methylsiloxanes in low yields. Dimethoxydimethylsilane is not a prerequisite intermediate for the desired conversion as anticipated. Methylation of the SiO_2 surface occurs via direct activation with subsequent conversion to the cyclic methylsiloxanes. However, cyclic methylsiloxanes can be easily electrochemically equilibrated, with the used solvent determining the product ring size.

Experimental Section

Synthesis of material: All described experiments were performed under argon inert gas atmosphere (<0.1 ppm O_2 and <0.1 ppm H_2O content). For screening experiments an undivided (25 mL) glass cell for the electrolysis was used. The active surface of the respective used platinum wire cathode was 0.009 cm^2, the geometric measurements of the platinum gauze anode were 20 mm in diameter. The separation of the electrode surfaces could be varied and was screened in the course of the project. The software used was IKA Labworldsoft 6.0. The glass cell compartment of the horizontal design was charged with 10 mL of a 0.1 M solution of Bu_4NOTf in THF (not stabilized by butylated hydroxytoluene). Methanol (81 μL, 2.0 mmol, 1.0 equiv.) was added and the cathode was placed in the glass cell compartment. The cathode was covered by quartz sand (1.0 g, 40–80 μm diameter), the anode was added, and both connected to the IKA power supply. As a blank sample, 0.3 mL of the reaction mixture was taken and filtered with n-pentane over silica gel and analyzed by a calibrated GC-MS method. Afterwards the reaction was conducted at room temperature without stirring. After termination of the electrolysis ($j=6.6$ A/cm^2, 0.5 *F*), a second aliquot of the reaction mixture was taken and filtered with n-pentane over silica gel and analyzed by a calibrated GC-MS method.

Characterization

NMR Spectroscopy of ^1H, ^{13}C and ^{29}Si spectra were recorded at 25 °C, using a Bruker Avance 500 (500 MHz, Analytische Messtechnik, Karlsruhe, Germany). Chemical shifts (δ) are reported in parts per million (ppm). Traces of CH_2Cl_2 in the corresponding deuterated solvent, or tetramethylsilane for ^{29}Si spectra were used as internal standard for calibration.

GC-MS measurements were carried out on an Agilent GC-A6890N using a HP-5 column (Agilent Technologies, Santa Clara, California), length: 30 m, inner diameter: 0.25 mm, film: 0.25 μm, carrier gas: helium. The chromatograph was coupled to a mass spectrometer Agilent MSD 5975C (Agilent, Santa Clara, California, USA).

Detailed information on general procedures, electrochemical conversions, cyclic voltammetry measurements and product characterization can be found in the Supporting Information.

Acknowledgements

Open Access funding enabled and organized by Projekt DEAL.

Conflict of Interest

The authors declare no conflict of interest.

Data Availability Statement

The data that support the findings of this study are available in the supplementary material of this article.

Keywords: electrochemistry · methylation · radicals · reduction · silicon

[1] E. Pouget, J. Tonnar, P. Lucas, P. Lacroix-Desmazes, F. Ganachaud, B. Boutevin, *Chem. Rev.* **2010**, *110*, 1233–1277.
[2] D. Seyferth, *Organometallics* **2001**, *20*, 4978–4992.
[3] R. M. Laine, K. Y. Blohowiak, T. R. Robinson, M. L. Hoppe, P. Nardi, J. Kampf, J. Uhm, *Nature* **1991**, *353*, 642–644.
[4] Y. Horii, K. Kannan, *Arch. Environ. Contam. Toxicol.* **2008**, *55*, 701–710.
[5] S. Varaprath, K. L. Salyers, K. P. Plotzke, S. Nanavati, *Anal. Biochem.* **1998**, *256*, 14–22.
[6] R. Wang, R. P. Moody, D. Koniecki, J. Zhu, *Environ. Int.* **2009**, *35*, 900–904.
[7] B. A. Kamino, T. P. Bender, *Chem. Soc. Rev.* **2013**, *42*, 5119–5130.
[8] W. Johnson, W. F. Bergfeld, D. V. Belsito, R. A. Hill, C. D. Klaassen, D. C. Liebler, J. G. Marks, R. C. Shank, T. J. Slaga, P. W. Snyder, F. A. Andersen, *Int. J. Toxicol.* **2011**, *30*, 149S-227S.
[9] P. C. Klykken, T. W. Galbraith, G. B. Kolesar, P. A. Jean, M. R. Woolhiser, M. R. Elwell, L. A. Burns-Naas, R. W. Mast, J. A. Mccay, K. L. White, A. E. Munson, *Drug Chem. Toxicol.* **1999**, *22*, 655–677.
[10] G. Zareba, R. Gelein, P. E. Morrow, M. J. Utell, *Skin Pharmacol. Appl. Skin Physiol.* **2002**, *15*, 184–194.
[11] K. Y. Blohowiak, D. R. Treadwell, B. L. Mueller, M. L. Hoppe, S. Jouppi, P. Kansal, K. W. Chew, C. L. S. Scotto, F. Babonneau, *Chem. Mater.* **1994**, *6*, 2177–2192.
[12] L. N. Lewis, F. J. Schattenmann, T. M. Jordan, J. C. Carnahan, W. P. Flanagan, R. J. Wroczynski, J. P. Lemmon, J. M. Anostario, M. A. Othon, *Inorg. Chem.* **2002**, *41*, 2608–2615.
[13] E. G. Rochow, *J. Am. Chem. Soc.* **1945**, *67*, 963–965.
[14] M. E. Kenney, G. B. Goodwin (Case Western Reserve University), US 4717773, **1988**.
[15] J. E. Dick, D. Chong, *J. Am. Chem. Soc.* **2014**, *136*, 6776; Retracted due to intellectual property rights concerns.
[16] A. Boudin, G. Cerveau, C. Chuit, R. J. P. Corriu, C. Reye, *Organometallics* **1988**, *7*, 1165–1171.
[17] A. Rosenheim, B. Raibmann, G. Schendel, *Z. Anorg. Allg. Chem.* **1931**, *196*, 160–176.
[18] A. Boudin, G. Cerveau, C. Chuit, R. J. P. Corriu, C. Reye, *Angew. Chem. Int. Ed.* **1986**, *25*, 473–474.
[19] H. Cheng, R. Tamaki, R. M. Laine, F. Babonneau, Y. Chujo, D. R. Treadwell, *J. Am. Chem. Soc.* **2000**, *122*, 10063–10072.
[20] E. Suzuki, M. Akiyama, Y. Ono, *J. Chem. Soc., Chem. Commun.* **1992**, 136–137.
[21] Y. Ono, M. Akiyama, E. Suzuki, *Chem. Mater.* **1993**, *5*, 442–447.
[22] M. Akiyama, E. Suzuki, Y. Ono, *Inorg. Chim. Acta* **1993**, *207*, 259–261.
[23] a) S. Möhle, M. Zirbes, E. Rodrigo, T. Gieshoff, A. Wiebe, S. R. Waldvogel, *Angew. Chem., Int. Ed.* **2018**, *57*, 6018–6041; *Angew. Chem.* **2018**, *130*, 6124–6149; b) A. Wiebe, T. Gieshoff, S. Möhle, E. Rodrigo, M. Zirbes, S. R. Waldvogel, *Angew. Chem. Int. Ed.* **2018**, *57*, 5594–5619; *Angew. Chem.* **2018**, *130*, 5694–5721.
[24] a) D. Pollok, S. R. Waldvogel, *Chem. Sci.* **2020**, *11*, 12386–12400; b) J. Seidler, J. Strugatchi, T. Gärtner, S. R. Waldvogel, *MRS Energy & Sustainability* **2020**, *7*, E42.

EurJOC
European Journal of Organic Chemistry

Research Article
doi.org/10.1002/ejoc.202201253

Chemistry Europe
European Chemical Societies Publishing

[25] a) A. D. Beck, S. Haufe, J. Tillmann, S. R. Waldvogel, *ChemElectroChem* **2022**, *9*, e202101374; b) A. D. Beck, S. Haufe, S. R. Waldvogel, *ChemElectroChem* **2022**, *9*, e202200840; c) J. L. Röckl, D. Pollok, R. Franke, S. R. Waldvogel, *Acc. Chem. Res.* **2020**, *53*, 45–61; d) S. R. Waldvogel, S. Lips, M. Selt, B. Riehl, C. J. Kampf, *Chem. Rev.* **2018**, *118*, 6706–6765.
[26] C. Huajun, F. Hongcheng, H. Jinghui, L. Liguo (Zhejiang Hesheng Silicon Industry Co), CN 103924259A, **2014**.
[27] J. Jianxiong, L. Zhifang, L. Mengxian, W. Chuan (Hangzhou Normal University), CN 104120442A, **2014**.
[28] L. Kai (Luo Kai), CN 103952716A, **2014**.
[29] a) S. B. Beil, D. Pollok, S. R. Waldvogel, *Angew. Chem. Int. Ed.* **2021**, *60*, 14750–14759; *Angew. Chem.* **2021**, *133*, 14874–14883; b) M. Klein, S. R. Waldvogel, *Angew. Chem., Int. Ed.* **2022**, e202204140; *Angew. Chem.* **2022**, e202204140.
[30] D. Mickewich, J. Turkevich, *J. Phys. Chem.* **1968**, *72*, 2703–2706.
[31] B. S. Evans, E. Whittle, *Int. J. Chem. Kinet.* **1978**, *10*, 745–757.
[32] R. Caporaso, S. Manna, S. Zinken, A. R. Kochnev, E. R. Lukyanenko, A. V. Kurkin, A. P. Antonchick, *Chem. Commun.* **2016**, *52*, 12486–12489.
[33] a) K.-S. Du, J.-M. Huang, *Green Chem.* **2018**, *20*, 1405–1411; b) U. Rudqvist, K. Torssell, P. N. Skancke, K. Hedberg, K. Schaumburg, L. Ehrenberg, *Acta Chem. Scand.* **1971**, *25*, 2183–2188.
[34] Z. Li, X. Cui, L. Niu, Y. Ren, M. Bian, X. Yang, B. Yang, Q. Yan, J. Zhao, *Adv. Synth. Catal.* **2017**, *359*, 246–249.
[35] R. Zhang, X. Shi, Q. Yan, Z. Li, Z. Wang, H. Yu, X. Wang, J. Qi, M. Jiang, *RSC Adv.* **2017**, *7*, 38830–38833.
[36] G. B. Garbutt, H. D. Gesser, *Can. J. Chem.* **1970**, *48*, 2685–2694.
[37] M. G. Voronkov, *J. Organomet. Chem.* **1998**, *557*, 143–155.

Manuscript received: October 27, 2022
Revised manuscript received: November 17, 2022
Accepted manuscript online: November 18, 2022

European Journal of Organic Chemistry

Supporting Information

Assessment of the Electrochemical Synthesis Route to Silicones Starting from Silica as Feedstock

Alexander D. Beck, Lukas Schäffer, Stefan Haufe, and Siegfried R. Waldvogel*

Contents

1 General Information

Used reagents were of high purity (≥97%) and obtained from commercial suppliers such as Aldrich, VWR, and Acros. Solvents were obtained in anhydrous quality and water content was checked by Karl-Fischer analysis. Quartz sand was dried under vacuum prior to electrolysis (180 °C, 24 h, $0.1x10^{-3}$ mbar). Electrochemical reactions were carried out at glassy carbon (GC), platinum (Pt), copper (Cu), and graphite (C). A platinum gauze (75x75 mm, 52 mesh woven from 0.1 mm diameter wire, 99.9% (metals basis), obtained from VWR International GmbH, Darmstadt, Germany), a platinum foil (75x75 mm, 0.025 mm; 99.9% (metals basis), obtained from chemPUR Feinchemikalien und Forschungsbedarf GmbH, Karlsruhe, Germany) and a platinum wire (50 cm, 0.4 mm in diameter, 99.9% (metals basis), obtained from chemPUR Feinchemikalien und Forschungsbedarf GmbH, Karlsruhe, Germany) were used. GC, Pt, Cu, and C electrodes were obtained from IKA (IKA-Werke GmbH & Co. KG, Staufen, Germany). The dimensions of all used IKA electrode materials were 7 cm x 1 cm x 0.3 cm. All descried reactions were performed under argon inert gas atmosphere (<0.1 ppm O_2 and <0.1 ppm H_2O content).

Gas chromatography was performed on an Agilent GC-A6890N (Agilent, Santa Clara, California, USA) using a RTX200 column (Agilent Technologies, Santa Clara, California, USA), length: 60 m + 30 m, inner diameter: 2 x 0.32 mm, film: 0.25 µm, carrier gas: helium. **GC-MS** measurements were carried out on an Agilent GC-A6890N using a HP-5 column (Agilent Technologies, Santa Clara, California), length: 30 m, inner diameter: 0.25 mm, film: 0.25 µm, carrier gas: helium. The chromatograph was coupled to a mass spectrometer Agilent MSD 5975 C (Agilent, Santa Clara, California, USA).

NMR Spectroscopy of ^{1}H, ^{13}C and ^{29}Si spectra were recorded at 25 °C, using a Bruker Avance 500 (500 MHz, Analytische Messtechnik, Karlsruhe, Germany). Chemical shifts (δ) are reported in parts per million (ppm). Traces of CH_2Cl_2 in the corresponding deuterated solvent, or tetramethylsilane for ^{29}Si spectra were used as internal standard for calibration.

Cyclic voltammetry was performed under inert gas in a 20 mL glass vial (SVC-3 voltammetry cell, ALS Co., Ltd., Tokyo, Japan) equipped with an SP-300 potentiostat (Bio-Logic Science Instruments, Seyssinet-Pariset, France) *WE*: GC / Pt electrode tip, 1.6 mm in diameter; *CE*: platinum wire; *RE*: Ag/Ag^+ in 0.01 M $AgNO_3$ / 0.1 M Bu_4NClO_4. Solvent: THF. v = 200 mV/s, T = 25 °C, supporting electrolyte: $n$$Bu_4NOTf$, c ($n$$Bu_4NOTf$) = 0.1 M.

2 Set-up and general protocols for electrochemical synthesis

Vertical design:
For screening experiments an undivided (250 mL) glass cell for electrolysis was used. The active surface of the respective used wire cathode was 0.009 cm^2, the geometric dimensions of the gauze anode were 75x75 mm and electrode surfaces were separated by about 0.3 cm.

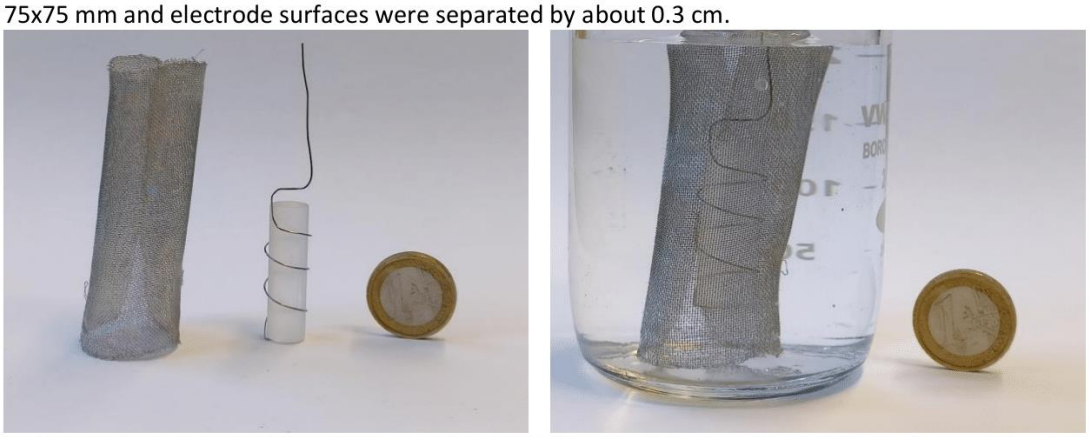

Figure 1: Vertical cell design for the reduction of SiO_2; left: 75x75 mm cylindrical platinum gauze anode, quartz piece (3 cm long, 8 mm in diameter), with 1 Euro coin for size comparison; right: setup emerged in electrolyte, with 1 Euro coin for size comparison.

Horizontal design:
For screening experiments an undivided (25 mL) glass cell for electrolysis was used. The active surface of the respective used wire cathode was 0.009 cm^2, the geometric measurements of the gauze anode were 20 mm in diameter. Separation of the electrode surfaces could be varied and was screened in course of the project.

Figure 2: Horizontal cell design for the reduction of SiO_2; left: 20mm diameter platinum gauze anode, platinum wire (5.6 cm helically coiled, 0.4 mm in diameter), with 1 Euro coin for size comparison; right: setup with cathode covered in quartz sand, with 1 Euro coin for size comparison.

Undivided PTFE Cell:
For screening experiments undivided (5 mL) PTFE cells for electrolysis with reaction block, stirrer, power supply were obtained as IKA Screening System (IKA-Werke GmbH & Co. KG, Staufen, Germany). The active surface of the respective used electrode was 1.3 cm^2, anode and cathode surface were separated by 0.5 cm. The software used was IKA Labworldsoft 6.0.

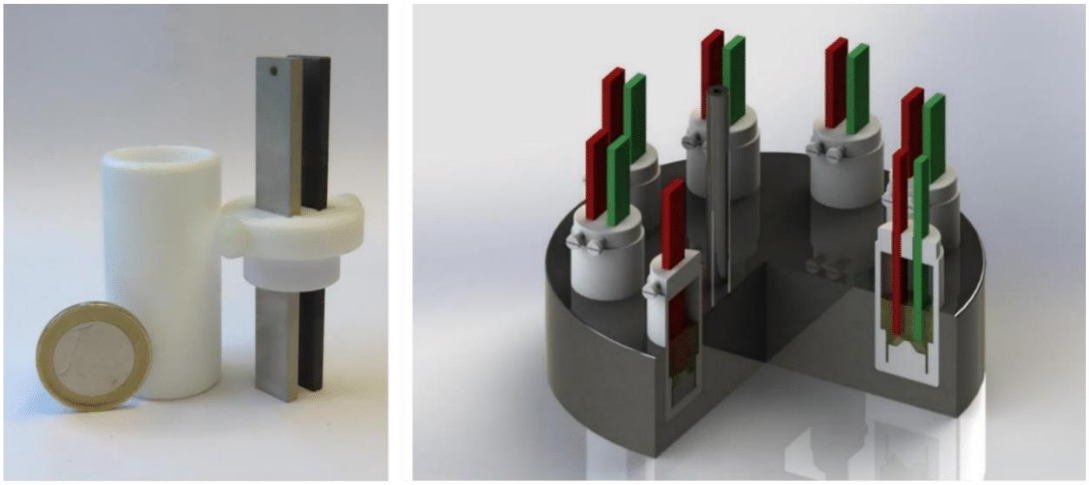

Figure 3: 5 mL PTFE cell; left: with 1 Euro coin for size comparison; right: schematic visualization of 5 mL PTFE cells in a screening block.

General procedure for optimization reactions in vertical cell design (GP1):
The glass cell compartment of the vertical design was charged with 200 mL of a 0.1 M solution of Bu_4NOTf in THF (not stabilized by butylated hydroxytoluene) under inter gas conditions in the glovebox. The used electrolyte was prepared and mixed in advance. Methanol (1.62 mL, 40.0 mmol, 1.0 eq.) was added, anode and cathode were placed in the glass cell compartment and connected to the IKA power supply. As blank sample, 0.3 mL of the reaction mixture was taken and filtered with n-pentane over silica gel and analyzed by a calibrated GC-MS method. Afterwards the reaction was conducted at room temperature without stirring. After termination of the electrolysis (j = 6.6 A/cm^2, 0.5 *F*), a second aliquot of the reaction mixture was taken and filtered with n-pentane over silica gel and analyzed by a calibrated GC-MS method. The general workup procedure consisted of carefully stripping off volatile compounds under cooling, washing of the organic layer with distilled water (3x25 mL) and back-washing with n-pentane (3x25 mL). The combined organic fractions were dried over Na_2SO_4 and filtered. Volatile compounds were carefully stripped off under cooling and the crude product was purified by HPLC.

General procedure for optimization reactions in horizontal cell design (GP2):
The glass cell compartment of the horizontal design was charged with 10 mL of a 0.1 M solution of Bu_4NOTf in THF (not stabilized by butylated hydroxytoluene) under inter gas conditions in the glovebox. The used electrolyte was prepared and mixed in advance. Methanol (81 µL, 2.0 mmol, 1.0 eq.) was added and the cathode was placed in the glass cell compartment (Figure 4, 1). The cathode was evenly covered by quartz sand (1.0 g, 40-80 µm in diameter) (Figure 4, 2). The anode was positioned and connected to an alligator clip. The inter-electrode gap was adjusted with a laboratory scissor jack and the cathode was connected to an alligator clip (Figure 4, 3). Both alligator clips were connected to the IKA power supply. As blank sample, 0.3 mL of the reaction mixture was taken and filtered with n-pentane over silica gel and analyzed by a calibrated GC-MS method. Afterwards the reaction was conducted at room temperature without stirring. After termination of the electrolysis (j = 6.6 A/cm^2, 0.5 *F*), a second aliquot of the reaction mixture was taken and filtered with n-pentane

over silica gel and analyzed by a calibrated GC-MS method. The workup procedure was analogue to GP1.

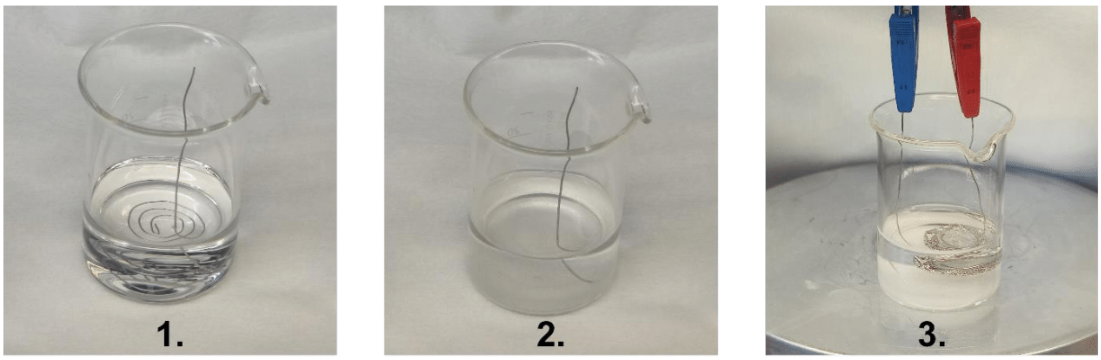

Figure 4. General procedure for optimization reactions in horizontal cell design: 1. the glass cell compartment was charged with the electrolyte and MeOH and the cathode was added; 2. the cathode was evenly covered with quartz sand; 3. the anode is connected to an alligator clip and after adjusting of the inter-electrode gap, the cathode is connected to an alligator clip.

General procedure for equilibration reactions (GP3):
The undivided PTFE cell compartment was charged with 5 mL of a 0.1 M solution of Bu_4NOTf in THF (not stabilized by butylated hydroxytoluene) under inter gas conditions in the glovebox. The used electrolyte was prepared and mixed in advance. Hexamethylcyclotrisiloxane (D_3) (445 mg, 2.0 mmol, 1.0 eq.) was added. The electrodes were connected to the IKA power supply, and the reaction was conducted at room temperature without stirring. After termination of the electrolysis (j = 10 mA/cm^2, 0.2 F), the product distribution was determined by direct ^{1}H and ^{29}Si NMR spectroscopy of samples of 300 µL of the reaction solution with a reference of 50 µL tetramethylsilane (TMS). For ^{29}Si NMR spectroscopy an additive of 8 mg $Cr(acac)_3$ as paramagnetic reagent for enhanced longitudinal relaxation was used. The workup procedure was analogue to GP1.

General procedure for Fenton-type reactions (GP4):
A 20 mL glass vial was charged with $FeCl_2$ (anhydrous, 63 mg, 0.5 mmol, 0.5 eq.), quartz sand (1.0 g, dried under vacuum prior to the Fenton-type reaction (180 °C, 24 h, 0.1x10^{-3} mbar)) and DMSO (anhydrous, 3 mL) under inter gas conditions in the glovebox. The mixture was stirred for some minutes until a homogeneous distribution of $FeCl_2$ and quartz sand is achieved. From this point on, the routes differ slightly depending on the peroxide used, due to aqueous or anhydrous conditions.
For the use of hydrogen peroxide, the glass vial was sealed with a septum and transferred out of the glovebox. Fresh hydrogen peroxide (30%, 5.0 mmol, 5.0 eq.) is added dropwise with a syringe under stirring. After the addition of peroxide, the reaction is stirred at room temperature for 24 h. Afterwards, the seal of the glass vial is removed, and the siloxane product distribution is extracted from the reaction mixture with 10 mL of n-pentane. A sample of 0.3 mL was taken and filtered with n-pentane over silica gel and analyzed by a calibrated GC-MS method.
For $K_2S_2O_8$ and *tert*-butyl hydroperoxide, the glass vial is kept in the glovebox. The respective anhydrous peroxide is added carefully under stirring (5.0 mmol, 5.0 eq.). Afterwards, the reaction is stirred at room temperature for 24 h. The product distribution is extracted with 10 mL of n-pentane and a sample of 0.3 mL was taken and filtered with n-pentane over silica gel and analyzed by a calibrated GC-MS method. The workup procedure was analogue to GP1.

3 General cyclic voltammetry protocol

The complete set-up was used in a Glovebox under argon inert gas atmosphere (<0.1 ppm O_2 and <0.1 ppm H_2O content), so no further degassing of the solvent was necessary. As supporting electrolyte non stabilized THF (water content <10 ppm, checked by Karl-Fischer analysis) containing 0.1 M Bu_4NOTf was placed in a 20 mL glass vial. Cyclic voltammetry was performed with a scan rate of 0.2 V/s otherwise noted, using glassy carbon or platinum working electrode (tip, 1.6 mm in diameter, each), a platinum wire as counter electrode and an Ag/Ag^+ reference electrode in 0.01 M $AgNO_3$ / 0.1 M Bu_4NClO_4 acetonitrile solution. Ferrocene/Ferrocenium (FcH/FcH^+) was used as internal reference (half-wave potential 0.09 V vs. Ag/Ag^+).

4 Calculation of current yield

The current yield was calculated (Equation 1) based on the number of electrons used for the respective cyclic methylsiloxanes with the assumption of one electron per methyl moiety, due to the previously postulated radical conversion.

$$CY = \frac{Z_{pr} \times F \times y \times 100}{I \times t}[\%] \qquad (1)$$

With Z_{pr} = product quantity [mmol], F = 96500 [As/mol], y = number of electrons, I = used current [A], t = electrolysis duration [s].

GC-MS was calibrated using dilutions of D_3, D_4 and D_5 in THF in the concentrations of 1 ppm, 5 ppm, 10 ppm, 25 ppm and 50 ppm with cycloheptane as internal standard. GC-MS calibration was regularly refreshed.

5 Results for the electrochemical screening reactions

The conversion was evaluated by GC-MS referenced to cycloheptane as internal standard after calibration and calculated via current yield respective to the methylated ammonium cation, presumably Bu_3MeN^+ (see chapter 4 on page S7).

5.1 Screening of supporting electrolyte combination in presence of MeOH

For the direct electrochemical conversion of silica raw materials to cyclic methylsiloxanes, the combination of supporting electrolyte was screened (Table 1) according to GP2 in presence of 0.2 M MeOH with a platinum wire cathode (surface area of 0.009 cm^2) and platinum gauze anode (20 mm in diameter) at room temperature without stirring. The inter-electrode gap was 2 mm, quartz sand (1.0 g) was used as SiO_2 source. A current density of 6.6 A/cm^2 was used with an applied charge of 0.5 *F*.

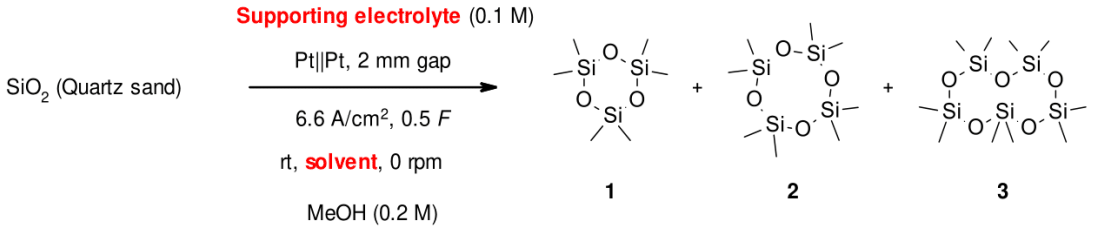

Scheme 1. Reaction conditions for the screening of supporting electrolyte combination in presence of 0.2 M MeOH for direct electrochemical conversion of silica raw materials to cyclic methylsiloxanes.

Table 1. Results for the screening of supporting electrolyte combination in presence of 0.2 M MeOH for direct electrochemical conversion of silica raw materials to cyclic methylsiloxanes.[a]

Entry	Solvent[b]	Supporting electrolyte[c]	[%] Yield and (µmol) of 1[d]	[%] Yield and (µmol) of 2[d]	[%] Yield and (µmol) of 3[d]
1	THF	Bu_4NOTf	0.8% (0.1)	0.6% (0.0)	0.5% (0.0)
2	MeCN	Bu_4NOTf	0.0% (0.0)	0.0% (0.0)	0.0% (0.0)
3	1,4-Dioxan	Bu_4NOTf	0.0% (0.0)	0.0% (0.0)	0.0% (0.0)
4	DME	Bu_4NOTf	0.0% (0.0)	0.0% (0.0)	0.0% (0.0)
5	THF	Bu_4NClO_4	0.0% (0.0)	0.0% (0.0)	0.0% (0.0)
6	THF	Bu_3MeNSO_4Me	0.0% (0.0)	0.0% (0.0)	0.0% (0.0)
7	THF	Bu_4NBF_4	0.0% (0.0)	0.0% (0.0)	0.0% (0.0)
8	THF	$Bu_3MeNNTF_2$	0.0% (0.0)	0.0% (0.0)	0.0% (0.0)

[a] Conditions for electrolysis and product range are depicted in Scheme 1. [b] THF = Tetrahydrofuran, MeCN = Acetonitrile, DME = 1,2-dimethoxyethane. [c] OTf = ($CF_3SO_3^-$), NTf_2 = [$(CF_3SO_2)_2N]^-$). [d] Yield (see Chapter 4) calculated based on the number of electrons used for the respective cyclic methylsiloxanes with the assumption of one electron per methyl moiety with Bu_3MeN^+ as methyl source, referenced to GC-MS calibration curve.

5.2 Screening of inter-electrode gap in presence of MeOH

For the direct electrochemical conversion of silica raw materials to cyclic methylsiloxanes, the inter-electrode gap (distance between cathode to anode surface) was screened (Table 2) according to GP2 in presence of 0.2 M MeOH with a platinum wire cathode (surface area of 0.009 cm^2) and platinum gauze anode (20 mm in diameter) at room temperature without stirring. Quartz sand (1.0 g) was used as SiO_2 source in a THF solvent with 0.1 M Bu_4NOTf. A current density of 6.6 A/cm^2 was used with an applied charge of 0.5 *F*.

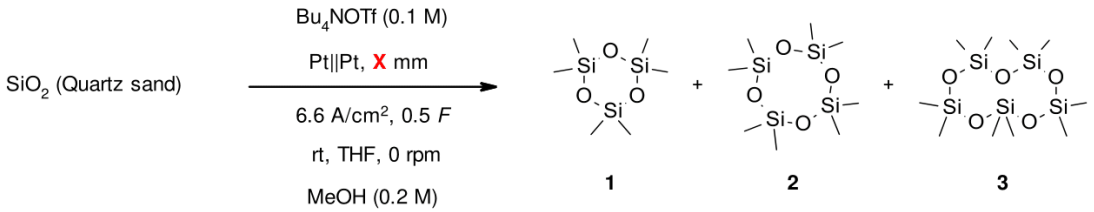

Scheme 2. Reaction conditions for the screening of inter-electrode gap in presence of 0.2 M MeOH for direct electrochemical conversion of silica raw materials to cyclic methylsiloxanes.

Table 2. Results for the screening of inter-electrode gap in presence of 0.2 M MeOH for direct electrochemical conversion of silica raw materials to cyclic methylsiloxanes.[a]

Entry	Inter-electrode gap [cm]	[%] Yield and (µmol) of 1[b]	[%] Yield and (µmol) of 2[b]	[%] Yield and (µmol) of 3[b]
1	0.2 cm	0.8% (0.1)	0.6% (0.0)	0.5% (0.0)
2	0.4 cm	0.8% (0.1)	0.6% (0.0)	0.5% (0.0)
3	0.7 cm	0.0% (0.0)	0.6% (0.0)	0.5% (0.0)
4	1.0 cm	0.0% (0.0)	0.6% (0.0)	0.0% (0.0)
5	1.5 cm	0.0% (0.0)	0.6% (0.0)	0.0% (0.0)

[a] Conditions for electrolysis and product range are depicted in Scheme 2. [b] Yield (see Chapter 4) calculated based on the number of electrons used for the respective cyclic methylsiloxanes with the assumption of one electron per methyl moiety with Bu_3MeN^+ as methyl source, referenced to GC-MS calibration curve.

5.3 Screening of current density in presence of MeOH

For the direct electrochemical conversion of silica raw materials to cyclic methylsiloxanes, the current density was screened (Table 3) according to GP2 in presence of 0.2 M MeOH with a platinum wire cathode (surface area of 0.009 cm^2) and platinum gauze anode (20 mm in diameter) at room temperature without stirring. The inter-electrode gap was 2 mm, quartz sand (1.0 g) was used as SiO_2 source in a THF solvent with 0.1 M Bu_4NOTf. The applied charge was 0.5 *F*.

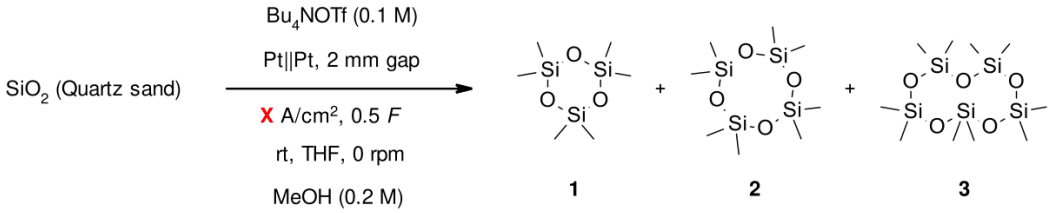

Scheme 3. Reaction conditions for the screening of current density in presence of 0.2 M MeOH for direct electrochemical conversion of silica raw materials to cyclic methylsiloxanes.

Table 3. Results for the screening of current density in presence of 0.2 M MeOH for direct electrochemical conversion of silica raw materials to cyclic methylsiloxanes.[a]

Entry	Current density [A/cm²]	[%] Yield and (µmol) of 1[b]	[%] Yield and (µmol) of 2[b]	[%] Yield and (µmol) of 3[b]
1[c]	0.01 A/cm²	0.0% (0.0)	0.0% (0.0)	0.0% (0.0)
2[c]	0.05 A/cm²	0.0% (0.0)	0.0% (0.0)	0.0% (0.0)
3[c]	0.1 A/cm²	0.0% (0.0)	0.0% (0.0)	0.5% (0.0)
4	0.5 A/cm²	0.0% (0.0)	0.0% (0.0)	0.5% (0.0)
5	1.1 A/cm²	0.0% (0.0)	0.0% (0.0)	0.5% (0.0)
6	3.3 A/cm²	0.0% (0.0)	0.6% (0.0)	0.5% (0.0)
7	6.6 A/cm²	0.8% (0.1)	0.6% (0.0)	0.5% (0.0)
8[d]	22 A/cm²	0.8% (0.1)	0.6% (0.0)	0.5% (0.0)

[a] Conditions for electrolysis and product range are depicted in Scheme 3. [b] Yield (see Chapter 4) calculated based on the number of electrons used for the respective cyclic methylsiloxanes with the assumption of one electron per methyl moiety with Bu_3MeN^+ as methyl source, referenced to GC-MS calibration curve. [c] Platinum sheet (3.2 cm^2 surface area) was used as cathode material for lower current densities, due to minimum current from power supply unit. [d] Maximum current density due to conductivity, current density decreases in the course of the reaction.

5.4 Screening of electrode material in presence of MeOH

For the direct electrochemical conversion of silica raw materials to cyclic methylsiloxanes, the cathode material was screened (Table 4) according to GP2 in presence of 0.2 M MeOH with a platinum gauze anode (20 mm in diameter) at room temperature without stirring. The inter-electrode gap was 2 mm, quartz sand (1.0 g) was used as SiO_2 source in a THF solvent with 0.1 M Bu_4NOTf. A current density of 6.6 A/cm² was used with an applied charge of 0.5 *F*.

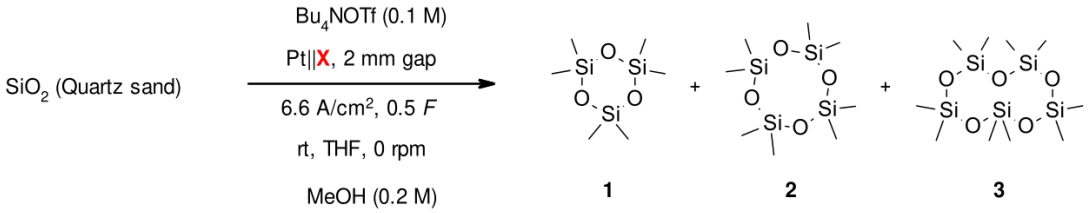

Scheme 4. Reaction conditions for the screening of cathode material in presence of 0.2 M MeOH for direct electrochemical conversion of silica raw materials to cyclic methylsiloxanes.

Table 4. Results for the screening of cathode material in presence of 0.2 M MeOH for direct electrochemical conversion of silica raw materials to cyclic methylsiloxanes.[a]

Entry	Cathode material	[%] Yield and (µmol) of 1[b]	[%] Yield and (µmol) of 2[b]	[%] Yield and (µmol) of 3[b]
1[c]	Platinum wire	0.8% (0.1)	0.6% (0.0)	0.5% (0.0)
2[d]	Platinum sheet	0.8% (0.1)	0.6% (0.0)	0.5% (0.0)
3[d]	Carbon plate	0.0% (0.0)	0.0% (0.0)	0.5% (0.0)
4[d]	Copper plate	0.0% (0.0)	0.0% (0.0)	0.0% (0.0)
5[c]	Copper wire	0.0% (0.0)	0.0% (0.0)	0.0% (0.0)
6[d, e]	Carbon coated copper plate	0.0% (0.0)	0.0% (0.0)	0.0% (0.0)

[a] Conditions for electrolysis and product range are depicted in Scheme 4. [b] Yield (see Chapter 4) calculated based on the number of electrons used for the respective cyclic methylsiloxanes with the assumption of one electron per methyl moiety with Bu_3MeN^+ as methyl source, referenced to GC-MS calibration curve. [c] Surface area of 0.009 cm². [d] Surface area of 3.2 cm², current density limited by power supply unit. [e] Exfoliation of the carbon coating in course of reaction.

5.5 Screening of SiO_2 source in presence of MeOH

For the direct electrochemical conversion of silica raw materials to cyclic methylsiloxanes, the SiO_2 source was screened (Table 5) according to GP2 in presence of 0.2 M MeOH with a platinum wire cathode (surface area of 0.009 cm^2) and a platinum gauze anode (20 mm in diameter) at room temperature without stirring. The inter-electrode gap was 2 mm, the electrolyte was THF solvent with 0.1 M Bu_4NOTf. A current density of 6.6 A/cm^2 was used with an applied charge of 0.5 *F*.

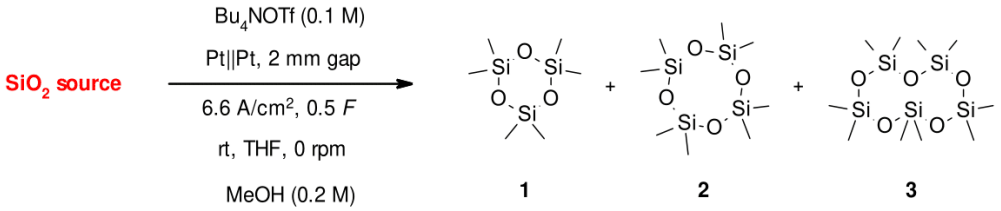

Scheme 5. Reaction conditions for the screening of SiO_2 source in presence of 0.2 M MeOH for direct electrochemical conversion of silica raw materials to cyclic methylsiloxanes.

Table 5. Results for the screening of SiO_2 source in presence of 0.2 M MeOH for direct electrochemical conversion of silica raw materials to cyclic methylsiloxanes.[a]

Entry	SiO_2 source	[%] Yield and (µmol) of 1[b]	[%] Yield and (µmol) of 2[b]	[%] Yield and (µmol) of 3[b]
1[c]	Quartz sand	0.8% (0.1)	0.6% (0.0)	0.5% (0.0)
2[d]	Quartz wool	0.8% (0.1)	0.6% (0.0)	0.5% (0.0)
3[d, e]	Fumed silica (HDK V-15)[f]	0.8% (0.1)	0.0% (0.0)	0.5% (0.0)
4[d, e]	Fumed silica (HDK H-15) [g]	1.6% (0.1)	0.6% (0.0)	0.5% (0.0)

[a] Conditions for electrolysis and product range are depicted in Scheme 5. [b] Yield (see Chapter 4) calculated based on the number of electrons used for the respective cyclic methylsiloxanes with the assumption of one electron per methyl moiety with Bu_3MeN^+ as methyl source, referenced to GC-MS calibration curve. [c] 1.0 g of substrate was used to cover the cathode. [d] 100 mg g of substrate was used to cover the cathode. [e] Formation of a colorless, opaque suspension. [f] Wacker HDK V-15: hydrophilic, amorphous fumed silica with a BET surface of 130 – 170 m^2/g. [g] Wacker HDK H-15: hydrophobic, amorphous fumed silica with a BET surface of 130 – 170 m^2/g.

5.6 Screening of applied charge in presence of MeOH

For the direct electrochemical conversion of silica raw materials to cyclic methylsiloxanes, the applied charge was screened (Table 6) according to GP2 in presence of 0.2 M MeOH with a platinum wire cathode (surface area of 0.009 cm^2) and a platinum gauze anode (20 mm in diameter) at room temperature without stirring. The inter-electrode gap was 2 mm, quartz sand (1.0 g) was used as SiO_2 source in THF solvent with 0.1 M Bu_4NOTf as supporting electrolyte. A current density of 6.6 A/cm^2 was used.

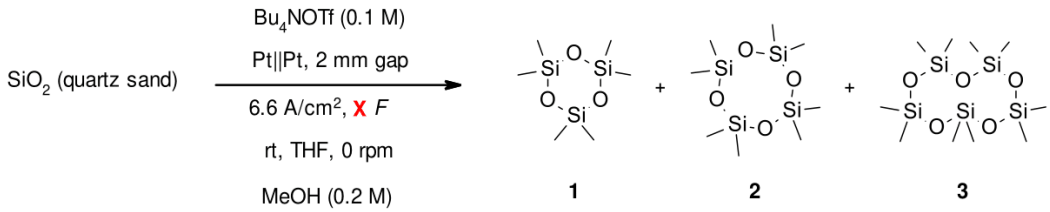

Scheme 6. Reaction conditions for the screening of applied charge in presence of 0.2 M MeOH for direct electrochemical conversion of silica raw materials to cyclic methylsiloxanes.

Table 6. Results for the screening of applied charge in presence of 0.2 M MeOH for direct electrochemical conversion of silica raw materials to cyclic methylsiloxanes.[a]

Entry	Applied charge [*F*]	[%] Yield and (µmol) of 1[b]	[%] Yield and (µmol) of 2[b]	[%] Yield and (µmol) of 3[b]
1	0.0 *F*	0.0% (0.0)	0.0% (0.0)	0.0% (0.0)
2	0.1 *F*	0.8% (0.1)	0.6% (0.0)	0.5% (0.0)
3	0.3 *F*	0.8% (0.1)	1.2% (0.0)	0.9% (0.0)
4	0.5 *F*	0.8% (0.1)	0.6% (0.0)	0.5% (0.0)
5	0.7 *F*	0.0% (0.0)	0.6% (0.0)	0.5% (0.0)
6	0.9 *F*	0.0% (0.0)	0.6% (0.0)	0.5% (0.0)

[a] Conditions for electrolysis and product range are depicted in Scheme 6. [b] Yield (see Chapter 4) calculated based on the number of electrons used for the respective cyclic methylsiloxanes with the assumption of one electron per methyl moiety with Bu_3MeN^+ as methyl source, referenced to GC-MS calibration curve.

5.7 Screening of the amount of MeOH

For the direct electrochemical conversion of silica raw materials to cyclic methylsiloxanes, the amount of MeOH was screened (Table 7) according to GP2 with a platinum wire cathode (surface area of 0.009 cm^2) and a platinum gauze anode (20 mm in diameter) at room temperature without stirring. The inter-electrode gap was 2 mm, quartz sand (1.0 g) was used as SiO_2 source in THF solvent with 0.1 M Bu_4NOTf as supporting electrolyte. A current density of 6.6 A/cm^2 was used with an applied charge of 0.3 *F*.

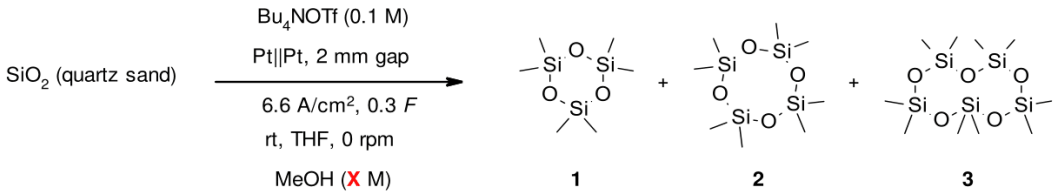

Scheme 7. Reaction conditions for the screening of the amount of MeOH for direct electrochemical conversion of silica raw materials to cyclic methylsiloxanes.

Table 7. Results for the screening of the amount of MeOH for direct electrochemical conversion of silica raw materials to cyclic methylsiloxanes.[a]

Entry	MeOH [mol/l]	[%] Yield and (µmol) of 1[b]	[%] Yield and (µmol) of 2[b]	[%] Yield and (µmol) of 3[b]
1	0.00 mol/l	2.3% (0.2)	6.3% (0.3)	5.0% (0.2)
2	0.05 mol/l	1.6% (0.1)	4.1% (0.2)	3.3% (0.1)
3	0.10 mol/l	0.8% (0.1)	2.3% (0.1)	1.9% (0.1)
4	0.20 mol/l	0.8% (0.1)	1.2% (0.0)	0.9% (0.0)
5	0.50 mol/l	0.0% (0.0)	0.0% (0.0)	0.0% (0.0)

[a] Conditions for electrolysis and product range are depicted in Scheme 7. [b] Yield (see Chapter 4) calculated based on the number of electrons used for the respective cyclic methylsiloxanes with the assumption of one electron per methyl moiety with Bu_3MeN^+ as methyl source, referenced to GC-MS calibration curve.

5.8 Screening of supporting electrolyte concentration in absence of MeOH

For the direct electrochemical conversion of silica raw materials to cyclic methylsiloxanes, the concentration of supporting electrolyte was screened (Table 8) according to GP2 in absence of MeOH with a platinum wire cathode (surface area of 0.009 cm^2) and platinum gauze anode (20 mm in diameter) at room temperature without stirring. The inter-electrode gap was 2 mm, quartz sand (1.0 g) was used as SiO_2 source in THF solvent with R_4NOTf as supporting electrolyte. A current density of 6.6 A/cm^2 was used with an applied charge of 0.3 *F*.

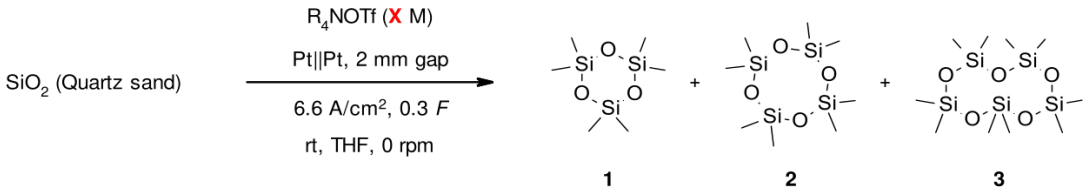

Scheme 8. Reaction conditions for the screening of supporting electrolyte concentration in absence of MeOH for direct electrochemical conversion of silica raw materials to cyclic methylsiloxanes.

Table 8. Results for the screening of supporting electrolyte concentration in absence of MeOH for direct electrochemical conversion of silica raw materials to cyclic methylsiloxanes.[a]

Entry	Amount of supporting electrolyte	[%] Yield and (µmol) of 1[b]	[%] Yield and (µmol) of 2[b]	[%] Yield and (µmol) of 3[b]
1	Bu_4NOTf (0.1 M)	2.3% (0.2)	6.3% (0.3)	5.0% (0.2)
2	Bu_4NOTf (0.2 M)	2.3% (0.3)	5.5% (0.6)	4.2% (0.4)
3	Bu_4NOTf (0.3 M)	2.6% (0.5)	5.8% (0.9)	4.3% (0.5)
4	Bu_4NOTf (0.4 M)	2.9% (0.8)	6.3% (1.4)	4.5% (0.8)
5	Bu_4NOTf (0.5 M)	1.8% (0.7)	4.1% (1.1)	2.9% (0.6)
6	Et_4NOTf (0.1 M)	0.0% (0.0)	0.0% (0.0)	0.0% (0.0)
7	NH_4OTf (0.1 M)	0.0% (0.0)	0.0% (0.0)	0.0% (0.0)

[a] Conditions for electrolysis and product range are depicted in Scheme 8. [b] Yield (see Chapter 4) calculated based on the number of electrons used for the respective cyclic methylsiloxanes with the assumption of one electron per methyl moiety with Bu_3MeN^+ as methyl source, referenced to GC-MS calibration curve.

5.9 Screening of supporting electrolyte concentration in presence of MeOH

For the direct electrochemical conversion of silica raw materials to cyclic methylsiloxanes, the concentration of supporting electrolyte was screened (Table 9) according to GP2 in presence of 0.2 M MeOH with a platinum wire cathode (surface area of 0.009 cm^2) and platinum gauze anode (20 mm in diameter) at room temperature without stirring. The inter-electrode gap was 2 mm, quartz sand (1.0 g) was used as SiO_2 source in THF solvent with Bu_4NOTf as supporting electrolyte. A current density of 6.6 A/cm^2 was used with an applied charge of 0.3 *F*.

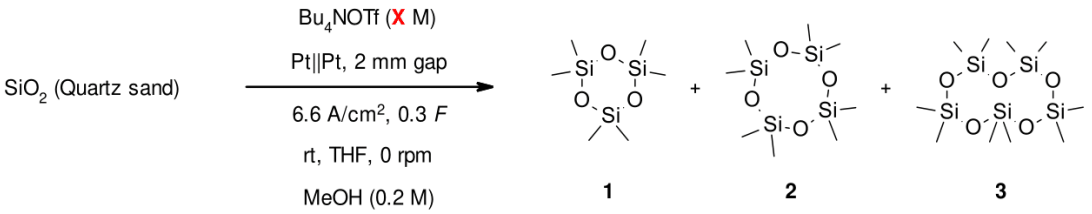

Scheme 9. Reaction conditions for the screening of supporting electrolyte concentration in presence of MeOH for direct electrochemical conversion of silica raw materials to cyclic methylsiloxanes.

Table 9. Results for the screening of supporting electrolyte concentration in presence of MeOH for direct electrochemical conversion of silica raw materials to cyclic methylsiloxanes.[a]

Entry	Amount of supporting electrolyte	[%] Yield and (µmol) of 1[b]	[%] Yield and (µmol) of 2[b]	[%] Yield and (µmol) of 3[b]
1	Bu_4NOTf (0.1 M)	0.8% (0.1)	1.2% (0.0)	0.9% (0.0)
2	Bu_4NOTf (0.2 M)	0.6% (0.1)	1.5% (0.1)	0.8% (0.1)
3	Bu_4NOTf (0.3 M)	0.6% (0.1)	1.5% (0.2)	0.9% (0.1)
4	Bu_4NOTf (0.4 M)	0.6% (0.1)	1.5% (0.3)	1.0% (0.1)
5	Bu_4NOTf (0.5 M)	0.5% (0.1)	1.2% (0.3)	0.6% (0.1)

[a] Conditions for electrolysis and product range are depicted in Scheme 9. [b] Yield (see Chapter 4) calculated based on the number of electrons used for the respective cyclic methylsiloxanes with the assumption of one electron per methyl moiety with Bu_3MeN^+ as methyl source, referenced to GC-MS calibration curve.

5.10 Screening of Bu_3MeN^+ additives in absence of MeOH

For the direct electrochemical conversion of silica raw materials to cyclic methylsiloxanes, Bu_3MeN^+ additives were screened (Table 10) according to GP2 in absence of MeOH with a platinum wire cathode (surface area of 0.009 cm^2) and platinum gauze anode (20 mm in diameter) at room temperature without stirring. The inter-electrode gap was 2 mm, quartz sand (1.0 g) was used as SiO_2 source in THF solvent with 0.1 M Bu_4NOTf as supporting electrolyte. A current density of 6.6 A/cm^2 was used with an applied charge of 0.3 *F*.

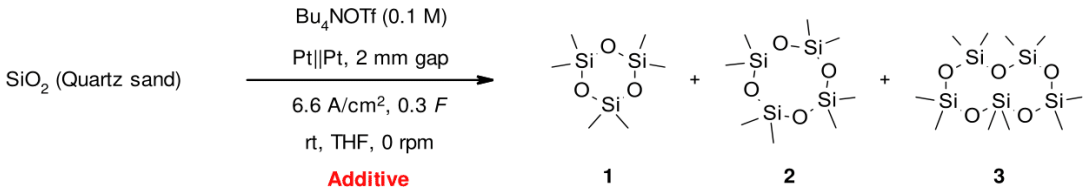

Scheme 10. Reaction conditions for the screening of Bu_3MeN^+ additives in absence of MeOH for direct electrochemical conversion of silica raw materials to cyclic methylsiloxanes.

Table 10. Results for the screening of Bu_3MeN^+ additives in absence of MeOH for direct electrochemical conversion of silica raw materials to cyclic methylsiloxanes.[a]

Entry	Additives [%][b]	[%] Yield and (µmol) of 1[c]	[%] Yield and (µmol) of 2[c]	[%] Yield and (µmol) of 3[c]
1	None	2.3% (0.2)	6.3% (0.3)	5.0% (0.2)
2	10% Bu_3MeNCl	0.8% (0.1)	2.3% (0.1)	1.9% (0.1)
3	20% Bu_3MeNCl	0.0% (0.0)	1.2% (0.0)	0.9% (0.0)
4	30% Bu_3MeNCl	0.0% (0.0)	0.0% (0.0)	0.0% (0.0)
5	10% $Bu_3MeNNTf_2$	1.6% (0.1)	4.7% (0.3)	3.7% (0.2)
6	20% $Bu_3MeNNTf_2$	1.6% (0.1)	2.9% (0.2)	2.3% (0.1)
7	30% $Bu_3MeNNTf_2$	0.8% (0.1)	1.7% (0.1)	1.4% (0.1)
8	10% Bu_3MeNSO_4Me	1.6% (0.1)	4.1% (0.2)	3.3% (0.1)
9	20% Bu_3MeNSO_4Me	0.8% (0.1)	2.3% (0.1)	1.9% (0.1)
10	30% Bu_3MeNSO_4Me	0.8% (0.1)	1.2% (0.0)	0.9% (0.0)

[a] Conditions for electrolysis and product range are depicted in Scheme 10. [b] The percentage is related to the supporting electrolyte Bu_4NOTf, OTf = ($CF_3SO_3^-$), NTf_2 = [$(CF_3SO_2)_2N]^-$). [c] Yield (see Chapter 4) calculated based on the number of electrons used for the respective cyclic methylsiloxanes with the assumption of one electron per methyl moiety with Bu_3MeN^+ as methyl source, referenced to GC-MS calibration curve.

5.11 Screening of the reaction conditions for Fenton like SiO_2 methylation

For the radial methylation of silica raw materials to cyclic methylsiloxanes, reaction conditions were screened (Table 11) according to GP4 at room temperature with stirring at 500 rpm. 3 mL DMSO was used as solvent and reagent with anhydrous $FeCl_2$ and hydrogen peroxide solution (30%) to yield cyclic methylsiloxanes. No electrical current was applied.

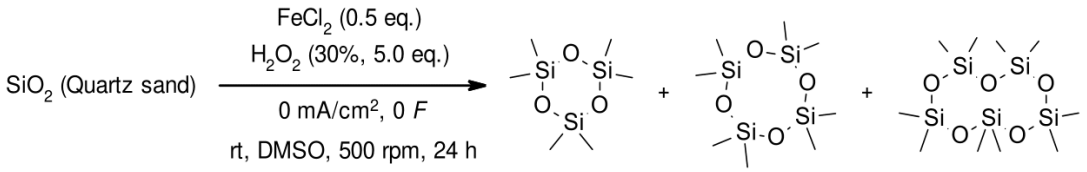

Scheme 11. Reaction conditions for the radial methylation of silica raw materials to cyclic methylsiloxanes.

Table 11. Results for the radial methylation of silica raw materials to cyclic methylsiloxanes.[a]

Entry	Deviation of standard conditions	[%] Yield and (µmol) of 1[b]	[%] Yield and (µmol) of 2[b]	[%] Yield and (µmol) of 3[b]
1	No Fe(II)	0.0% (0.0)	0.0% (0.0)	0.0% (0.0)
2	No SiO_2	0.0% (0.0)	0.0% (0.0)	0.0% (0.0)
3	No H_2O_2	0.0% (0.0)	0.0% (0.0)	0.0% (0.0)
4	O_2, moisture	0.0% (0.0)	0.0% (0.0)	0.0% (0.0)
5	$FeCl_2$ (0.1 eq)	0.0% (0.0)	0.1% (0.7)	0.1% (0.5)
6	$FeCl_2$ (0.5 eq)	0.1% (0.9)	0.3% (2.1)	0.1% (0.5)
7	$FeCl_2$ (1.0 eq)	0.1% (0.9)	0.2% (1.4)	0.1% (0.5)
8	50 °C	0.1% (0.9)	0.3% (2.1)	0.1% (0.5)
9	Fumed silica[c]	0.2% (1.8)	0.8% (5.3)	0.2% (1.1)
10	TEMPO added[d]	0.0% (0.0)	0.0% (0.0)	0.0% (0.0)

[a] Reaction conditions and product range are depicted in Scheme 11. [b] Quantification of the yield was referenced to GC-MS calibration curve. [c] Wacker HDK H-15. [d] TEMPO = (2,2,6,6-Tetramethylpiperidin-1-yl)oxyl, (5 mmol, 781 mg, 5 eq.).

5.12 Screening of the equilibration of cyclic methylsiloxanes via catalytic conditions

For the equilibration of cyclic methylsiloxanes, catalytic conditions of the electrolyte, platinum electrode surface and temperature were screened (Table 12) according to GP3 in presence of platinum electrodes at different temperatures without stirring. The inter-electrode gap was 5 mm, cyclic methylsiloxane (2.0 mmol, 1.0 eq.) was used in THF solvent with 0.1 M Bu_4NOTf supporting electrolyte. No electrical current was applied.

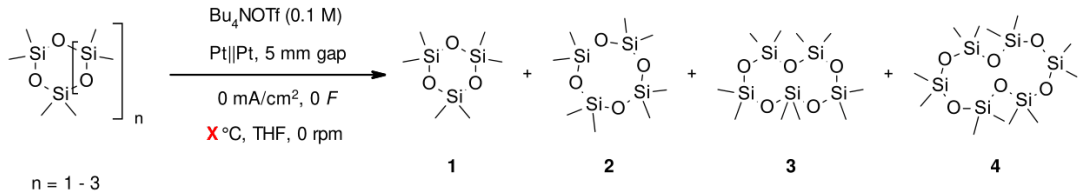

Scheme 12. Reaction conditions for the equilibration of cyclic methylsiloxanes via catalytic conditions.

Table 12. Results for the equilibration of cyclic methylsiloxanes via catalytic conditions.[a]

Entry	Time [h] / Temp. [°C]	Educt species	[%] Yield and (mmol) of 1[b]	[%] Yield and (mmol) of 2[b]	[%] Yield and (mmol) of 3[b]	[%] Yield and (mmol) of 4[b]
1	0.5 h / 25 °C	D_3	100% (2.0)	0% (0.0)	0% (0.0)	0% (0.0)
2	1.0 h / 25 °C	D_3	100% (2.0)	0% (0.0)	0% (0.0)	0% (0.0)
3	5.0 h / 25 °C	D_3	100% (2.0)	0% (0.0)	0% (0.0)	0% (0.0)
4	1.0 h / 25 °C	D_4	0% (0.0)	100% (2.0)	0% (0.0)	0% (0.0)
5	1.0 h / 25 °C	D_5	0% (0.0)	0% (0.0)	100% (2.0)	0% (0.0)
6[c]	1.0 h / 66 °C	D_3	100% (2.0)	0% (0.0)	0% (0.0)	0% (0.0)
7[c]	1.0 h / 66 °C	D_4	0% (0.0)	100% (2.0)	0% (0.0)	0% (0.0)
8[c]	1.0 h / 66 °C	D_5	0% (0.0)	0% (0.0)	100% (2.0)	0% (0.0)

[a] Reaction conditions and product range are depicted in Scheme 12. [b] Quantification of the yield was performed by ^{29}Si NMR relative to tetramethylsilane as internal standard. [c] Temperature was limited due to boiling point of the electrolyte.

5.13 Screening of the equilibration of cyclic methylsiloxanes via peroxidic species

For the equilibration of cyclic methylsiloxanes, peroxidic species were used to evaluate the influence of the decomposition of OTf^- supporting electrolyte anion via a peroxidic intermediate and subsequent reaction with cyclic methylsiloxanes. Peroxidic species were screened (Table 13) according to GP3 in presence of platinum electrodes at room temperature for different durations without stirring. The inter-electrode gap was 5 mm, hexamethylcyclotrisiloxane (445 mg, 2.0 mmol, 1.0 eq.) was used in THF solvent with 0.1 M Bu_4NOTf supporting electrolyte and peroxide (2.0 mmol, 1.0 eq.). No electrical current was applied.

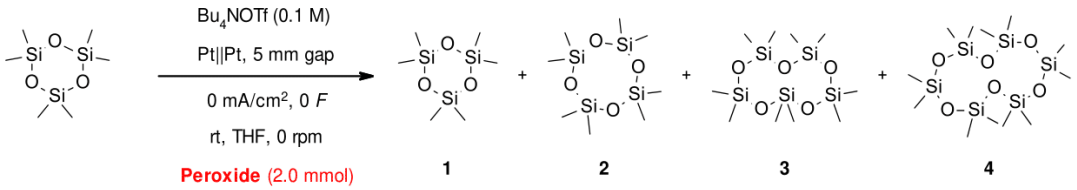

Scheme 13. Reaction conditions for the equilibration of hexamethylcyclotrisiloxane via peroxidic species.

Table 13. Results for the equilibration of hexamethylcyclotrisiloxane via peroxidic species.[a]

Entry	Peroxide / Time [h]	[%] Yield and (mmol) of 1[b]	[%] Yield and (mmol) of 2[b]	[%] Yield and (mmol) of 3[b]	[%] Yield and (mmol) of 4[b]
1	H_2O_2 (30%) / 1.0 h	98% (2.0)	1% (0.0)	0% (0.0)	1% (0.0)
2	H_2O_2 (30%) / 12 h	97% (2.0)	2% (0.0)	0% (0.0)	1% (0.0)
3	H_2O_2 (30%) / 24 h	95% (1.9)	3% (0.1)	0% (0.0)	2% (0.0)
4	$K_2S_2O_8$ / 1.0 h	99% (2.0)	0% (0.0)	0% (0.0)	1% (0.0)
5[c]	*t*BuOOH / 1.0 h	99% (2.0)	0% (0.0)	0% (0.0)	1% (0.0)

[a] Reaction conditions and product range are depicted in Scheme 13. [b] Quantification of the yield was performed by ^{29}Si NMR relative to tetramethylsilane as internal standard. [c] *t*BuOOH = *tert*-butyl hydroperoxide (anhydrous solution in decane).

5.14 Screening of the electrochemical equilibration of cyclic methylsiloxanes

For the electrochemical equilibration of cyclic methylsiloxanes current density and applied charge were screened (Table 14) according to GP3 with platinum electrodes at room temperature without stirring. The inter-electrode gap was 5 mm, cyclic methylsiloxanes (2.0 mmol, 1.0 eq.) were used in THF solvent with 0.1 M Bu_4NOTf supporting electrolyte.

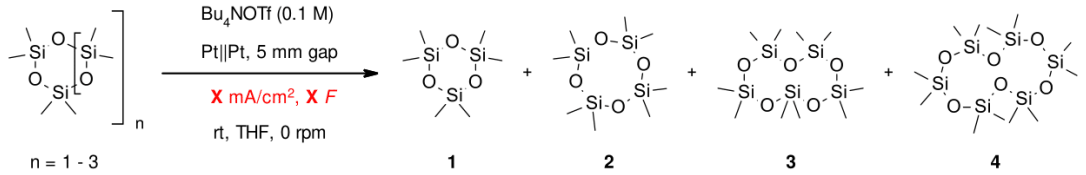

Scheme 14. Reaction conditions for the electrochemical equilibration of cyclic methylsiloxanes.

Table 14. Results for the electrochemical equilibration of cyclic methylsiloxanes.[a]

Entry	Current density [mA/cm²]	Applied charge [*F*]	Educt species	[%] Yield and (mmol) of 1[b]	[%] Yield and (mmol) of 2[b]	[%] Yield and (mmol) of 3[b]	[%] Yield and (mmol) of 4[b]
1	10 mA/cm²	0.2 *F*	D_3	46% (0.9)	15% (0.3)	8% (0.2)	31% (0.6)
2	10 mA/cm²	0.5 *F*	D_3	34% (0.7)	21% (0.4)	10% (0.2)	35% (0.7)
3	10 mA/cm²	1.0 *F*	D_3	3% (0.1)	39% (0.8)	12% (0.2)	46% (0.9)
4	10 mA/cm²	2.0 *F*	D_3	1% (0.0)	40% (0.8)	12% (0.2)	47% (0.9)
5	20 mA/cm²	1.0 *F*	D_3	2% (0.0)	42% (0.8)	13% (0.3)	43% (0.9)
6	35 mA/cm²	1.0 *F*	D_3	2% (0.0)	46% (0.9)	11% (0.2)	41% (0.8)
7	10 mA/cm²	0.2 *F*	D_4	0% (0.0)	98% (2.0)	2% (0.0)	0% (0.0)
8	10 mA/cm²	1.0 *F*	D_4	2% (0.2)	94% (1.9)	4% (0.1)	0% (0.0)
9	10 mA/cm²	2.0 *F*	D_4	5% (0.1)	87% (1.7)	8% (0.2)	0% (0.0)
10	20 mA/cm²	1.0 *F*	D_4	5% (0.1)	88% (1.8)	7% (0.1)	0% (0.0)
11	35 mA/cm²	1.0 *F*	D_4	6% (0.1)	86% (1.7)	8% (0.2)	0% (0.0)
12	10 mA/cm²	0.2 *F*	D_5	0% (0.0)	7% (0.1)	93% (1.9)	0% (0.0)
13	10 mA/cm²	1.0 *F*	D_5	0% (0.0)	16% (0.3)	84% (1.7)	0% (0.0)
14	10 mA/cm²	2.0 *F*	D_5	0% (0.0)	21% (0.4)	79% (1.6)	0% (0.0)
15	20 mA/cm²	1.0 *F*	D_5	0% (0.0)	26% (0.5)	74% (1.5)	0% (0.0)

16	35 mA/cm^2	1.0 *F*	D_5	0% (0.0)	34% (0.7)	66% (1.3)	0% (0.0)

[a] Conditions for electrolysis and product range are depicted in Scheme 14. [b] Quantification of the yield was performed by ^{29}Si NMR relative to tetramethylsilane as internal standard.

5.15 Screening of the hydrolysis of dimethoxydimethylsilane (DMDMS)

For the hydrolysis of dimethoxydimethylsilane (DMDMS) the amount of water was screened (Table 15) according to GP3 in presence of platinum electrodes at room temperature without stirring. The inter-electrode gap was 5 mm, dimethoxydimethylsilane (278 µL, 2.0 mmol, 1.0 eq.) was used in THF solvent with 0.1 M Bu_4NOTf supporting electrolyte. No electrical current was applied.

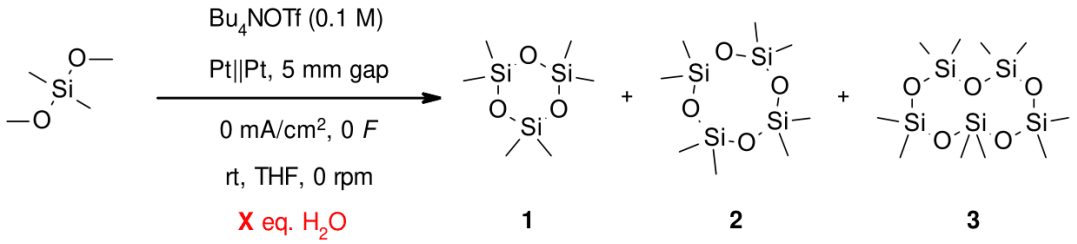

Scheme 15. Reaction conditions for the hydrolysis of dimethoxydimethylsilane.

Table 15. Results for the hydrolysis of dimethoxydimethylsilane.[a]

Entry	Time [h] / Amount of H_2O (eq.)	[%] Yield and (µmol) of 1[b]	[%] Yield and (µmol) of 2[b]	[%] Yield and (µmol) of 3[b]
1	1.0 h / 1.0 eq.	0% (0.0)	0% (0.0)	0% (0.0)
2	6.0 h / 1.0 eq.	0% (0.0)	0% (0.0)	0% (0.0)
3	24 h / 1.0 eq.	0% (0.0)	0% (0.0)	0% (0.0)
4	24 h / 2.0 eq.	0% (0.0)	0% (0.0)	0% (0.0)
5	24 h / 5.0 eq.	0% (0.0)	0% (0.0)	0% (0.0)
6	24 h / 10 eq.	0% (0.0)	0% (0.0)	0% (0.0)

[a] Reaction conditions and product range are depicted in Scheme 15. [b] Quantification of the yield was performed by ^{29}Si NMR relative to tetramethylsilane as internal standard.

6 Cyclic voltammetry data

6.1 Reduction potential of methyl sources and derivatives

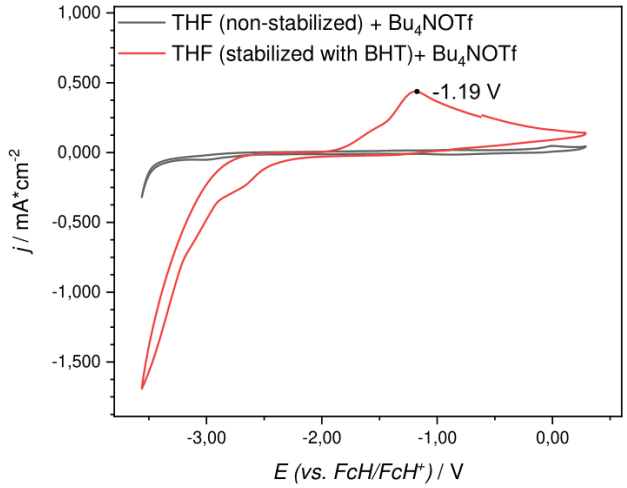

Figure 5. Cyclic voltammogram of the used electrolyte with Bu_4NOTf and THF non-stabilized (black) and stabilized by butylated hydroxytoluene (red). W.E. Pt (A = 8.0 mm²), *v* = 0.2 V/s. Peak potential of butylated hydroxytoluene: −1.19 V vs. FcH/FcH^+.

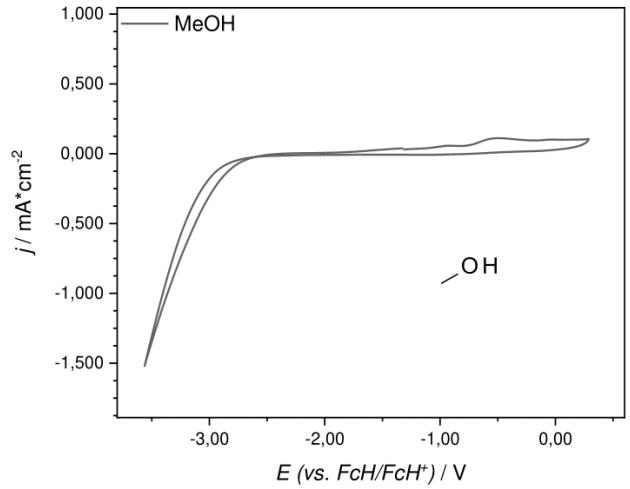

Figure 6. Cyclic voltammogram of 40 mM methanol in 0.1 M Bu_4NOTf and THF (non-stabilized). W.E. Pt (A = 8.0 mm²), *v* = 0.2 V/s. No peak potential of methanol in the range of cathodic reduction.

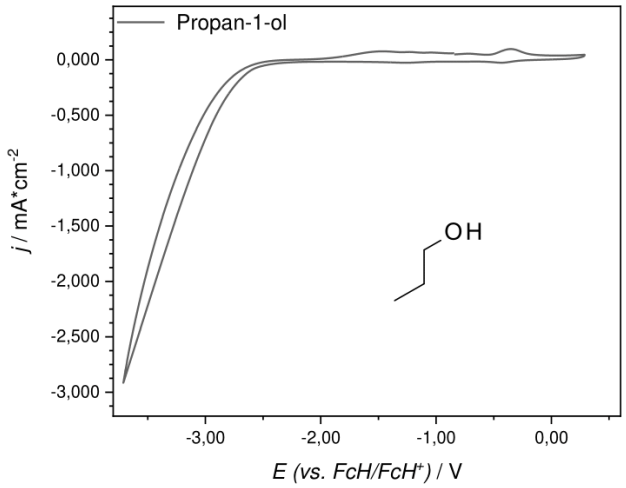

Figure 7. Cyclic voltammogram of 40 mM propan-1-ol in 0.1 M Bu_4NOTf and THF (non-stabilized). W.E. Pt (A = 8.0 mm²), *v* = 0.2 V/s. No peak potential of propan-1-ol in the range of cathodic reduction.

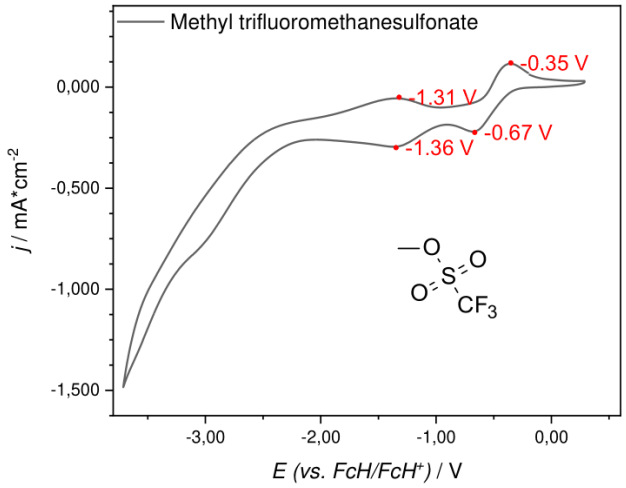

Figure 8. Cyclic voltammogram of 40 mM methyl trifluoromethanesulfonate in 0.1 M Bu_4NOTf and THF (non-stabilized). W.E. Pt (A = 8.0 mm²), *v* = 0.2 V/s. Peak potentials of methyl trifluoromethanesulfonate: −1.31 V vs. FcH/FcH^+, −0.35 V vs. FcH/FcH^+, −0.67 V vs. FcH/FcH^+ and −1.36 V vs. FcH/FcH^+.

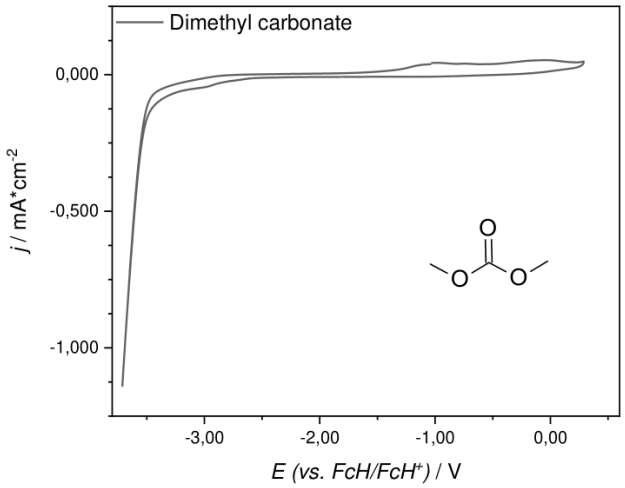

Figure 9. Cyclic voltammogram of 40 mM dimethyl carbonate in 0.1 M Bu_4NOTf and THF (non-stabilized). W.E. Pt (A = 8.0 mm²), *v* = 0.2 V/s. No peak potential of dimethyl carbonate in the range of cathodic reduction.

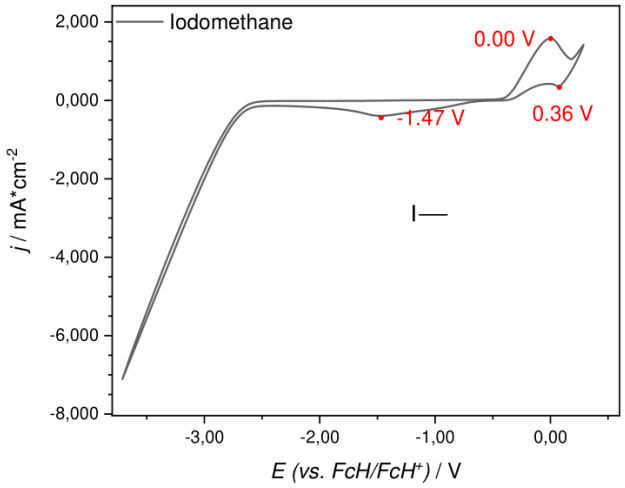

Figure 10. Cyclic voltammogram of 40 mM iodomethane in 0.1 M Bu_4NOTf and THF (non-stabilized). W.E. Pt (A = 8.0 mm²), *v* = 0.2 V/s. Peak potentials of iodomethane: 0.00 V vs. FcH/FcH^+, 0.36 V vs. FcH/FcH^+ and −1.47 V vs. FcH/FcH^+.

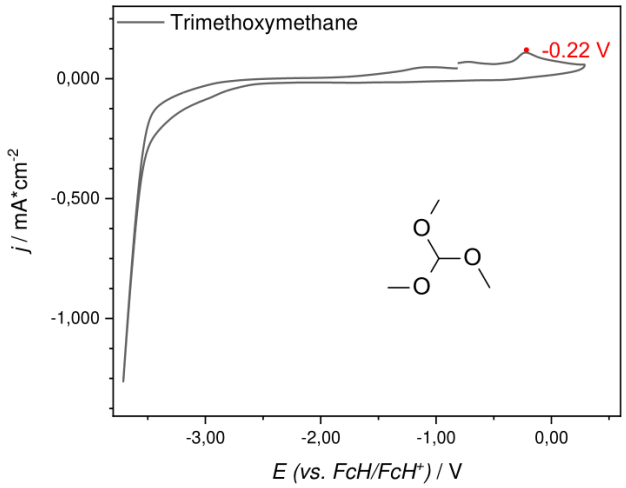

Figure 11. Cyclic voltammogram of 40 mM trimethoxymethane in 0.1 M Bu_4NOTf and THF (non-stabilized). W.E. Pt (A = 8.0 mm²), *v* = 0.2 V/s. Peak potentials of trimethoxymethane: −0.22 V vs. FcH/FcH^+.

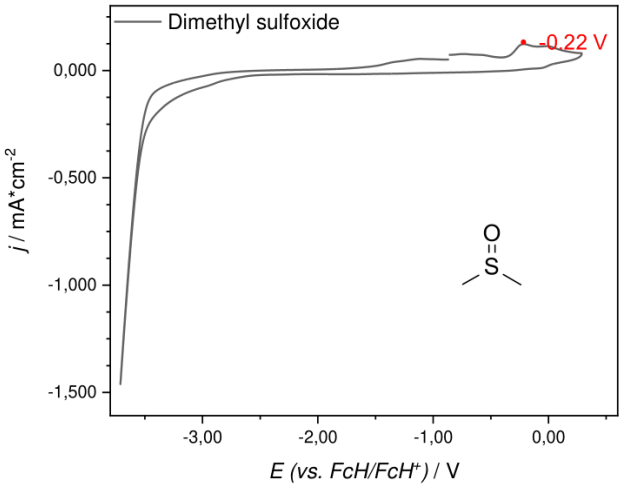

Figure 12. Cyclic voltammogram of 40 mM dimethyl sulfoxide in 0.1 M Bu_4NOTf and THF (non-stabilized). W.E. Pt (A = 8.0 mm²), *v* = 0.2 V/s. Peak potentials of dimethyl sulfoxide: −0.22 V vs. FcH/FcH^+.

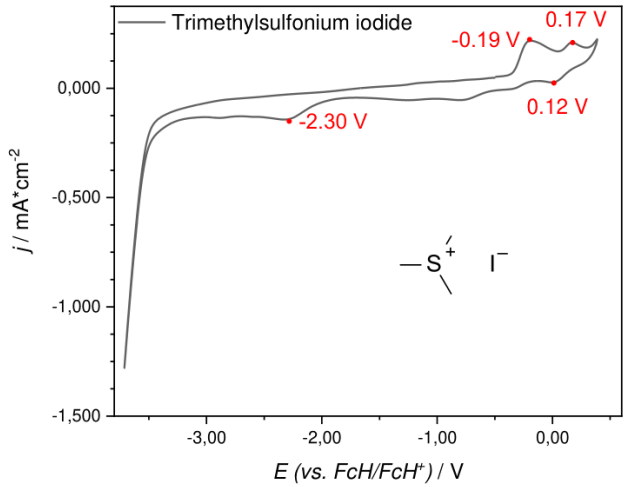

Figure 13. Cyclic voltammogram of 40 mM trimethylsulfonium iodide in 0.1 M Bu_4NOTf and THF (non-stabilized). W.E. Pt (A = 8.0 mm²), *v* = 0.2 V/s. Peak potentials of trimethylsulfonium iodide: −0.19 V vs. FcH/FcH^+, 0.17 V vs. FcH/FcH^+,0.12 V vs. FcH/FcH^+ and −2.30 V vs. FcH/FcH^+.

6.2 Reduction potential of (cyclic) siloxanes

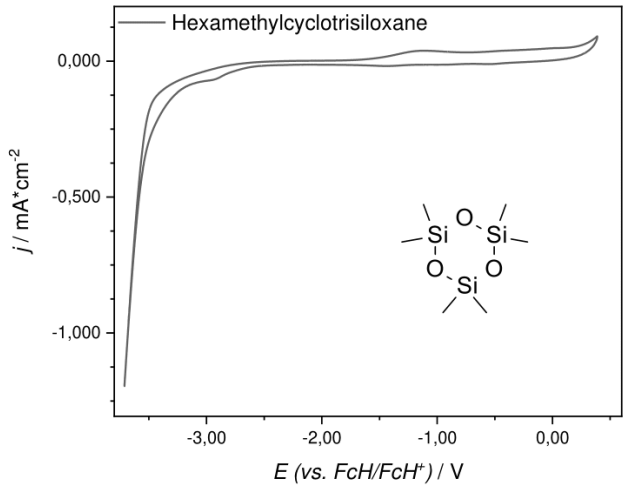

Figure 14. Cyclic voltammogram of 40 mM hexamethylcyclotrisiloxane (D_3) in 0.1 M Bu_4NOTf and THF (non-stabilized). W.E. Pt (A = 8.0 mm²), *v* = 0.2 V/s. No peak potential of hexamethylcyclotrisiloxane in the range of cathodic reduction.

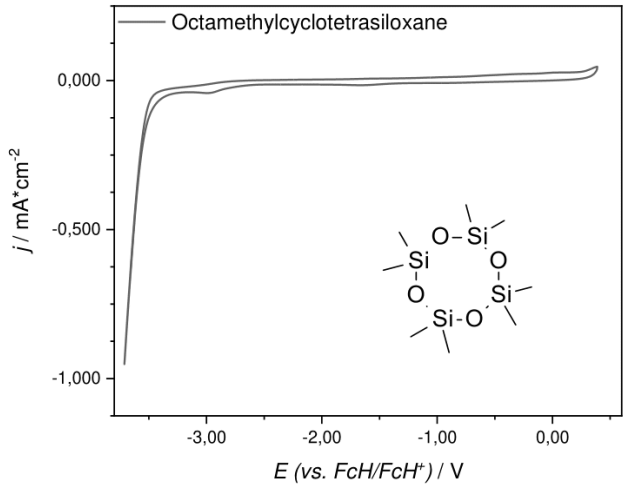

Figure 15. Cyclic voltammogram of 40 mM octamethylcyclotetrasiloxane (D_4) in 0.1 M Bu_4NOTf and THF (non-stabilized). W.E. Pt (A = 8.0 mm²), *v* = 0.2 V/s. No peak potential of octamethylcyclotetrasiloxane in the range of cathodic reduction.

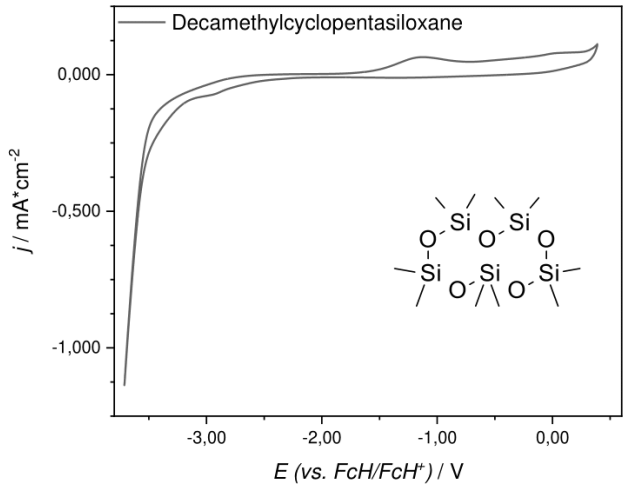

Figure 16. Cyclic voltammogram of 40 mM decamethylcyclopentasiloxane (D_5) in 0.1 M Bu_4NOTf and THF (non-stabilized). W.E. Pt (A = 8.0 mm²), *v* = 0.2 V/s. No peak potential of decamethylcyclopentasiloxane in the range of cathodic reduction.

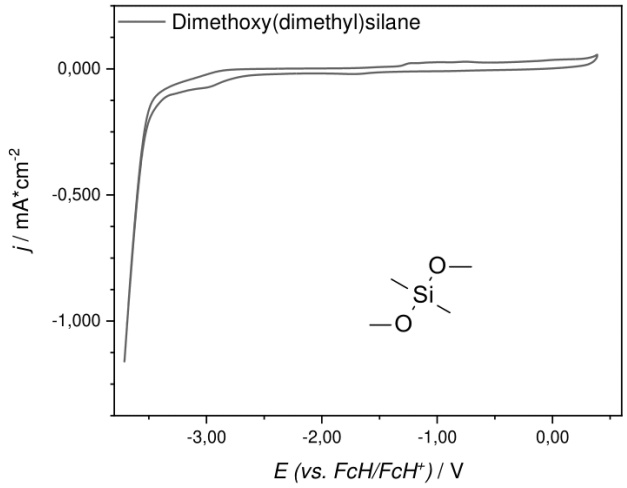

Figure 17. Cyclic voltammogram of 40 mM dimethoxy(dimethyl)silane in 0.1 M Bu_4NOTf and THF (non-stabilized). W.E. Pt (A = 8.0 mm²), *v* = 0.2 V/s. No peak potential of dimethoxy(dimethyl)silane in the range of cathodic reduction.

7 Product Characterization

7.1 Hexamethylcyclotrisiloxane (D_3) (1)

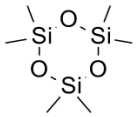

1

^{1}H NMR (500 MHz, CD_2Cl_2): δ [ppm] = 0.17 (s, 18H).
^{13}C NMR (125 MHz, CD_2Cl_2): δ [ppm] = 1.1.
^{29}Si NMR (100 MHz, CD_2Cl_2): δ [ppm] = −8.9.
MS m/z = 207 $[M-CH_3]^+$
Data are in agreement with literature.[1–5]

7.2 Octamethylcyclotetrasiloxane (D_4) (2)

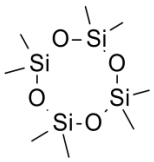

2

^{1}H NMR (500 MHz, CD_2Cl_2): δ [ppm] = 0.11 (s, 24H)
^{13}C NMR (125 MHz, CD_2Cl_2): δ [ppm] = 0.9.
^{29}Si NMR (100 MHz, CD_2Cl_2): δ [ppm] = −19.2.
MS m/z = 281 $[M-CH_3]^+$
Data are in agreement with literature.[1–5]

7.3 Decamethylcyclopentasiloxane (D_5) (3)

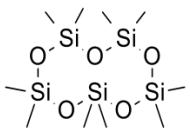

3

^{1}H NMR (500 MHz, CD_2Cl_2): δ [ppm] = 0.10 (s, 30H).
^{13}C NMR (125 MHz, CD_2Cl_2): δ [ppm] = 1.0.
^{29}Si NMR (100 MHz, CD_2Cl_2): δ [ppm] = −21.7.
MS m/z = 355 $[M-CH_3]^+$
Data are in agreement with literature.[3,4,6]

7.4 Dodecamethylcyclohexasiloxane (D_6) (4)

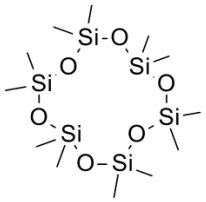

4

^{1}H NMR (500 MHz, CD_2Cl_2): δ [ppm] = 0.10 (s, 36H).
^{13}C NMR (125 MHz, CD_2Cl_2): δ [ppm] = 1.1.
^{29}Si NMR (100 MHz, CD_2Cl_2): δ [ppm] = −22.3.
MS m/z = 429 $[M]^+$
Data are in agreement with literature.[3,4]

7.5 Octane (5)

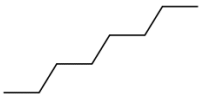

5

^{1}H NMR (500 MHz, CD_2Cl_2): δ [ppm] = 1.22 – 1.42 (m, 12H), 0.86 – 0.97 (m, 6H).
^{13}C NMR (125 MHz, CD_2Cl_2): δ [ppm] = 32.6, 30.0, 23.4, 14.5.
MS m/z = 114 $[M]^+$
Data are in agreement with literature.[7]

7.6 Tributylamine (6)

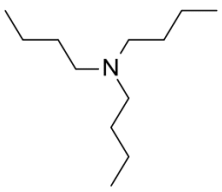

6

^{1}H NMR (500 MHz, CD_2Cl_2): δ [ppm] = 2.32 – 2.42 (m, 2H), 1.36 – 1.48 (m, 2H), 1.24 – 1.36 (m, 2H), 0.92 (t, *J* = 7.3 Hz 3H).
^{13}C NMR (125 MHz, CD_2Cl_2): δ [ppm] = 54.5, 30.1, 21.2, 14.4.
MS m/z = 185 $[M]^+$
Data are in agreement with literature.[8]

7.7 Dimethyl sulfone (7)

7

^{1}H NMR (500 MHz, CD_2Cl_2): δ [ppm] = 2.94 (s, 6H).
^{13}C NMR (125 MHz, CD_2Cl_2): δ [ppm] = 42.9.
MS m/z = 94 $[M]^+$
Data are in agreement with literature.[9]

7.8 Butane (8)

8

Butane was referenced to authentic samples by GC and GC-MS.
MS m/z = 58 $[M]^+$
Data are in agreement with literature.[10]

8 NMR Spectra

^{29}Si NMR spectrum of the crude reaction mixture after the electrochemical conversion according to GP2.

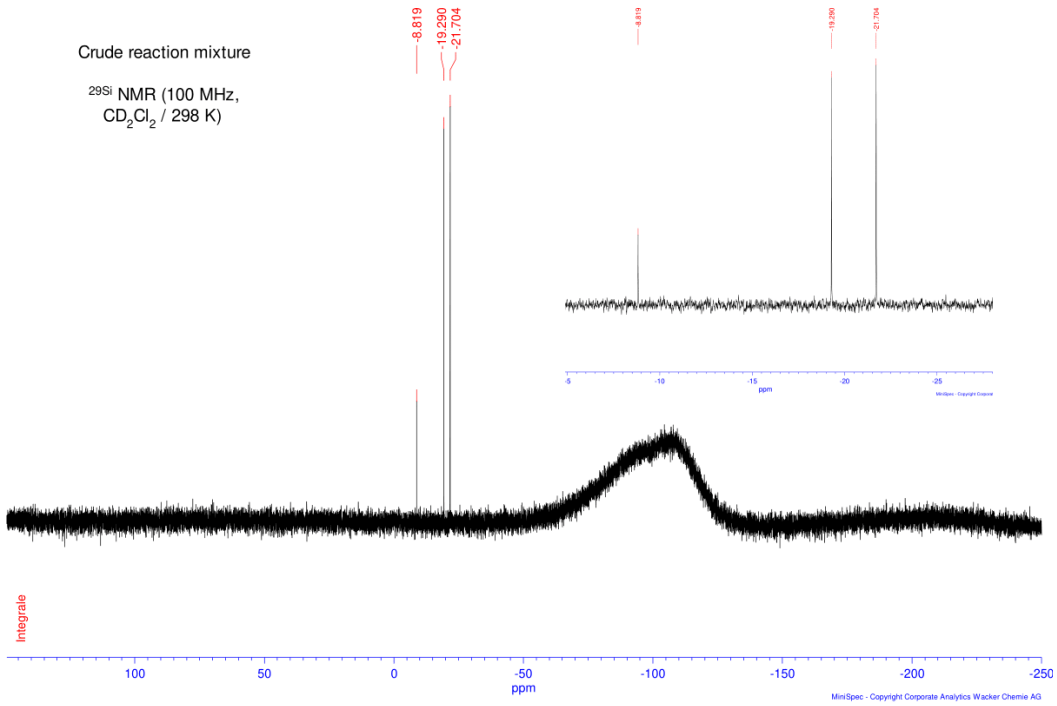

8.1 NMR Spectra of all isolated compounds

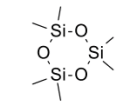

^{1}H NMR (500 MHz, CD_2Cl_2 / 298 K): **1**

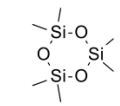

^{13}C NMR (125 MHz, CD_2Cl_2 / 298 K): **1**

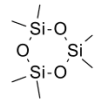

^{29}Si NMR (100 MHz, CD_2Cl_2 / 298 K): **1**

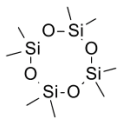

^{1}H NMR (500 MHz, CD_2Cl_2 / 298 K): **2**

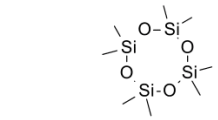

^{13}C NMR (125 MHz, CD_2Cl_2 / 298 K): **2**

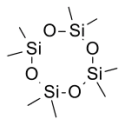

^{29}Si NMR (100 MHz, CD_2Cl_2 / 298 K): **2**

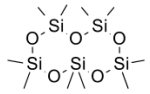

^{1}H NMR (500 MHz, CD_2Cl_2 / 298 K): **3**

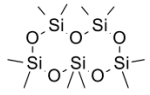

^{13}C NMR (125 MHz, CD_2Cl_2 / 298 K): **3**

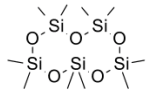

^{29}Si NMR (100 MHz, CD_2Cl_2 / 298 K): **3**

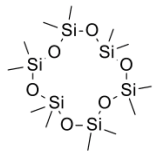

^{1}H NMR (500 MHz, CD_2Cl_2 / 298 K): **4**

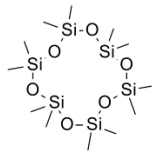

^{13}C NMR (125 MHz, CD_2Cl_2 / 298 K): **4**

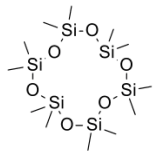

^{29}Si NMR (100 MHz, CD_2Cl_2 / 298 K): **4**

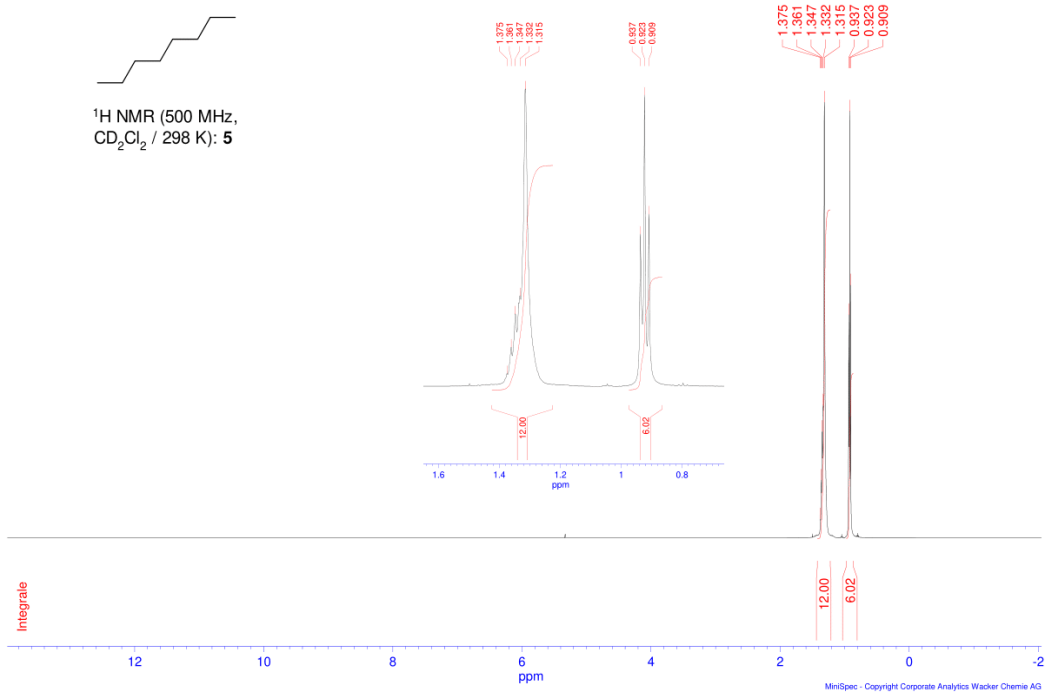

^{1}H NMR (500 MHz, CD_2Cl_2 / 298 K): **5**

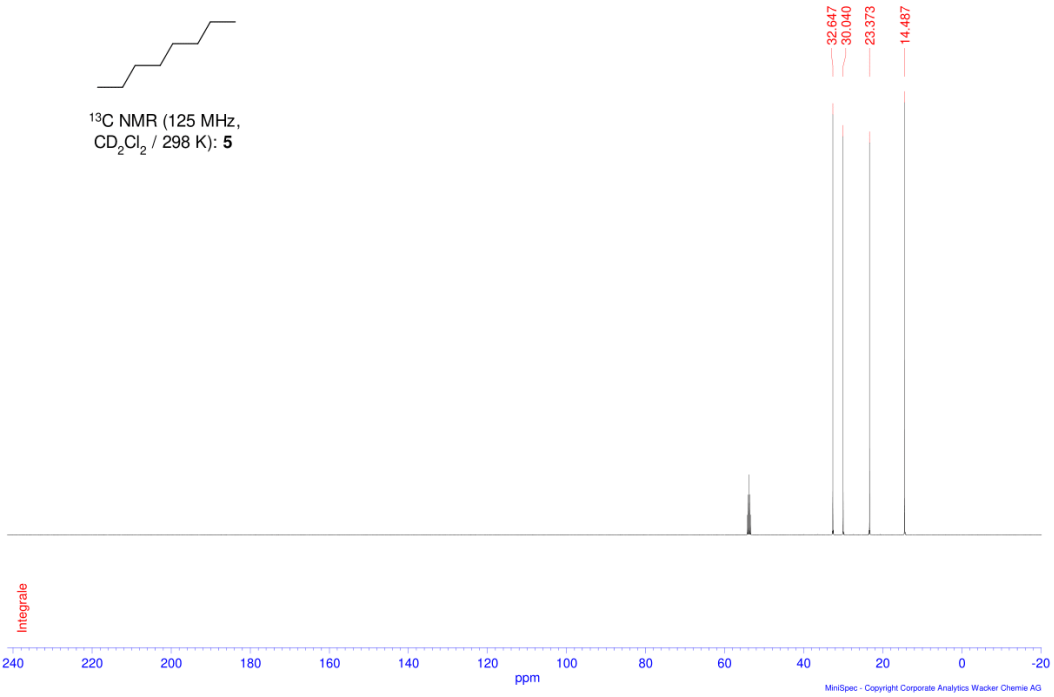

^{13}C NMR (125 MHz, CD_2Cl_2 / 298 K): **5**

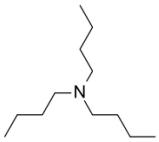

^{1}H NMR (500 MHz, CD_2Cl_2 / 298 K): **6**

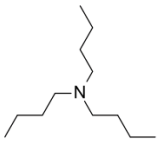

^{13}C NMR (125 MHz, CD_2Cl_2 / 298 K): **6**

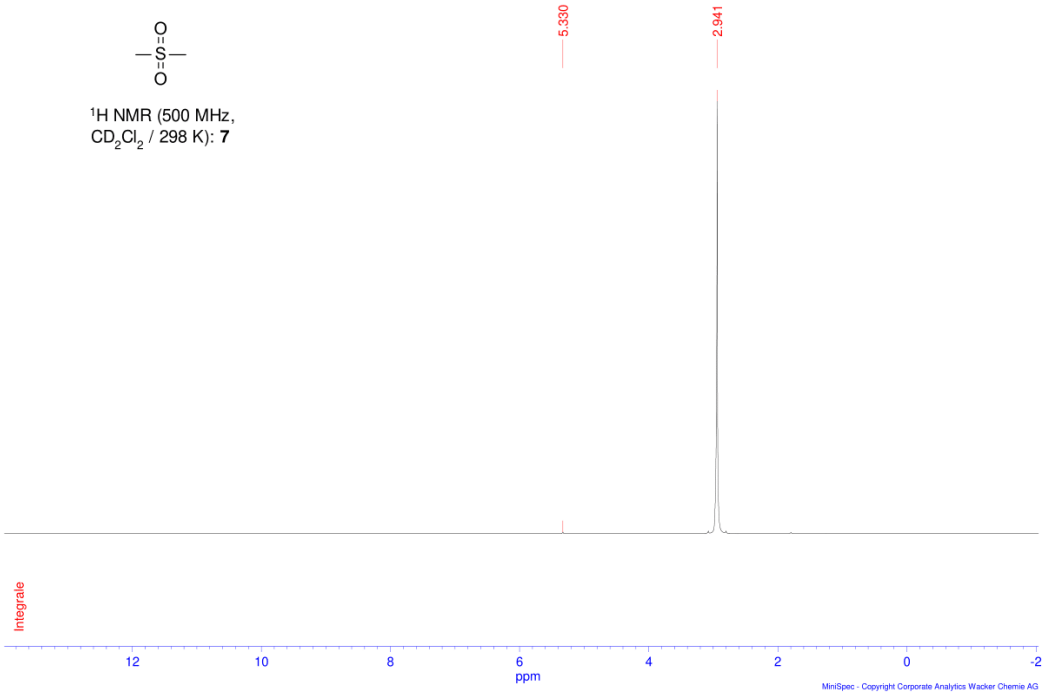

^{1}H NMR (500 MHz, CD_2Cl_2 / 298 K): **7**

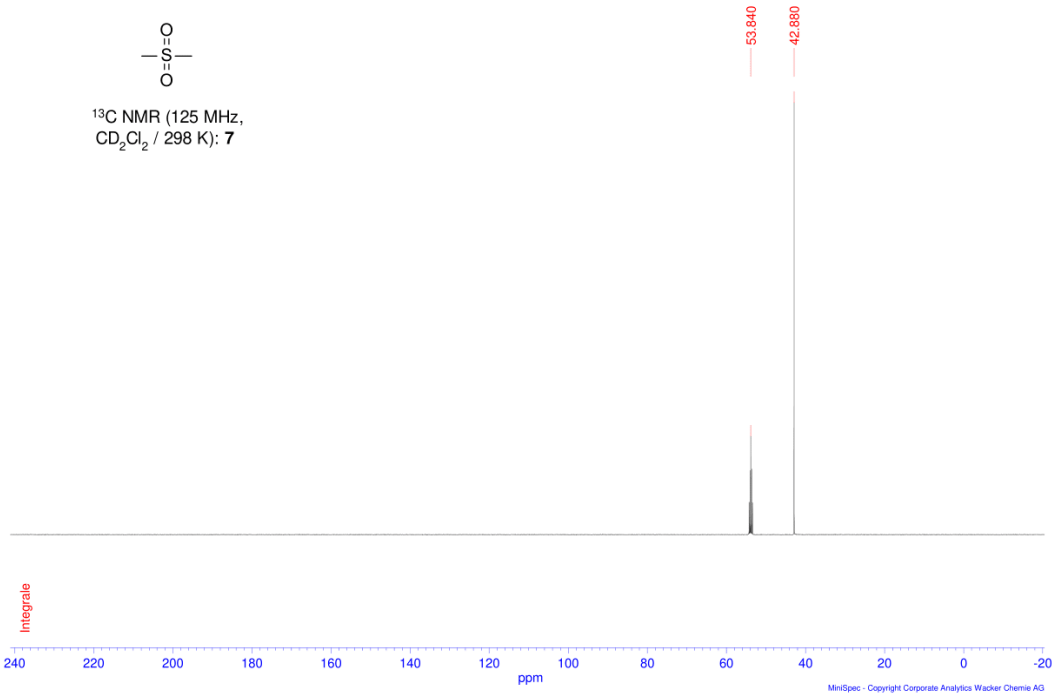

^{13}C NMR (125 MHz, CD_2Cl_2 / 298 K): **7**

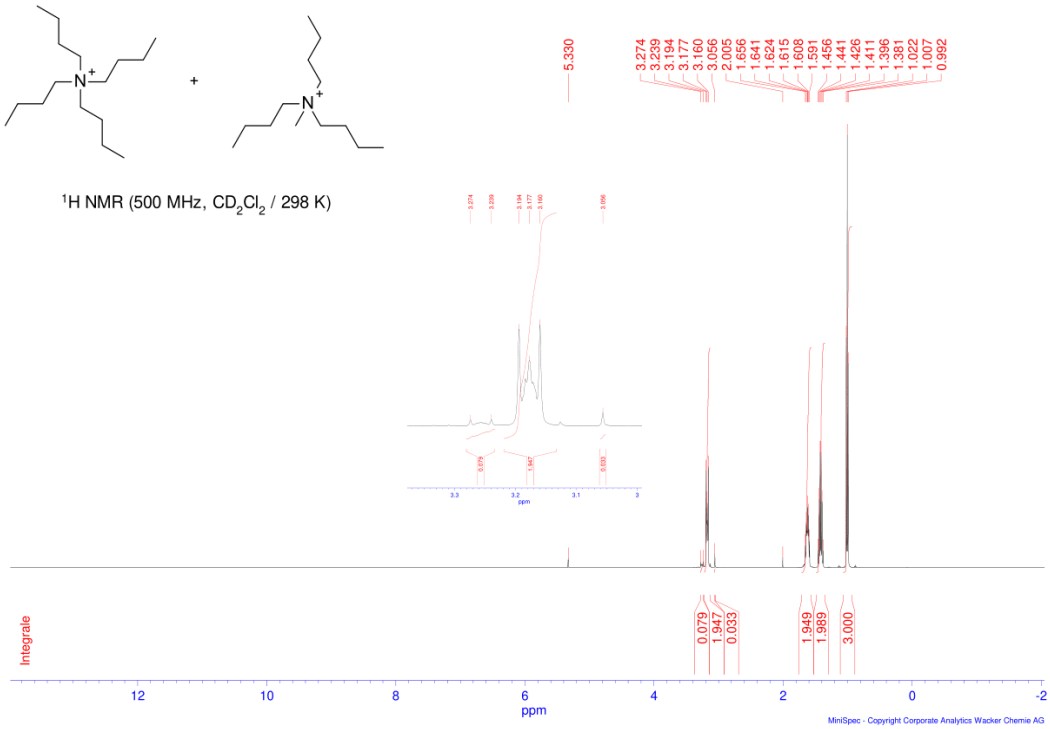

^{1}H NMR (500 MHz, CD_2Cl_2 / 298 K)

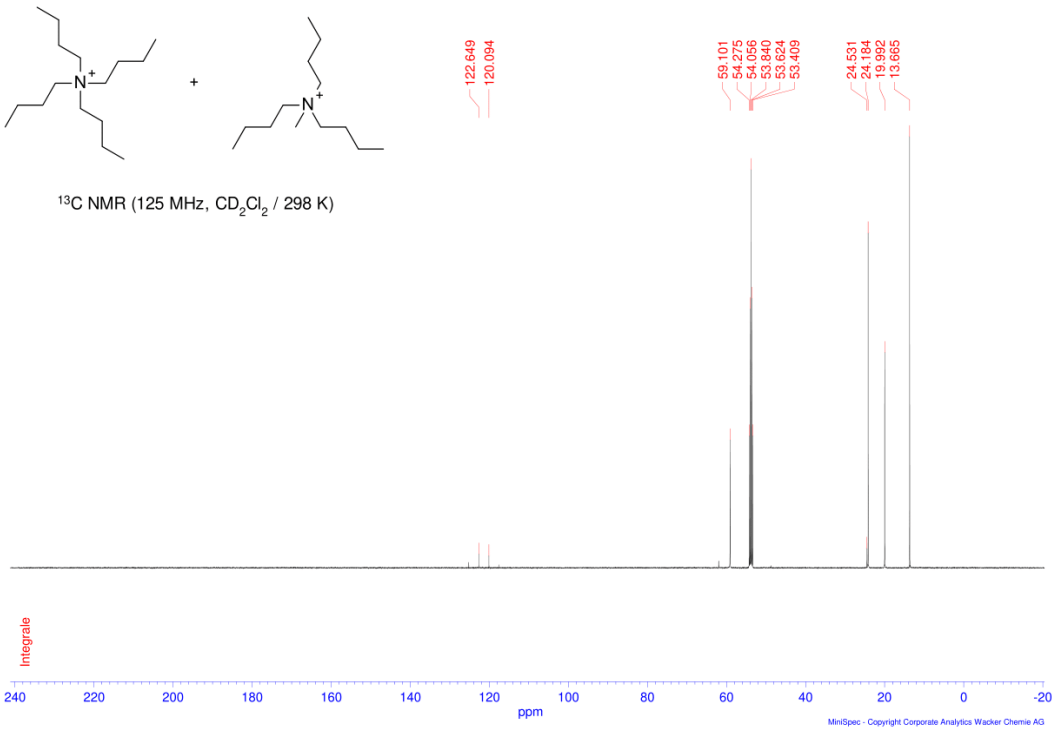

^{13}C NMR (125 MHz, CD_2Cl_2 / 298 K)

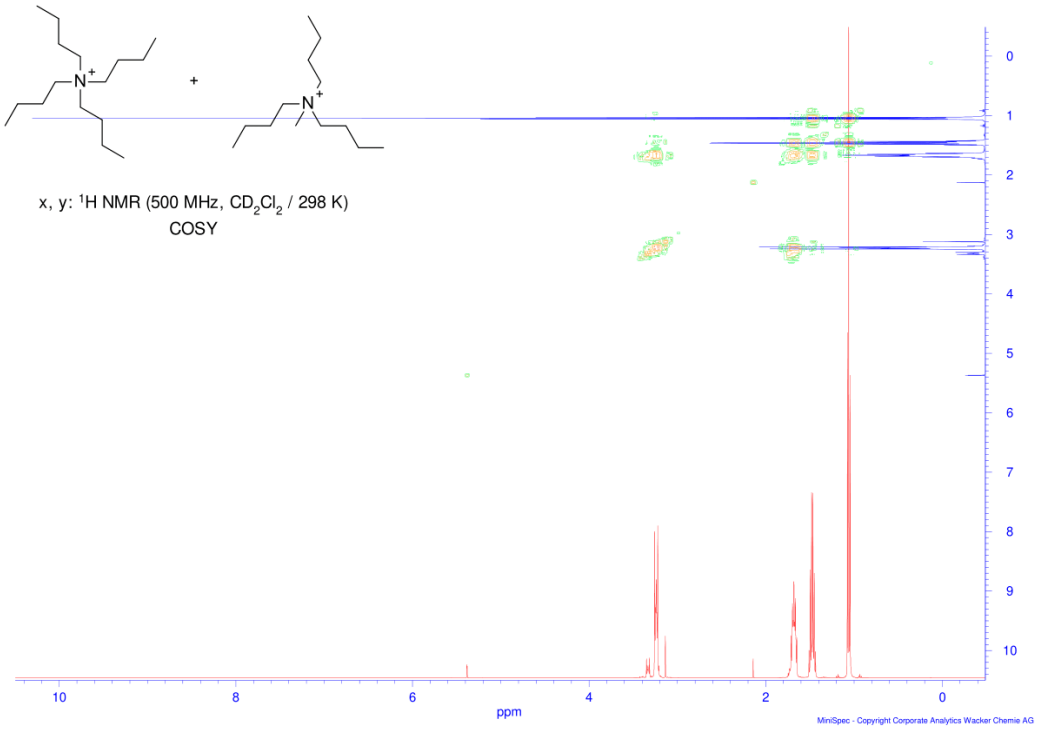
x, y: ¹H NMR (500 MHz, CD_2Cl_2 / 298 K)
COSY
ppm
MiniSpec - Copyright Corporate Analytics Wacker Chemie AG

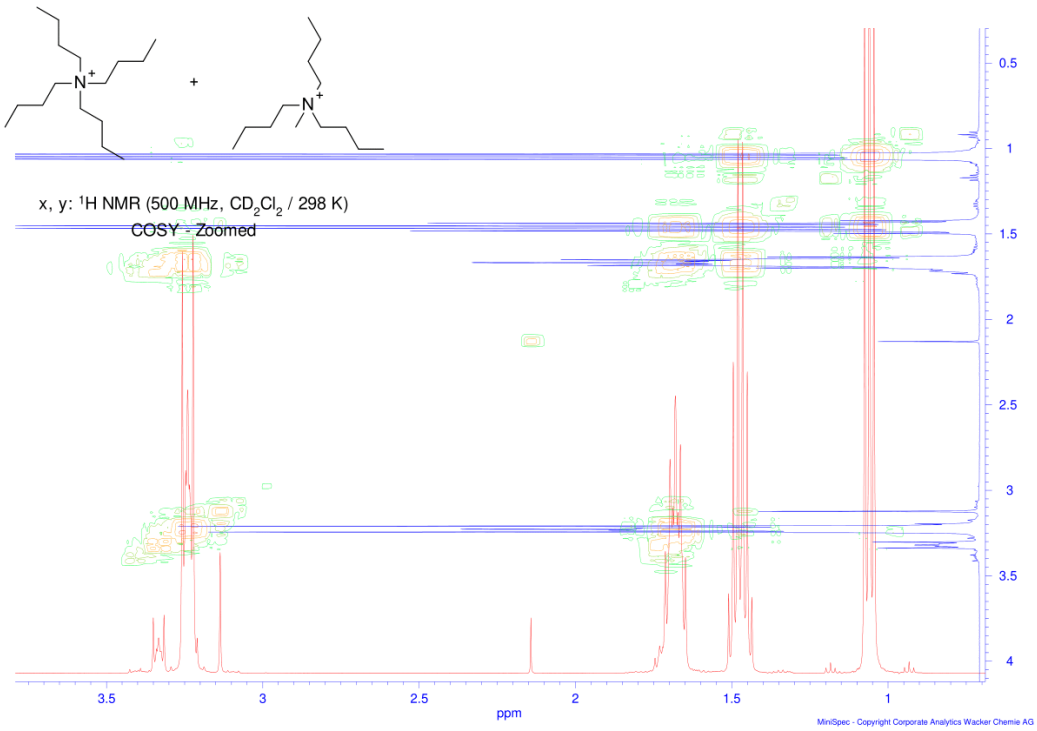
x, y: ¹H NMR (500 MHz, CD_2Cl_2 / 298 K)
COSY - Zoomed
ppm
MiniSpec - Copyright Corporate Analytics Wacker Chemie AG

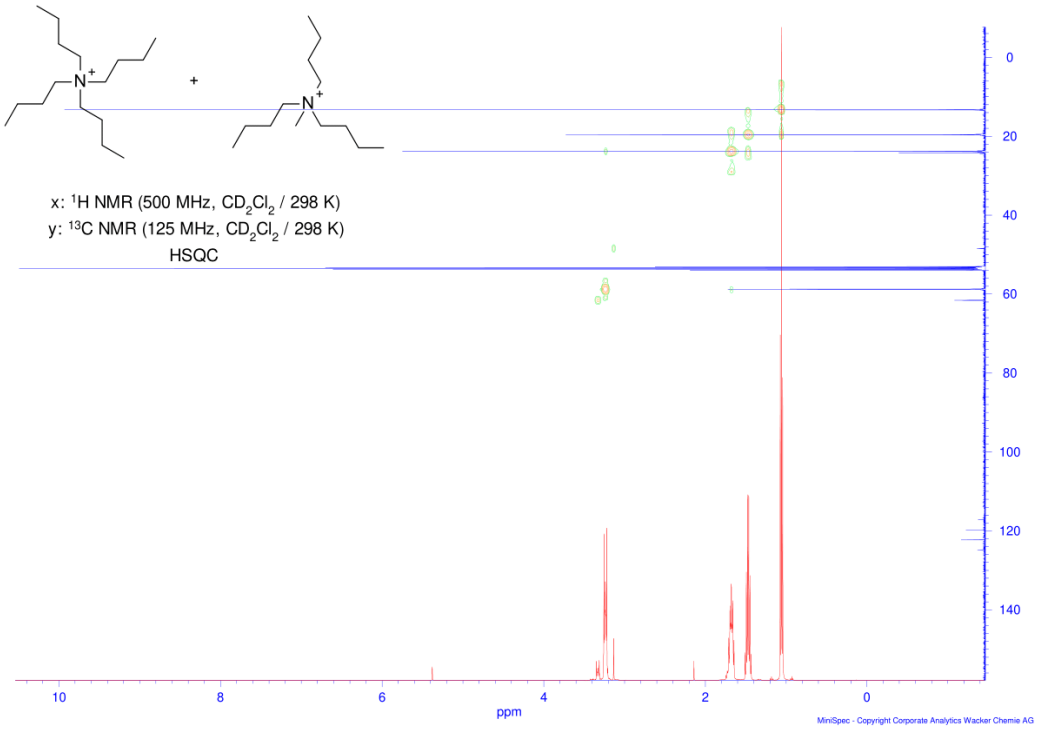
x: ^{1}H NMR (500 MHz, CD_2Cl_2 / 298 K)
y: ^{13}C NMR (125 MHz, CD_2Cl_2 / 298 K)
HSQC
ppm
MiniSpec - Copyright Corporate Analytics Wacker Chemie AG

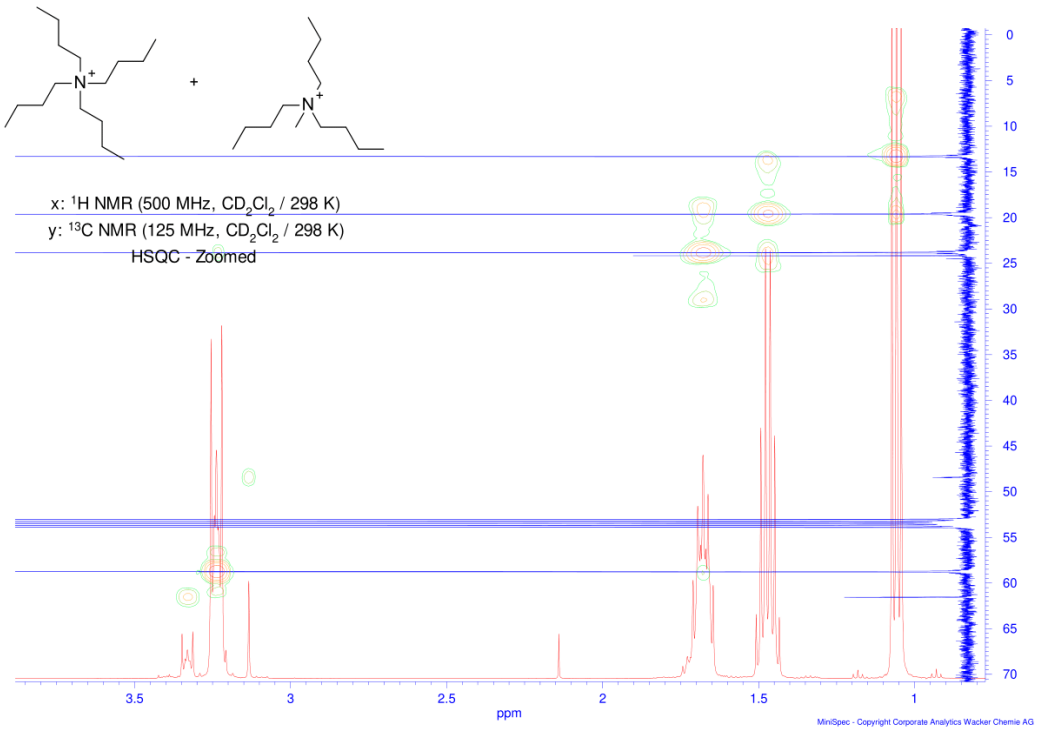
x: ^{1}H NMR (500 MHz, CD_2Cl_2 / 298 K)
y: ^{13}C NMR (125 MHz, CD_2Cl_2 / 298 K)
HSQC - Zoomed
ppm
MiniSpec - Copyright Corporate Analytics Wacker Chemie AG

9 References

[1] R. A. Assink, A. K. Hays, R. W. Bild, B. L. Hawkins, *J. Vac. Sci. Technol., A* **1985**, *3*, 2629–2633.

[2] T. B. Casserly, K. K. Gleason, *J. Phys. Chem. B* **2005**, *109*, 13605–13610.

[3] J. C. Reynolds, G. J. Blackburn, C. Guallar-Hoyas, V. H. Moll, V. Bocos-Bintintan, G. Kaur-Atwal, M. D. Howdle, E. L. Harry, L. J. Brown, C. S. Creaser, C. L. P. Thomas, *Anal. Chem.* **2010**, *82*, 2139–2144.

[4] A. R. Bassindale, K. H. Pannell, *J. Chem. Soc., Perkin Trans. 2* **1990**, 1801–1804.

[5] Z. Zhang, B. P. Gorman, H. Dong, R. A. Orozco-Teran, D. W. Mueller, R. F. Reidy, *J. Sol-Gel Sci. Technol.* **2003**, *28*, 159–165.

[6] J. Souček, G. Engelhardt, K. Stránský, J. Schraml, *Collect. Czech. Chem. Commun.* **1976**, *41*, 234–238.

[7] a) L. M. Bull, D. G. Gillies, S. J. Matthews, L. H. Sutcliffe, A. J. Williams, *Magn. Reson. Chem.* **1991**, *29*, 273–281; b) J. J. Eisch, S. Dutta, *Organometallics* **2005**, *24*, 3355–3358; c) E. Marotta, C. Paradisi, *J. Am. Soc. Mass. Spectrom.* **2009**, *20*, 697–707.

[8] a) R. J. Abraham, J. J. Byrne, L. Griffiths, M. Perez, *Magn. Reson. Chem.* **2006**, *44*, 491–509; b) H. Eggert, C. Djerassi, *J. Am. Chem. Soc.* **1973**, *95*, 3710–3718.

[9] a) R. J. Abraham, J. J. Byrne, L. Griffiths, *Magn. Reson. Chem.* **2008**, *46*, 667–675; b) G. Barbarella, P. Dembech, A. Garbesi, A. Fava, *Magn. Reson. Chem.* **1976**, *8*, 108–114; c) A. H. Fawcett, K. J. Ivin, C. D. Stewart, *Magn. Reson. Chem.* **1978**, *11*, 360–369.

[10] R. M. Souto, J. L. Rodríguez, E. Pastor, *Chem. - Eur. J.* **2005**, *11*, 3309–3317.

4 Zusammenfassung

In dieser Arbeit wurden drei Routen zur Elektrifizierung wertschöpfender Prozesse hin zu WACKER-relevanten Produkten unter Verzicht auf Opferelektrodenmaterialien, krebserregender organischer Verbindungen und mit möglichem Einbinden der Verfahren in bestehende Kreislaufprozesse untersucht (Schema 15). Zur Untersuchung dieser Thematiken war der Ausschluss von Sauerstoff und Feuchtigkeit notwendig. Alle Arbeiten, von Messungen durch Cyclovoltammetrie, über Synthesen bis zu Aufarbeitung und Analytik der Produkte, wurden vollständig unter Inertgas-Atmosphäre in einer Glovebox durchgeführt. Trotz synthetischer Herausforderungen konnte ein wichtiger Zugang zu Allylsilanen geschaffen werden, der ausgehend von Hydrosilanen ein neues Mediator-System im Bereich der anodischen Oxidation von Silanen darstellt. Die Aktivierung durch Lewis-saure Borane konnte sowohl im Bereich der Si-C-, wie auch der Si-Si-Bindung gezeigt werden.

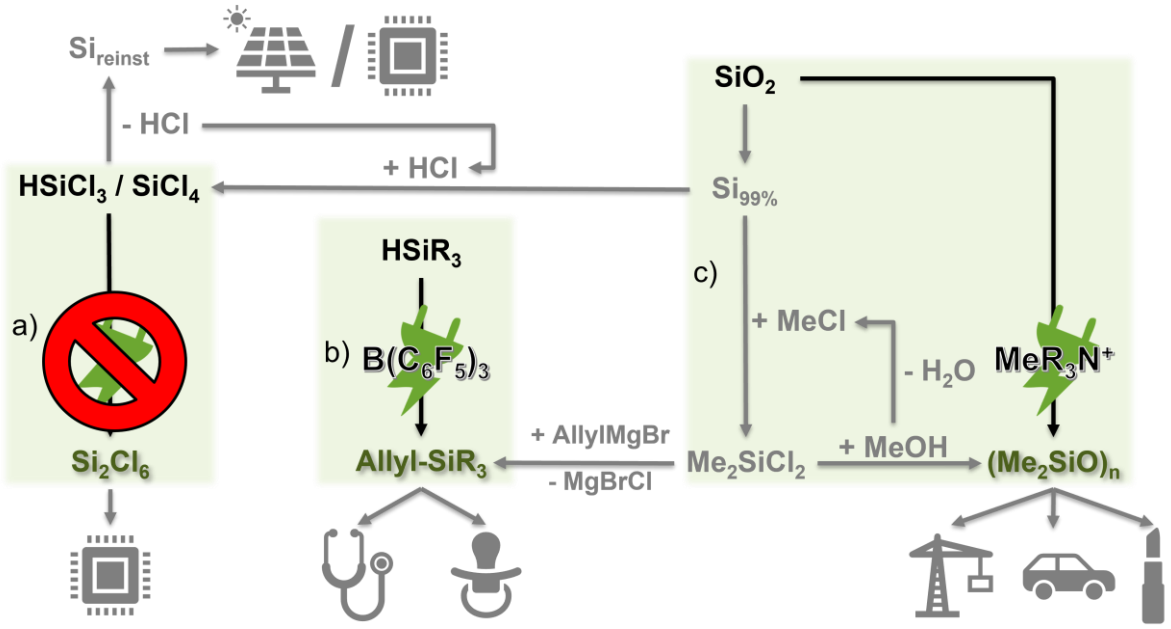

Schema 15. Zusammenfassung der Elektrifizierung möglicher Syntheserouten und -zugänge für WACKER-relevante Produkte: a) Zugang zu Si_2Cl_6 ausgehend von $SiCl_4$ und $HSiCl_3$ ist elektrochemisch versperrt; b) Zugang zu Allylsilanen ausgehend von Hydrosilanen kann durch Lewis-saures Boran als Mediator erreicht werden; c) Direkter Zugang zu Siloxanen ausgehend von SiO_2 ist durch MeR_3N^+ als Methylquelle möglich.

Start dieser Arbeit war die elektrochemische Dimerisierung von $SiCl_4$ und $HSiCl_3$ (Schema 15, a), wie in Kapitel 3.1 beschrieben. Die leichte Überreduktion hin zu Polysilanen, welche die Kathode im Reaktionsverlauf beschichten und damit die

Reaktion unterbinden, stellte eine der primären Problemstellungen dieser Untersuchung dar. Eine weitere Herausforderung ist durch das Zielprodukt Si_2Cl_6 selbst gegeben, welches sich unter diversen Bedingungen, wie in Anwesenheit von freien Halogeniden, nukleophilen Aminen, in einer Vielzahl von aprotischen Lösemitteln und *N*-Oxylen instabil verhält. Während diverse Ansätze auf Basis von Cyclovoltammetrie Messungen zu Beginn vielversprechend wirken, ist der synthetische Zugang aufgrund der Produktinstabilität und der Überreduktion der Edukte eine Hürde, die elektrochemische Protokolle ausschließt. Die Aktivierung von Hydrosilanen durch das Lewis-saure Boran $B(C_6F_5)_3$ zeigt Potential, konnte jedoch für die Si-Si-Bindungsknüpfung nicht zur Steigerung der Ausbeute oder der Etablierung eines Syntheseprotokolls für das selbst Lewis-saure $HSiCl_3$ eingesetzt werden.

Fortgesetzt wurden diese Arbeiten auf dem Gebiet elektronenreicherer Hydrosilane (Kapitel 0), deren Konversion zu Allylsilanen untersucht werden sollte (Schema 15, b). Basierend auf Erkenntnissen im Bereich der Si-H-Aktivierung durch die erste Thematik, konnte eine Syntheseroute beschrieben werden, die eine Domino-Reaktion, parallel an Anode und Kathode, nutzt. Benzyl- und Allylsilane sind über diesen Reaktionsweg zugänglich, besonders für die Darstellung von Allylsilanen ist die Si-H-Aktivierung durch den Lewis-sauren Boran-Mediator obligatorisch, um das Produkt vor Überoxidation zu schützen. In diesen Arbeiten konnte zusätzlich demonstriert werden, dass das Lewis-saure Boran nicht vollständig durch koordinierende Ionen des Leitsalzes deaktiviert wird. Die Anwesenheit von entsprechenden Leitsalz-Ionen ist sogar notwendig, um das Intermediat zu stabilisieren. Weiterhin kann über diese Route auf Opferanoden verzichtet werden und freiwerdender Chlorwasserstoff lässt sich leicht in bestehende Kreislaufprozesse einbinden.

Weitergeführt wurde die Arbeit zu Si-C-Bindungsknüpfungen durch den direkten Zugang zu Siloxanen ausgehend von SiO_2 (Kapitel 0), was auf bisherigen Forschungsergebnissen[1] und Patentanmeldungen[2] basiert (Schema 15, c). Die Reproduktion der Ergebnisse war durch das Elektrolysesetup herausfordernd. Entscheidend für eine entsprechende Konversion sind sowohl die hohe Stromdichte wie auch der Abstand von Anode zu Kathode und von Kathode zu SiO_2 Substrat für die reduktive Umsetzung. Dies konnte durch Etablieren eines reproduzierbaren Setups, mittels Anschwemm-Elektrode, gelöst werden, die auch unlösliche Substrate zugänglich macht. In synthetischen Arbeiten stellte sich heraus, dass Methylradikale die relevante Spezies sind und dadurch hohe Anforderungen an den Elektrolyten, bezüglich

elektrochemischer Stabilität, Stabilisierung der Methylradikalspezies und Koordination durch das Anion gestellt werden. Darüber hinaus geht die gewünschte Methylierung, entgegen bisherigen Vermutungen nicht von Methanol, sondern von Methylammoniumionen aus dem Leitsalz aus. Durch FENTON-analoge Reaktionsführung konnte die Methylradikal-gesteuerte Konversion von SiO_2 zu Methylsiloxanen untermauert werden. Die Ausbeuten des Protokolls sind bisher sehr gering und die Zersetzung des Elektrolyten über kathodische und anodische Konversion stellt den „grünen“ Ansatz elektrochemischer Umsetzungen in Frage.

[1] J. E. Dick, D. Chong, *J. Am. Chem. Soc.* **2014**, *136*, 6776; Zurückgezogen aufgrund von Bedenken bezüglich der Rechte an geistigem Eigentum.

[2] a) C. Huajun, F. Hongcheng, H. Jinghui, L. Liguo (Zhejiang Hesheng Silicon Industry Co), CN 103924259 A, **2014**; b) J. Jianxiong, L. Zhifang, L. Mengxian, W. Chuan (Hangzhou Normal University), CN 104120442 A, **2014**; c) L. Kai (Luo Kai), CN 103952716 A, **2014**.

5 Ausblick

Die elektrochemische Dimerisierung zu Si_2Cl_6 lässt auf Basis der gewonnenen Erkenntnisse keine erfolgversprechenden Ansätze zu. Die Konversion von Chlorsilanen ist jedoch ein wichtiges und aktuelles Thema für die elektrochemische Synthese.[1] Wie im Verlauf dieser Arbeit aufgezeigt, basiert die kathodische Konversion von Chlorsilanen bisher beinahe ausschließlich auf dem Einsatz von Opferanoden zum Abfangen des freigesetzten Chlorids (Schema 16). Während dieser Prozess nicht für industrielle Anwendungen geeignet ist, stellt der zusätzliche Eingriff in das Reaktionsverhalten der Intermediate ein Problem der Skalierung und Übertragbarkeit auf Metallionen-freie Syntheserouten dar. Es wäre daher von großem Interesse, Alternativen für den Einsatz von Opferanoden in der Konversion von Chlorsilanen zu etablieren.

Dies könnte durch die Verwendung von Gasanoden, wie der Wasserstoff-Anode, ermöglicht werden. Wie bereits durch GROGGER[2,3] demonstriert wurde, lassen sich damit freie Chloride aus der Reaktion als Chlorwasserstoff entfernen (Schema 16). Diese könnten in bestehenden Prozessen als Edukt wiederverwendet werden. Der bisherige Aufbau der Wasserstoff-Anode ist jedoch komplex und manuelles Beschichten der porösen Oberfläche stellt eine geeignete Reproduzierbarkeit in Frage. Das Aufkommen von elektrochemischen Thematiken, bei denen die Konversion von Gasen ein zentraler Aspekt ist, wie in der CO_2-Elektrolyse,[4] rückt Anwendung und Einsatz von Gas-Diffusionselektroden in den Mittelpunkt. Der zunehmende kommerzielle Zugang zu geeigneten Anodensystemen könnte die Forschungsaktivität in diesem Bereich für die Konversion von Chlorsilanen verstärken und so einen wichtigen Schritt in der Elektrifizierung von industriellen Prozessen schaffen.

Der Einsatz von Alkenen als Halogenidfänger, wie WALDVOGEL und Mitarbeiter[5] kürzlich für Halogenid-Shuttle demonstrierten, könnte einen weiteren Schritt in der Konversion von Chlorsilanen, mit Verzicht auf Opferanodenmaterialien, darstellen (Schema 16). Während von dieser Möglichkeit bereits mit zyklischen Verbindungen berichtet wurde,[2] konnten sich die Halogenid-Shuttle bisher nicht in der Synthese von Chlorsilanen etablieren. Die gute Transportfähigkeit und hohe Sicherheit der halogenierten Strukturen, im Vergleich zu den reaktiven Halogenen,[6] könnten für zukünftige Anwendungen von Interesse sein.[5]

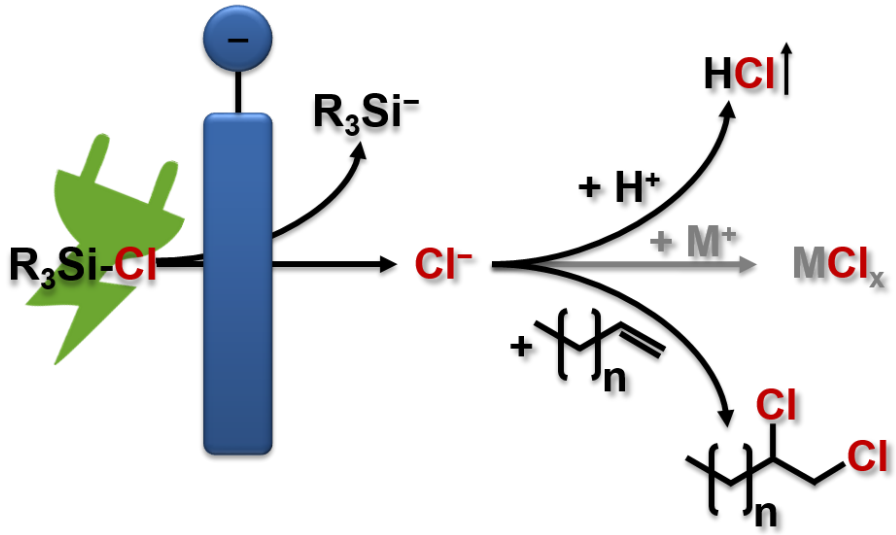

Schema 16. Abbildung zu Möglichkeiten des Halogenid-Fangs in der elektrochemischen Konversion von Chlorsilanen (M = Metall).

Die Einführung eines Lewis-sauren Borans als Mediator in der anodischen Konversion von Hydrosilanen stellt in dieser Arbeit eine neuartige Syntheseroute für andernfalls schwer zugängliche Silane dar. Die Konversion ist dabei stark von den stabilisierenden Eigenschaften des anionischen Intermediats abhängig, sodass bisher nur eine überschaubare Anzahl entsprechender Verbindungen synthetisiert werden konnte. Es ist daher von hohem Interesse ein breiteres Substratspektrum relevanter Verbindungen zu schaffen. Der Einsatz von Monochlorhydrosilanen sollte aufgrund der geringeren Lewis-Azidität[7] für die gewünschte Konversion geeignet sein und erlaubt weitere Funktionalisierung der Halogengruppe. Silylamine, die als wichtige Vertreter organofunktioneller Silane zählen,[8] könnten über entsprechende Hydrosilanverbindungen, durch den Boran-Mediator, zugänglich sein. Neben den Allyl- und Benzylsystemen sind Vinylstrukturen und weitere substituierte Vertreter mit kathodisch erreichbarem Reduktionspotential denkbar für industriell relevante Substrate. Eine zusätzliche Stabilisierung des Anions durch Zugabe von Mg^{2+} oder vergleichbare komplexierende Additive sollte für die Konversion von Hydrosilanen geprüft werden.

[1] L. Lu, J. C. Siu, Y. Lai, S. Lin, *J. Am. Chem. Soc.* **2020**, *142*, 21272–21278.

[2] C. Jammegg, S. Graschy, E. Hengge, *Organometallics* **1994**, *13*, 2397–2400.

[3] A. Popp, R. Weidner, H. Stüger, C. Grogger, B. Loidl (Consortium für elektrochemische Industrie GmbH), DE 10 2004 029 258 A1, **2004**.

[4] a) T. N. Nguyen, C.-T. Dinh, *Chem. Soc. Rev.* **2020**, *49*, 7488–7504; b) D. Wakerley, S. Lamaison, J. Wicks, A. Clemens, J. Feaster, D. Corral, S. A. Jaffer, A. Sarkar, M. Fontecave, E. B. Duoss, S. Baker, E. H. Sargent, T. F. Jaramillo, C. Hahn, *Nat. Energy* **2022**, *7*, 130–143.

[5] X. Dong, J. L. Roeckl, S. R. Waldvogel, B. Morandi, *Science* **2021**, *371*, 507–514.

[6] a) M. Eissen, D. Lenoir, *Chem. - Eur. J.* **2008**, *14*, 9830–9841; b) I. Saikia, A. J. Borah, P. Phukan, *Chem. Rev.* **2016**, *116*, 6837–7042.

[7] A. Šimarek, M. Lamač, M. Horáček, J. Pinkas, *Appl. Organomet. Chem.* **2018**, *32*, e4442.

[8] C. Grogger, B. Loidl, H. Stueger, T. Kammel, B. Pachaly, *J. Organomet. Chem.* **2006**, *691*, 105–110.

6 Abkürzungsverzeichnis

ALD	Atomlagenabscheidung (*atomic layer deposition*)
A	Ampere
Bu	Butyl
CV	Cyclovoltammetrie
D_3	Hexamethylcyclotrisiloxan
D_4	Octamethylcyclotetrasiloxan
D_5	Decamethylcyclopentasiloxan
D_6	Dodecamethylcyclohexasiloxan
DMDMS	Dimethyldimethoxysilan
DMSO	Dimethylsulfoxid
FcH/FcH^+	Ferrocen/Ferrocenium
FLP	frustrierte Lewis Paar (*frustrated Lewis pair*)
HAT	Wasserstoff Atom Transfer (*hydrogen atom transfer*)
HMPT	Hexamethylphosphorsäuretriamid
Mes	Mesityl
M	molar
mV	Millivolt
NHPI	*N*-Hydroxyphthalimid
nm	Nanometer
OTf	Trifluormethansulfonat
PINO	Phthalimido-*N*-oxyl
ROP	Ringöffnungspolymerisation
SCE	Kalomelelektrode (*saturated calomel electrode*)
SEI	Festkörper-Elektrolyt-Interphase (*solid electrolyte interphase*)
THF	Tetrahydrofuran
vs.	versus